AUGMENTATION OF CONDENSATION HEAT TRANSFER OF R-11

BY INTERNALLY FINNED TUBES

by

K.S. VENKATESH

B.E., Mechanical Engineering, Bangalore University, India, 1979

A MASTER'S THESIS

Submitted in partial fulfilment of the

requirements for the degree

MASTER OF SCIENCE

Department of Mechanical Engineering

KANSAS STATE UNIVERSITY

Manhattan, Kansas

1984

Approved by :

M. Z. Azer

Major Professor

LD
2668
.T4
1984
.V46
c. 2

A11202 665865

TABLE OF CONTENTS

LIST OF FIGURES

Figure | Page

LIST OF TABLES

Chapter I

INTRODUCTION

In-tube condensation occurs in a variety of engineering situations such as airconditioning and refrigeration, petrochemical, process and numerous other industries. The use of more efficient heat exchangers in the fields of nuclear and conventional power plants, space ships, and naval ships has become a necessity in the modern world. Economic and energy considerations have motivated the interest of different investigators to explore the use of various techniques to augment heat transfer in heat exchangers. The goals of these investigators were either to reduce the size of heat exchangers for a given heat load, thereby reducing their cost, or to increase the heat capacity of existing heat exchangers. In a report published in 1975 by Bergles [1], it was estimated that the investment in heat exchanger equipment in the U.S. was approaching one billion dollars yearly. Ten to twenty percent reduction in capital cost could produce savings in the 100 million dollar range.

Usually, in-tube condensation results in high heat transfer coefficients. However, fluids, such as certain organic liquids as well as fluro-carbon refrigerants, have thermophysical and transport properties which usually result in low condensation heat transfer coefficients. Augmenting the condensation heat transfer of these fluids could significantly improve the efficiency and performance of condensers.

During the past several decades numerous techniques have been tried to improve the heat transfer in heat exchangers. These techniques can be broadly classified into active and passive techniques. Vibration of the heat transfer surface and the application of electrostatic fields are among the active techniques. As active techniques of augmenting the heat transfer required external power application, they received little attention by investigators. Roughened, corrugated, fluted, and internally finned tubes, and tubes with vortex generator inserts such as twisted tapes and static in-line mixers are a few among the passive techniques for augmenting heat transfer. Most investigations in the past were directed toward passive techniques because they do not require external power. These passive techniques are easy to incorporate, relatively simple to operate and pose less problems in maintenance. Commercial production of most of these passive augmented tubes are currently in vogue. One of the factors which is limiting the use of some of these techniques is the lack of reliable design correlations for predicting the heat transfer and pressure drop. Considerable amount of testing is needed before most of these techniques can be put into full scale industrial use.

The main concern of the present study was to investigate the enhancement of in-tube condensation of R-11 by internally finned tubes. It was an extension of the investigation of Said [2] in which he studied the augmentation of in-tube condensation of R-113 by internally finned tubes. The tubes tested by Said [2] were also tested in the present study using R-11 test fluid.

The objectives of the present study were:

1. To take different sets of heat transfer and pressure drop data for condensation of R-11 inside internally finned tubes at different flow parameters.
2. To compare the experimental results with the predictions of existing correlations in order to identify the correlation which best predicts the experimental results of the present study.

Chapter II

LITERATURE SURVEY

A bibliography of world literature on augmentation was published by Bergles et al. [3]. Over 1900 references were cited in this bibliography. The references were grouped under two major classifications:

1. Techniques of Augmentation: Active, requiring external power, or passive requiring no external power.

2. Modes of heat transfer.

Considering the vast scope of augmentation, the present literature survey had to be limited to in-tube condensation (mode of heat transfer) inside internally finned tubes (technique of augmentation). A preliminary review of the subject matter revealed that design correlations of internally finned tubes for condensation heat transfer and pressure drop are only the extensions of smooth tube correlations. Also, the development of design correlations for condensation is closely related to single-phase flow inside tubes. So, a few single-phase flow studies inside tubes were also included in the present study.

As a first step, the literature surveys of recent studies of different investigators such as Royal [4], Luu [5] and Said [2] were reviewed. Royal [4] studied experimentally the augmentation of in-tube condensation of steam with internally finned tubes and twisted tape inserts. Luu [5] and Said [2] experimentally studied the augmentation of condensation heat transfer of R-113 by internally finned tubes and twisted tape inserts. Luu [5] also conducted experiments with rough tubes.

Royal [4] surveyed the condensation literature in general and augmentation of condensation inside tubes in particular. He classified the general condensation literature into two categories, dropwise and filmwise condensation. Filmwise condensation is the most common in condensation processes. He classified filmwise condensation literature into condensation outside tubes and condensation inside tubes. The literature on augmentation of inside film condensation was again classified according to augmentation techniques into passive and active techniques. Passive augmentation techniques cited were surface roughness, extended surfaces, and vortex generators. Also, he categorized the references according to flow conditions, such as laminar or turbulent, and according to whether the design correlations developed were experimental or analytical. He cited over 40 references dealing with predicting in-tube condensation heat transfer coefficients and over 70 references on augmentation of condensation. Royal's [4] literature survey was a comprehensive attempt at reviewing the condensation literature available prior to 1975.

Luu [5] studied the literature systematically according to subject matter. The broad headings under which he reviewed the literature were:

1. Flow regime studies in two-phase flow
2. Heat transfer studies of single and two-phase flow
3. Augmentation of heat transfer using twisted tapes, internally finned tubes, and rough tubes.

In the heat transfer studies of two-phase flow, Luu included references pertaining to vertical film condensation and in-tube condensation. In-tube condensation literature was then critically reviewed to include various parametric effects on heat transfer and pressure drop, such as inlet superheat, heat flux, tube inclination, pressure level, diameter to length ratio of condenser, and fluid properties. The literature of augmentation heat transfer using internally finned tubes included single and two-phase flow. Luu's [5] literature survey cited over 200 references published prior to 1980.

Said [2] attempted to update the condensation literature incorporating work done up to 1982. Omitting some of the basic references which were already reviewed thoroughly by Royal [4] and Luu [5], he included the references relevant to his study.

Considering the objectives of the present study and realizing the extent to which the literature has been reviewed, an attempt to review the widely used design correlations for heat transfer and pressure drop during condensation inside smooth and internally finned tubes was made. More interested readers are urged to refer to references [2,3,4,5].

SMOOTH TUBES

Several correlations are available in the literature for predicting local and overall average condensation heat transfer coefficients inside smooth tubes. In general, these correlations were either based on single-phase flow heat transfer correlations or on analogy between heat and momentum transfer in the condensate film. The correlations of Akers et al. [6], Boyko and Kruzhilin [7], Rosson and Myers [8], Traviss et al. [9], Soliman et al. [10], Azer et al. [11], Cavallini and Zecchin [12], and Shah [13] are a few of the several correlations available for predicting heat transfer coefficients during in-tube condensation. Reference to the correlations of Akers et al. [6], Boyko and Kruzhilin [7], and Shah [13] will be made in a later chapter.

Pressure drop during two-phase flow inside a horizontal tube is a combination of frictional and momentum parts. The correlations of

Lockhart-Martinelli [14], Dukler et al. [15,16], and Hughmark [17], are widely used for the estimation of the frictional pressure drop. The momentum pressure drop requires the knowledge of the void fraction variation in the direction of flow. The void fraction correlations of the homogeneous model [18], Lockhart-Martinelli [14], Baroczy [19], Thom [20], Zivi [21], Turner-Wallis [22], and Hughmark [23] are among the correlations available in the literature. Reference will be made to these correlations in a later chapter.

INTERNALLY FINNED TUBES

In recent years, manufacturing techniques have been well developed to produce a wide variety of internally finned tubes. Numerous experimental and analytical studies on the effects of these tubes on heat transfer and pressure drop in single-phase as well as two-phase flow were conducted by different investigators.

Single-Phase-Studies.

Watkinson et al. [24,25,26] experimentally investigated the heat transfer and pressure drop with internally finned tubes of different diameters and fin geometries in single-phase flow. An enhancement of heat transfer as high as 170% at the same Reynolds number and up to 80% at constant pumping power was reported [24] for turbulent flow of water in internally finned tubes. A 95% enhancement of heat transfer for air [25] and 224% for laminar flow of oil [26] was obtained using internally finned tubes. In the above papers, it was also reported that spiralling the fins improved the heat transfer with only moderate pressure drop increase.

Carnavos [27,28,29] conducted experiments to cool air, and to heat water using internally finned tubes. In his study of cooling air [27], he used 21 tubes of integral spiral and longitudinal fins. The finned tubes were reported to perform better than smooth tubes by factors of 1.2-2.0 at constant pumping power. He also presented correlating equations to pre-predict the heat transfer and friction factor for internally finned tubes. In [28], Carnavos experimentally investigated the heat transfer performance of five composite tubes, made by mechanically coupling in parallel individual copper tubes having continuous integral internal spiral and longitudinal fins, for cooling air in turbulent flow. He reported that at constant pumping power, the composite tubes performed better than smooth tubes by factors of 1.7 to 10. Correlations to predict heat transfer and pressure drop were also presented. In [29], Carnavos experimentally investigated the heat transfer performance of heating water and/or a 50%-50% ethylene glycol-water solution in turbulent flow by tubes having internal spiral and longitudinal fins and found that these tubes performed better than smooth tubes.

Compared to the experimental investigations, the analytical studies of heat transfer and pressure drop were limited.

Hu and Chang [30] studied the heat transfer of fully developed laminar flow in internally finned tubes analytically. The fins considered had fictitious zero thickness. They concluded that the presence of internal fins improves the heat transfer performance for laminar flow more than turbulent flow and the Nusselt number of laminar flow in tubes with optimum number of internal fins of particular height can surpass that of many cases of turbulent flow in finless tubes.

Nandakumar and Masliyah [31] used the finite element method of analysis to solve the momentum equation describing the laminar fluid flow in a finned tube. They developed empirical correlations, covering a wide range of fin parameters, for the friction factor f and the Nusselt number. In a later paper [32], they obtained the heat transfer coefficients for forced convection, fully developed laminar flow in an internally finned tube, with axial uniform heat flux and with peripherally uniform temperature, using the finite element method. They concluded that the Nusselt number of a triangular finned tube was higher than that of a finless tube, and was a strong function of fin length and fin thickness.

Soliman and Feingold [33] conducted an analysis of fully developed laminar flow in internally finned tubes by solving the momentum equation using infinite series coefficients matching method to obtain the velocity profile and friction factor. They reported that the values of the dimensionless velocity at any location within the tube was found to depend mainly on the number of fins and their height, and to a lesser degree on the fin half-angle. In a later paper [34], they analytically solved the energy equation of fully developed laminar flow to obtain the temperature profile and heat transfer, and concluded that the Nusselt number increases with the increase of the number of fins up to a critical fin number beyond which a reversal of trend occurs.

Two-Phase Flow Studies.

A limited number of studies on augmentation of in-tube condensation has been reported in the literature. Owing to the complexity of the condensation mechanism in internally finned tubes, no analytical studies have been attempted. The correlations developed to predict the heat transfer and pressure drop during condensation inside internally finned tubes are based on smooth tube correlations and are semi-empirical in nature.

Reisbig [35] studied the condensation of R-12 inside horizontal tubes with internal longitudinal fins. He reported a 40% increase in heat transfer compared to smooth tubes. He also found that the finned tubes performed best in two-phase flow and that these tubes were not advantageous at extreme qualities.

Kroger [36] studied the laminar condensation heat transfer of R-12 inside smooth and internally finned tubes. His experimental study included examination of the effects of tube inclination, and different tube diameters to length ratios. He noted that in a horizontal position, the rate of heat transfer for a large diameter tube having twelve fins was almost the same as that for a smaller tube having nine fins. The heat transfer rate at an inclination of 10 degrees was found to be up to 200% greater than that of an equivalent smooth horizontal tube.

Vrable et al. [37,38,39] investigated the condensation heat transfer and pressure drop during condensation of R-12 inside two longitudinally finned tubes. They reported that the addition of extended surfaces on the inner surface of the tubes resulted in approximately 20% increase in the average tube side heat transfer coefficient. They also proposed a heat transfer correlation based on Cavallini and Zecchin [12,40] correlation for smooth tubes.

Royal and Bergles [41-43] conducted an experimental investigation on in-tube condensation of steam with three augmentation techniques: tube inclination, twisted tape inserts, and internally finned tubes. Their conclusions were: (a) the effects of tube inclination on in-tube heat transfer coefficients were small. An inclination of 10 degrees downwards in the direction of flow increased the heat transfer coefficient by a maximum of 10% over the horizontal value, on a nominal area basis. (b) twisted tape inserts enhanced the heat transfer coefficients by as much as 30% above smooth tubes, on a nominal area basis. (c) internally finned tubes enhanced the heat transfer coefficients by as much as 150% above smooth tube values, on a nominal area basis. The heat transfer and pressure drop correlations developed by Royal and Bergles for internally finned tubes are discussed in Chapter V.

Luu and Bergles [5,44-46] condensed R-113 inside rough tubes, tubes with twisted tape inserts, and internally finned tubes. They reported that twisted tape inserts increased the heat transfer coefficients, on a nominal area basis, by approximately 30% and pressure drop by 250%, over by smooth tube results. Internally finned tubes increased the heat transfer as much as 120% over that of smooth tube with only a modest pressure drop increase. They concluded that the improvement in heat transfer performance of internally finned tubes were far better than that of twisted tape inserts. They developed correlations to predict the heat transfer and pressure drop during condensation inside internally finned tubes and tubes with twisted tape inserts. The correlations of internally finned tubes are discussed in Chapter V.

Said and Azer [2,47] investigated the effects of twisted tape inserts and internally finned tubes on augmenting the condensation heat transfer of R-113. The twisted-tapes selected were of different pitch to diameter ratios. The four internally finned tubes tested had different outside diameters and fin geometries. Their results showed an improvement in heat transfer coefficients by internally finned tubes as high as 51% over smooth tube results, on a nominal area basis. The heat transfer was accompanied by a modest increase in the pressure drop. The twisted tape inserts enhanced the heat transfer coefficients by approximately 23% over the smooth tube, on a nominal basis, and was accompanied by a significant increase in the pressure drop. The correlation equations proposed for heat transfer and pressure drop during condensation by Said and Azer are discussed in Chapter V.

Chapter III

EXPERIMENTAL INVESTIGATION

The primary objectives of this experimental investigation were:

1. to obtain experimental heat transfer and pressure drop data for condensation of R-11 inside horizontal tubes with and without internal fins.
2. to correlate the experimental heat transfer and pressure drop results with the existing correlations and to identify among these correlations the ones that correlate best with the data.

3.1 TEST FACILITY

The apparatus used in the study was originally constructed by Said [2] for studying the enhancement of in-tube condensation by internally finned tubes and tubes with twisted tape inserts. He used R-113 as the condensing fluid. A minor modification was made on the test facility to allow for using R-11 as the condensing fluid. This modification required the installation of a liquid R-11 cooler between the liquid receiver and the circulating pump. Figure 3.1 shows a photographic view of the test facility.

3.2 R-11 FLOW LOOP

Figure 3.2 shows a schematic diagram of R-11 flow loop. It includes the following components:

1. an electrically heated boiler
2. a superheater
3. a liquid circulating gear pump
4. a liquid-vapor separator

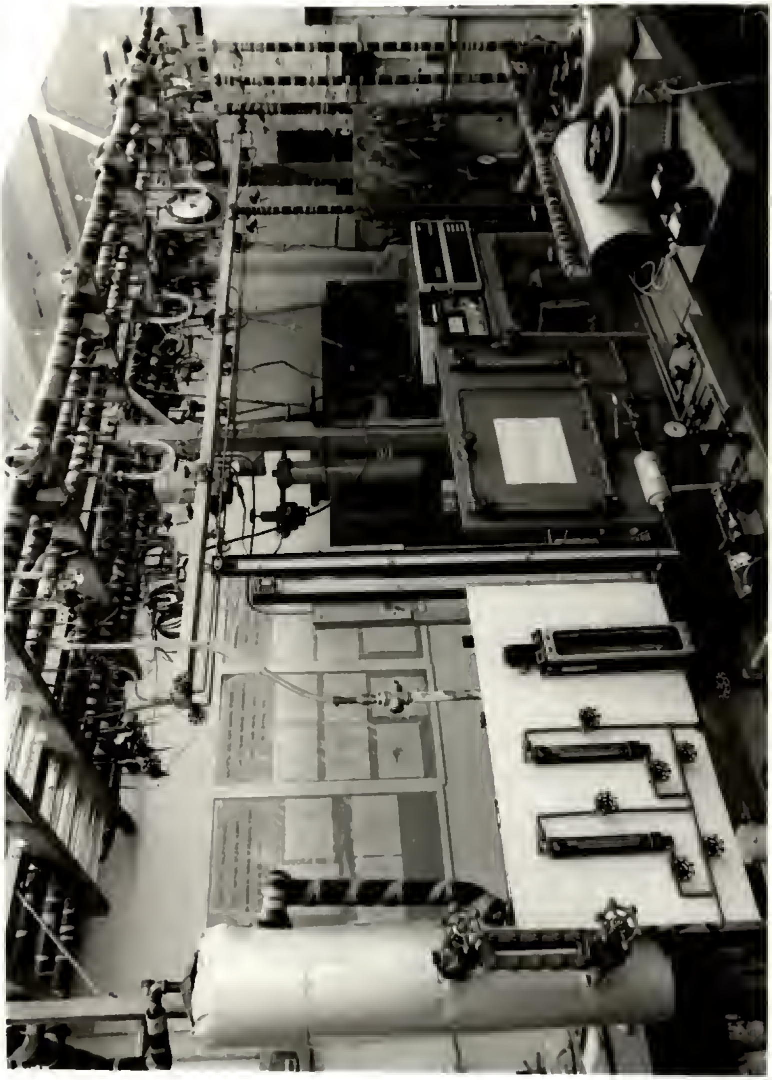

Fig. 3.1 Photographic View of the Entire Test Facility

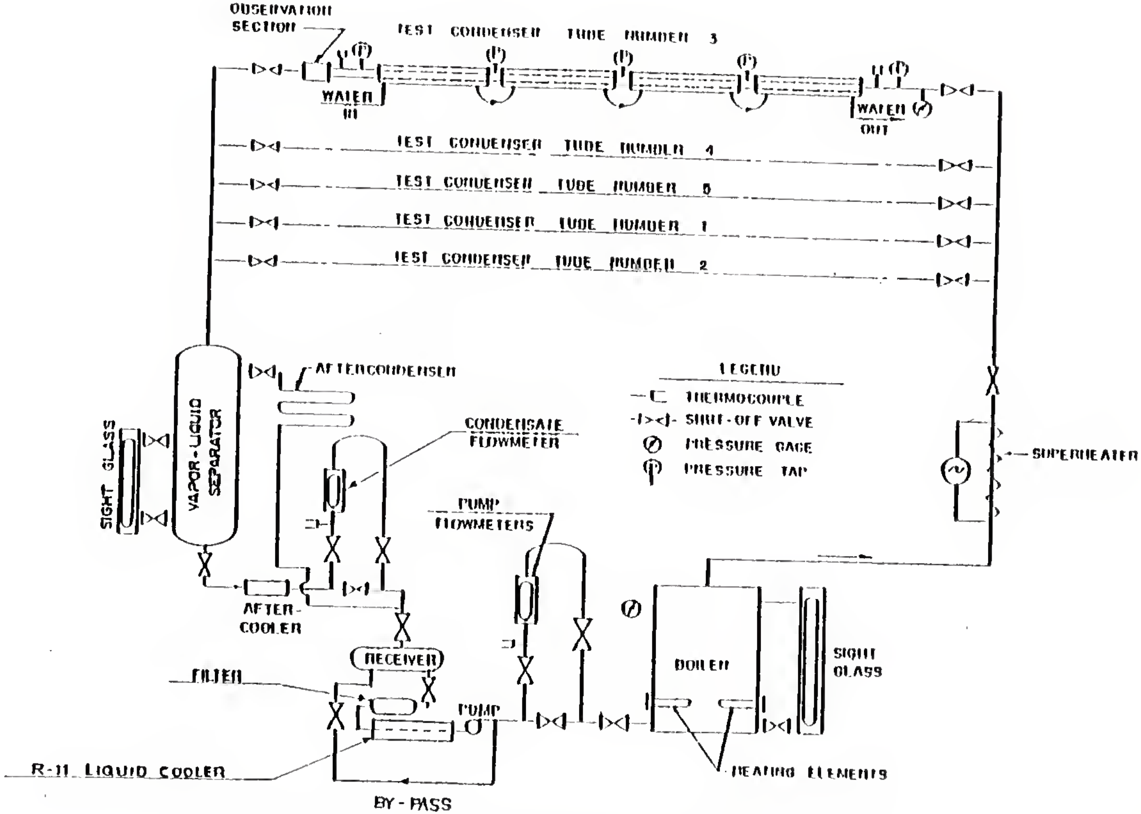

Fig. 3.2 A Schematic Diagram of the R-11 Flow Circuit.

5. an after condenser
6. a liquid receiver
7. liquid flowmeters
8. a liquid drier

In addition to the above components, the test facility included five test condensers which were mounted horizontally in parallel as shown in Fig. 3.2. Each test condenser consisted of four subsections. Each subsection was a double pipe counter flow heat exchanger where R-11 condensed inside the inner tube and the coolant flowed in the annulus. Among the five inner tubes, one was smooth, the second had straight internal fins, the third, fourth and fifth had spiral internal fins with different helix angles and outside diameters.

3.2.1 Test Condenser Construction and Instrumentation

The geometric parameters of the smooth tube and the internally finned tubes tested are given in Table 3.1. Figure 3.3 shows a photograph of the finned tubes tested.

Each test condenser was constructed out of one single inner tube where R-11 condensed. Each condenser consisted of four subsections. These subsections were constructed by soldering four equal lengths of copper tubing around the outside surface of the test condenser using proper fittings and connections. Each subsection represented a double-pipe counter-flow heat exchanger. The width of the annular space in each of the subsections was 2.54 cms (1 in.) in all the test condenser tubes. The outer tube of each of the four subsections was provided with coolant inlet and outlet connections and connections to measure the outside surface temperature of the inner tube. The connection between two subsections of test condenser was done by plastic tubing as shown in Fig. 3.4. An observation section was

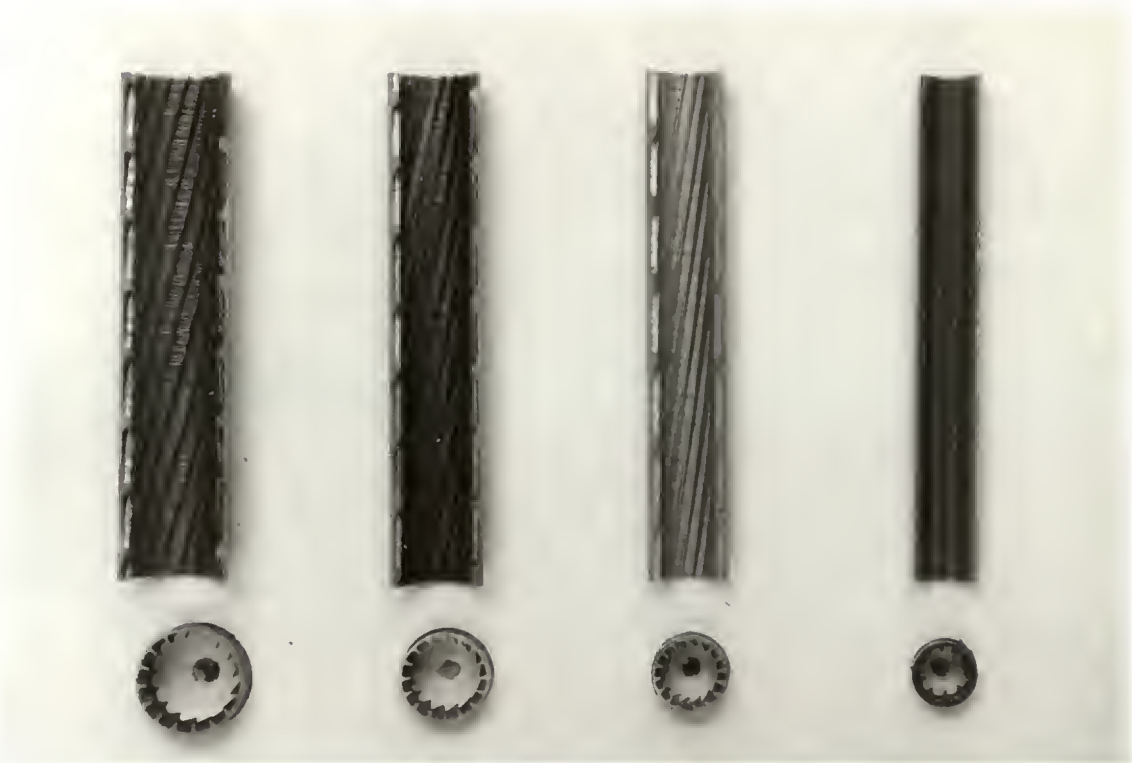

Fig. 3.3 Photograph of the Test Condenser Tubes, Left to Right: Tubes 5, 4, 3 and 2.

TABLE 3-1. Geometric Parameters of the Experimental Tubes#

Tube No.	1	2	3	4	5
Type	Smooth	Straight Finned	Spiral Finned	Spiral Finned	Spiral Finned
Material	cu	cu	cu	cu	cu
No. of fins, n	———	10	16	16	16
Outside diameter, D_o	1.5875	1.5850	1.9012	2.2162	2.6568
Inside diameter, D_i	1.3843	1.4199	1.7145	2.0384	2.5375
Equivalent diameter, D_e	1.3843	1.36	1.666	1.987	2.457
Hydraulic diameter, D_h	1.3843	0.853	0.858	1.13	1.50
Fin height, b	———	0.1575	0.1803	0.1981	0.2134
Wall thickness	0.1016	0.0826	0.0934	0.0889	0.0597
Fin height/ inside diameter	———	0.1109	0.1052	0.0972	0.0841
Actual flow area, A_{fa}**	1.5050	1.4527	2.1799	3.1009	4.7413
Nominal flow area, A_{fn}**	1.5050	1.5835	2.3087	3.2634	5.0571
Core flow area, A_{fc}**	———	0.9588	1.4397	2.1181	3.4987
Actual area, A_a***	4.3489	6.68	10.2	11.3	13.1
Nominal area, A_n***	4.3489	4.4607	5.3863	6.4038	7.9718
Inter-fin spacing, W	———	0.297	0.206	0.305	0.363
Helix angle, α	———	0°	9.71°	12.34°	19.36°

TABLE 3-1. Geometric Parameters of the Experimental Tubes (continued)

Tube No.	1	2	3	4	5
Pitch, cm/360°	______	ST	22.2	20.3	15.2

* all lengths and areas are in cm and cm^2 respectively, as appropriate.

** area in cm^2

***area in cm^2/cm

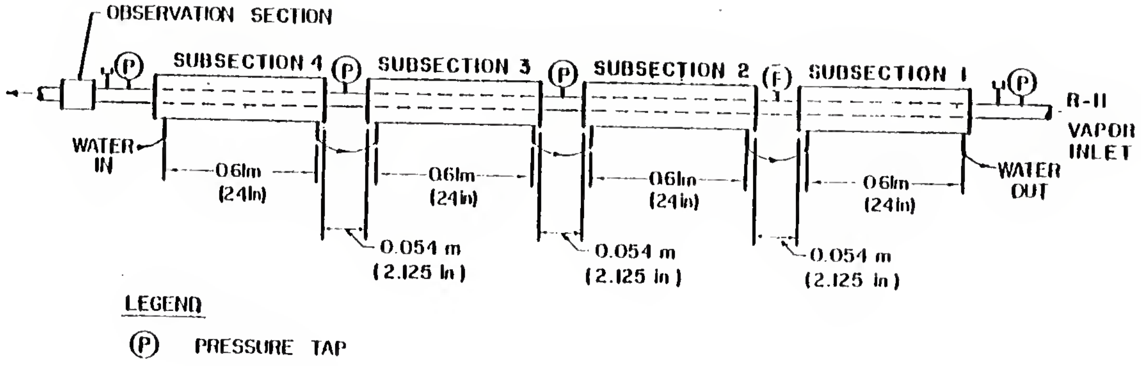

Fig. 3.4 A Schematic Diagram of the Test Condenser

installed at the exit of each condenser, made of high pressure clear glass, to observe the condensate flow. Each test condenser had a flexible copper vibration eliminator section attached to it to accommodate any expansion due to heating during operation.

Each test condenser was instrumented to measure the inlet and outlet temperatures of the cooling water in each subsection, inlet pressure and temperature, and the exit temperature of R-11. All temperatures were measured by copper-constantan B and S 24 gage thermocouples. All thermocouples were connected to a data acquisition system which gave a printout of all temperature readings. All thermocouples were calibrated at two points, the boiling water and melting ice temperatures. The inlet pressure was measured with a Heise pressure gage type H28832.

There were five pressure taps to measure the pressure drop across each subsection. The location of these pressure taps are shown in Fig. 3.5. All the pressure taps had four holes, each 0.16 cms (1/16 in.) diameter, spaced 90° apart around the circumference of the test condenser. These holes were covered with a copper sleeve which had a clearance of about 0.48 cms (3/16 in.). The sleeve was silver brazed to the condenser tube. A 0.32 cms (1/8 in.) I.D. copper tube was attached to the sleeve and connected to the pressure measurement device.

The pressure drop across any two pressure taps was measured by a properly calibrated Foxboro Differential Pressure (D/P) cell type 13A. The D/P cell pressure drop measurements were checked against the measurements of a Pace Wianco pressure transducer (P/T) model KP15. The P/T was connected to a Pace Wianco digital indicator, model CD25, which gave the pressure difference across any two taps directly. Figure 3.6 shows a schematic diagram of the piping circuit for pressure measurements. In general the D/P cell and P/T measurements agreed. Even when they differed,

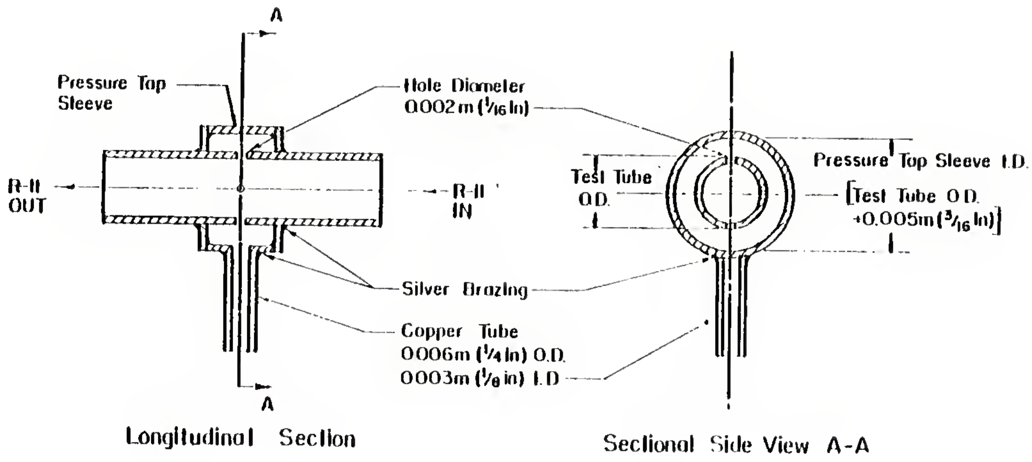

Fig. 3.5 Pressure Tap Construction Details.

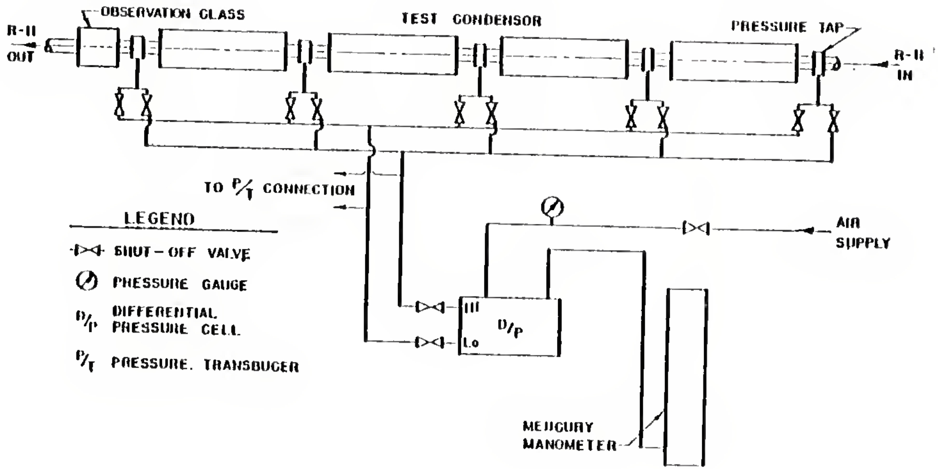

Fig. 3.6 Schematic Diagram for Pressure Drop Measurement.

the difference was small and then the average of two readings were taken.

The average wall temperature of each test condenser tube of each subsection was measured by four thermocouples attached as shown in Fig. 3.7. Two thermocouples were attached at the top, the other two at the bottom. An axial distance of 0.61m (24 in.) was maintained between the two thermocouple stations located at 0.152m (6 in.) from the coolant's inlet and outlet. The construction details of each thermocouple junction is shown in Fig. 3.8. Conical grooves, slightly larger than the bead of thermocouple, were drilled and the beads were silver brazed in these grooves. Fast drying epoxy (a product of Armstrong company type A-36/B-36) was applied to the silver brazed portion of thermocouple and a short length of nylon heat shrink tubing was slid from the other end towards the junction until it touched the outside surface of the condenser test tube and covered the junction. More epoxy was added to secure the nylon tube to the outside surface. This arrangement ensured the elimination of contact between the thermocouple junction and cooling water. The outer surface of the condenser was then covered with fiber glass insulating tape near the thermocouple junction. The thermocouple leads were then tied to the test condenser tube using nylon cable tie. Additional epoxy was used to cover the thermocouple leads between the junction and nylon tie. The fiber glass tape protected the thermocouple leads from getting heated at the portion where they were tied to condenser tube and the nylon tie prevented the detachment of the thermocouple junction by accidental pulling of the thermocouple leads from the other end. The thermocouple leads were then led through the outside tube as shown in Fig. 3.8. The space between the leads and the copper tube attached to the outer tube of each subsection was filled with

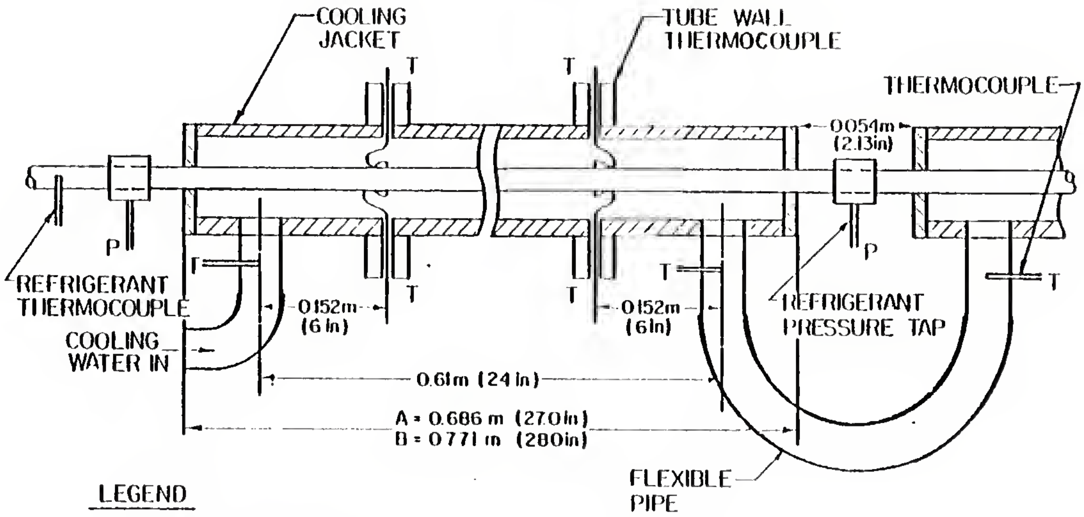

LEGEND

A FOR TUBES No. 1 and 2.
B FOR TUBES No. 3, 4 and 5.
P PRESSURE TAP
T THERMOCOUPLE

Fig. 3.7 A Schematic View of a Subsection.

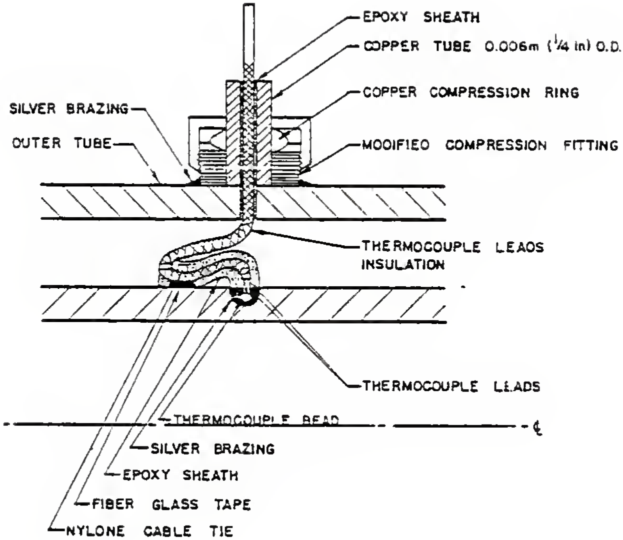

Fig. 3.8 Thermocouple Mounting Detail.

epoxy to prevent any coolant leaks. The thermocouple junctions were checked for good thermal contact after their completion.

The flow of R-11 leaving the circulating pump was measured by two Fisher and Porter variable area flowmeters. The flowmeters were mounted vertically in parallel so that they could be used individually or simultaneously to measure the flow rate. One had a range of 0.0-0.35 g.p.m. and the other 0.0-0.55 g.p.m. There was a similar flowmeter connected between the vapor-liquid separator and the liquid receiver to measure the flow rate of the uncondensed vapor inside the test condenser. In the present study complete condensation was achieved inside the test condenser in all runs and hence this was never used. Electric heating elements were used to heat R-11 in the vapor generator. The power was controlled by a powerstat variable transformer. The power input to each of the heating elements was measured by measuring the current and voltage across each heating circuit. Appendix A lists additional details about the components of the refrigerant flow circuit.

Individual test condensers and the entire refrigerant circuit was leak-proof tested under pressurized and evacuated conditions. A layer of rubber insulation, 0.064m (2.5 in.) thick, prevented heat loss from the test condenser tube to the ambient. The vapor generator was also insulated with 0.019m (3/4 in.) thick layer of fiber glass insulation.

3.3 Cooling Water Loop

City supply water was used as a coolant. Figure 3.9 shows a schematic diagram of the cooling water flow loop. The city water was supplied to a mixing tank from the water main. The water was pumped through a circulating pump to the main test condenser, after condenser, and the R-11

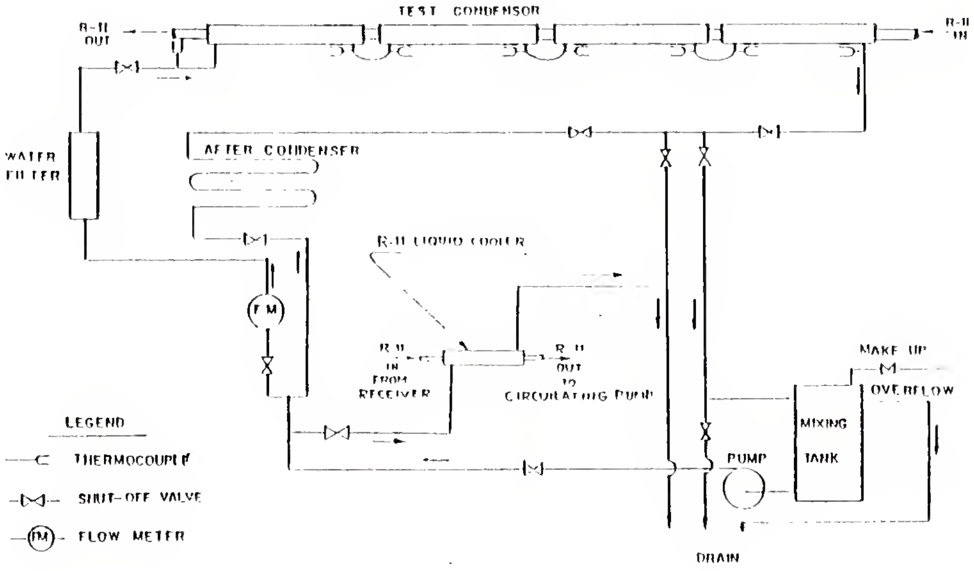

Fig. 3.9 A Schematic Diagram of the Cooling Water Circuit.

liquid cooler. The water flow rate to the test condenser was measured by Brooks Rotameter (range 0.0 to 3.0 g.p.m.). The design of the cooling water loop permitted control of the flow through test condenser, the R-11 liquid cooler and the cooling water inlet temperature. The R-11 liquid cooler, installed between the liquid receiver and the refrigerant circulating pump, ensured the liquid phase of R-11 at the inlet of the refrigerant pump. The coolant's inlet temperature was achieved by mixing appropriate quantities of supply water from the mains and return water from the test condenser, in the mixing tank.

3.4 Operation of Test Facility and Data Acquisition

The entire system was evacuated down to 1000 microns by a vacuum pump and then charged with R-11. The process of evacuation and charging was repeated two to three times to rid the system out of non-condensables.

The circulating water pump was put into operation and the flow rate was adjusted to the desired level. Before applying the electric power to the heating elements of the vapor generator, it was ensured that the heating elements were well immersed in the liquid by checking liquid level through the sight glass attached to it. If the liquid level was low, R-11 was pumped from the liquid receiver into the vapor generator until the desired level was achieved. Electric power was then gradually applied to the heating elements inside the vapor generator. When the liquid level started decreasing in the vapor generator, the refrigerant circulating pump was put into operation. The balance of flow into and out of the vapor generator was achieved by adjusting the bypass valve after the refrigerant circulating pump. Once the flow balance was achieved, electric power was then applied to superheater. The desired flow rate of R-11 into the test condenser, its inlet pressure and superheat for any experimental run, was achieved by adjusting the electric power to the vapor generator and the superheater, controlling the liquid flow rate from the refrigerant pump, and by controlling cooling water flow rate and its inlet temperature. For each experimental run, steady state condition was established when the readings of all temperatures, pressures, flow rates, and liquid level in the vapor generator and liquid receiver remained constant for a period of least two hours.

During each experimental run, the following measurements were taken.

1. Water flow rate to the test condenser in kg/s (g.p.m.)
2. R-11 inlet gage pressure to the test condenser kPa (psia)
3. The inlet and outlet temperatures of R-11 of the test condenser, in deg C (deg F)
4. The temperature of liquid R-11 leaving the flowmeter, in deg C (deg F)
5. The temperature of sixteen thermocouples attached to the outer wall of the test condenser, deg C (deg F)
6. The flow rate of refrigerant into the test condenser in kg/s (g.p.m.)
7. The inlet and outlet water temperatures of each subsection
8. The pressure drop across the test condenser (for tubes 1, 2 and 3) in mm Hg (in. of Hg)

The pressure drop across the test condenser was not taken for tubes 4 and 5, as these tubes had larger diameters compared to the other tubes tested and consequently, their pressure drops were too low to be measured accurately.

The flow rates of R-11, measured by the variable area flowmeters, were corrected according to the manufacturer's recommendation to account for density variations of the fluid tested, since these flow meters were originally calibrated to handle R-113.

Heat balance error of ±5% was set as the criterion for acceptability of any experimental run before documentation. The heat balance was calculated as the ratio of the difference between heat gain rate of the cooling water and the rate of heat loss of the condensing fluid to the rate of heat gain of the cooling water. The heat gain rate of the cooling water was calculated from its flow rate and its temperature rise. The rate of heat loss of the condensing fluid was calculated from its flow rate and its enthalpy change between its inlet and outlet. In all the experimental runs, R-11 was slightly superheated at the inlet of the test condenser and slightly subcooled at the exit of test condenser.

The heat balance error for the experimental runs rarely exceeded ±5%. However, a few runs with heat balance error slightly higher than the above limits were also included in the data reported in this study.

The ranges of experimental parameters covered in this study were dictated by the various limitations of the existing experimental set up. The ranges of the experimental parameter are listed in Table 3.2.

TABLE 3.2 Ranges of Experimental Parameters Covered

Refrigerant's Mass Flux (based on nominal inside area)	$17.14(1.264x10^4) - 85.55(6.308x10^4)$ $\frac{Kg}{s-m^2}$ $(lbm/hr-ft^2)$
Overall Condensing Heat Transfer Coefficient	1044.2(183.9) - 3456.4(608.7) $\frac{W}{m^2-{}^oC}$ $(Btu/hr-ft^2-{}^oF)$
Overall Heat Transfer Rate	1268(4331) - 2924(9983) W (Btu/hr)
Inlet Coolant Temperature	14.7(58.64) - 25.0(75.56) ^oC (^oF)
Test Fluid Inlet Pressure	127.2(18.45) - 172.7(25.04) kPa(psia)
Test Fluid Inlet Superheat	2.46(4.42) - 9.86(17.74) ^oC (^oF)
Outlet Quality	-.158 (Subcooled) - 0.0

Chapter IV

EXPERIMENTAL RESULTS

4.1 Introduction

During the present investigation, fifty-two experimental runs were taken for the smooth tube (tube 1), fifty-two runs for the straight finned tube (tube 2), fifty-nine, thirty-three and thirty-six runs for the spirally finned tubes, tubes 3, 4 and 5, respectively. For the reasons discussed earlier, pressure drop data were taken only for the smooth tube (tube 1), the straight finned tube (tube 2) and the spirally finned tube (tube 3). Nineteen pressure drop readings were taken for the smooth tube, nineteen for the straight finned tube and eighteen for the spirally finned tube. In these pressure drop measurements, only the total drop across the entire test condenser tube was recorded.

The sectional and overall average heat transfer coefficients were calculated from the following equation.

$$\overline{h} = \left[\frac{\pi \; D_i \; \Delta z \; (\overline{T}_s - \overline{T}_{wo})}{\dot{m}_{wa} Cp_{wa} \; (T_{wao} - T_{wai})} - \frac{D_i}{2K} \ln \left(\frac{D_o}{D_i} \right) \right]^{-1} \qquad (4\text{-}1)$$

In the above equation, Eq. (4-1), $\overline{T}_s$ is the saturation temperature corresponding to the inlet pressure of the test condenser tube since the pressure drop in all experimental runs was small enough to have no significant effect on the change in saturation temperature.

While computing the sectional heat transfer coefficients for section 1 (refer to Fig. 3.4.), for each test condenser using Eq. (4-1), it was found that the resulting heat transfer coefficient was very high. The reason for such results was due to the fact that the temperature difference $(\overline{T}_s - T_{wo})$ was very small to yield very high $\overline{h}$. It was then reasoned that basing the heat transfer coefficient of such a temperature difference was not realistic due to the fact that R-11 entered this section superheated and its temperature remained above the saturation temperature $\overline{T}_s$ over a major portion of this section. It was then decided to base $\overline{h}$ for this section on the difference $[(\overline{T}_s + T_{sup})/2 - T_{wo}]$ where T_{sup} is the inlet superheat temperature of R-11.

In calculating the overall heat transfer coefficient of the entire test condenser from Eq. (4-1), Δz was replaced by L, the combined lengths of four sections. $\overline{T}_{wo}$ was taken as the arithmetic mean of the sixteen thermocouples attached to the outside wall temperature of the test condenser tube. The total energy transfer was taken as the sum of energy gain rate of the cooling water for the entire test condenser.

A sample of the calculation procedure is given in Appendix B. Appendix C gives the computer program for the data reduction, and Appendix D gives the reduced data of all the experimental runs. The estimation of experimental uncertainties of the computed overall average heat transfer coefficient is given in Appendix E. The uncertainty was estimated to be ±16.15%.

4.2 Heat Transfer Results

From the reduced data of the experimental runs, the following general observations can be made on the heat transfer results.

1. The average sectional heat transfer coefficients of each subsection nearest to the inlet was highest among all subsections and decreased in the direction of flow for the remaining three subsections.
2. Heat gained by water in the four subsections were close enough in

majority of experimental runs which indicated that the quality of condensing vapor decreased linearly in the direction of flow.

3. Also, by carrying out the energy balance on each subsection, starting from the one nearest to the inlet and then proceeding to the next subsection in the direction of flow, it was possible to estimate the exit quality of all the subsections.

4.2.1 Smooth Tube and Internally Finned Tubes

The experimental runs were carried out at three nominal inlet pressures, 1.32 bar (19.19 psia.), 1.47 bar (21.29 psia.), and 1.67 bar (24.17 psia.)(1 bar = 10^2 kPa). The mass flux based on the inside nominal area ranged from 41.33 (3.05×10^4) to 85.55 (6.31×10^4) kg/s.m^2 (lbm/hr.ft^2) for tube 1, 54.00 (3.98×10^4) to 84.57 (6.24×10^4) kg/s.m^2 (lbm/hr.ft^2) for tube 2, 37.20 (2.74×10^4) to 66.46 (4.90×10^4) kg/s.m^2 (lbm/hr.ft^2) for tube 3, 26.35 (1.94×10^4) to 47.01 (3.47×10^4) kg/s.m^2 (lbm/hr.ft^2) for tube 4, and 17.14 (1.26×10^4) to 28.45 (2.10×10^4) kg/s.m^2 (lbm/hr.ft^2) for tube 5.

Constant inlet pressures of the condensing fluid could not be maintained precisely because of the practical difficulties in trying to maintain reasonable inlet superheat and exit subcooling for the desired ranges of mass fluxes. The variation of the inlet pressures of all the tubes reported for different mass fluxes of the condensing fluid were within ±0.028 bar (±0.40 psia.) from the nominal pressures. The mass flux ranges for different tubes were dictated by the practical limitations of the test facility.

The overall average heat transfer coefficients at three nominal inlet pressures for the smooth tube are plotted versus mass flux in Figs. 4.1 through 4.3. Figures 4.5 through 4.7 are the plots of the overall heat transfer coefficient versus the mass flux at different nominal inlet

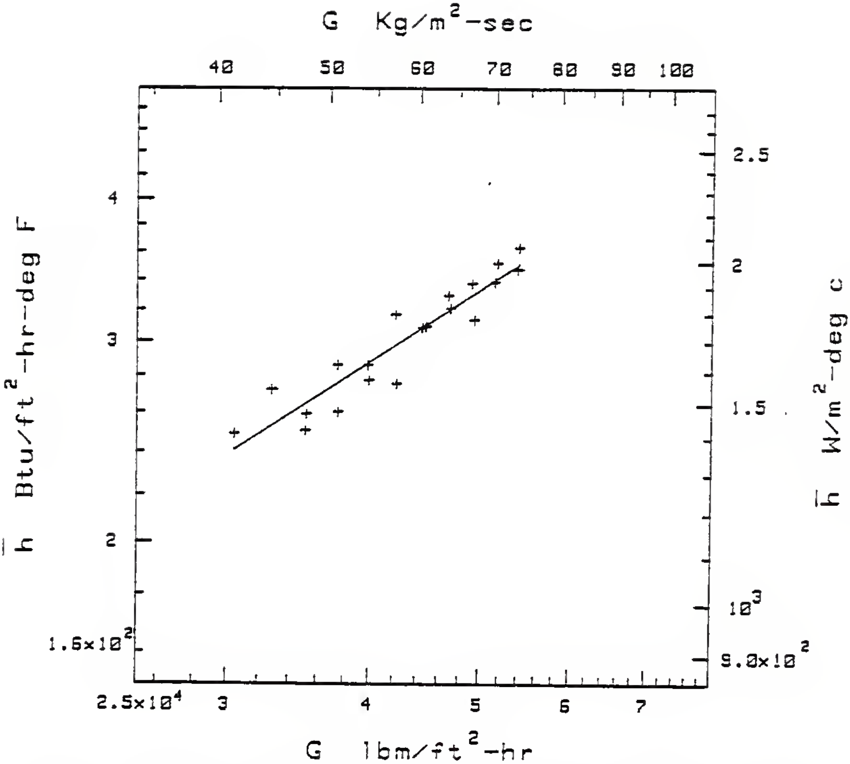

Fig 4.1 Experimental overall average heat transfer coefficients versus mass flux, Tube 1, Pin=1.32 bar (19.19 Psia)

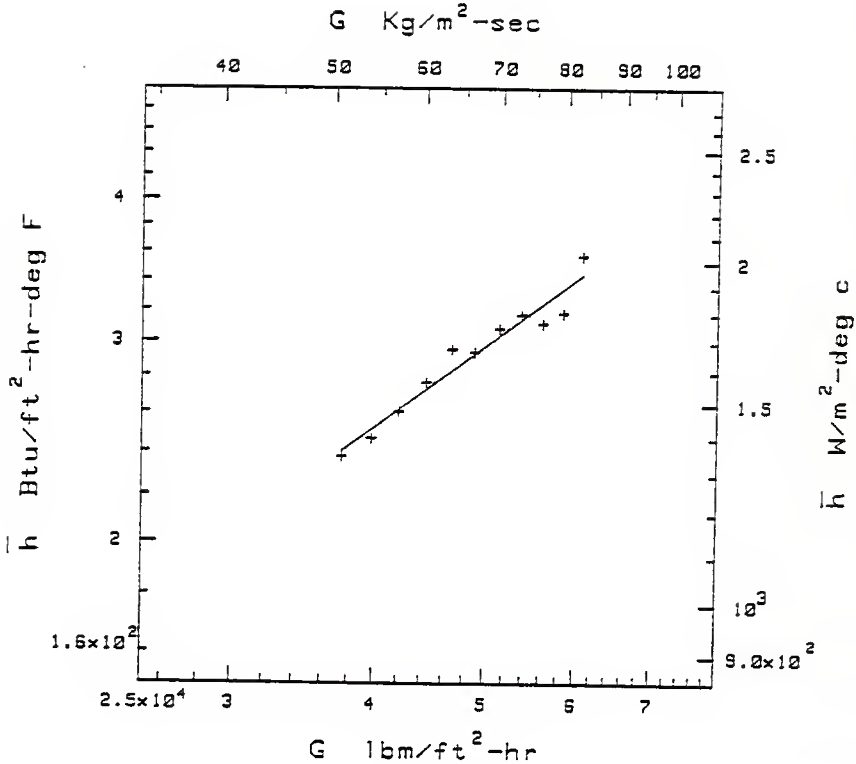

Fig 4.2 Experimental overall average heat transfer coefficients versus mass flux, Tube 1, Pin=1.47 bar (21.29 Psia)

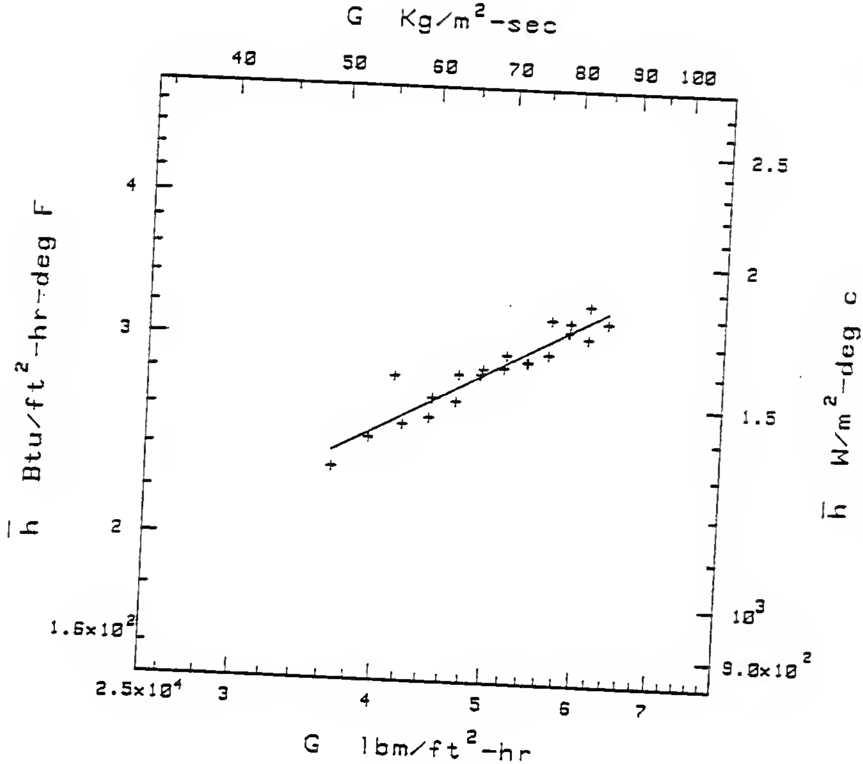

Fig 4.3 Experimental overall average heat transfer coefficients versus mass flux, Tube 1, Pin=1.67 bar (24.17 Psia)

pressures for tube 2, Figs. 4.9 through 4.11 are similar plots for tube 3, Figs. 4.13 through 4.15 for tube 4, and Figs. 4.17 through 4.19 for tube 5.

Because of the trend of the data, it was possible to correlate the results of all the tubes at each nominal pressure by the following equation:

$$\overline{h} = C\ G^{n} \tag{4-2}$$

where C and n are constants obtained by the least square regression analysis. Values of C and n are given in Appendix F, Table F.1, for all the tubes at all nominal inlet pressures. Figure 4.4 shows a plot of the regression equations of $\overline{h}$ versus G at all inlet pressures for tube 1. Similarly, the regression equations of $\overline{h}$ versus G at all inlet pressures are shown in Fig. 4.8 for tube 2, Fig. 4.12 for tube 3, Fig. 4.16 for tube 4, and Fig. 4.20 for tube 5. The results of all the tubes show that, for the same mass flux, $\overline{h}$ decreased with the increase in pressure. This is due to the fact that, for a given G, the density decreases as the pressure decreases and as a result the velocity of the condensing fluid increases resulting in the increase of the $\overline{h}$ value.

4.3 Pressure Drop Results

As reported earlier, pressure drop data were taken for tubes 1, 2, and 3 only. Nineteen runs of pressure drop for tube 1, nineteen for tube 2, and eighteen for tube 3 were taken at two nominal inlet pressures, 1.32 bar (19.19 psia.) and 1.67 bar (24.17 psia.).

The total pressure drop, Δp at the two nominal inlet pressures for the smooth tube are plotted versus the mass flux in Figs. 4.21 and 4.22. Figures 4.24 and 4.25 are plots of the total pressure drop versus mass flux at the two nominal inlet pressures for tube 2, and Figs. 4.27 and 4.28 for tube 3. The results were correlated by the equation

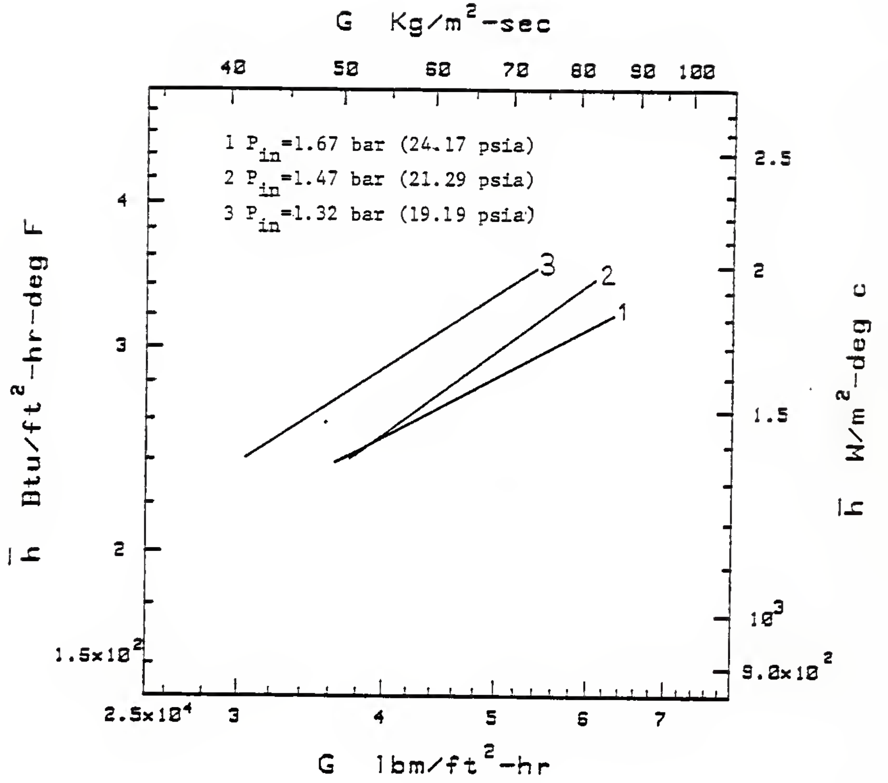

Fig 4.4 Experimental overall average heat transfer coefficients versus mass flux, Tube 1, at all pressures

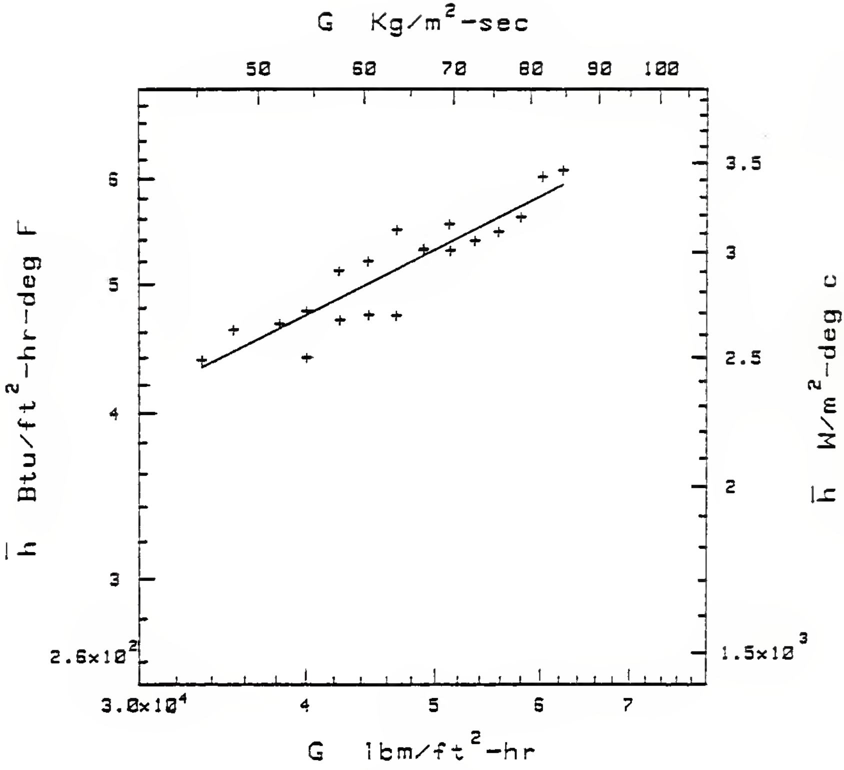

Fig 4.5 Experimental overall average heat transfer coefficients versus mass flux, tube 2, P_{in}=1.32 bar (19.19 psia)

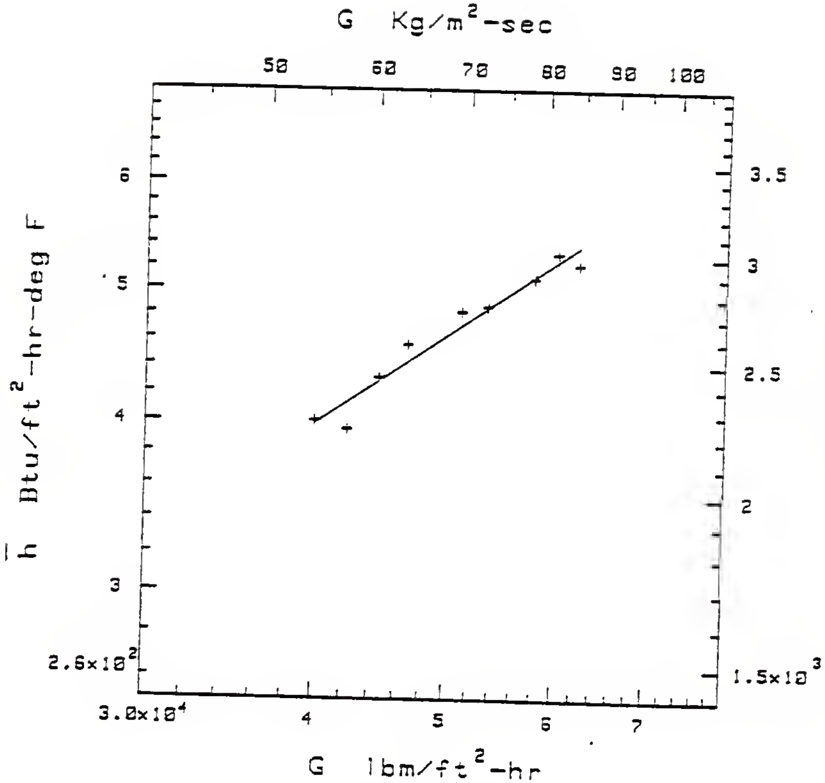

Fig 4.6 Experimental overall average heat transfer coefficients versus mass flux, Tube 2, P_{in}=1.47 bar (21.29 psia)

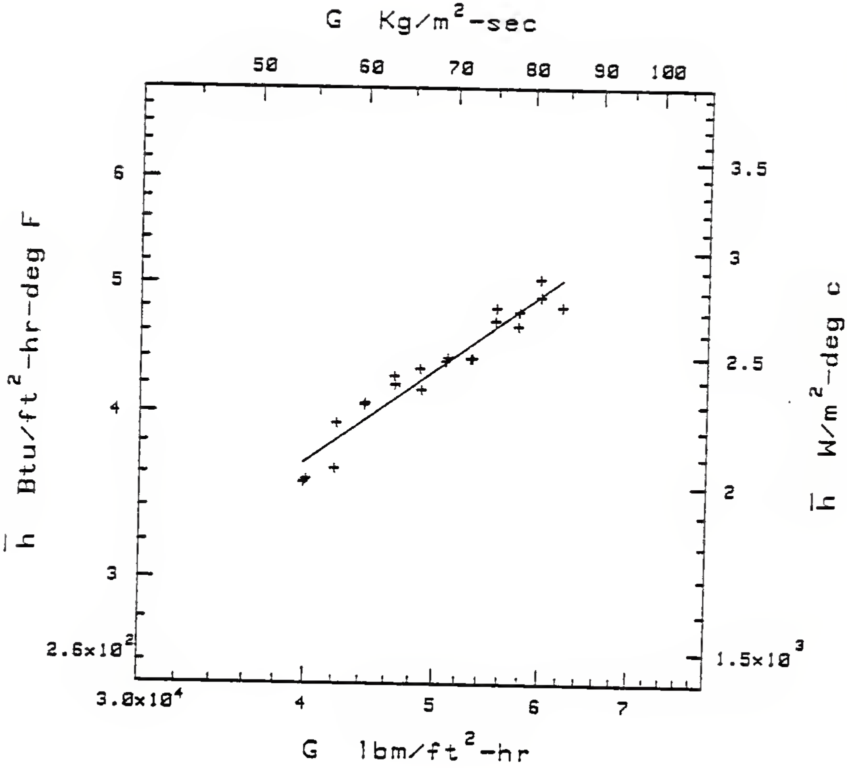

Fig 4.7 Experimental overall average heat rransfer coefficients versus mass flux, tube 2, P_{in}=1.67 bar (24.17 psia)

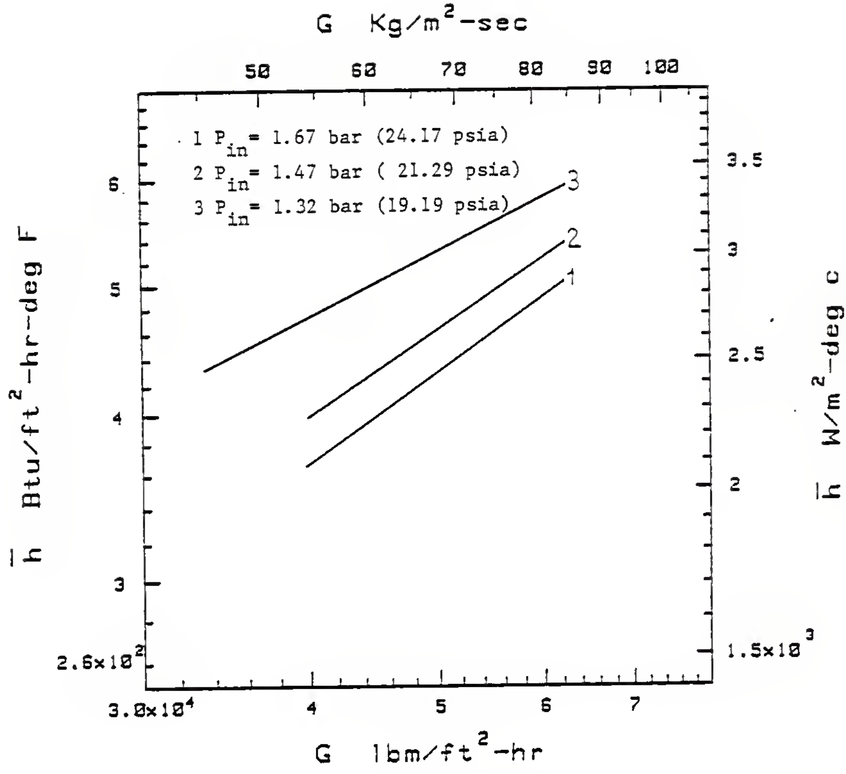

Fig 4.8 Experimental overall average heat transfer coefficients versus mass flux, Tube 2, at all pressures

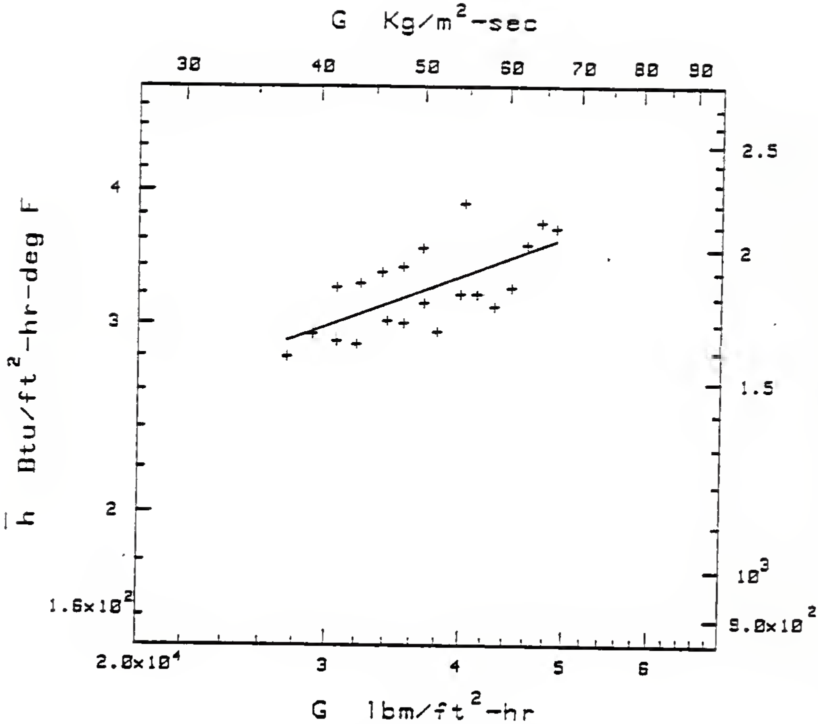

Fig 4.9 Experimental overall average heat transfer coefficients versus mass flux, Tube 3, Pin=1.32 bar (19.19 Psia)

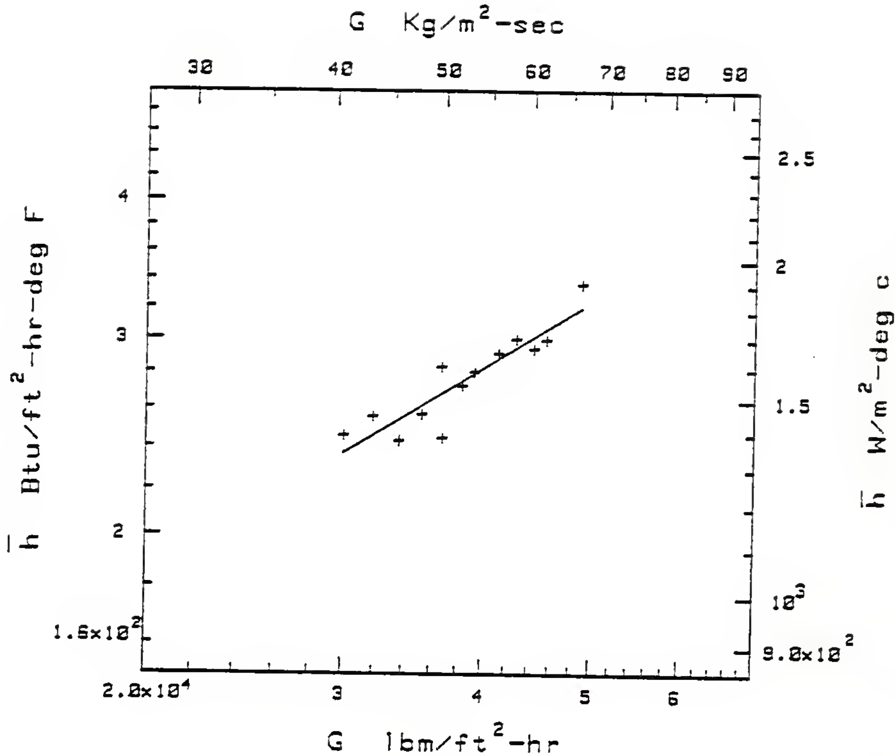

Fig 4.10 Experimental overall average heat transfer coefficients versus mass flux, Tube 3, Pin=1.47 bar (21.29 Psia)

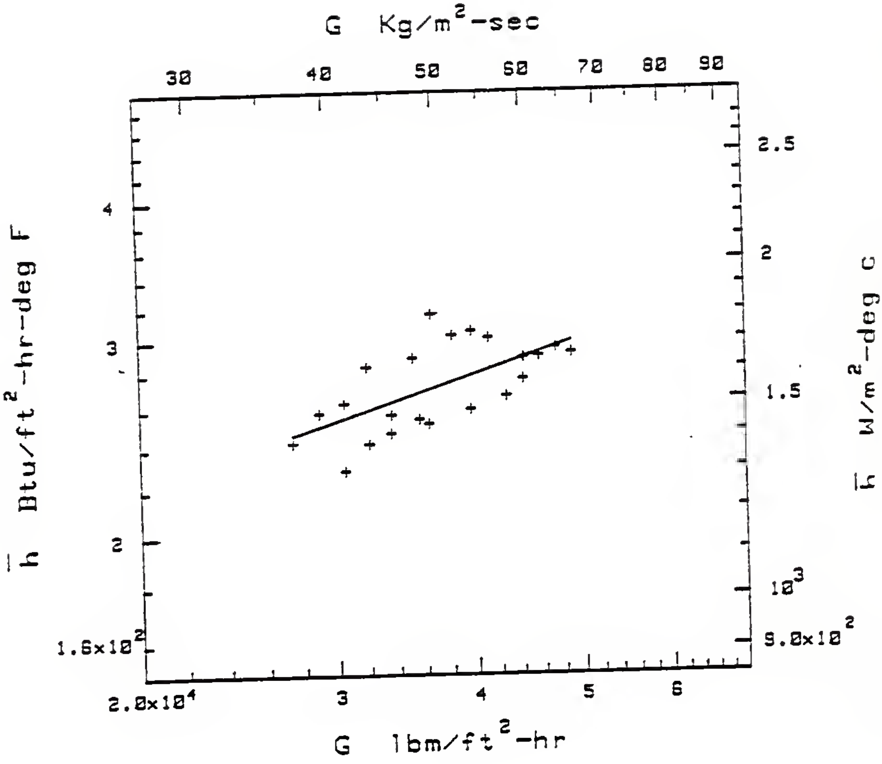

Fig 4.11 Experimental overall average heat ransfer coefficients versus mass flux, Tube 3, Pin=1.67 bar (24.17 Psia)

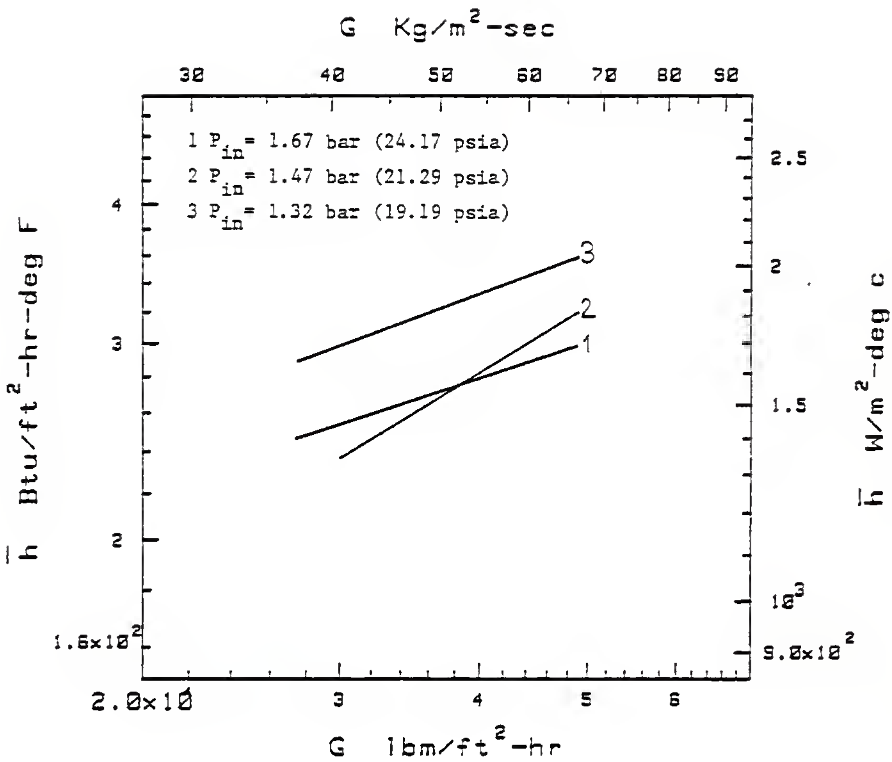

Fig 4.12 Experimental overall average heat transfer coefficients versus mass flux, Tube 3, at all pressures

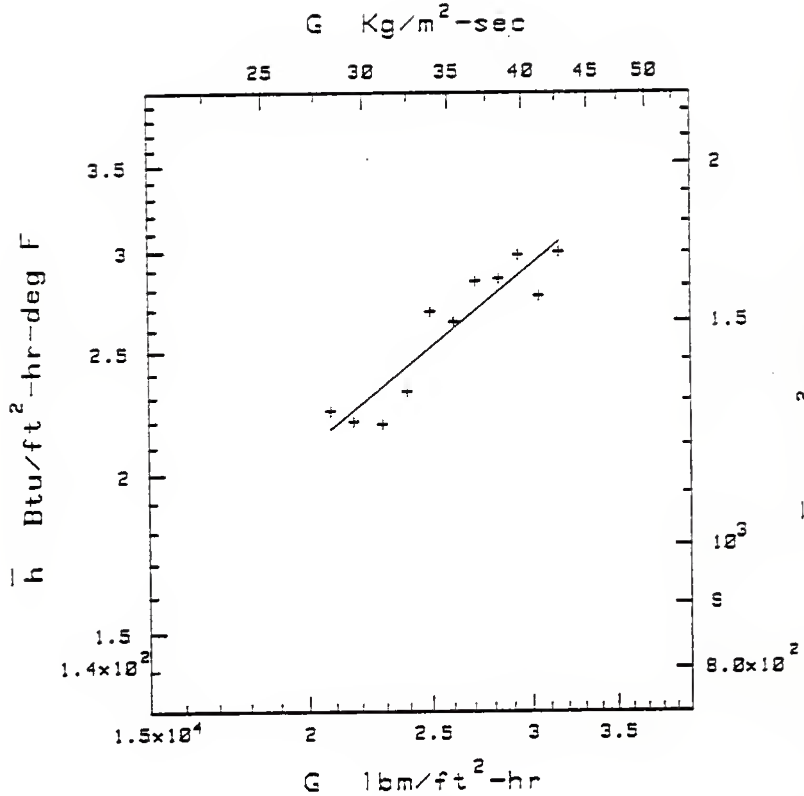

Fig 4.13 Experimental overall average heat transfer coefficients versus mass flux, Tube 4, Pin=1.32 bar (19.19 Psia)

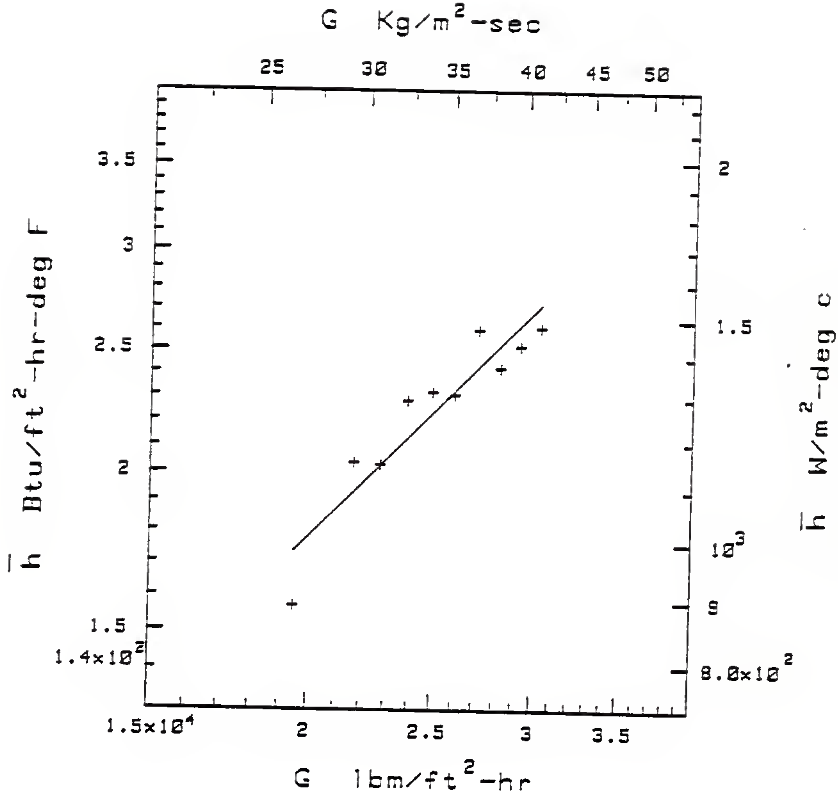

Fig 4.14 Experimetnal overall average heat transfer coefficients versus mass flux, Tube 4, Pin=1.47 bar (21.29 Psia)

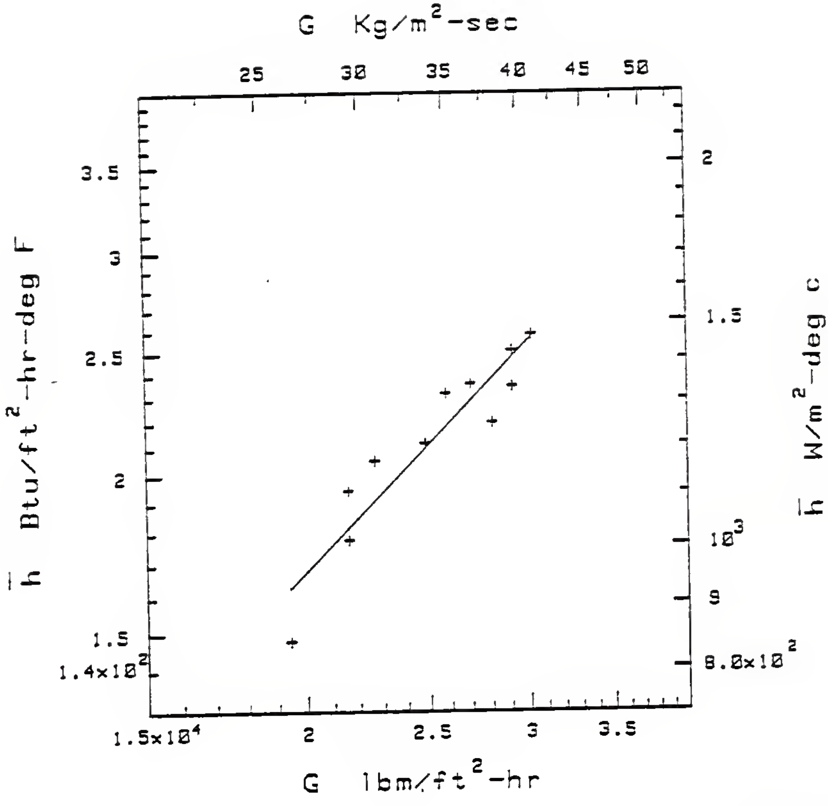

Fig 4.15 Experimental overall average heat transfer coefficients versus mass flux , Tube 4, Pin=1.67 bar (24.17 Psia)

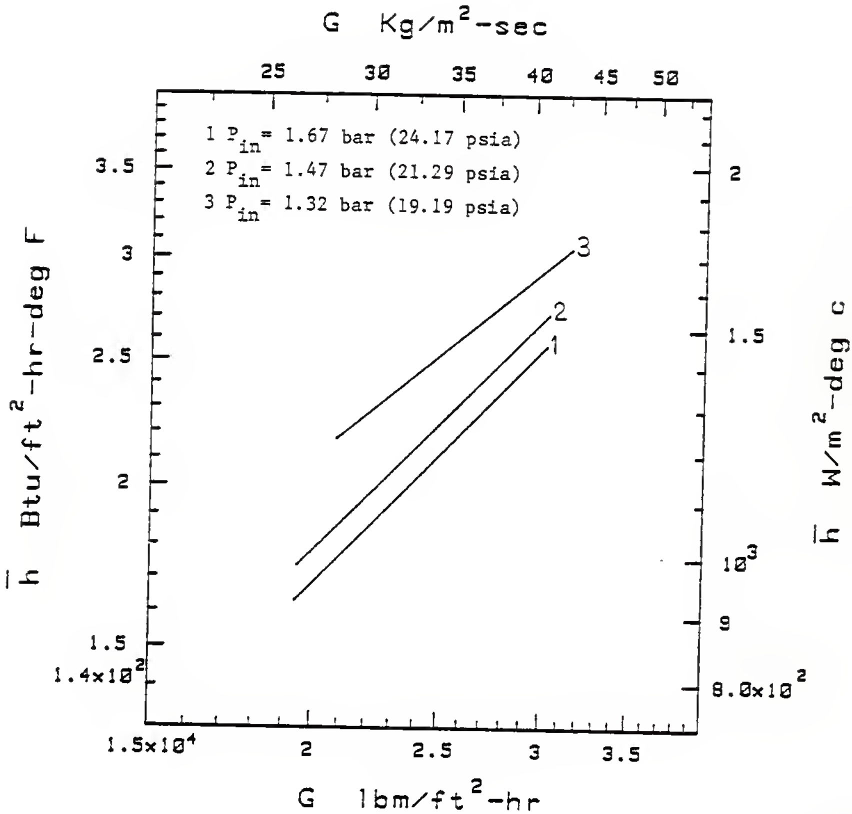

Fig 4.16 Experimental overall average heat transfer coefficients versus mass flux, Tube 4, at all pressures

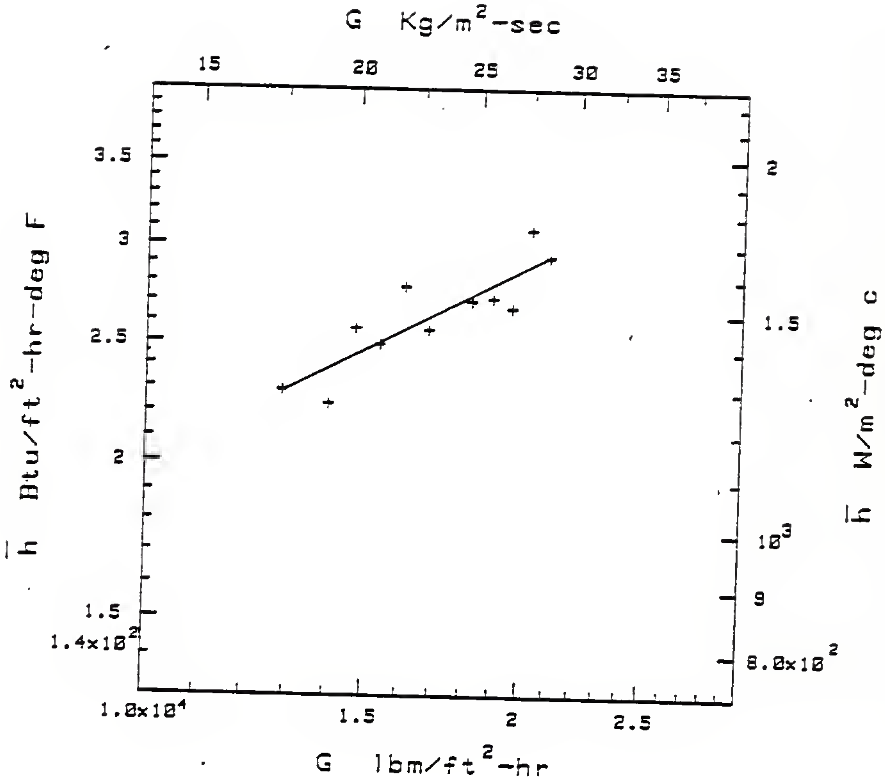

Fig 4.17 Experimental overall average heat transfer coefficients versus mass flux, Tube 5, Pin= 1.32 bar (19.19 Psia)

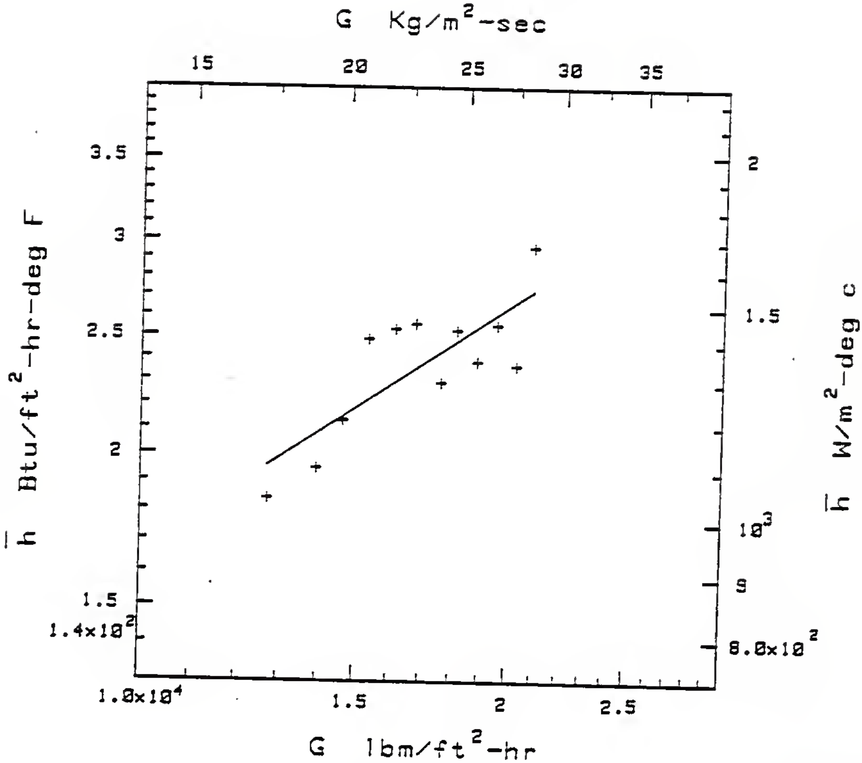

Fig 4.18 Experimental overall average heat transfer coefficients versus mass flux, Tube 5, Pin=1.47 bar (21.29 Psia)

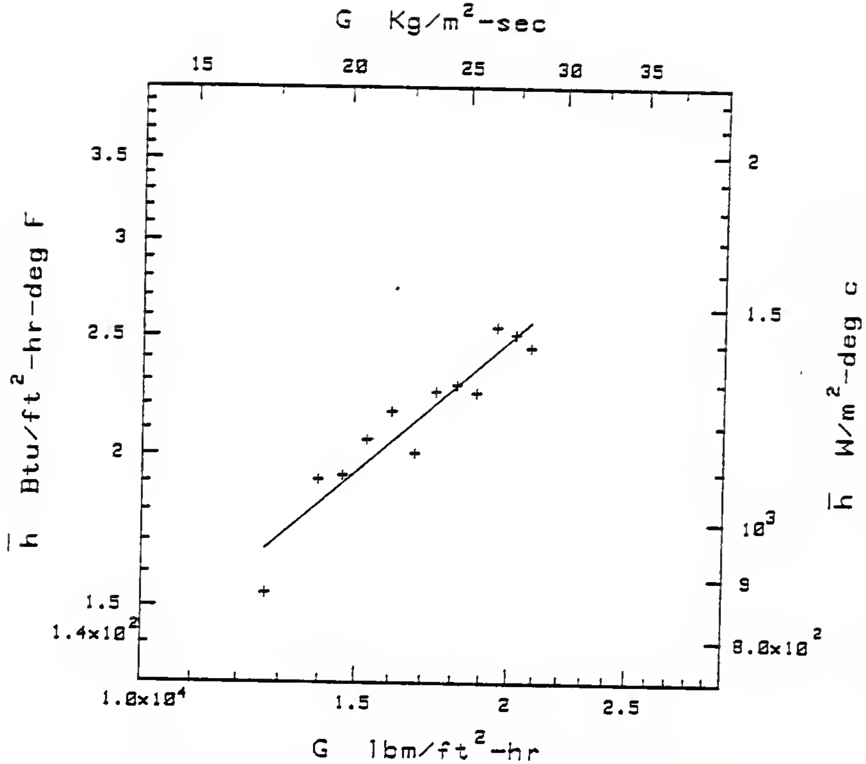

Fig 4.19 Experimental overall average heat transfer coefficients versus mass flux, Tube 5, Pin=1.67 bar (24.17 Psia)

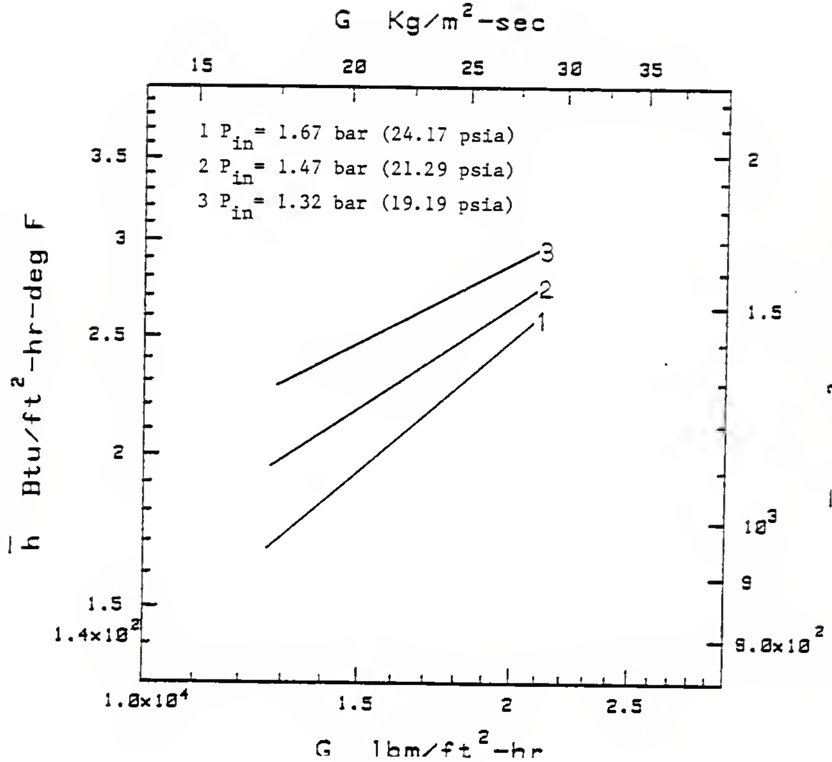

Fig. 4.20 Experimental overall average heat transfer coefficients versus mass flux, tube 5, at all pressures

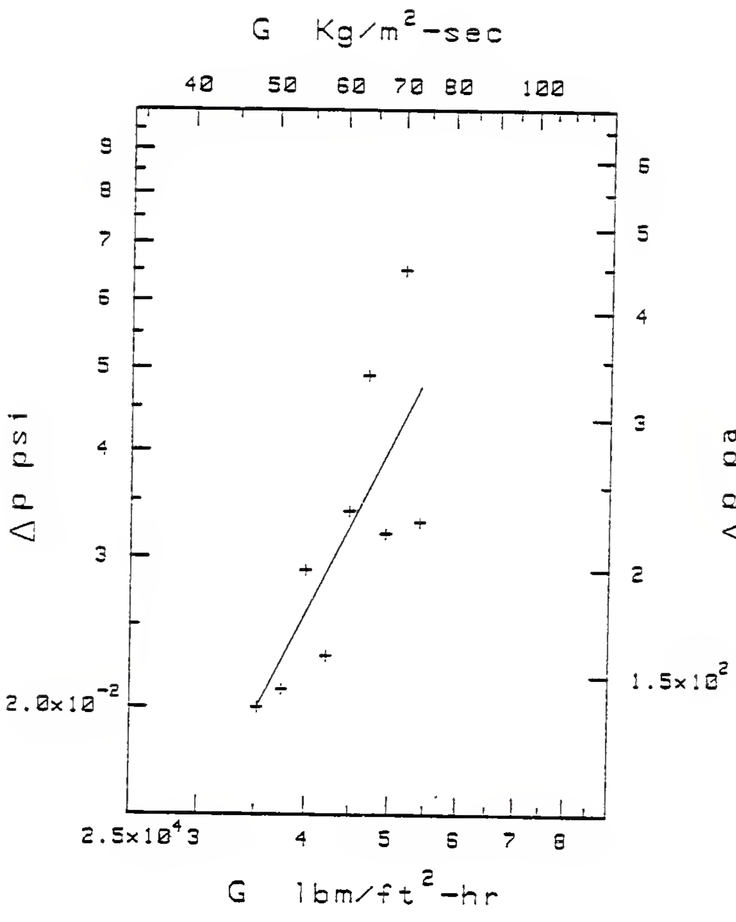

Fig 4.21 Experimental total pressure drop versus mass flux, Tube 1, Pin=1.32 bar (19.19 Psia)

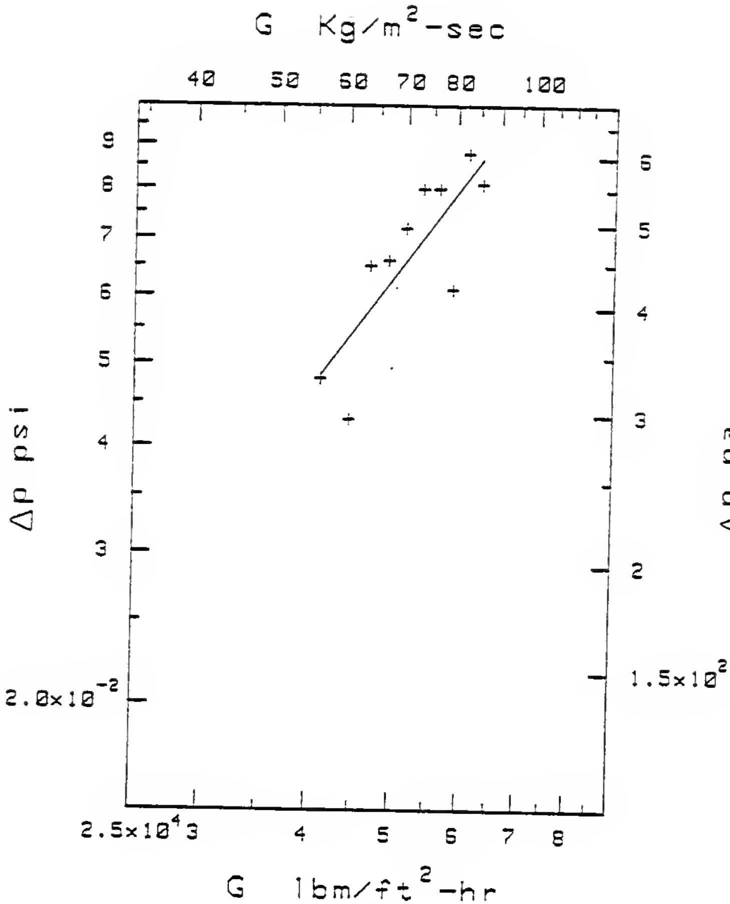

Fig 4.22 Experimental total pressure drop versus mass flux, Tube 1, Pin=1.67 bar (24.17 Psia)

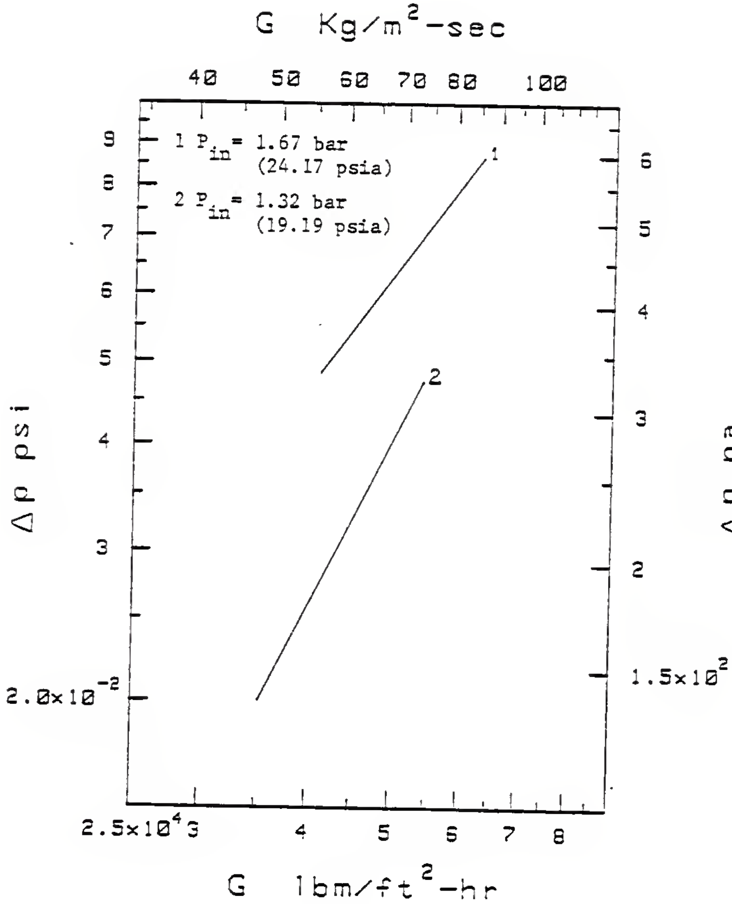

Fig 4.23 Experimental total pressure drop versus mass flux, tube 1, at all pressures

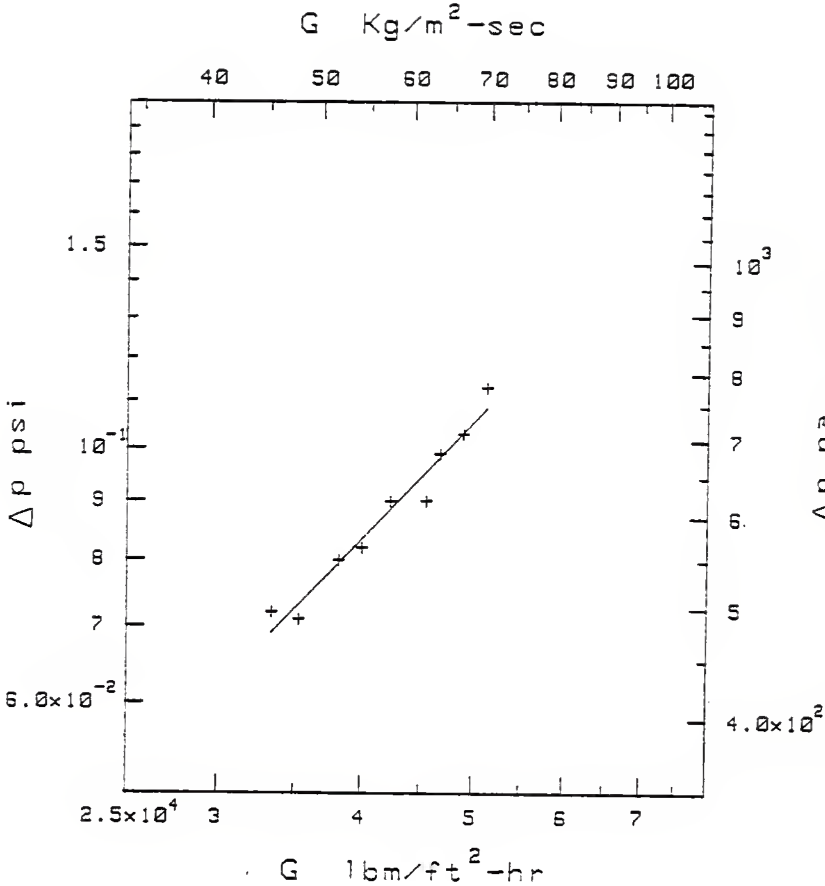

Fig 4.24 Experimental total pressure drop versus mass flux, Tube 2, Pin=1.32bar (19.19 Psia)

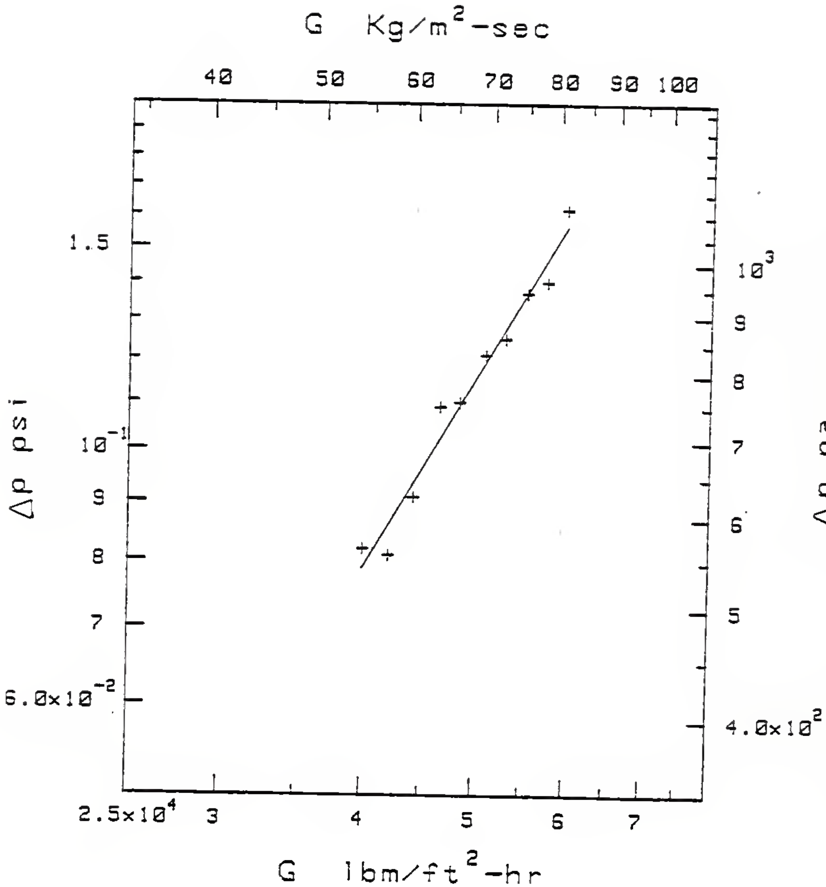

Fig 4.25 Experimental total pressure drop versus mass flux, Tube 2, Pin=1.67 bar (24.17 Psia)

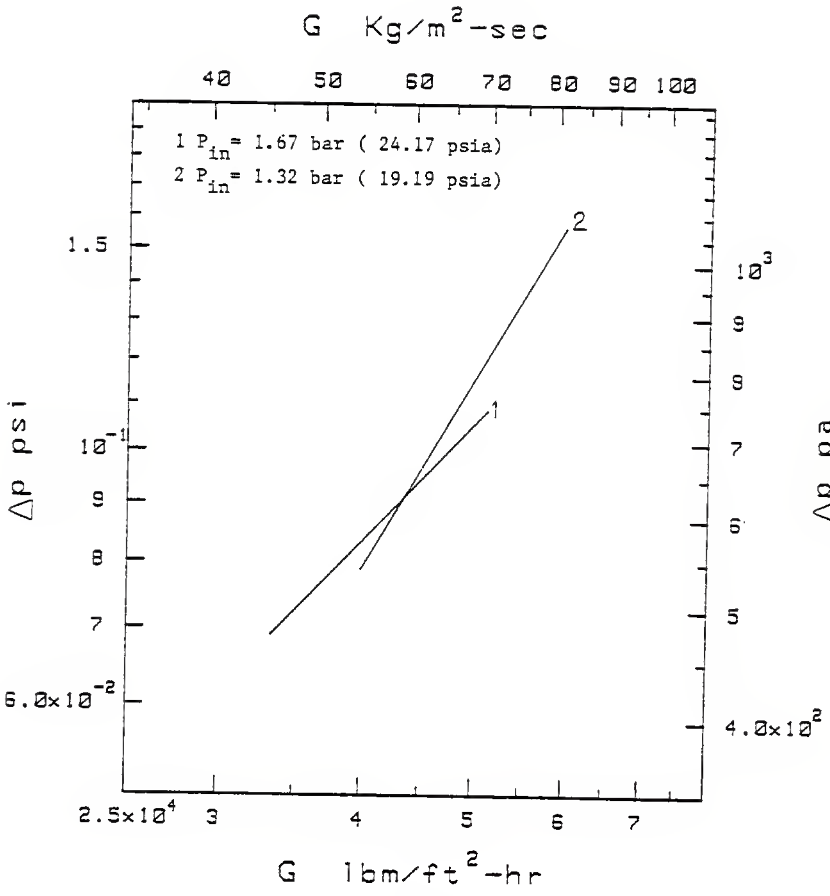

Fig 4.26 Experimental total pressure drop versus mass flux, Tube 2, at all pressures

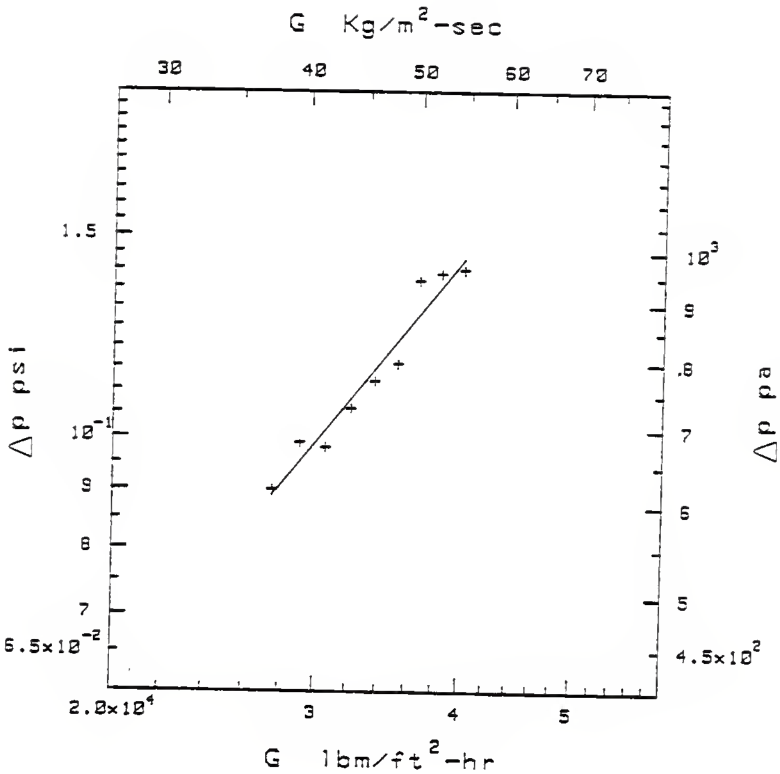

Fig 4.27 Experiment total pressure drop versus mass flux, Tube 3, Pin=1.32 bar (19.19 Psia)

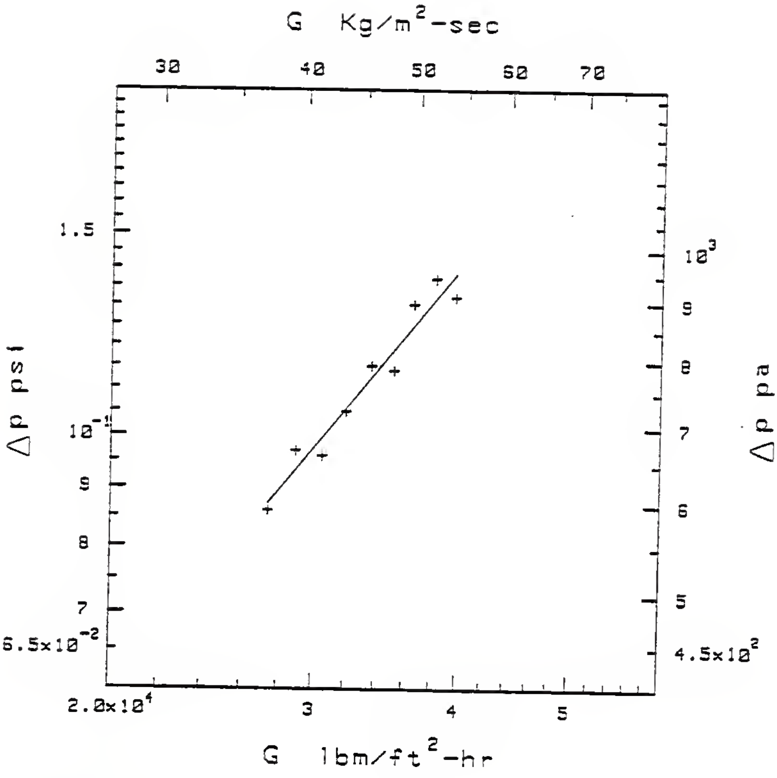

Fig 4.28 Experimental total pressure drop versus mass flux,
Tube 3, Pin=1.67 bar (24.17 Psia)

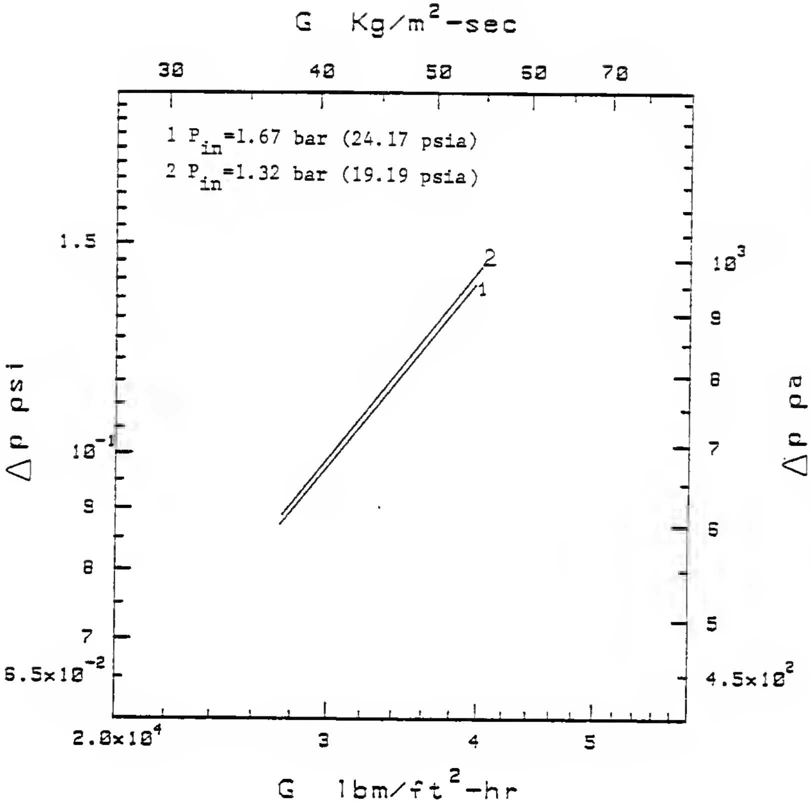

Fig 4.29 Experimental total pressure drop versus mass flux, Tube 3, at all pressures

$$\Delta P = C' \, G^{n'} \tag{4-3}$$

The constants C' and n' were obtained by the least square regression technique. The values of C' and n' for the tubes 1, 2 and 3 tested at all pressures are given in Appendix F, Table F.2. Figure 4.23 shows the least square regression lines for the smooth tube at two different pressures. For the smooth tube, it was observed that higher inlet pressures resulted in higher pressure drops. The regression lines at the two different inlet pressures are shown in Fig. 4.26 for tube 2, and Fig. 4.29 for tube 3. For the straight finned tube (tube 2), the total pressure drop was high at the lower inlet pressure and higher mass flux compared to that at higher inlet pressure. For the spiral finned tube (tube 3) higher inlet pressure yielded marginally lower total pressure drop. In all the above plots, results show that Δp increased as G increased for the two nominal inlet pressures.

The performance of all the tubes tested in terms of their heat transfer and the associated pressure drop, will be evaluated in Chapter VI.

Chapter V

CORRELATION OF EXPERIMENTAL DATA

5.1 Introduction

There are numerous correlations available for predicing the heat transfer and pressure drop during in-tube condensation. Before relying on these correlations for commercial design usage, these correlations should predict the data of different investigators over a wide range of flow conditions for different fluids within reasonable degree of accuracy. Different heat transfer and pressure drop correlations were tested to identify the correlations which properly predicted the data of the present study.

5.2 Smooth Tube Correlations

5.2.1 Heat Transfer

The smooth tube experimental data were compared with the predictions of the correlations of Akers et al. [6], Boyko and Kruzhilin [7], and Shah [13]. A summary of these correlations follows.

The overall average heat transfer coefficient of Akers _et al_. [6] is given by

$$\bar{h} = C \frac{k_\ell}{D_i} Re_e^n \; Pr_\ell^{1/3} \qquad (5\text{-}1)$$

where

$C = 0.0265$, $n = 0.8$ for $Re_e > 5 \times 10^4$

$C = 5.03$, $n = 1/3$ for $Re_e < 5 \times 10^4$

$$Re_e = \left(\frac{G_e D_i}{\mu_\ell}\right) \qquad (5\text{-}2)$$

$$G_e = G\left[\bar{x}\left(\frac{\rho_\ell}{\ell_v}\right)^{0.5} + (1 - \bar{x})\right] \quad (5\text{-}3)$$

The above correlation is recommended by ASHRAE Handbook of Fundamentals [48].

The overall average heat transfer coefficients of Boyko and Kruzhilin [7] is given by

$$\bar{h} = 0.024\,\frac{k_\ell}{D_i}\,Re_L^{0.8}\,Pr_\ell^{0.43}\left[\frac{(\rho/\rho_m)_{in}^{0.5} + (\rho/\rho_m)_{out}^{0.5}}{2}\right] \quad (5\text{-}4)$$

where

$$\left(\frac{\rho}{\rho_m}\right) = 1 + x\left(\frac{\rho_\ell}{\rho_v} - 1\right) \quad (5\text{-}5)$$

The local heat transfer coefficient of Shah [13] is given by

$$h_z=0.023\left(\frac{k_\ell}{D_i}\right) Re_L^{0.8}\,Pr_\ell^{.4}\left[(1-x)^{0.8}+3.8x^{0.76}(1-x)^{0.04}\,.\,P_{rc}^{-0.38}\right] \quad (5\text{-}6)$$

All the properties in the above correlations are evaluated at the saturation temperature. Shah also suggested that an approximate expression for the average $\bar{h}$ for complete condensation can be obtained by substituting average $\bar{x}$ in Eq. (5-6). After analyzing the experimental results of several investigators, Shah suggested that an approximate expression for the average $\bar{h}$ for complete condensation can be obtained by substituting $\bar{x}$=0.5 in Eq. (5-6). He also pointed out that $\bar{h}$ obtained from this expression differed by no more than 5% from averaging the values obtained by the predictions of Eq. (5-6). After evaluation of Shah's correlation, Said selected $\bar{x}$=0.4 and when it was substituted in Eq. (5-6) the following expression resulted.

$$\bar{h}=0.023\left(\frac{k_\ell}{D_i}\right) Re_L^{0.8}\,Pr_\ell^{0.4}\,[0.665 + 1.86\,P_{rc}^{-0.38}] \quad (5\text{-}7)$$

The average heat transfer coefficient of the predictions of Eq. (5-6) can be evaluated by integration using the following equation.

$$\frac{1}{\bar{h}} = \frac{1}{(x_{in} - x_{out})} \int_{x_{out}}^{x_{in}} \frac{dx}{h_z} \qquad (5\text{-}8)$$

Equation (5-8) is based on energy balance with the assumption that the difference between the condensing fluid and the inner wall temperature is constant for entire length of the tube. Said [2], in his investigation of in-tube condensation with R-113, correlated his experimental data of $\bar{h}$ with the predicted values from Eq. (5-7) and the prediction of Eq. (5-6) averaged by Eq. (5-8). Eq. (5-7) predicted his data well. Hence in the present study, it was decided to use Eq. (5-7) for correlating the data of the present study.

Figures 5.1 and 5.2 show the comparison between the predictions of Akers et al. [6], Eq. (5-1), and the overall experimental values and the experimental overall and sectional values, respectively, of the heat transfer coefficients. Figure 5.1 shows that the predictions of the overall heat transfer coefficients were within ±30% of experimental results for 83% of the experimental runs. Also, the correlation predicted reasonably well the sectional average heat transfer coefficient values shown in Fig. 5.2. The sectional average values of the heat transfer coefficients of section 1 were not included in Fig. 5.2 for two reasons. First, Eq. (5-1) substantially underpredicted the values obtained experimentally. Secondly, the temperature difference on which basis the overall average and sectional averages of sections 2, 3, and 4 were calculated, were different than those of section 1 as outlined earlier.

Figure 5.3 shows the comparison between the experimental overall heat transfer coefficients and predictions of Boyko and Kruzhilin's

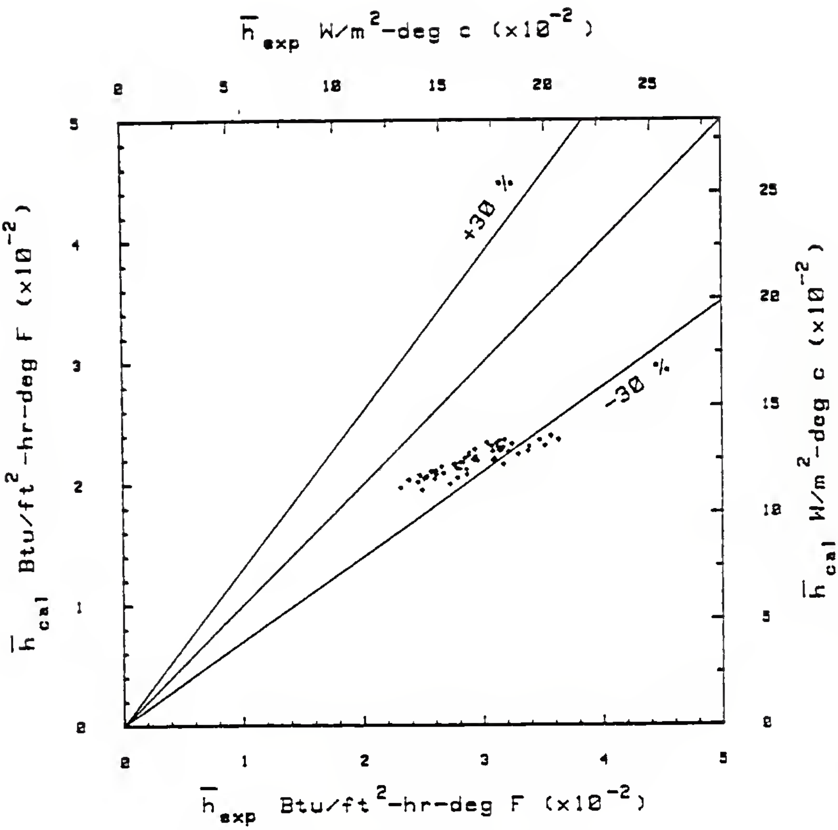

Fig 5.1 Comparison of experimental overall heat transfer coefficient with predictions of the correlation of Akers et al. [6], Eq.(5-1), Tube 1

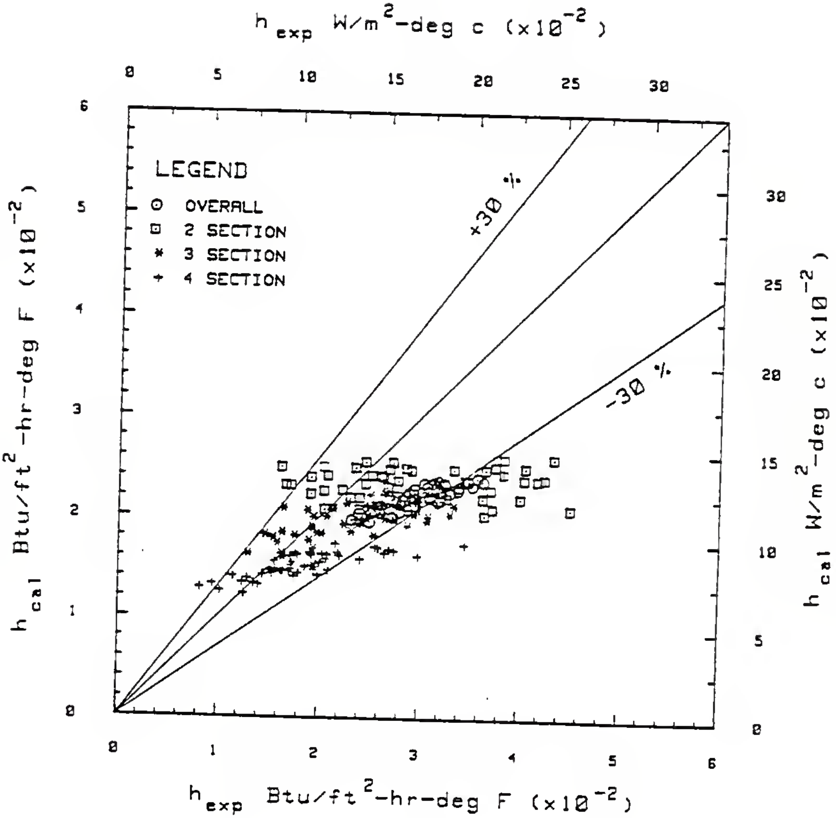

Fig 5.2 Comparison of experimental sectional and overall heat transfer coefficients with predictions of the correlation of Akers et al. [6], Eq.(5-1), tube 1

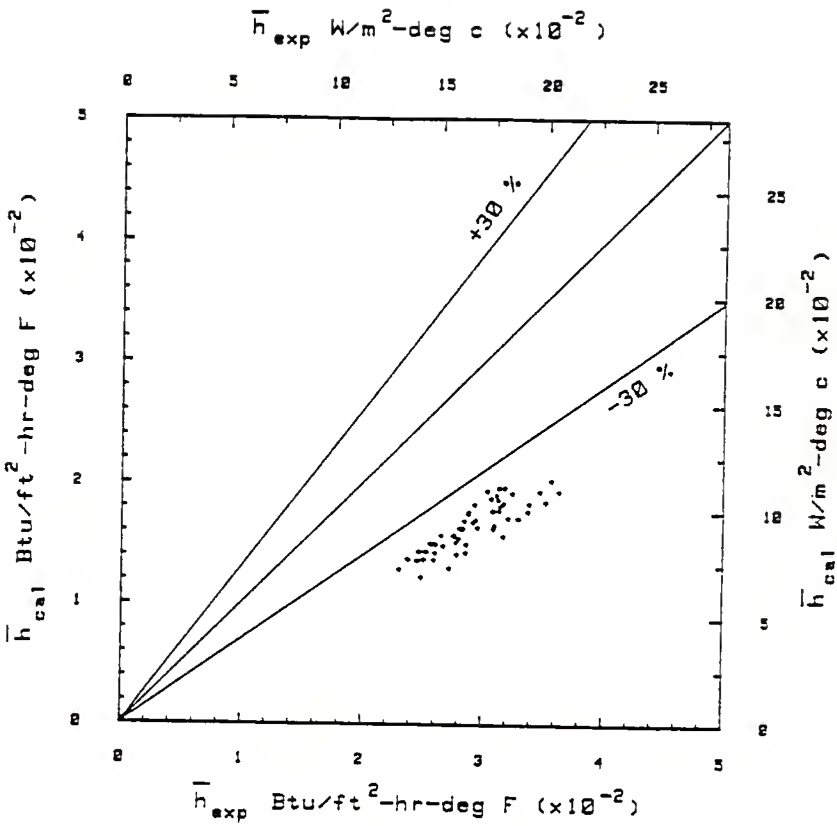

Fig 5.3 Comparison of experimental overall heat transfer coefficients with predictions of the correlation of Boyko and Kruzhilin [7], Eq.(5-4), tube 1

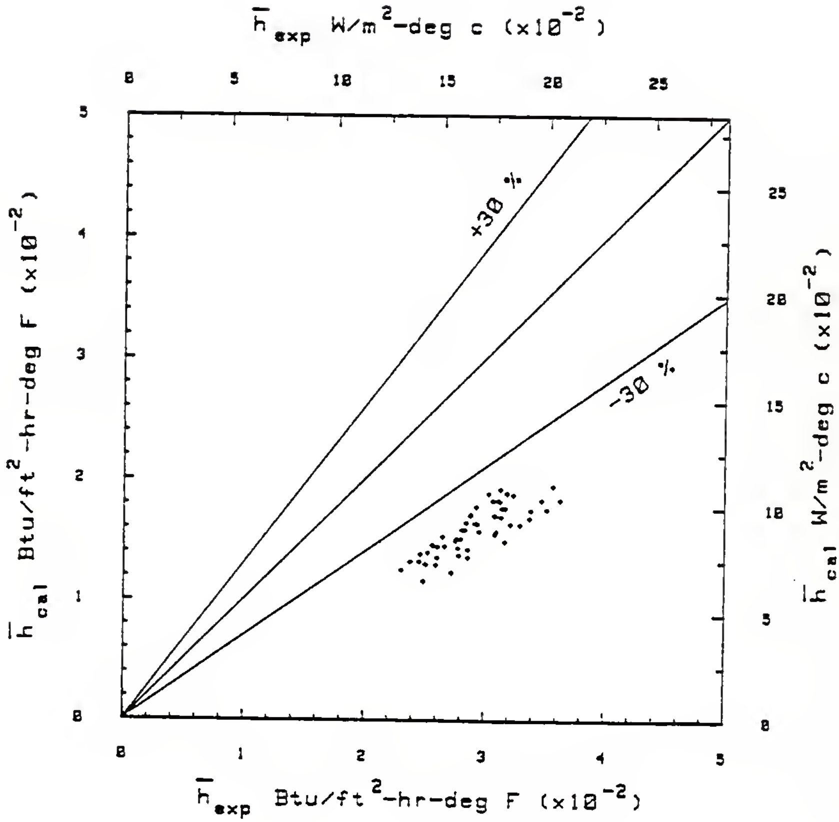

Fig 5.4 Comparison of experimental overall heat transfer coefficients with predictions of the correlation of Shah [13], Eq.(5-7), tube 1

correlation [7], Eq. (5-4). The correlation underpredicted the experimental overall heat transfer values.

The comparison between the experimental overall heat transfer results and predictions of Shah's correlation [13], Eq. (5-7), is shown in Fig. 5.4. The correlation also underpredicted the measured values.

The results of the above comparisons are summarized below:

1. The correlation of Akers et al. [6], Eq. (5-1), correlated 83% of experimental overall heat transfer values within ±30%. It also correlated the sectional heat transfer values reasonably well, except section 1.

2. The correlation of Boyko and Kruzhilin [7], and Shah [13] predicted overall heat transfer values lower than measured values.

It is worth noting that among the recent investigations of in-tube condensation by Royal and Bergles [4,42], Luu and Bergles [5,45,46], and Said and Azer [2,47], the smooth tube data obtained by Royal and Bergles, and Said and Azer correlated best with predictions of Akers et al. [6]. Luu and Bergles data correlated well with the predictions of Boyko and Kruzhilin [7].

5.2.2 Pressure Drop

The pressure gradient during two-phase flow inside a horizontal tube is usually divided into two parts, friction and momentum terms.

$$\left(\frac{dp}{dz}\right) = \left(\frac{dp}{dz}\right)_f + \left(\frac{dp}{dz}\right)_m \qquad (5\text{-}9)$$

The main factors involved in the frictional pressure drop are probably the viscous dissipation in the liquid film and the pressure drop associated with gas flow over the wavy interface. The momentum recovery part of the pressure drop is due to the deposition of faster moving vapor on the slower moving condensate flow.

The literature survey revealed that two basic models are usually used in analyzing the two-phase pressure drop. In the first model, the two phases are assumed homogeneous with the same gas and liquid velocities. The frictional pressure drop in this model is developed by introducing modifiers to the single phase friction coefficient. In the second model, the two phases are considered to have different velocities and hence are separated.

1. The frictional pressure gradient correlations

Among the well recognized frictional pressure gradient correlations are those of Lockhart-Martinelli [14] and Dukler [16]. A summary of these correlations follows.

Lockhart-Martinelli [14] defined a parameter X given by

$$X = \left[\left(\frac{dp}{dz}\right)_\ell \Big/ \left(\frac{dp}{dz}\right)_v \right]^{0.50} \qquad (5\text{-}10)$$

where

$\left(\frac{dp}{dz}\right)_\ell$ = frictional pressure gradient assuming that liquid alone is flowing in the pipe

$\left(\frac{dp}{dz}\right)_v$ = frictional pressure gradient assuming that gas (or vapor in case of condensation) alone is flowing in the pipe

In two-phase flow, four combinations of flows are possible. (a) Liquid viscous, gas viscous, (b) Liquid viscous, gas turbulent, (c) Liquid turbulent, gas viscous, and (d) Liquid turbulent, gas turbulent. Liquid turbulent, gas turbulent flow is the one usually encountered during in-tube condensation. For turbulent flow of the two phases during condensation, the parameter X can be replaced by X_{tt} and written as

$$X_{tt} = \left(\frac{1 - x}{x}\right)^{0.9} \left(\frac{\mu_\ell}{\mu_v}\right)^{0.1} \left(\frac{\rho_v}{\rho_\ell}\right)^{0.5} \tag{5-11}$$

Lockhart and Martinelli also defined the parameter ϕ_v as

$$\phi_v = \left[\left(\frac{dp}{dz}\right)_f \Big/ \left(\frac{dp}{dz}\right)_v\right]^{0.5} \tag{5-12}$$

For condensation

$$\left(\frac{dp}{dz}\right)_v = -\frac{2 f_o (x G)^2}{\rho_v D_i} \tag{5-13}$$

where

$$f_o = 0.045 \Big/ \left(\frac{GxD_i}{\mu_v}\right)^{0.2} \tag{5-14}$$

f_o is the friction factor for adiabatic two-phase flow. Lockhart and Martinelli reported the relationship between ϕ_v and X graphically by analyzing the pressure drop data of simultaneous adiabatic flow of air and various liquids. Soliman et al. [10] approximated the graphical results of ϕ_v versus X_{tt} by

$$\phi_v = [1 + 2.85 X_{tt}^{0.523}] \tag{5-15}$$

The frictional pressure gradient in the Dukler II correlation [16] is given by

$$\left(\frac{dp}{dz}\right)_f = -\frac{2 G^2 f_o \alpha(\lambda)\beta}{D_i \rho_{NS}} \tag{5-16}$$

where

f_o = single phase friction coefficient evaluated at the two phase Reynolds number

$$= 0.0014 + 0.125 \left(\frac{4\, \dot{M}_T\, \beta}{\pi D_i \mu_{NS}}\right)^{-0.32} \qquad (5\text{-}17)$$

$$\alpha(\lambda) = 1 - (\ell n\lambda)/[1.281 + 0.478\ \ell n\lambda + 0.444\ (\ell n\lambda)^2 + 0.094\ (\ell n\lambda)^3 + 0.00843\ (\ell n\lambda)^4] \qquad (5\text{-}18)$$

$$\beta = \left[\left(\frac{\rho_\ell}{\rho_{NS}}\right) \frac{\lambda^2}{(1-\psi)} + \left(\frac{\rho_v}{\rho_{NS}}\right) \frac{(1-\lambda)^2}{\psi}\right] \qquad (5\text{-}19)$$

$$\rho_{NS} = [\rho_\ell\, \lambda + \rho_v(1-\lambda)] \qquad (5\text{-}20)$$

$$\mu_{NS} = [\mu_\ell\, \lambda + \mu_v(1-\lambda)] \qquad (5\text{-}21)$$

and

$$\lambda = 1/[1 + \frac{1}{(1-x)} (\frac{\rho_v}{\rho_\ell})] \qquad (5\text{-}22)$$

The correlations of Lockhart-Martinelli and Dukler were originally developed for adiabatic two-phase flow. For the condensation process, Luu and Bergles [5,45] modified the friction coefficients in Eq. (5-13) and Eq. (5-16) by using modifiers suggested by Silver and Wallis [49]. They replaced the friction coefficient f_o by f_{co} and they were related by

$$(f_{co}/f_o) = \left[e^{(\xi/2f_o)} - \frac{\xi}{f_o}\right] \qquad (5\text{-}23)$$

where

$$\xi = \left(\frac{D_i}{2x}\right) \left[\left(\psi - \frac{x}{2}\frac{d\psi}{dx}\right) / \sqrt{\psi}\right] \left(\frac{dx}{dz}\right) \qquad (5\text{-}24)$$

2. The momentum pressure gradient $\left(\frac{dp}{dz}\right)_m$

The correlation of Lockhart-Martinelli and Dukler II are based on the separated two phase flow model. The momentum pressure gradient based on the same model as outlined by Said [2] is given by

$$\left(\frac{dp}{dz}\right)_m = -G^2 \left(\frac{dx}{dz}\right)\left\{\frac{2x}{\rho_v \psi} - \frac{2(1-x)}{\rho_\ell(1-\psi)} + \frac{d\psi}{dx}\left[\frac{(1-x)^2}{\rho_\ell(1-\psi)^2} - \frac{x^2}{\rho_v \psi^2}\right]\right\} \qquad (5\text{-}25)$$

To calculate the momentum pressure gradient, one needs to know the void fraction ψ and the quality gradient $\left(\frac{dx}{dz}\right)$. In the present study, the void fraction correlations of the homogeneous model [18], Lockhart-Martinelli [14], Baroczy [19], Thom [20], Zivi [21], and Turner-Wallis [22] were selected. Butterworth [50] suggested a generalized expression for ψ given by

$$\psi = \frac{1}{1 + A_1 \left(\frac{1 - x}{x}\right)^{q_1} \left(\rho_v/\rho_\ell\right)^{r_1} \left(\mu_\ell/\mu_v\right)^{S_1}} \tag{5-26}$$

The constants A_1, q_1, r_1, and S_1 are listed in Table 5.1 for various correlations.

By differentiating Eq. (5-26) with respect to x and substituting in Eq. (5-25) the following expression is obtained.

$$\left(\frac{dp}{dz}\right)_m = - G^2 \left(\frac{dx}{dz}\right) \left\{\frac{2x}{\rho_v \psi} - \frac{2\ (1-x)}{\rho_\ell\ (1-\psi)} + q_1 \left[\frac{\psi(1-x)}{x(1-\psi)\rho_\ell} - \frac{x(1-\psi)}{\psi(1-x)\rho_v}\right]\right\} \tag{5-27}$$

Table 5.1 The Constants in Eq. (5-26) for the Different Void Fraction Correlations

Model	A_1	q_1	r_1	S_1
Homogeneous [18]	1.0	1.0	1.0	0
Lockhart-Martinelli [14]	0.28	0.64	0.36	0.07
Baroczy [19]	1.0	0.74	0.65	0.13
Thom [20]	1.0	1.0	0.89	0.18
Zivi [21]	1.0	1.0	0.67	0
Turner-Wallis [22]	1.0	0.72	0.40	0.08

To predict the total pressure drop during condensation, the following procedure was adopted.

a) The test condenser was divided into a number of small increments (80 increments) of constant lengths.

b) A linear change in quality was assumed for which $\left(\frac{dx}{dz}\right) = (-1/L)$ where L = total length of test condenser.

c) Since the total pressure drop involved was very small, the properties of liquid phase were calculated at inlet pressure conditions.

d) The frictional pressure gradient was calculated separately using Lockhart-Martinelli and Dukler II correlations, and for momentum using Eq. (5-27) for various void fractions, for each incremental length.

e) The pressure drop for each incremental length was calculated by multiplying the pressure gradients of friction and momentum with incremental length.

f) By repeating steps (d) and (e) for all incremental lengths, the total pressure drop for the entire test condenser tube was calculated. The above scheme was implemented in a digital computer program.

As mentioned in Chapter IV, the quality at exit of each subsection could be estimated by energy balance of the condensing fluid and cooling water. This information can be used to find $\left(\frac{dx}{dz}\right)$ for each subsection to calculate the momentum pressure gradient from Eq. (5-27). Said [2] used both methods of quality variation to calculate the momentum and hence, the total pressure drop in the test condenser tube. He concluded that the best agreement between the predicted and the measured pressure drops were obtained by assuming the quality gradient to be equal to (-1/L) for the entire test condenser tube. This was the approach followed in calculating the pressure drop in the present study.

In the present study, all possible combinations of the frictional pressure gradients of Lockhart-Martinelli [14], and Dukler II [16] with and without the modification of Eqs. (5-23) and (5-24), and the momentum pressure gradients based on the void fraction correlations of the homogeneous model [18], Lockhart-Martinelli [14], Baroczy [19], Thom [20], Zivi [21], and Turner and Wallis [22], were tried to predict the pressure drop of the experimental runs of tube 1. The best agreement between the experimental pressure drop and the predictions were obtained without applying the modified friction coefficient given by Eq. (5-23). In general, the Lockhart-Martinelli [14] frictional pressure drop correlation predicted reasonably well the experimental pressure drop measurements with any of the six void fraction correlations used. The pressure drop predictions using the Dukler II [16] frictional pressure drop correlation was relatively sensitive to the choice of the void fraction correlations. Only, the void fraction correlation of Zivi in combination with the Dukler II frictional correlation predicted well the experimental overall pressure drop results.

Figure 5.5 shows a comparison between the experimental overall pressure drop and the predictions of the combination of Lockhart-Martinelli correlation for frictional pressure drop and the void fraction correlation of Zivi. The results show that the predictions were within ±40% from the experimental overall pressure drop for 64% of data points. Figure 5.6 shows a comparison between the experimental and predicted overall pressure drops for the combination of Dukler II/Zivi correlations. 53% of data points of the predicted values in Fig. 5.6 were within ±40% from the experimental overall pressure drop measurements.

It is of interest to point out that Royal and Bergles [4,43] reported that the best predictor of their pressure drop measurements of steam was

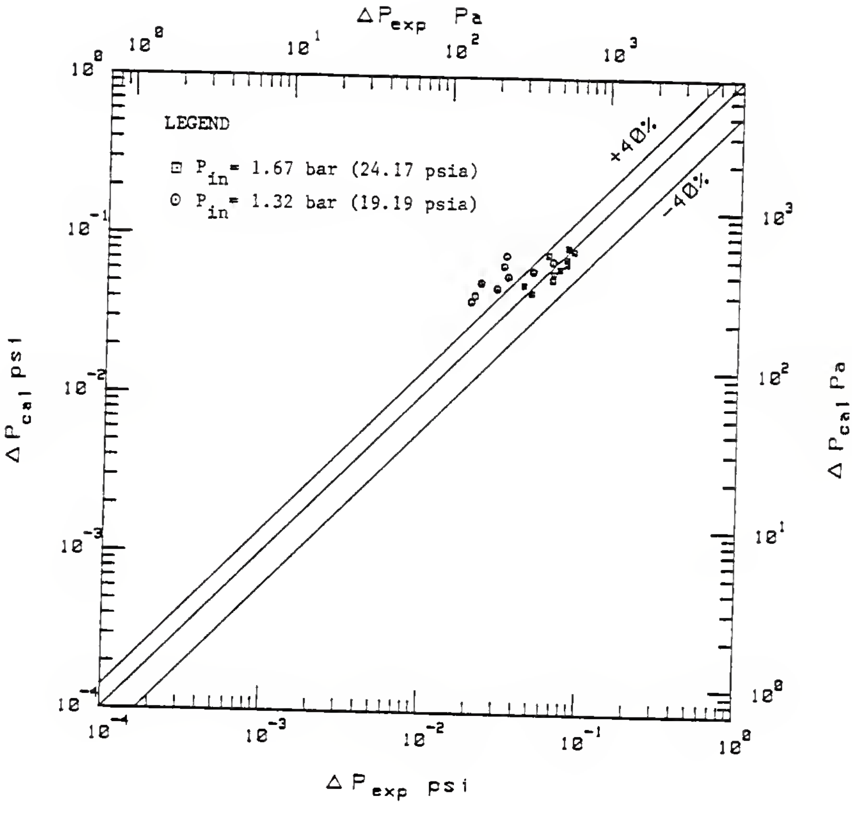

Fig 5.5 Comparison of experimental overall pressure drop with predictions of the correlations of Lockhart-Martinelli [14] for friction and Zivi [21] for void fraction, tube 1

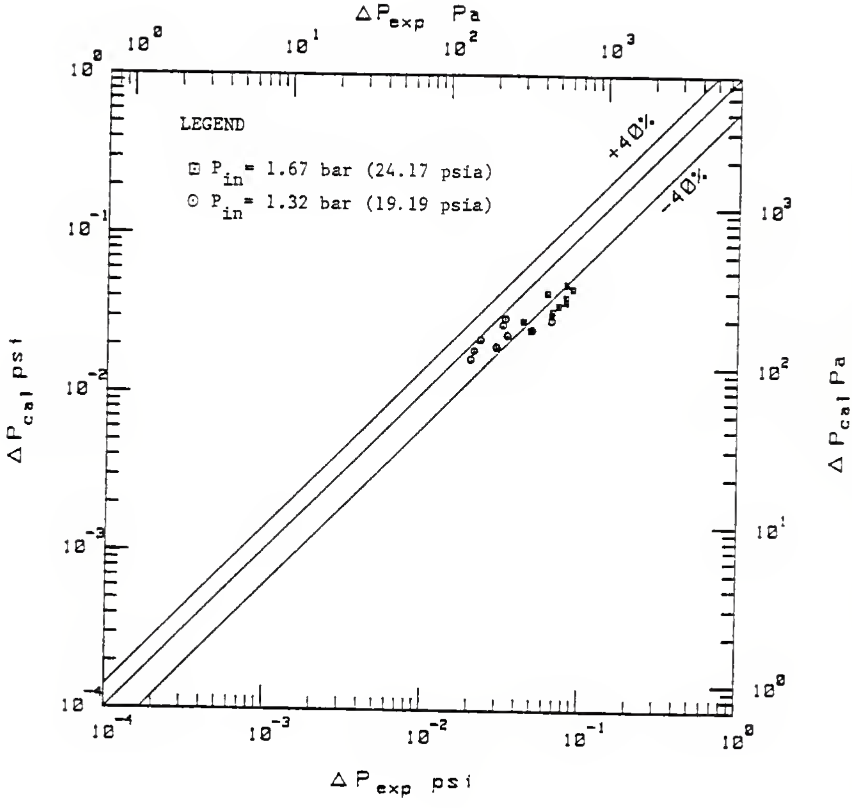

Fig 5.6 Comparison of experimental overall pressure drop with predictions of the correlations of Dukler II [16] for friction and Zivi [21] for void fraction, tube 1

the combination of the Dukler II [16] and the Hughmark [23] void fraction correlation. Luu and Bergles reported that Lockhart-Martinelli [14] and Dukler II [16] correlations for frictional pressure drop and the homogeneous [18] void fraction correlation for momentum pressure drop predicted their data best. They also reported that the calculated momentum pressure drops were insensitive to the void fraction values predicted by different void fraction correlations. Hence they used the homogeneous void fraction correlation for simplicity. Said and Azer [2,47] tested their data with various frictional and momentum pressure drop correlations and concluded that the Lockhart-Martinelli correlation [14] for frictional pressure drop and the homogeneous [18] void fraction for momentum pressure drop predicted their smooth tube data best.

5.3 Internally Finned Tubes

All the internally finned tubes tested gave higher heat transfer coefficients compared to the smooth tube. Also, internally finned tubes yielded higher overall pressure drops compared to the smooth tube results. These results may be attributed to the altered flow mechanism in in-tube condensation due to the presence of internal fins besides the increase in heat transfer area. The performance evaluation of the internally finned tubes, taking into consideration the increased heat transfer coefficients at the expense of the overall pressure drop, will be made in the next chapter.

5.3.1 Heat Transfer

Finned tube correlations.

The development of internally finned tube heat transfer correlations were based upon applying modifying factors to the smooth tube correlations to bring about the best agreement between the predictions and the experimental results. Various modifiers based on certain geometric parameters of the finned tube such as (W/D_h), (H/D_h), and $b^2/WD_i)$ were introduced by various investigators.

The following correlations have been suggested for in-tube condensation inside internally finned tubes.

The correlation of Royal and Bergles [42] is given by

$$\bar{h}=0.0265\ (k_\ell/D_h)\left(\frac{G_e D_h}{\mu_\ell}\right)^{0.8} Pr_\ell^{0.33}\left[1+160\left(\frac{b^2}{WD_i}\right)^{1.91}\right] \tag{5-28}$$

where

$$G_e = G\left[(1-\bar{x}) + \bar{x}\ \frac{\rho_\ell}{\rho_v}\right]^{0.5} \tag{5-29}$$

Royal and Bergles used this correlation to correlate their heat transfer data of steam condensed inside horizontal tubes with straight and spiral internal fins. This correlation was based on applying a modifying factor, which is a function of (b^2/WD_i), to the smooth tube correlations of Akers et al. [6].

Luu and Bergles [46] proposed the following correlation which best predicted their R-113 condensation data inside internally finned tubes.

$$\bar{h}=0.024\ (k_\ell/D_h)\left(\frac{GD_h}{\mu_\ell}\right)^{0.8} Pr_\ell^{0.43}\left[\frac{(\rho/\rho_m)_{in}^{0.5} + (\rho/\rho_m)_{out}^{0.5}}{2}\right]\left(\frac{b^2}{WD_i}\right)^{-0.22} \tag{5-30}$$

where

$$\left(\frac{\rho}{\rho_m}\right) = 1 + x\left(\frac{\rho_\ell}{\rho_v} - 1\right) \tag{5-31}$$

This correlation was based on modifying the smooth tube correlation of Boyko and Kruzhilin [7] by the factor $(b^2/WD_i)^{-0.22}$.

Said and Azer [47] introduced the factors F_1, F_2, and F_3 as modifiers to the smooth tube correlations of Akers et al. [6] to get the best agreement between the experimental and predicted values of the condensation heat transfer coefficients. Their correlation is given by

$$\bar{h}=0.0265(k_\ell/D_i)\left(\frac{G_e D_i}{\mu_\ell}\right)^{0.8} Pr_\ell^{0.333}\,[1 + 0.93\, F_1^{0.23}\, F_2^{0.58}\, F_3^{4.17}\, Re_\ell^{0.054}] \tag{5-32}$$

where

$$G_e = G[(1 - \bar{x}) + \bar{x}\left(\frac{\rho_\ell}{\rho_v}\right)^{0.5}] \tag{5-33}$$

and

$$Re_\ell = G\, D_i(1 - \bar{x})/\mu_\ell \tag{5-34}$$

The geometric factors F_1, F_2, and F_3 were originally introduced by Carnavos [28,29] in his study of single phase heat transfer and friction coefficient of finned tubes to get the best agreement between the experimental measurements and the predictions. These modifying factors are defined as follows.

$$F_1 = A_{fa}/A_{fc} \tag{5-35}$$

$$F_2 = A_n/A_a \tag{5-36}$$

$$F_3 = \sec\alpha \tag{5-37}$$

where

A_{fa} = actual free flow area, $\frac{\pi D_e^2}{4}$, cm^2

A_{fc} = open core free flow area, $\frac{\pi D_c^2}{4}$, cm^2

A_n = nominal heat transfer area based on D_i as if fins were not present, cm^2/cm

A_a = actual heat transfer area, cm^2/cm

The equivalent diameter D_e and core diameter D_c are defined by

$$\frac{\pi D_e^2}{4} = \frac{\pi D_i^2}{4} - nbt/\cos\alpha \tag{5-38}$$

$$\frac{\pi D_c^2}{4} = \frac{\pi}{4}(D_i - 2b)^2 \tag{5-39}$$

Hydraulic diameter is defined by

$$D_h = 4A_{fa}/A_a \tag{5-40}$$

With the above definitions, it can be shown that

$$F_1 = A_{fa}/A_{fc} = \left(\frac{D_e}{D_i}\right)^2 / [1 - (2b/D_i)]^2$$
$$= \frac{[1 - (4nbt)/(\pi D_i^2 \cos\alpha)]}{[1 - 2b/D_i]^2} \tag{5-41}$$

and

$$F_2 = A_n/A_a = (D_i D_h/D_e^2)$$
$$= \frac{\pi D_i}{[\pi D_i + 2nb/\cos\alpha]} \tag{5-42}$$

The values of F_1, F_2, and F_3 for the tubes tested in the present study are given in Table 5.2. Also the various geometric parameters of the finned tubes are shown in Fig. 5.7.

Table 5.2 Computed Values of F_1, F_2, and F_3

F Value	Tube Tested			
	2	3	4	5
F_1	1.515	1.514	1.464	1.355
F_2	0.6678	0.5281	0.5667	0.6085
F_3	1.0	1.0145	1.0236	1.0599

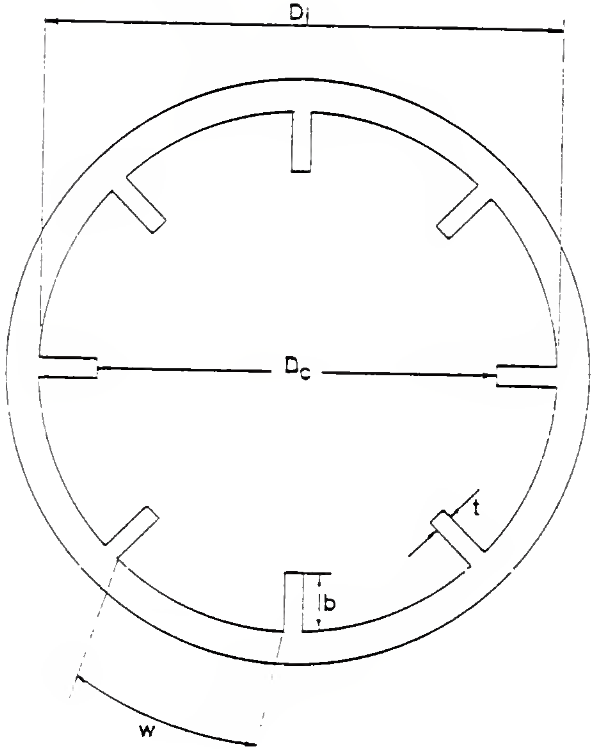

Fig. 5.7 Cross Section of Internally Finned Tube.

Figures 5.8 through 5.16 show comparisons between the predictions of Royal and Bergles correlation [42] with experimental measurements. Figures 5.8, 5.10, 5.12 and 5.14 show overall average heat transfer coefficients. Except for tube 3, Fig. 5.10, the correlation underpredicted $\bar{h}$ for tubes 2, 4, and 5. Similarly Figs. 5.9, 5.11, 5.13 and 5.15 show sectional averages and overall heat transfer coefficients for tubes 2, 4 and 5, respectively. Except for tube 3, all the sectional heat transfer coefficients were underpredicted by the correlation. For tube 3, as shown in Fig. 5.11, the correlation overpredicted the sectional averages of section 1 and underpredicted the sectional averages of section 4. A comparison of the predictions of Royal and Bergles with the experimental values for all the finned tubes is shown in Fig. 5.16. It is clear from the figure that the correlation underpredicted $\bar{h}$ for all finned tubes except tube 3.

Figures 5.17 through 5.25 show comparisons between the experimental measurements and the predictions of Luu and Bergles correlation [46] for the heat transfer coefficients. Figures 5.17, 5.19, 5.21, and 5.23 show comparisons for the overall heat transfer coefficients. The correlation predicted $\bar{h}$ within ±30% from experimental values for 79% of the data points for tube 2, 100% for tubes 3 and 4. The correlation underpredicted $\bar{h}$ for tube 5. Figures 5.18, 5.20, 5.22 and 5.24 show the comparisons of the experimental sectional averages and the overall heat transfer coefficients with the predictions. The correlation had a tendency to overpredict the sectional average heat transfer coefficients for section 1, except for tube 5 where they were underpredicted. For tubes 3, 4, and 5, the correlation tended to underpredict the sectional average heat transfer coefficient for section 4. The large scatter in the sectional heat transfer

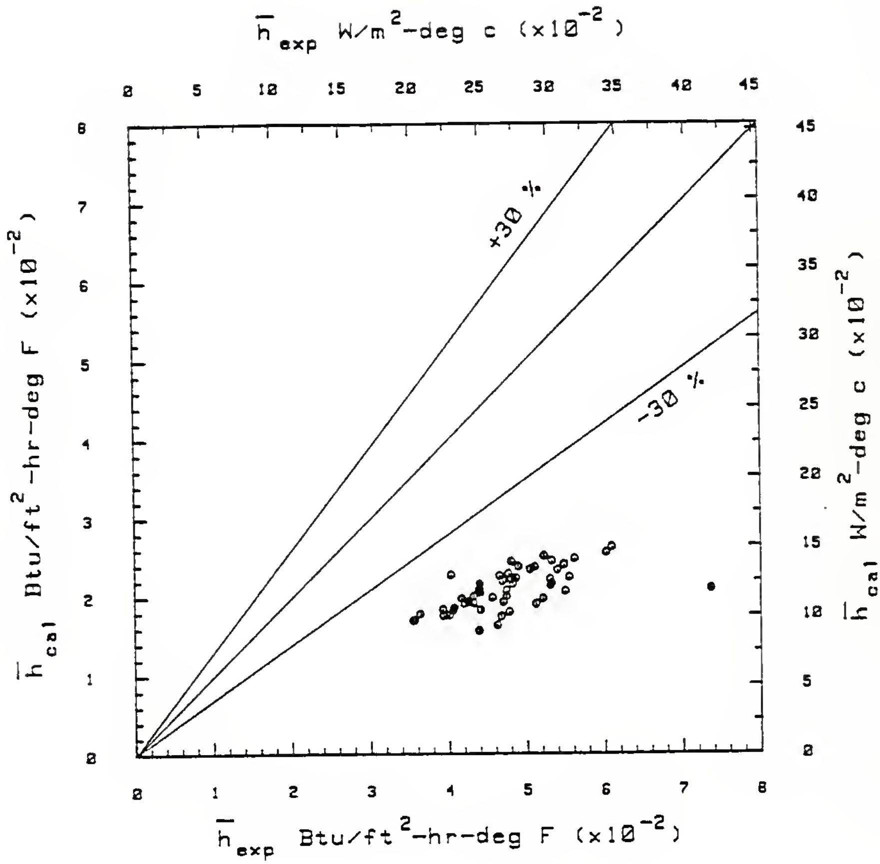

Fig 5.8 Comparison of experimental overall heat transfer coefficients with predictions of the correlation of Royal and Bergles [42], Eq.(5-28), tube 2

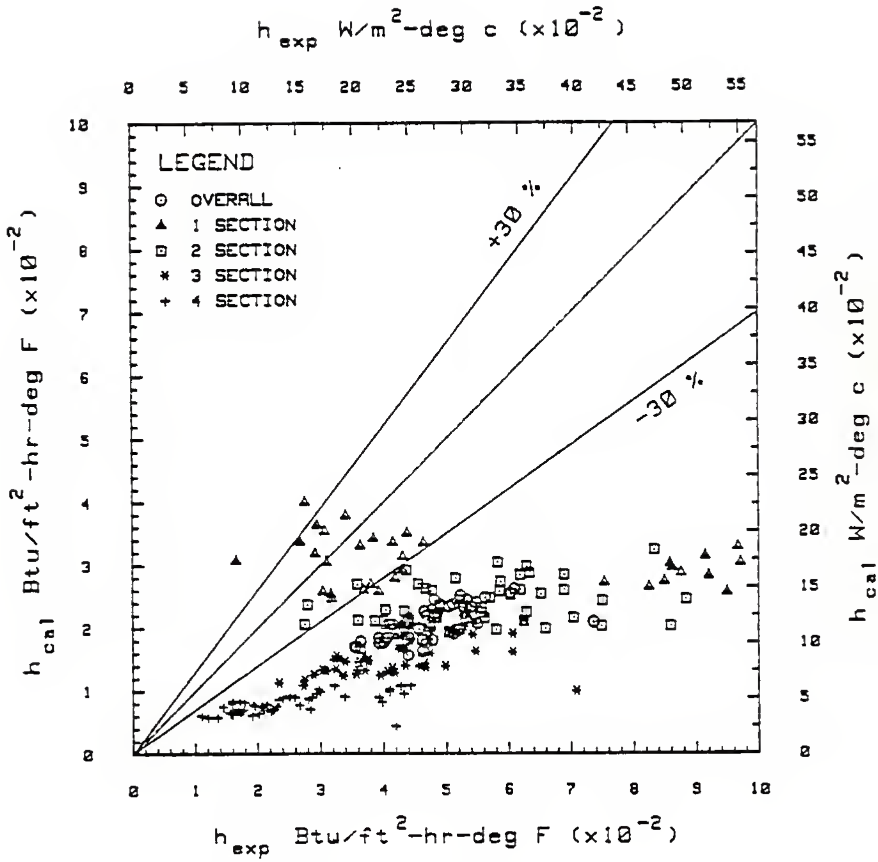

Fig 5.9 Comparison of experimental sectional and overall heat transfer coefficients with predictions of the correlation of Royal and Bergles [42], Eq.(5-28), tube 2

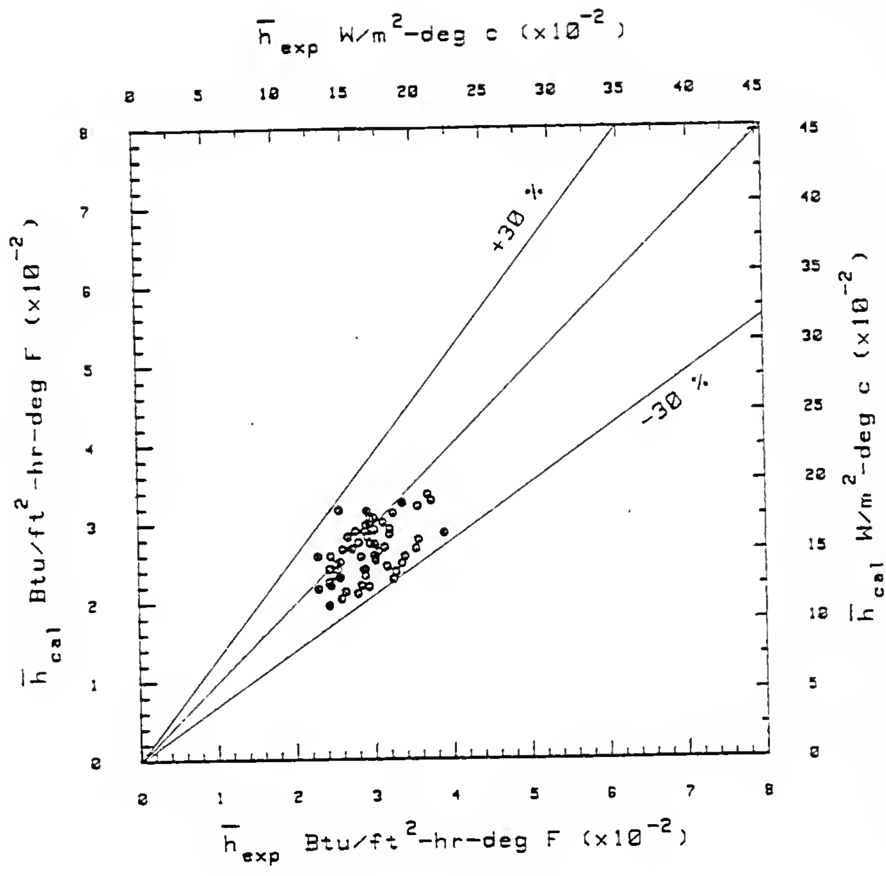

Fig 5.10 Comparison of experimental overall heat transfer coefficients with predictions of the correlation of Royal and Bergles [42], Eq.(5-28), tube 3

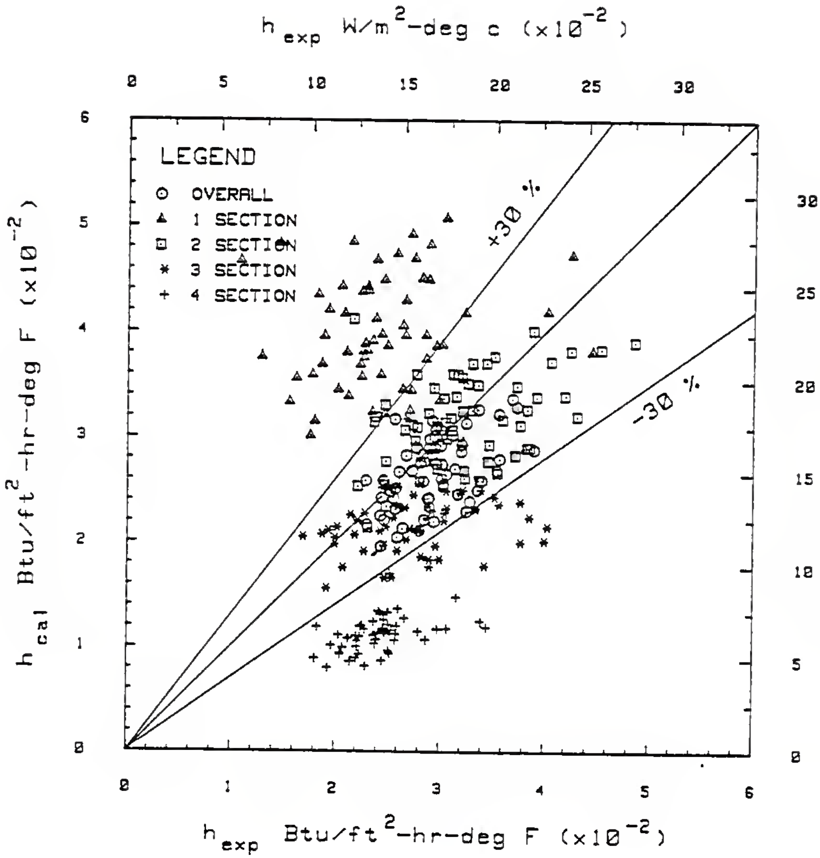

Fig 5.11 Comparison of experimental sectional and overall heat transfer coefficients with predictions of the correlation of Royal and Bergles [42], Eq.(5-28), tube 3

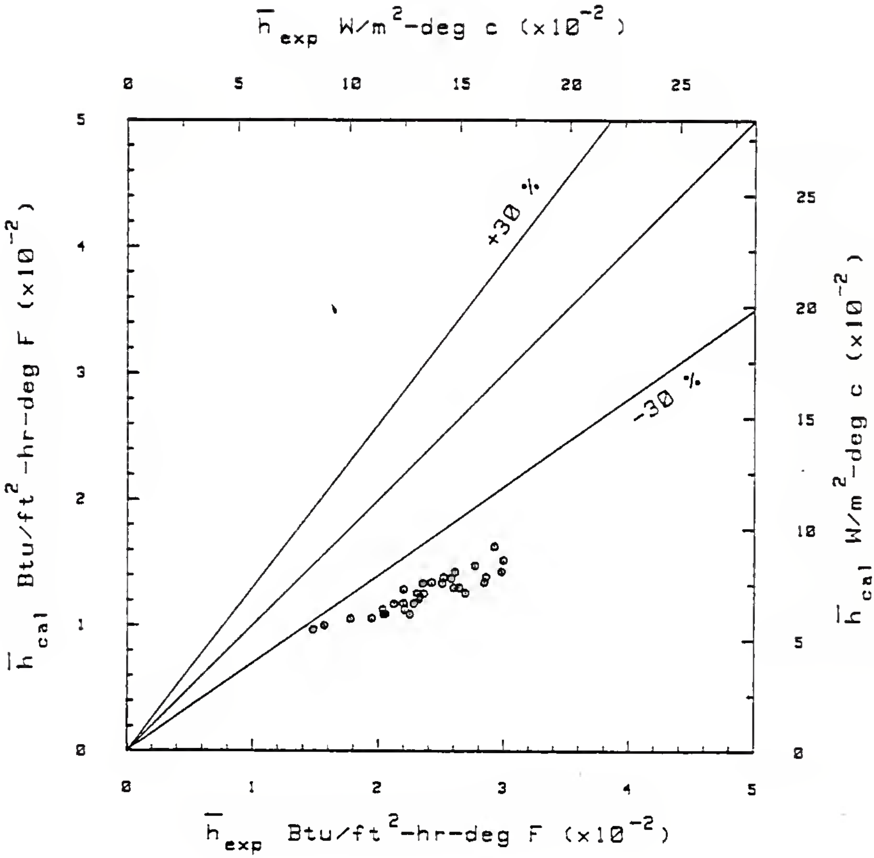

Fig 5.12 Comparison of experimental overall heat transfer coefficients with predictions of the correlation of Royal and Bergles [42], Eq.(5-28), tube 4

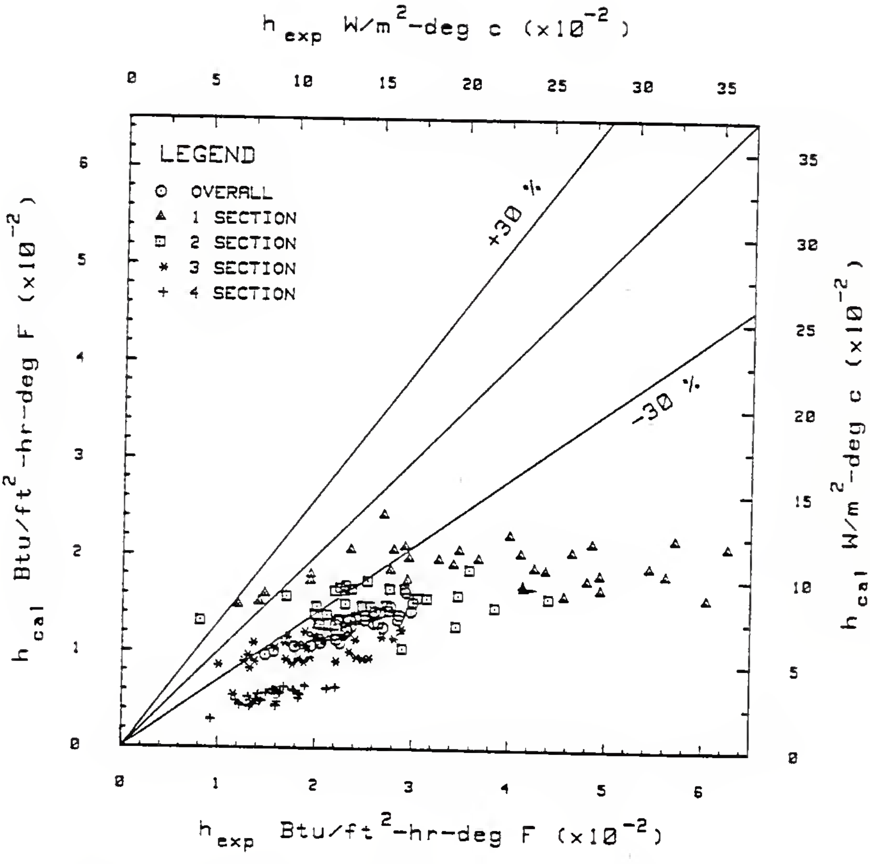

Fig 5.13 Comparison of experimental sectional and overall heat transfer coefficients with predictions of the correlation of Royal and Bergles [42], Eq.(5-28), tube 4

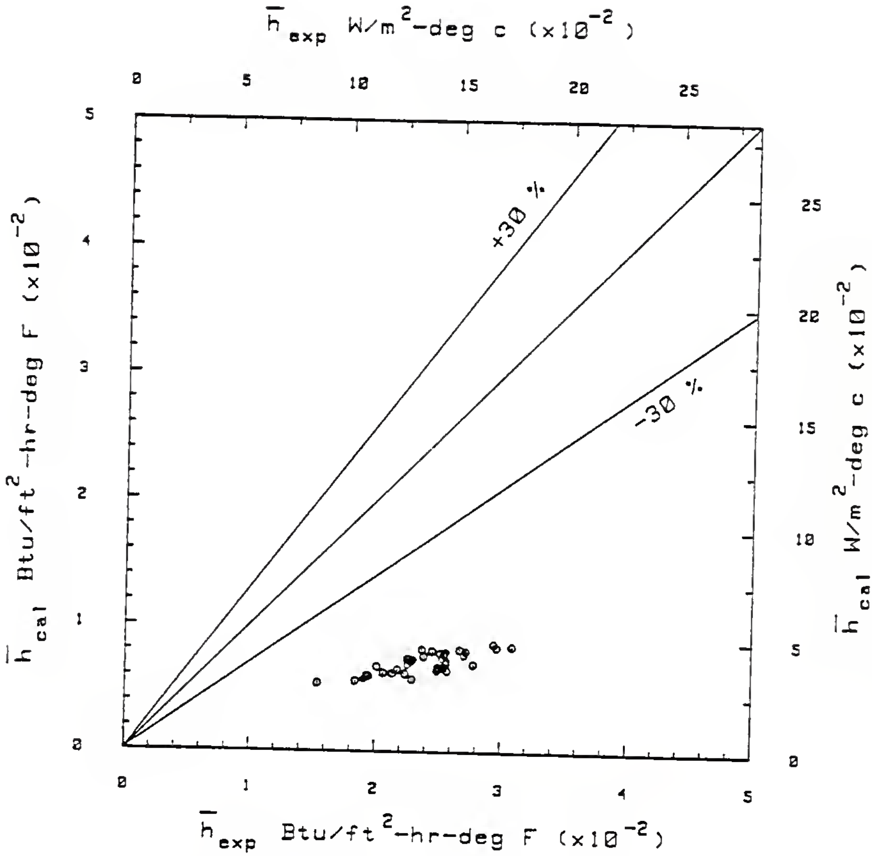

Fig 5.14 Comparison of experimental overall heat transfer coefficients with predictions of the correlation of Royal and Bergles [42], Eq.(5-28), tube 5

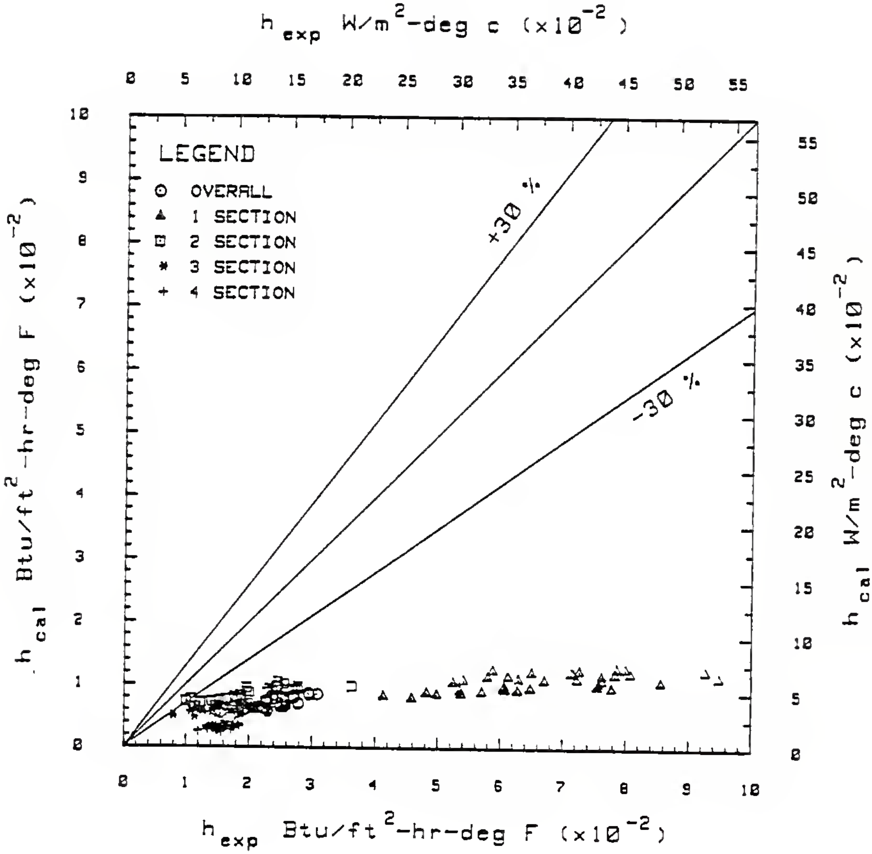

Fig 5.15 Comparison of experimental sectional and overall heat transfer coefficients with predictions of the correlation of Royal and Bergles [42], Eq.(5-28), tube 5

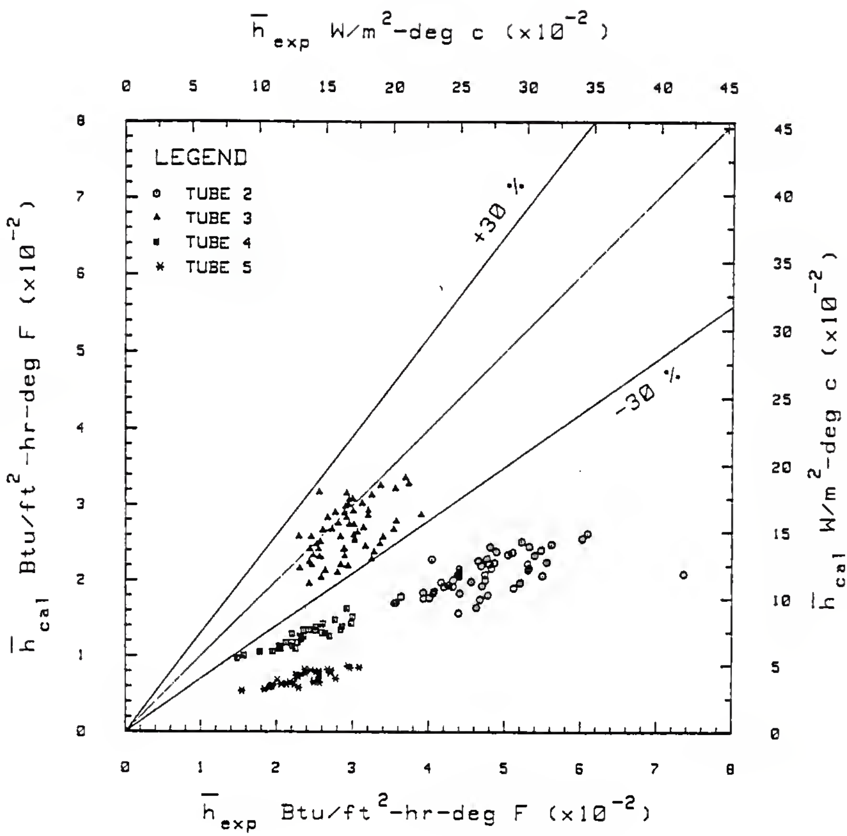

Fig 5.16 Comparison of experimental overall heat transfer coefficients with predictions of the correlation of Royal and Bergles [42], Eq.(5-28), all finned tubes

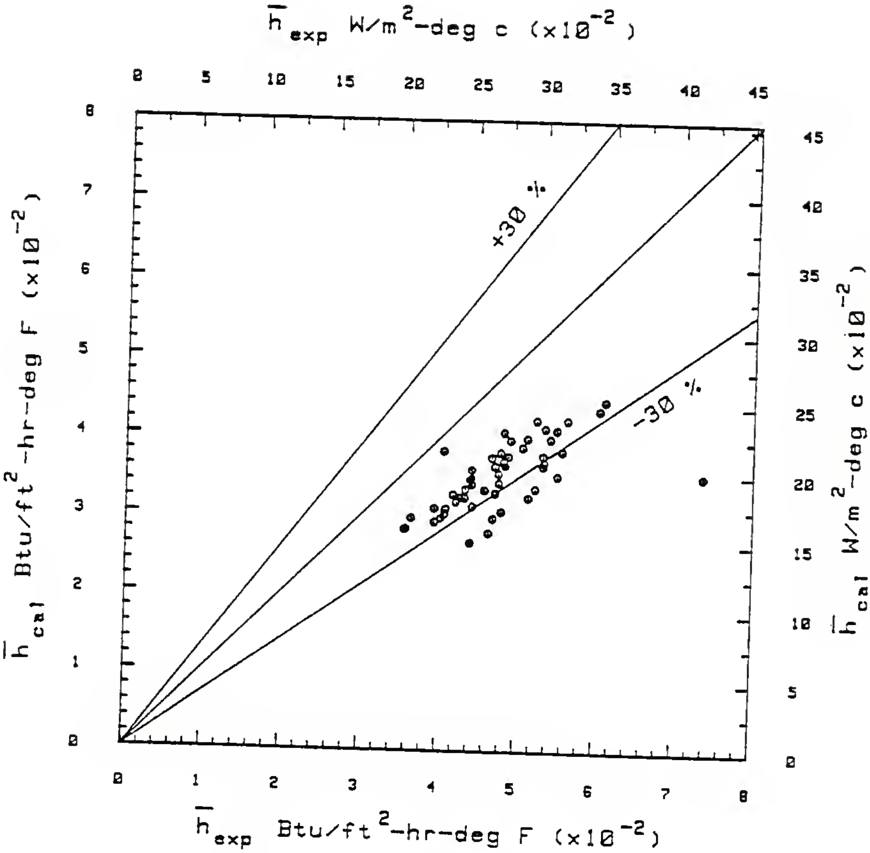

Fig 5.17 Comparison of experimental overall heat transfer coefficients with predictions of the correlation of Luu and Bergles [46], Eq.(5-30), tube 2

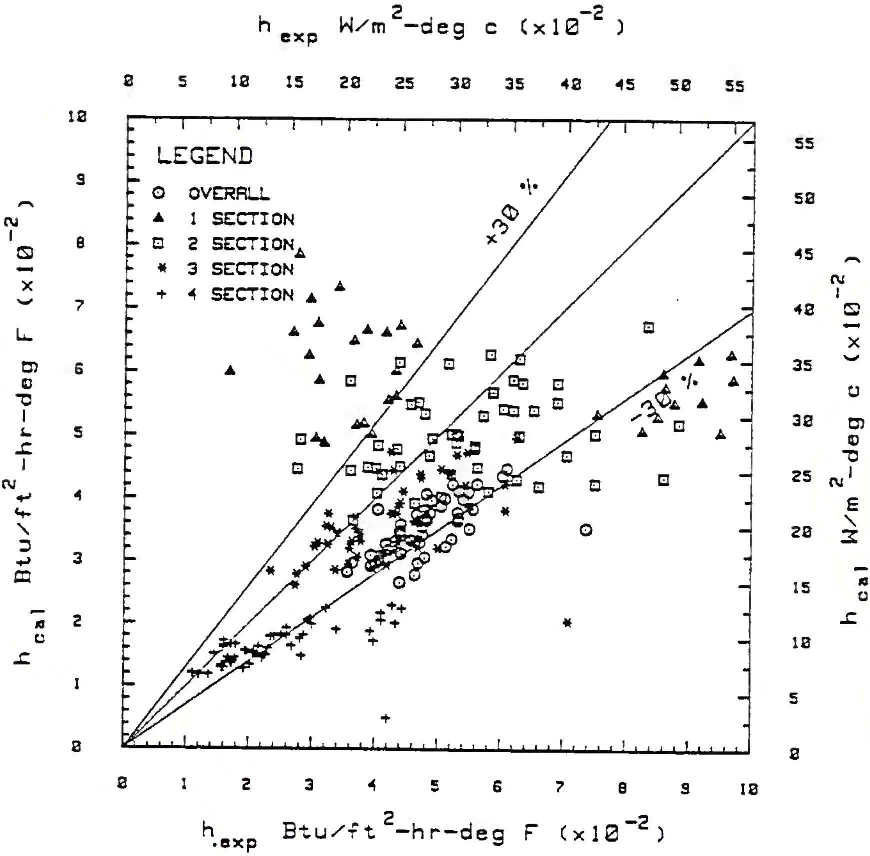

Fig 5.18 Comparison of experimental sectional and overall heat transfer coefficients with predictions of the correlation of Luu and Bergles [46], Eq.(5-30), tube 2

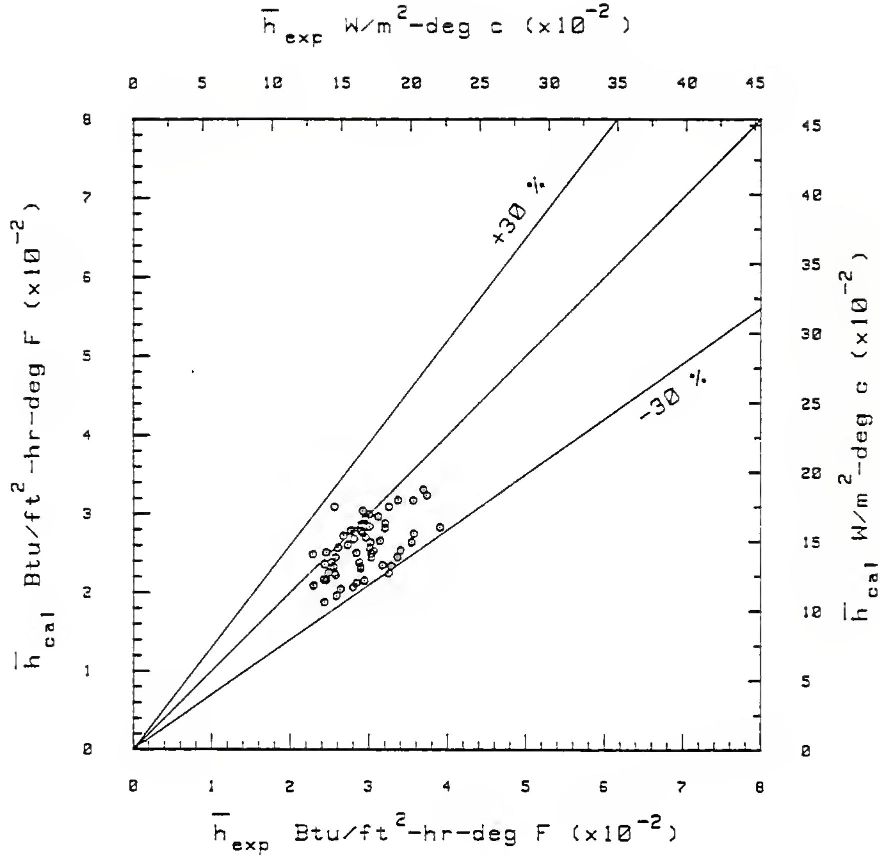

Fig 5.19 Comparison of experimental overall heat transfer coefficients with predictions of the correlation of Luu and Bergles [46], Eq.(5-30), tube 3

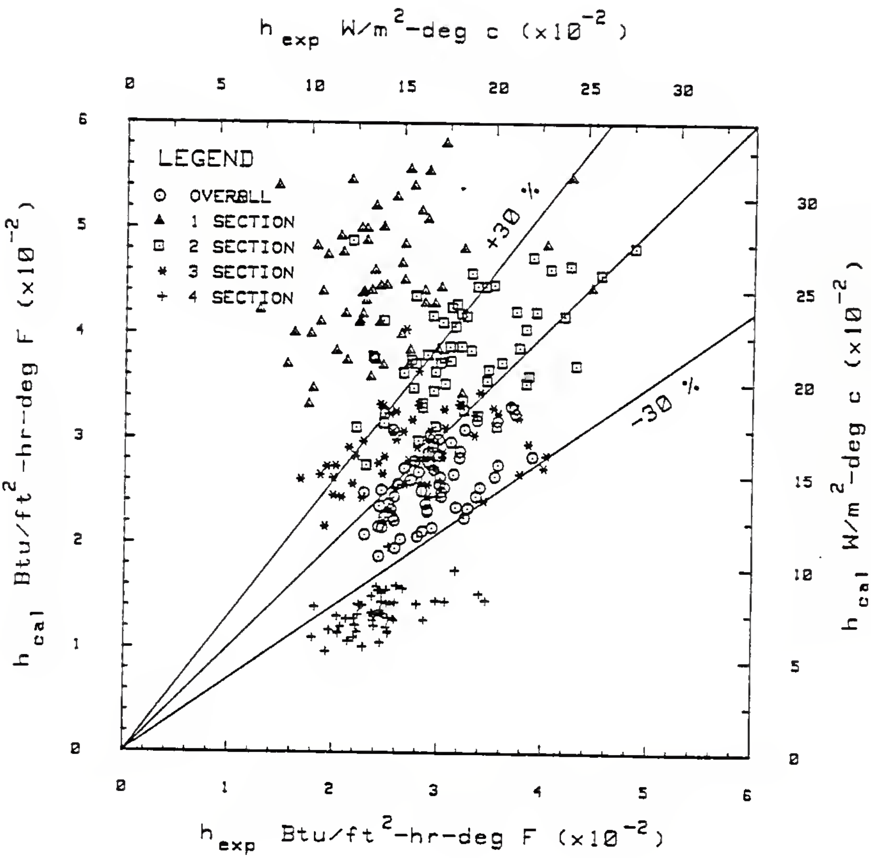

Fig 5.20 Comparison of experimental sectional and overall heat transfer coefficients with predictions of the correlation of Luu and Bergles [46], Eq.(5-30), tube 3

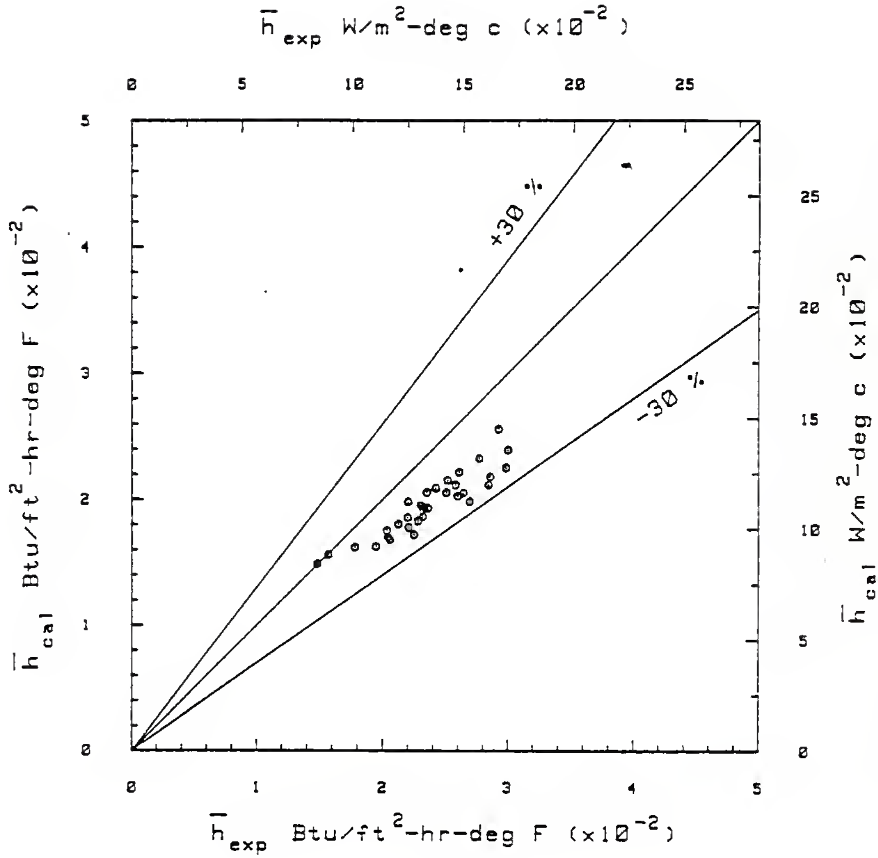

Fig 5.21 Comparison of experimental overall heat transfer coefficients with predictions of the correlation of Luu and Bergles [46], Eq.(5-30), tube 4

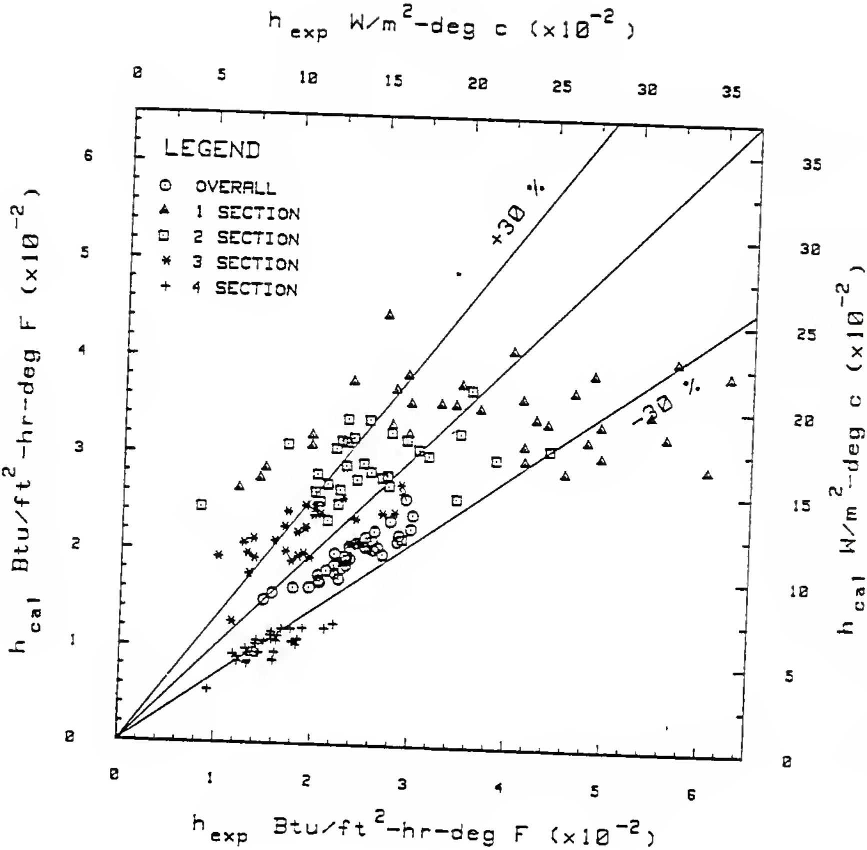

Fig 5.22 Comparison of experimental sectional and overall heat transfer coefficients with predictions of the correlation of Luu and Bergles [46], Eq.(5-30), tube 4

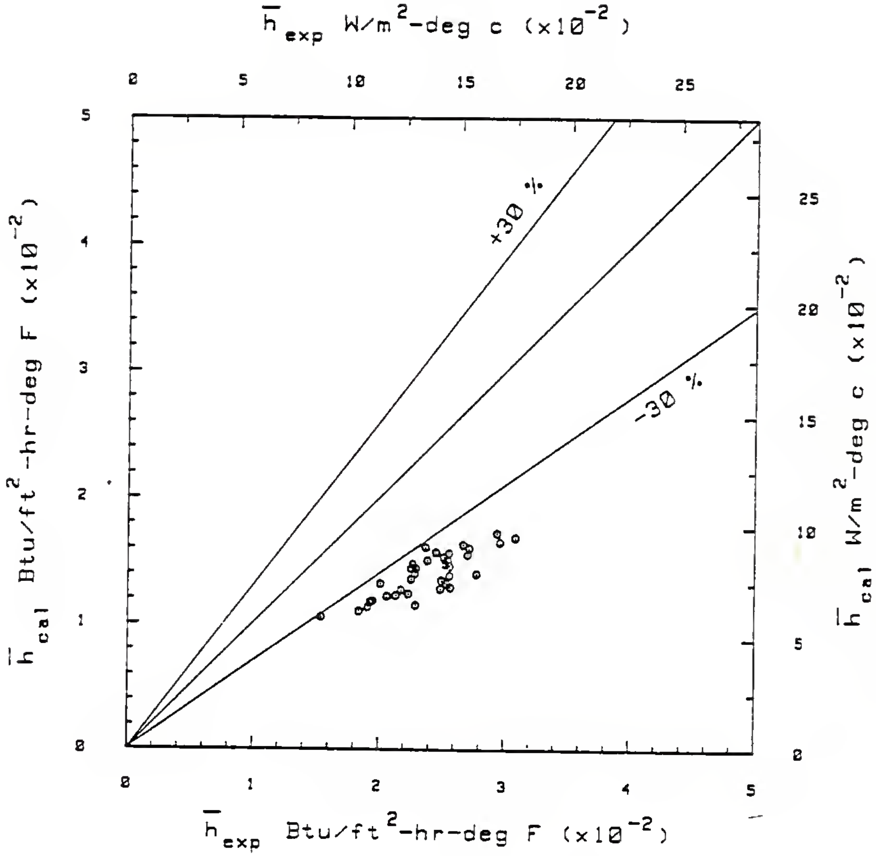

Fig 5.23 Comparison of experimental overall heat transfer coefficients with predictions of the correlation of Luu and Bergles [46], Eq.(5-30), tube 5

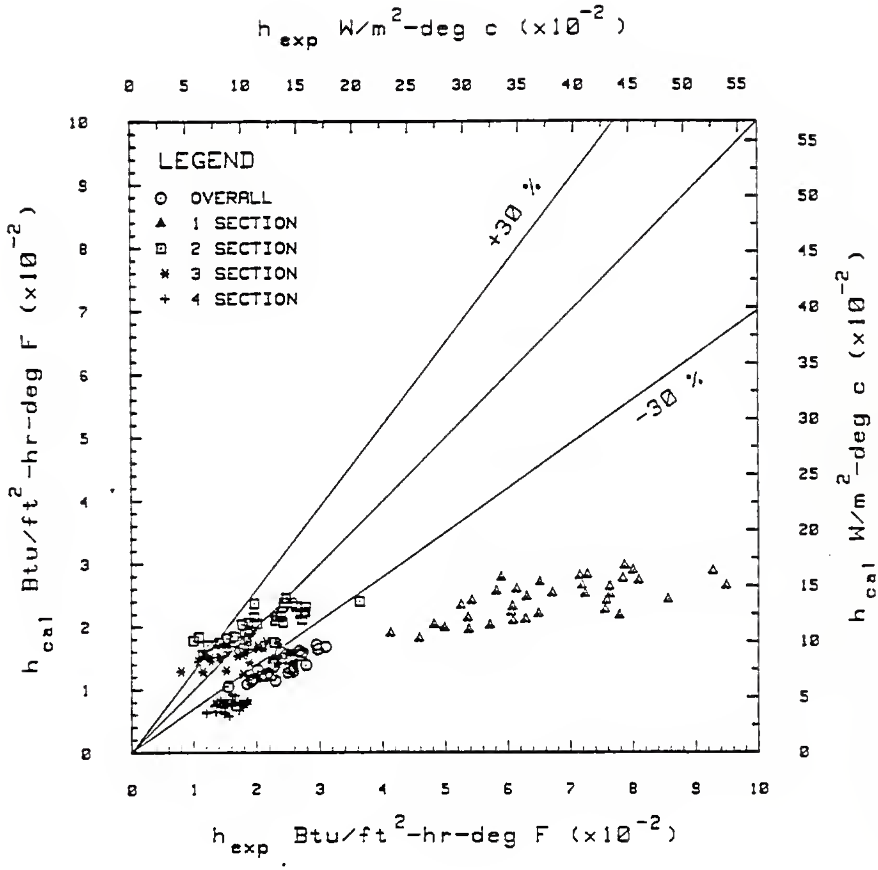

Fig 5.24 Comparison of experimental sectional and overall heat transfer coefficients with predictions of the correlation of Luu and Bergles [46], Eq.(5-30), tube 5

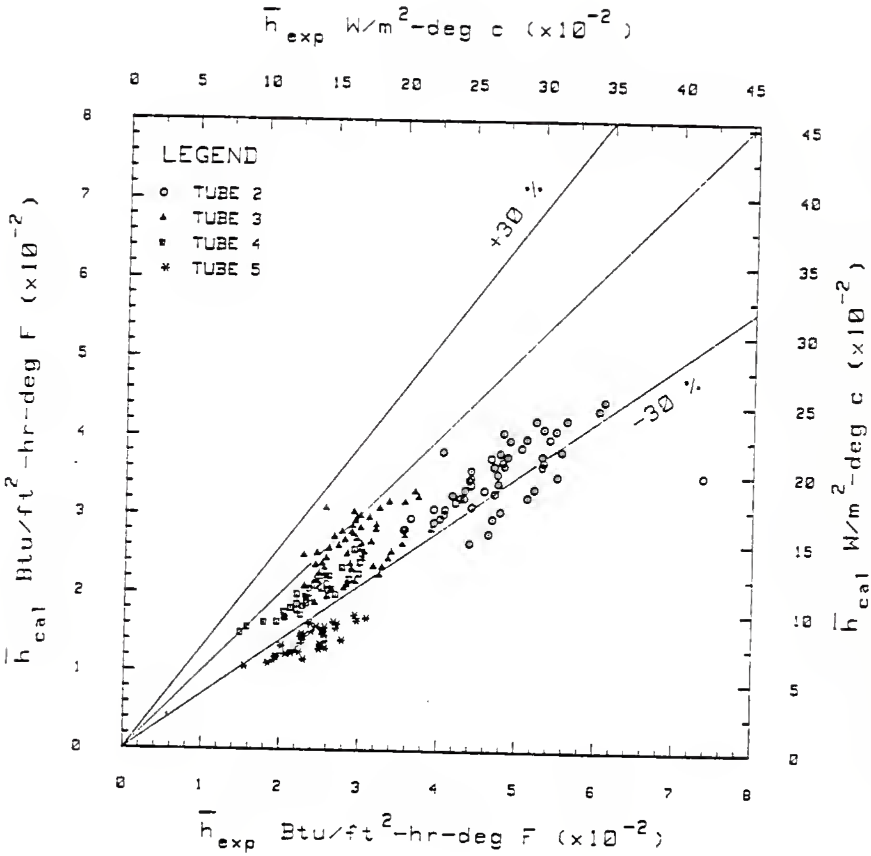

Fig 5.25 Comparison of experimental overall heat transfer coefficients with predictions of the correlation of Luu and Bergles [46], Eq.(5-30), all finned tubes

coefficients of section 1 may be due to the method of their calculation adopted, as discussed earlier. In general Luu and Bergles correlation predicted $\overline{h}$ values fairly well for all the tubes as shown in Fig. 5.25.

Figures 5.26 through 5.34 show comparisons between the experimental heat transfer coefficients with the predictions of the correlation of Said and Azer [47]. The correlation underpredicted the heat transfer coefficients for all the tubes. Figure 5.27, 5.29, 5.31 and 5.33 are plots of predicted $\overline{h}$ versus experimental measurements for tubes 2, 3, 4, and 5, respectively. Figure 5.35 includes comparison of predicted $\overline{h}$ of all the finned tubes versus the experimental values. It is evident from Figs. 5.26, 5.28, 5.30, 5.32, and 5.34 that the correlation underpredicted the $\overline{h}$ values. Figures 5.27, 5.29, 5.31, and 5.33 show comparison between the experimental and the predicted sectional and overall average heat transfer coefficients for all tubes tested. It is interesting to note that although Said and Azer [2,47] developed their correlation from condensing R-113 inside the same internally finned tubes tested in the present study, their correlation underpredicted the measurements for R-11. It should be mentioned that the range of flow rates with which Said [2] conducted his experiments with R-113 was higher than the flow rates covered in the present study.

5.3.2 Pressure Drop

Finned Tube Correlations

Royal and Bergles [43] had a limited success in predicting their pressure drop measurements of condensation of steam inside internally finned tubes, by merely replacing the inside nominal diameter by the hydraulic diameter of the finned tube in the Dukler II [16] frictional pressure

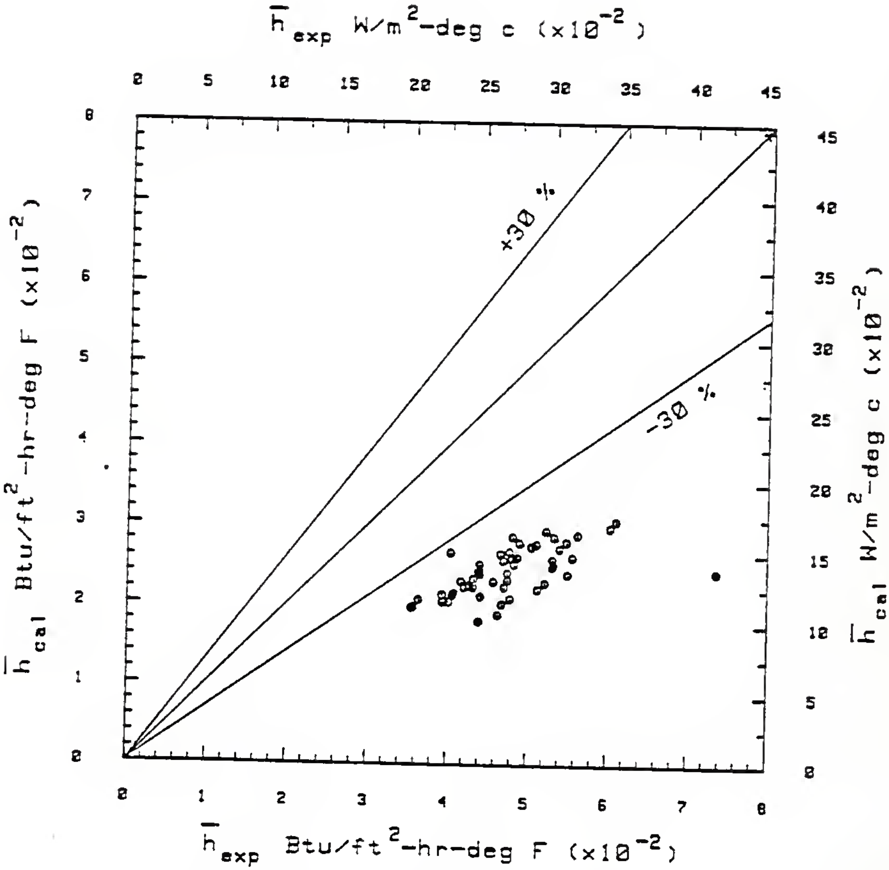

Fig 5.26 Comparison of experimental overall heat transfer coefficients with predictions of the correlation of Said and Azer [47], Eq.(5-32), tube 2

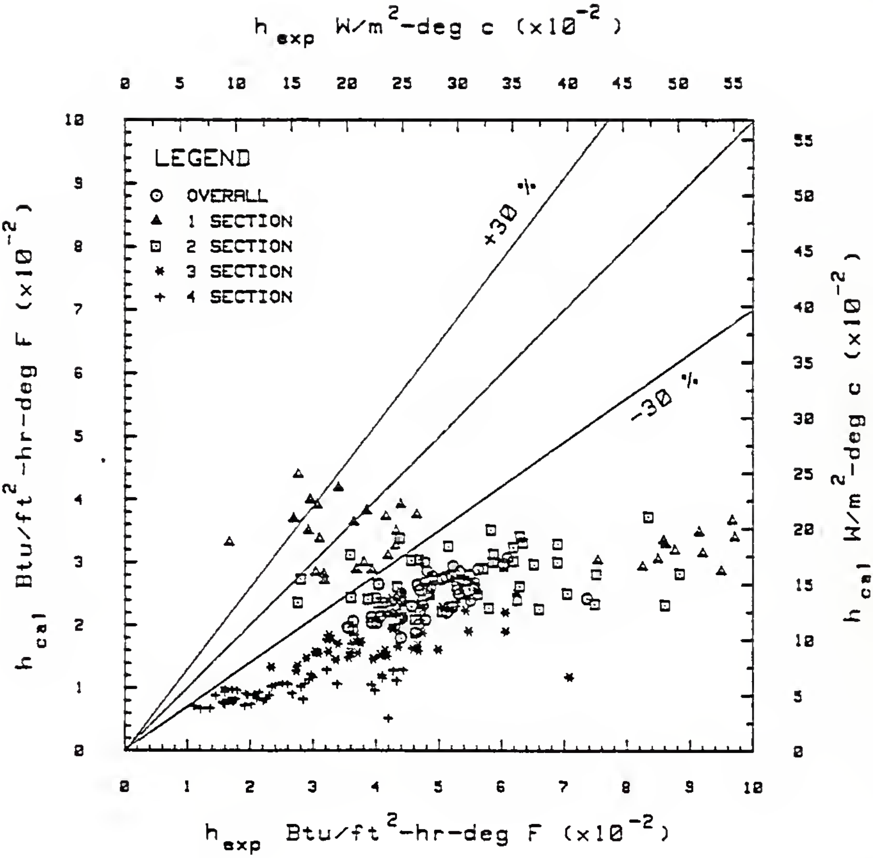

Fig 5.27 Comparison of experimental sectional and overall heat transfer coefficients with predcitions of the correlation of Said and Azer [47], Eq.(5-32), tube 2

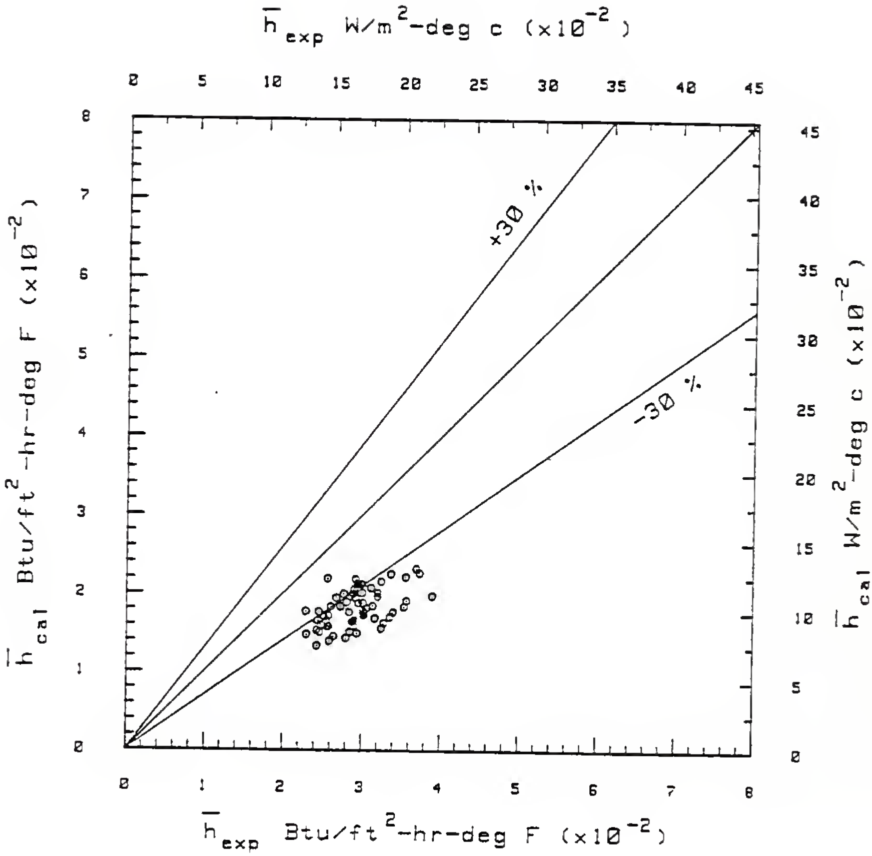

Fig 5.28 Comparison of experimental overall heat transfer coefficients with predictions of the correlation of Said and Azer [47], Eq.(5-32), tube 3

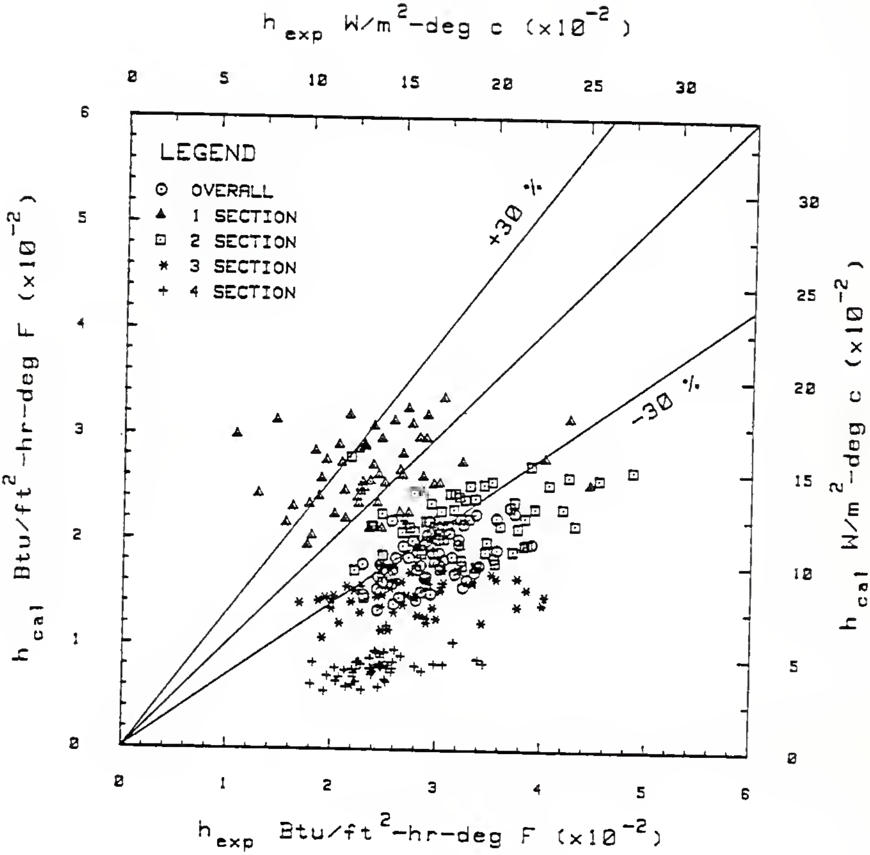

Fig 5.29 Comparison of experimental sectional and overall heat transfer coefficients with predictions of the correlation of Said and Azer [47], Eq.(5-32), tube 3

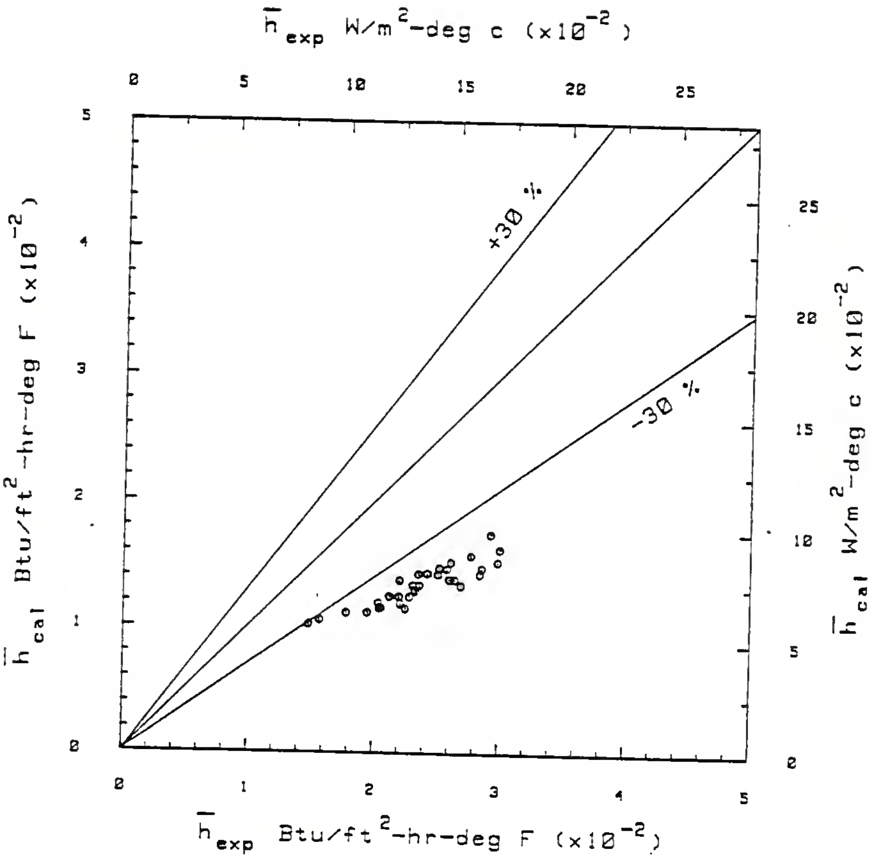

Fig 5.30 Comparison of experimental overall heat transfer coefficients with predictions of the correlation of Said and Azer [47], Eq.(5-32), tube 4

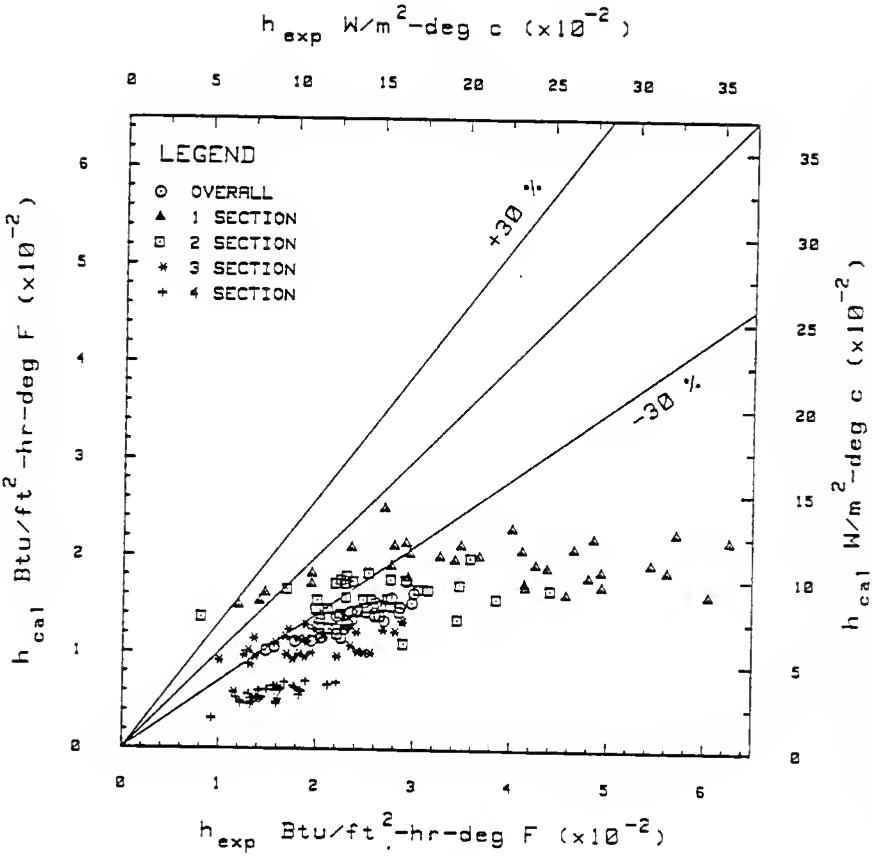

Fig 5.31 Comparison of experimental sectional and overall heat transfer coefficients with predictions of the correlation of Said and Azer [47], Eq.(5-32), tube 4

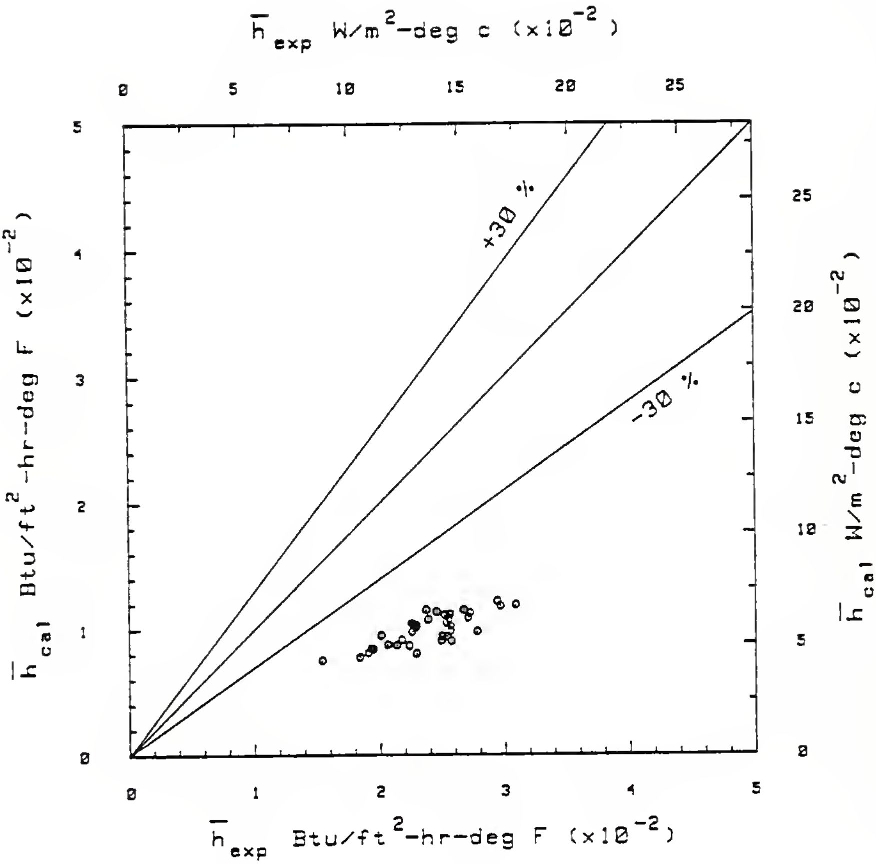

Fig 5.32 Comparison of experimental overall heat transfer coefficients with predictions of the correlation of Said and Azer [47], Eq.(5-32), tube 5

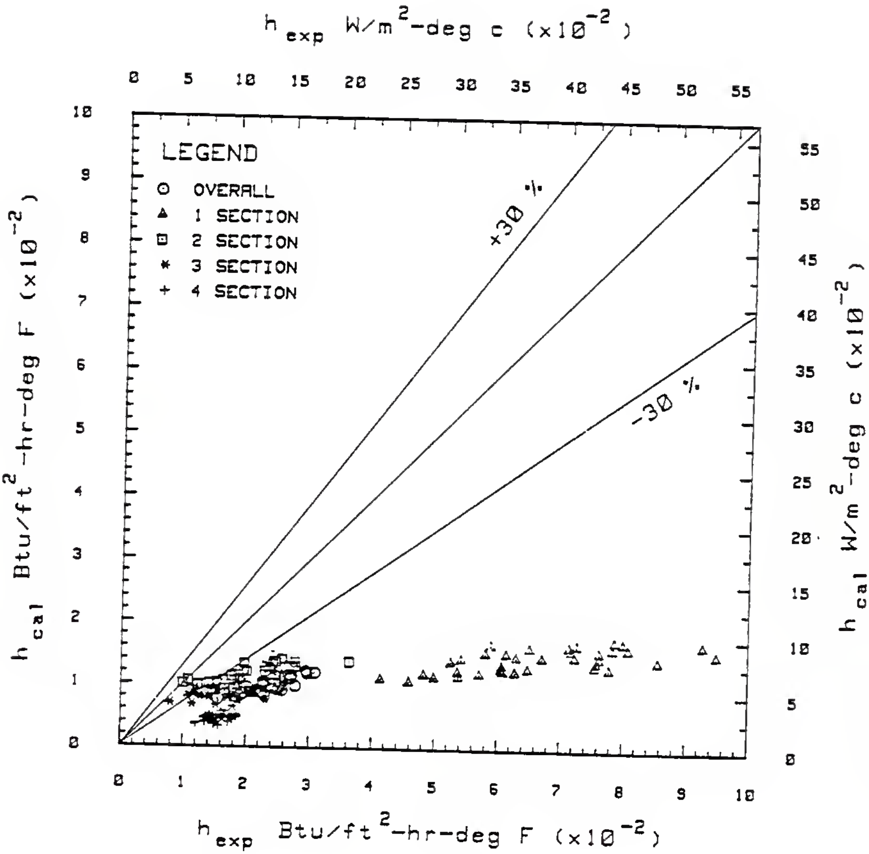

Fig 5.33 Comparison of experimental sectional and overall heat transfer coefficients with predictions of the correlation of Said and Azer [47], Eq.(5-32), tube 5

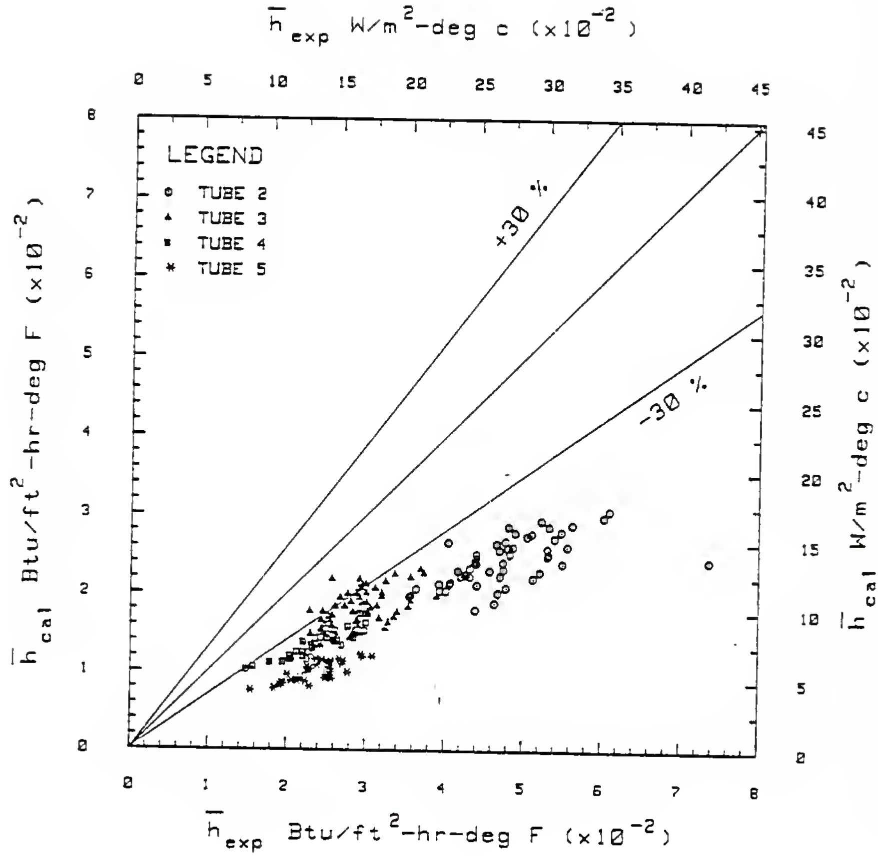

Fig 5.34 Comparison of experimental sectional and overall heat transfer coefficients with predictions of the correlation of Said and Azer [47], Eq.(5-32), all finned tubes

drop correlation along with the homogeneous [18] void fraction correlation. Luu and Bergles [5,45,46] applied the modification of Eq. (5-23) to the friction coefficient in the Dukler II correlation [16]. They were able to correlate reasonably well their pressure drop data of R-113 with the combination of the modified Dukler correlation and the homogeneous model of void fraction. They used also the hydraulic diameter in the Dukler's correlation. Said and Azer [2,47] introduced the following modifier to the friction coefficient of the Dukler correlation.

$$f_{fc} = f_o \, (1 + F_3^{3.37} \, F_4^{0.521}) \qquad (5\text{-}43)$$

f_{fc} replaces f_o in Eq. (5-16) and f_o is calculated by Eq. (5-17). F_4 is a factor given by:

$$F_4 = A_{fa}/A_{fn} = \left(\frac{D_e}{D_i}\right)^2$$

$$= [1 - (4nbt)/(\pi D_i^2 \cos\alpha)] \qquad (5\text{-}44)$$

where

A_{fn} = nominal flow area based on D_i as if fins were not present, $\frac{\pi D_i^2}{4}$, cm^2

F_4 was introduced by Carnavos [28,29] while correlating the pressure drops of single phase flow inside internally finned tubes. Table 5.3 gives the value of F_4 for the tubes tested.

Table 5.3 Computed Values of F_4

F Value	Tube Tested			
	2	3	4	5
F_4	0.9174	0.9442	0.9502	0.9376

Said and Azer retained D_i rather than replacing it by D_h in the Dukler II [16] correlation.

After careful examination of these existing finned tube pressure drop correlations, it was decided to test the following correlations to predict pressure drop in the present study.

A. Lockhart-Martinelli frictional pressure drop [14] correlation with D_h replacing D_i along with a combination of various void fraction correlations tried for smooth tube predictions. Lockhart-Martinelli frictional pressure drop correlation was tried with and without the friction coefficient modification of Eq. (5-23).

B. Dukler II [16] frictional pressure drop correlation with D_h replacing D_i along with a combination of various void fraction correlations. Dukler II friction pressure drop correlation was tried with and without the friction coefficient modification of Eq. (5-23).

C. Dukler II [16] friction pressure drop correlation with friction coefficient f_{fc} calculated from Eq. (5-43) as suggested by Said and Azer [2,47] along with a combination of various void fraction correlations.

The results of these correlations are summarized in the following.

1. Lockhart-Martinelli correlation [14] with any of the void fraction correlations predicted the measured pressure drop fairly well. The introduction of friction coefficient modification of Eq. (5-23) in Lockhart-Martinelli frictional pressure drop correlation overpredicted the measured pressure drop.
2. Dukler II correlation [16] for frictional pressure drop predictions was relatively sensitive to the void fraction correlation. Only Zivi's [21] void fraction correlation with Dukler II correlation for friction, predicted the measured pressure drop well. The

modification of friction coefficient of Eq. (5-23) yielded better predictions with Dukler II correlation.

3. Dukler II [16] frictional pressure correlation with friction coefficient f_{fc} for finned tubes as suggested by Said and Azer [2,47] in combination with Zivi void fraction correlation predicted the measured pressure drop of tube 3 within ±40% from experimental values, but overpredicted the pressure drop for tube 2.

4. As in smooth tube, momentum pressure drop was insensitive to the void fraction correlation used.

Figures 5.35, 5.36, and 5.37 show comparisons between the predictions of the Lockhart-Martinelli/Zivi void and experimental measurements. The results show that 58% of predicted values for tube 2, and all the predicted values for tube 3 are within ±40% from experimental pressure drop measurements. Figure 5.37 is a plot of the predicted values versus experimental measurements for tubes 2 and 3. Figures 5.38, 5.39, and 5.40 show comparisons between modified Dukler II/Zivi void correlation and experimental pressure drops. The results show that 79% of data points of tube 2 and 94% of data points of tube 3 agree within ±40% with the predicted values. It is clear from Fig. 5.40 that the modified Dukler II/Zivi void correlation predicted the finned tube condensation pressure drop best. Figures 5.41, 5.42, and 5.43 compares predicted pressure drops of Dukler II/Zivi with Said and Azer [2,47] friction coefficient of Eq. (5-43), and experimental measurements. The results show that the correlation predicted pressure drops of tube 3 well, but overpredicted the pressure drop of tube 2. Figure 5.44 shows comparison between the predictions and experimental measurements for tubes 2 and 3.

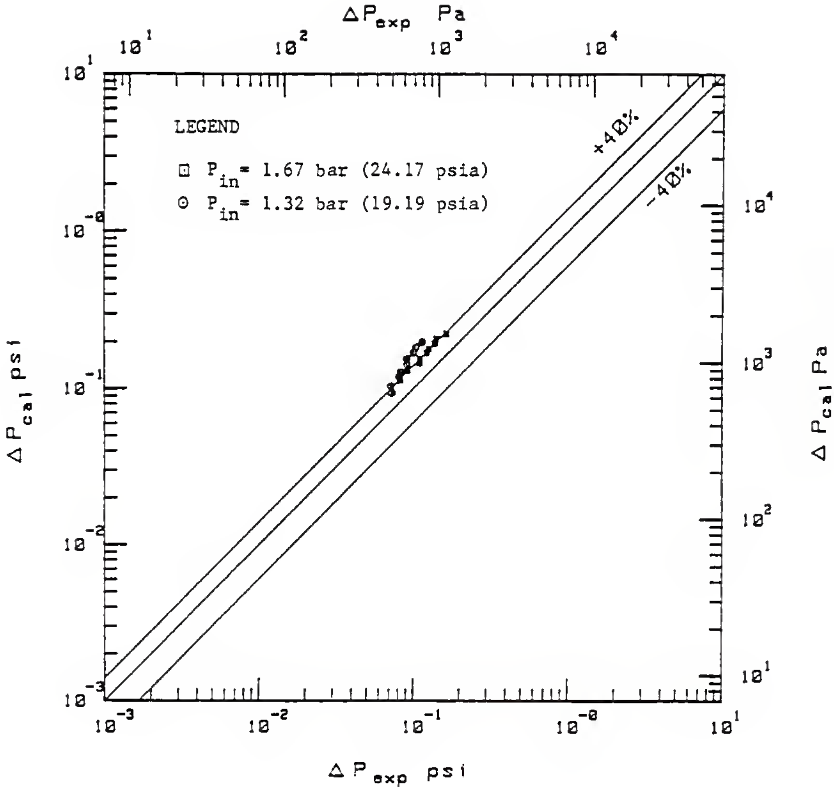

Fig 5.35 Comparison between experimental pressure drop and predictions of the combination of Lockhart-Martinelli [14] and Zivi [21] void fraction correlations, tube 2

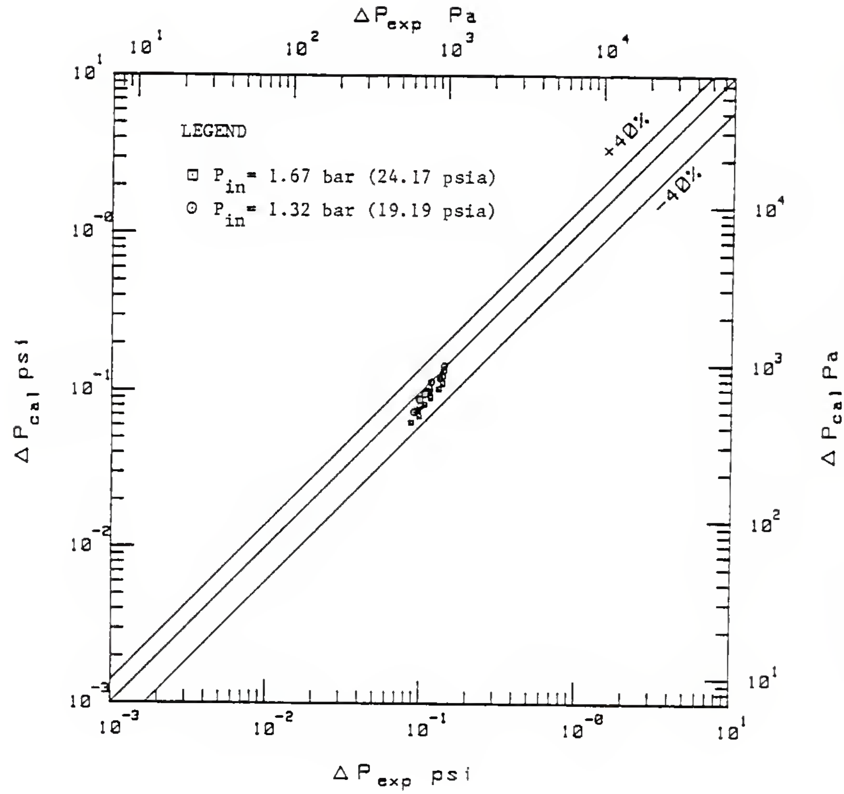

Fig 5.36 Comparison between experimental pressure drop and predictions of the combination of Lockhart-Martinelli [14] and Zivi [21] void fraction correlations, tube 3

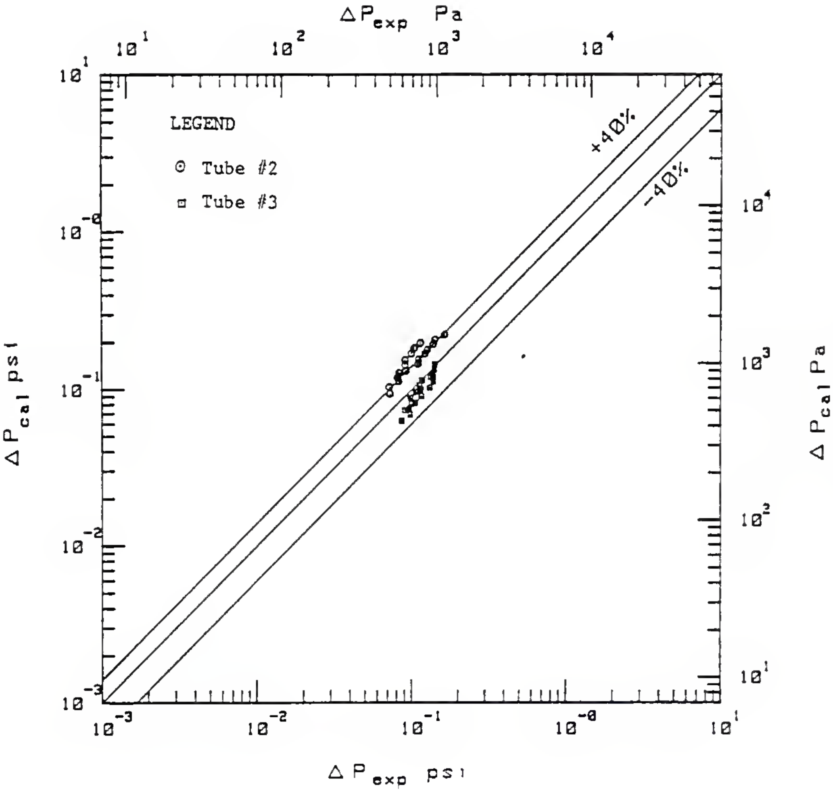

Fig 5.37 Comparison between experimental pressure drop and predictions of the combination of Lockhart-Martinelli [14] and Zivi [21] void fraction correlations, tube 2 and 3

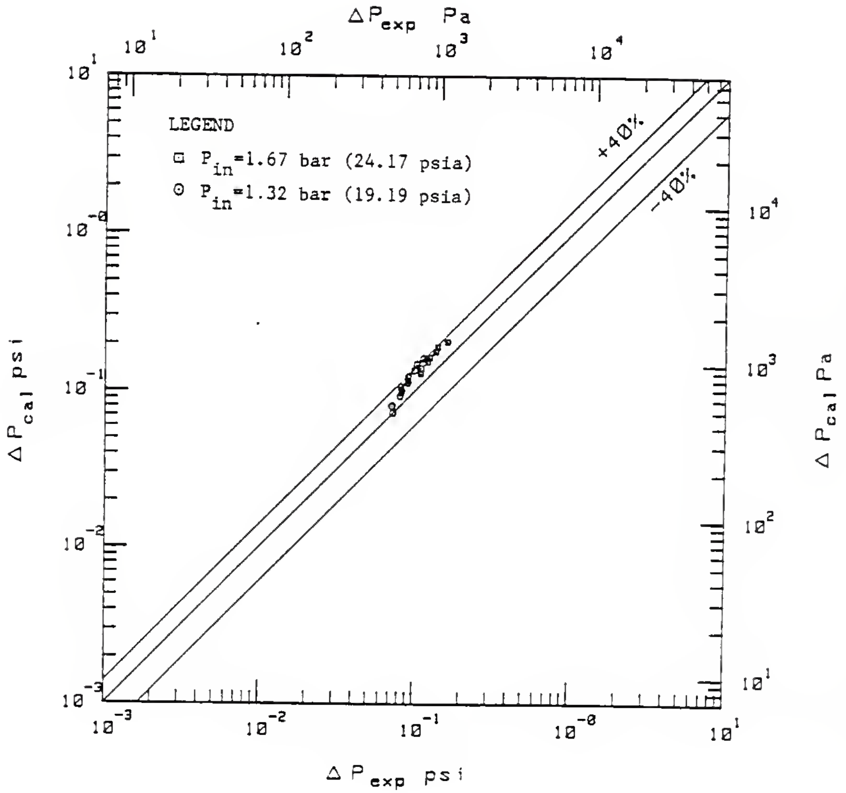

Fig 5.38 Comparison between experimental pressure drop and predictions of the combination of Dukler II [16] correlation, modified by Eq.(5-23) as suggested by Luu and Bergles, and Zivi [21] void fraction, tube 2

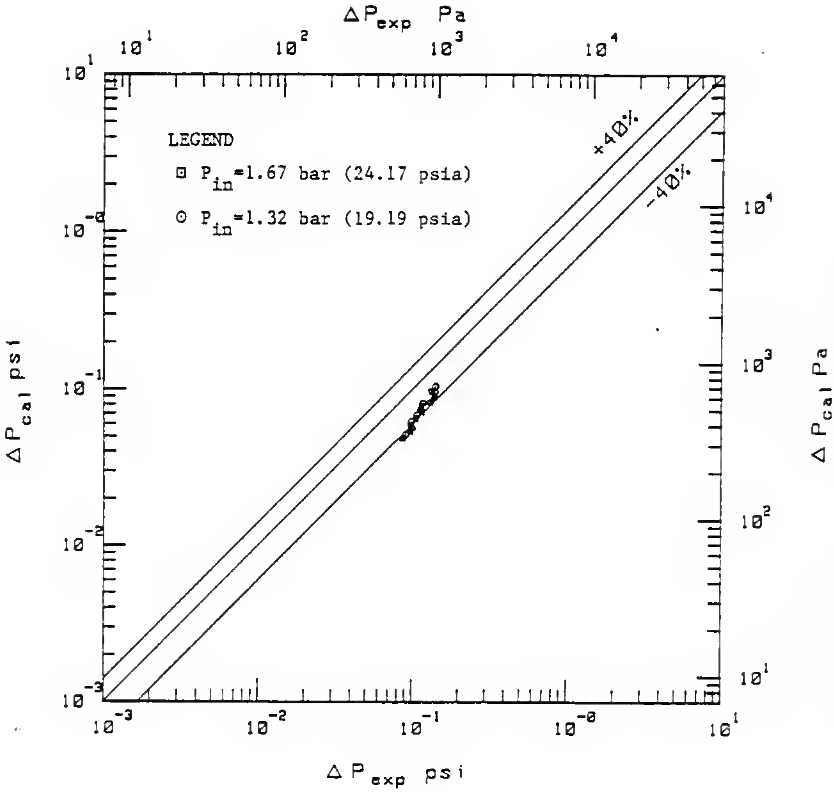

Fig 5.39 Comparison between experimental pressure drop and predictions of the combination of Dukler II [16] correlation, modified by Eq.(5-23),as suggested by Luu and Bergles, and Zivi [21] void fraction, tube 3

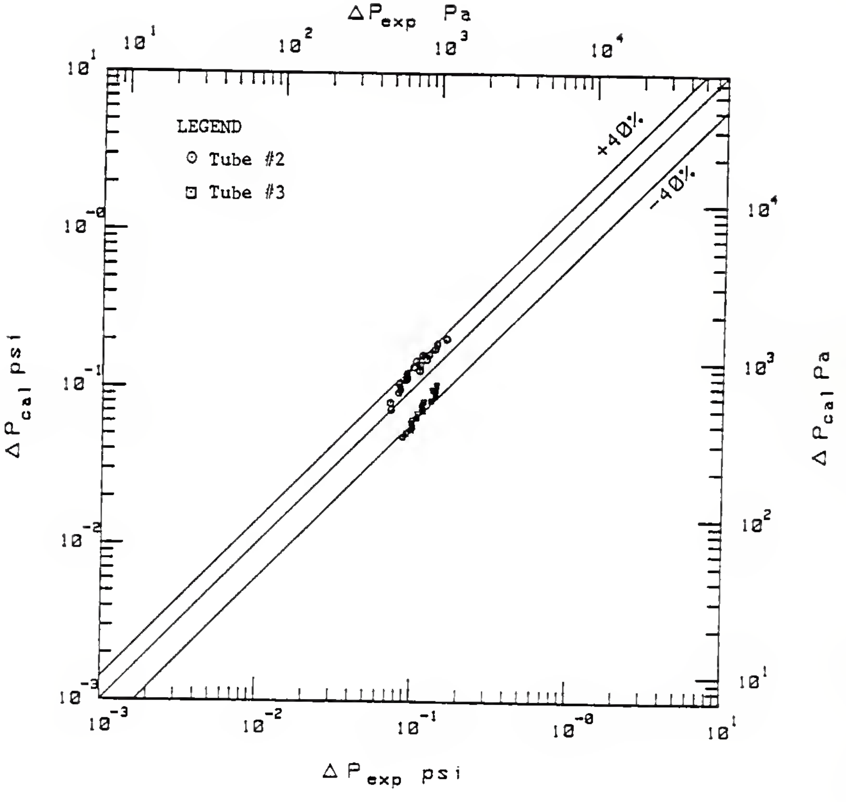

Fig 5.40 Comparison between experimental pressure drop and predictions of the combination of Dukler II [16] correlation, modified by Eq.(5-23), as suggested by Luu and Bergles, and Zivi [21] void fraction, tubes 2 and 3

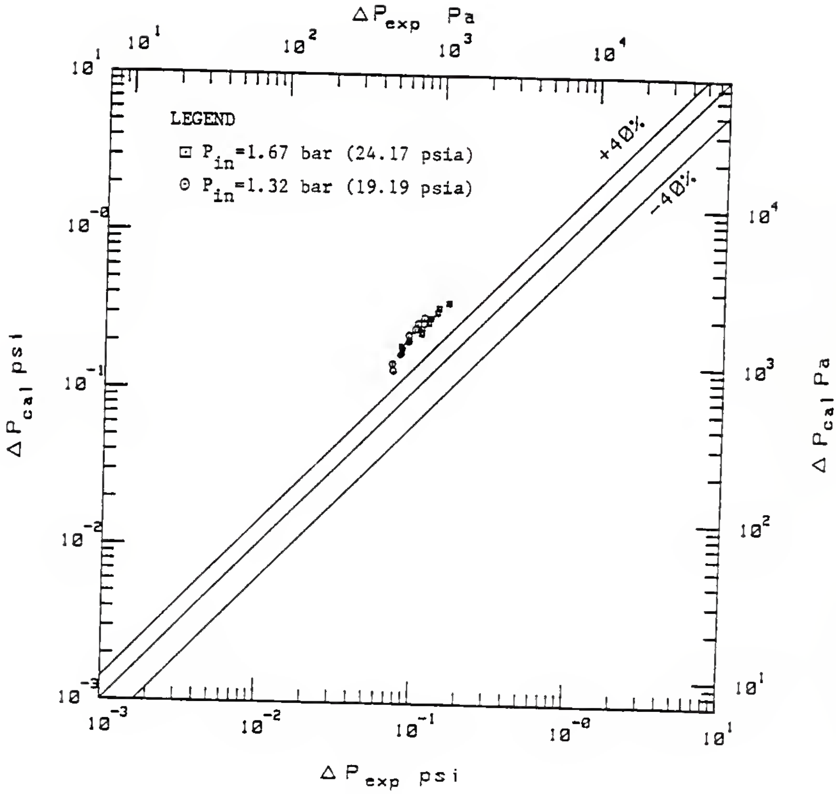

Fig 5.41 Comparison between experimental pressure drop and predictions of the combination of Dukler II [16] correlation, modified by Eq.(5-43), as suggested by Said and Azer, and Zivi [21] void fraction, tube 2

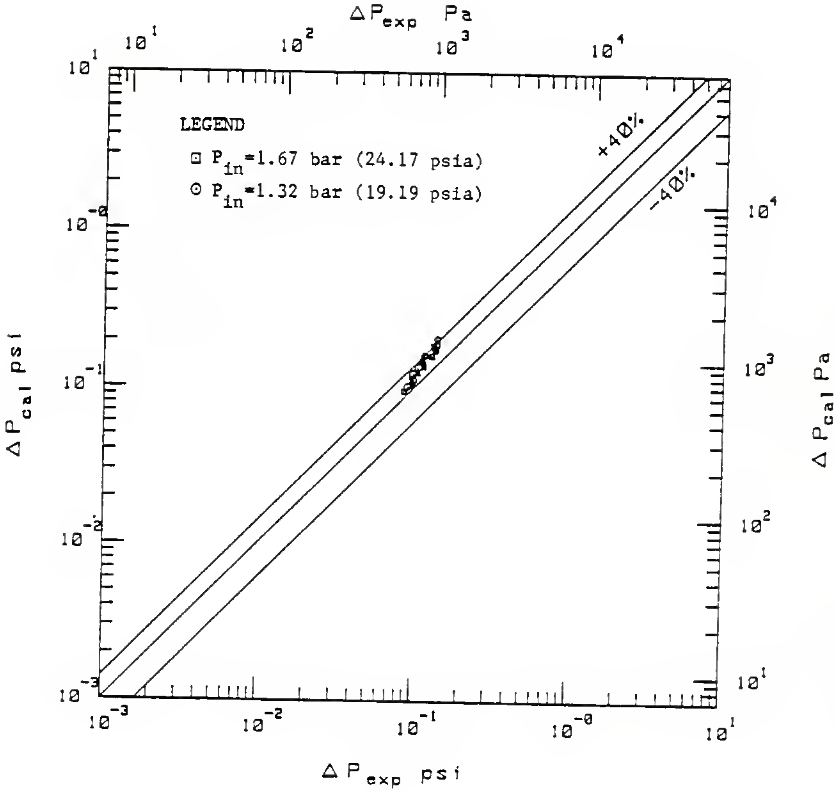

Fig 5.42 Comparison between experimental pressure drop and predictions of the combination of Dukler II [16] correlation, modified by Eq.(5-43), as suggested by Said and Azer, and Zivi [21] void fraction, tube 3

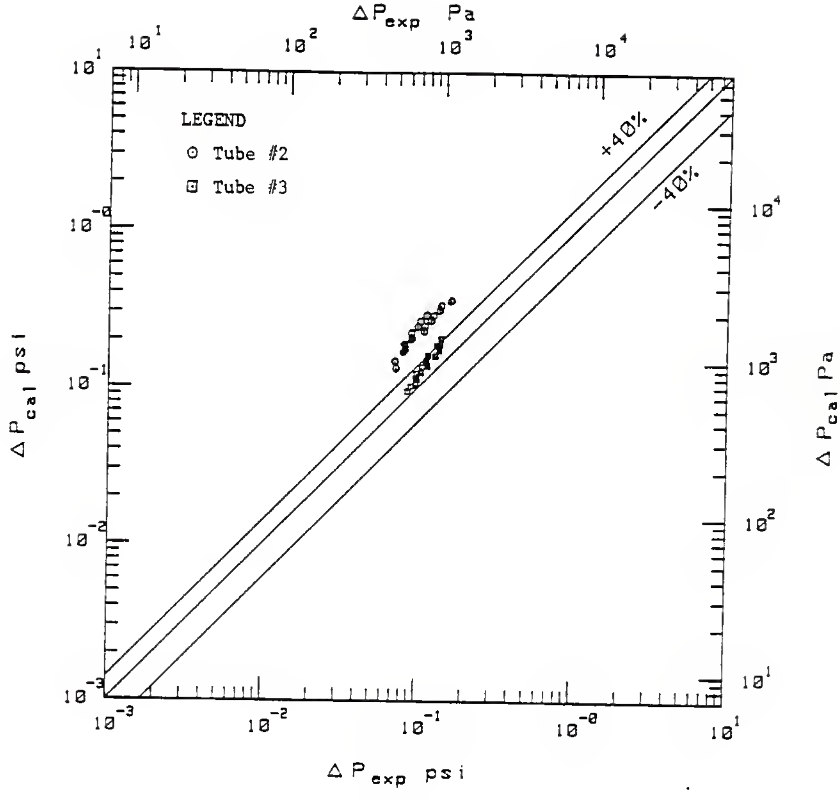

Fig 5.43 Comparison between experimental pressure drop and predictions of the combination of Dukler II [16] correlation, modified by Eq.(5-43), as suggested by Said and Azer, and Zivi [21] void fraction, tube 2 and 3

Chapter VI

PERFORMANCE EVALUATION

6.1 Introduction

The primary objective of this part of the study was to evaluate the performance of the internally finned tubes in agumenting in-tube condensation of R-11. For meaningful performance evaluation, the increase in heat transfer coefficients with internally finned tubes should be considered along with the penalty of increased pressure drop. In order to compare the increase in heat transfer coefficients and pressure drops, the overall heat transfer coefficients and pressure drops versus mass flux were combined in composite plots for same inlet pressures, as shown in Figures 6.1, through 6.5, for all the tubes tested. Figures 6.1, 6.2 and 6.3 show plots of the regression equations of the experimental overall average heat transfer coefficients $\overline{h}$ versus mass flux G for all tubes at the three different nominal pressures tested. The best performer among the finned tubes was tube 2 followed by tube 3. Due to the limitation of the test facility, it was not possible to cover the same range of mass flux for all tubes. As the inside diameter of the test condenser increased, the range of mass flux decreased as indicated in Figs. 6.1 through 6.5. On a nominal area basis, tubes 2 and 3 enhanced the heat transfer, on the average, by 55% and 13% respectively. Tube 5 performed better than tube 4. Since the range of mass flux for tubes 4 and 5 were less than tube 1, no direct comparison could be made. Figures 6.4 and 6.5 show plots of the regression lines of the experimental pressure drop versus the mass flux for tubes 1, 2, and 3. The results show that tube 3 had the highest pressure drop followed by tube 2. So, it is

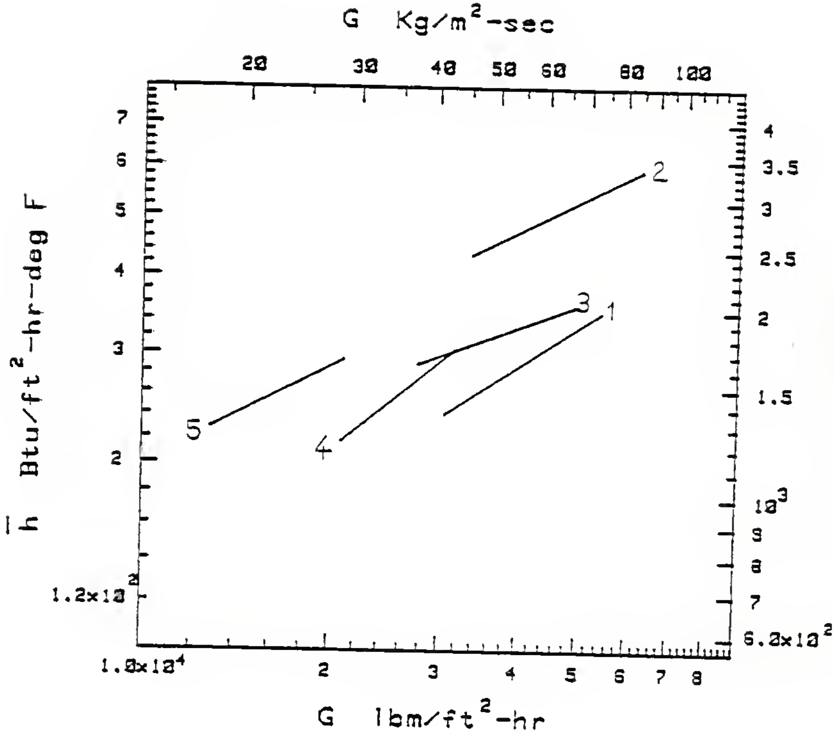

Fig 6.1 Experimental overall heat transfer coefficient versus mass flux G, for all tubes, P_{in}=1.32 bar (19.19 psia)

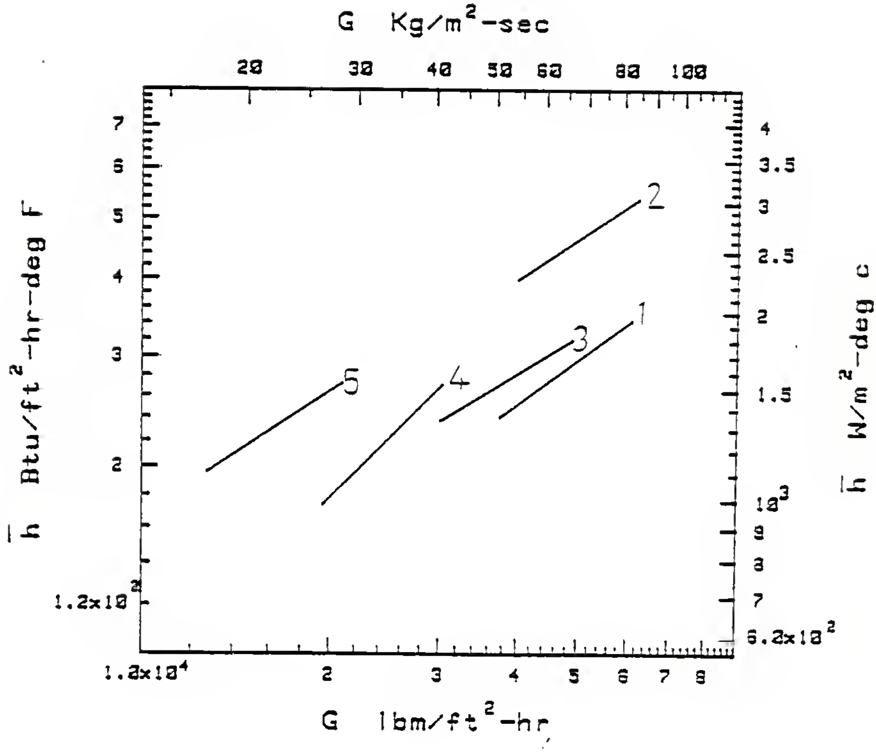

Fig 6.2 Experimental overall heat transfer coefficient versus mass flux G, for all tubes, P_{in}=1.47 bar (21.29 psia)

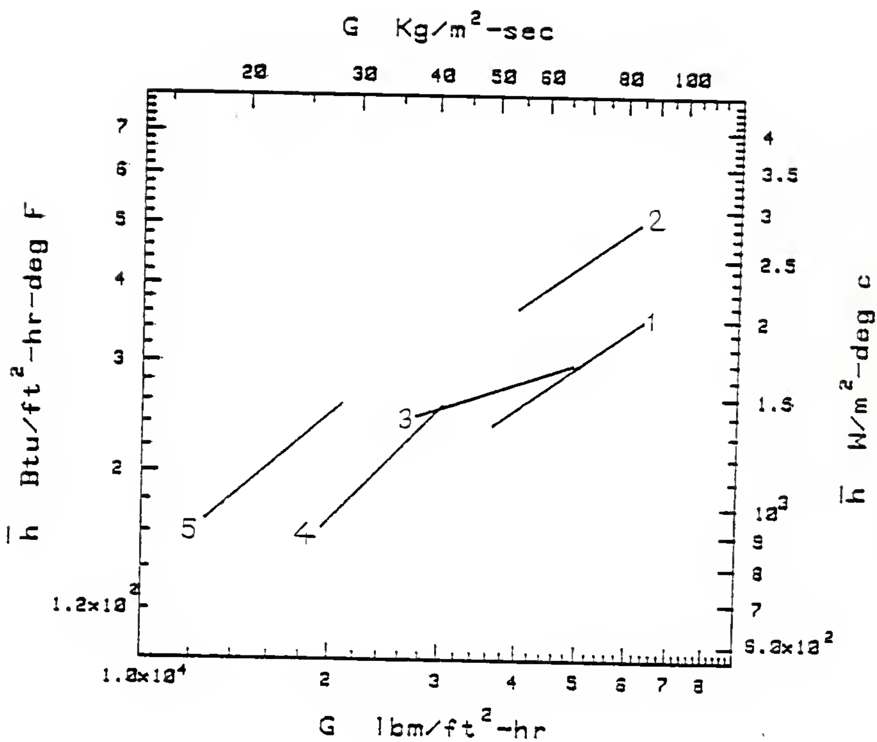

Fig 6.3 Experimental overall heat transfer coefficient versus mass flux G, for all tubes, P_{in}=1.67 bar (24.17 psia)

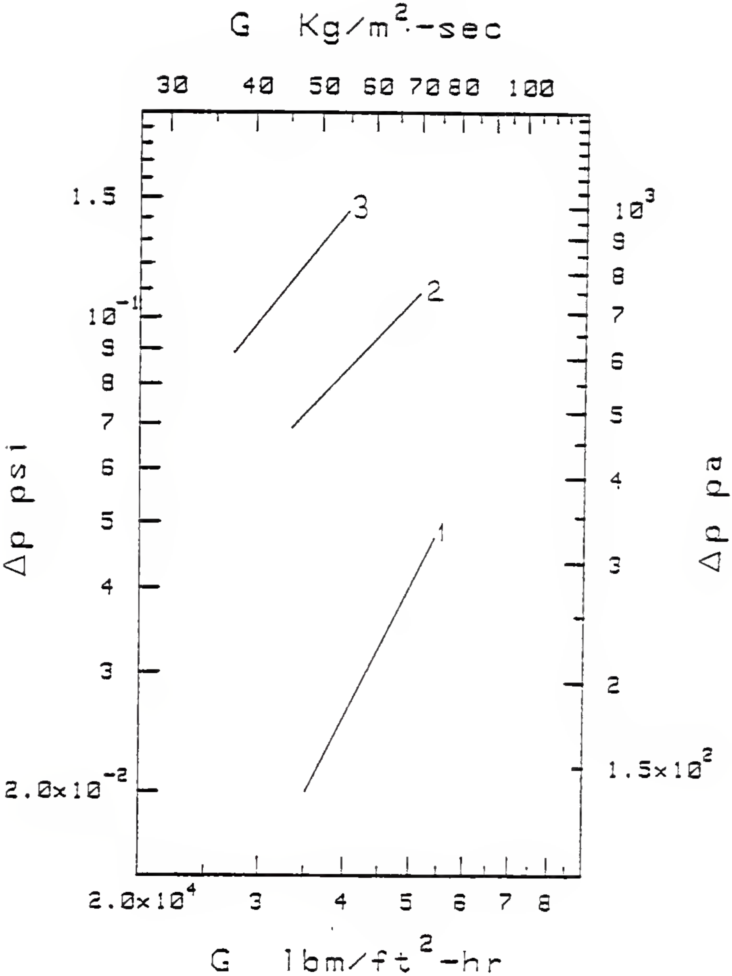

Fig 6.4 Experimental overall pressure drop versus mass flux G, for tubes 1, 2 and 3, P_{in} = 1.32 bar (19.19 psia)

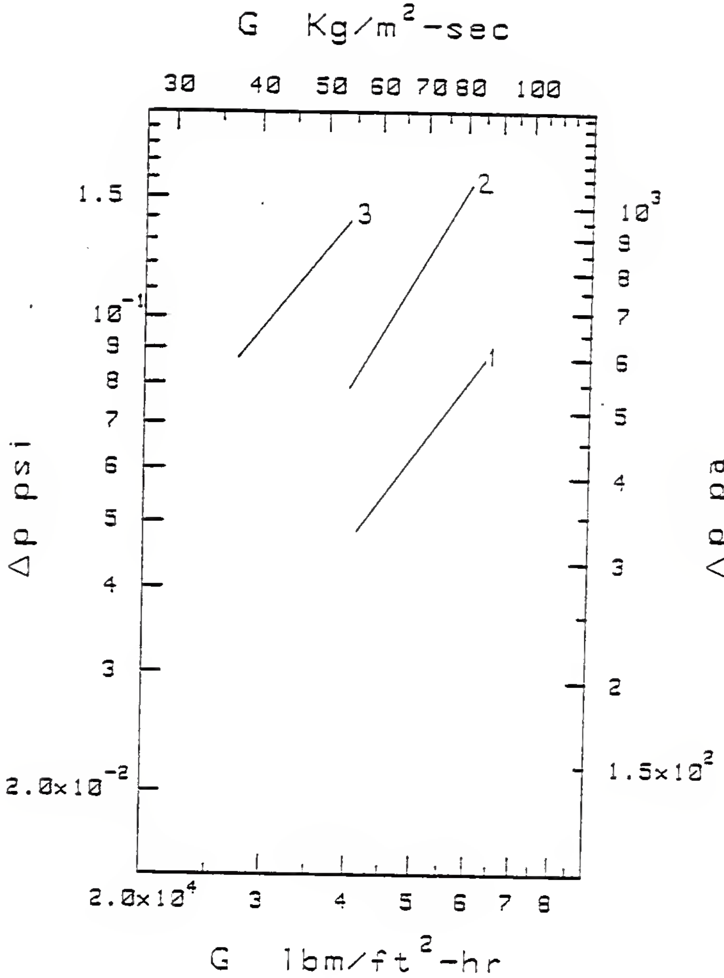

Fig 6.5 Experimental overall pressure drop versus mass flux G, for tubes 1, 2 and 3, P_{in} = 1.67 bar (24.17 psia)

obvious that heat transfer was enhanced with the penalty of increasing the pressure drop.

6.2 Performance Indices

There have been numerous attempts to develop indices to evaluate the performance of augmented surfaces. Bergles et al. [51,52] suggested nine performance indices for augmentation of heat transfer in single phase flow. They listed the objectives of augmentation as the increase in heat transfer, reduction in pumping power, and reduction in size of equipment. They also listed the controlling parameters with which these objectives can be achieved such as basic geometry, flow rate, pressure drops, pumping power, and heat duty. In developing the indices, they broadly divided the performance indices into two basic groups. In the first group, the performance indices were directed towards enhancement of heat transfer for existing heat exchangers. Therefore, the basic geometry was fixed. In the second group, the performance indices were directed towards heat transfer augmentation in the design of new heat exchangers with the objective of reducing their size.

Due to the difficulty of imposing some of the constraints on the performance indices, Royal [4] used two of these indices to evaluate the performance of internally finned tubes and tubes with twisted tapes during augmentation of condensation heat transfer of steam. These indices were the condenser size reduction index R_h and the pressure drop index $R_{\Delta p}$, and they are given by

$$R_h = (A_{aug}/A_{sm}) = (h_{sm}/h_{aug}) \tag{6-1}$$

and

$$R_{\Delta p} = (\Delta P_{aug}/\Delta P_{sm}) \tag{6-2}$$

In the above indices it was assumed that the external resistance of condensing surface is negligible or the condensing side thermal resistance controls the heat transfer. Also, R_h and $R_{\Delta p}$ were evaluated under the constraints of fixed heat duty, nominal diameter, and constant temperature difference.

Luu [5] used the same indices of Eq. (6-1) and Eq. (6-2) in evaluating the performance of internally finned tubes and tubes with twisted tape inserts in augmenting in-tube condensation of R-113.

In the present study, it was estimated that the outside heat transfer coefficients were of the same order of magnitude of the inside heat transfer coefficient. Hence the assumption of zero external resistance is unrealistic and the use of performance indices of Eq. (6-1) and Eq. (6-2) with negligible external resistance could not be justified. Said [2] arrived at the same conclusion while evaluating the performance of the internally finned tubes with R-113 as the condensing fluid.

Azer et al. [53] and Lin [54] used the ratio of the pumping power to the rate of heat transfer $\mathbb{P}/Q$ as an evaluating index in determining the performance of static in-line mixers while augmenting the condensation heat transfer. Said [2] also used the above ratio as a performance index in determining the performance of internally finned tubes and tubes with twisted tape inserts. The index ($\mathbb{P}/Q$) was evaluated under the constraints of fixed geometry, same mass flow rate of condensing fluid, and same temperature and mass flow rate of the coolant. The pumping power was obtained from the product of the volume flow rate of the liquid at the circulating pump and the pressure drop across the test condenser. The rate of heat transfer was evaluated from the temperature rise and flow rate of the coolant. The same index was used in the present study.

Only the smooth tube, tube 1, and the straight finned tube, tube 2, satisfied the constraint of fixed geometry, which required that the length and the inside diameter of the tube, augmented or unaugmented, be the same. Therefore, only tubes 1 and 2 were evaluated.

The constraints of same temperature and flow rate were replaced by the constraints that the inlet pressure P_{in} and the flow rate of condensing fluid were the same. The constraints of the constant P_{in} and mass flow rate imply a constant heat load when condensation is complete with the following assumptions.

1. Pressure change during condensation has negligible effect on the latent heat.
2. The effect of inlet superheat and exit subcooling on total energy transfer is negligible.

After careful examination, experimental runs of tube 1 and tube 2 with the same mass flow rate and the same inlet pressure were selected for the evaluation of performance of tube 2. Figures 6.6 and 6.7 show plots of $\mathbb{P}/Q$ versus Re for tubes 1 and 2 at two nominal inlet pressures, 1.32 bar (19.19 psia) and 1.67 bar (24.17 psia), respectively. Re_L was based on the liquid flowing alone, the inside diameter D_i, and the dynamic viscosity of the saturated liquid. The lower the index, the lower the power demand per unit heat transfer. It is clear from Figs. 6.6 and 6.7 that power demand for tube 2 was more than that of tube 1. It is obvious that enhancement of heat transfer was accompanied by an increase in pressure drop.

Azer and Shivakumar [55] used another performance index to evaluate performance of internally finned tubes during saturated boiling heat transfer. They defined the performance index r as the ratio of heat trans-

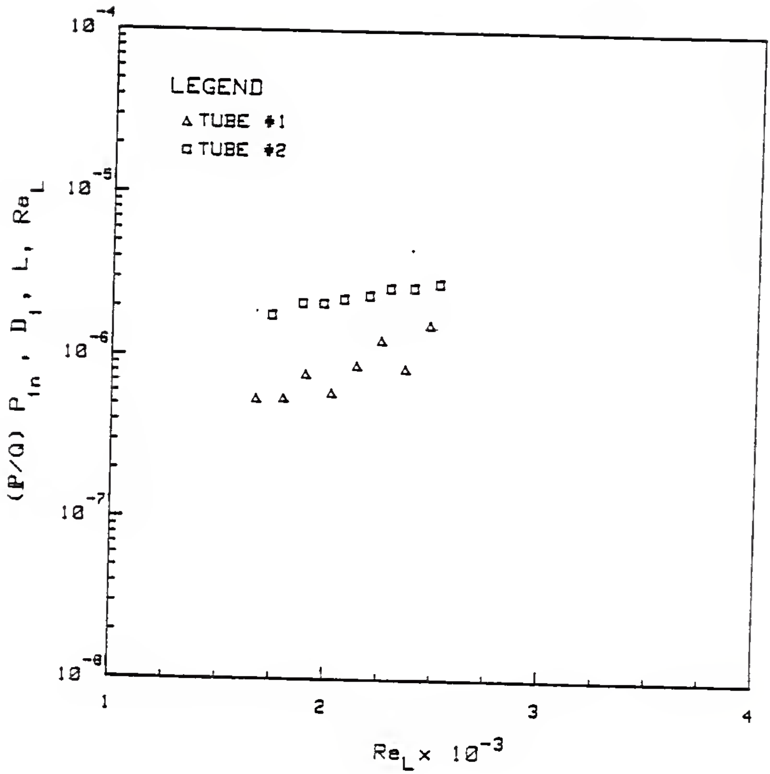

Fig 6.6 Pumping power per unit heat transfer rate versus Reynolds Number at P_{in} = 1.32 bar (19.19 psia)

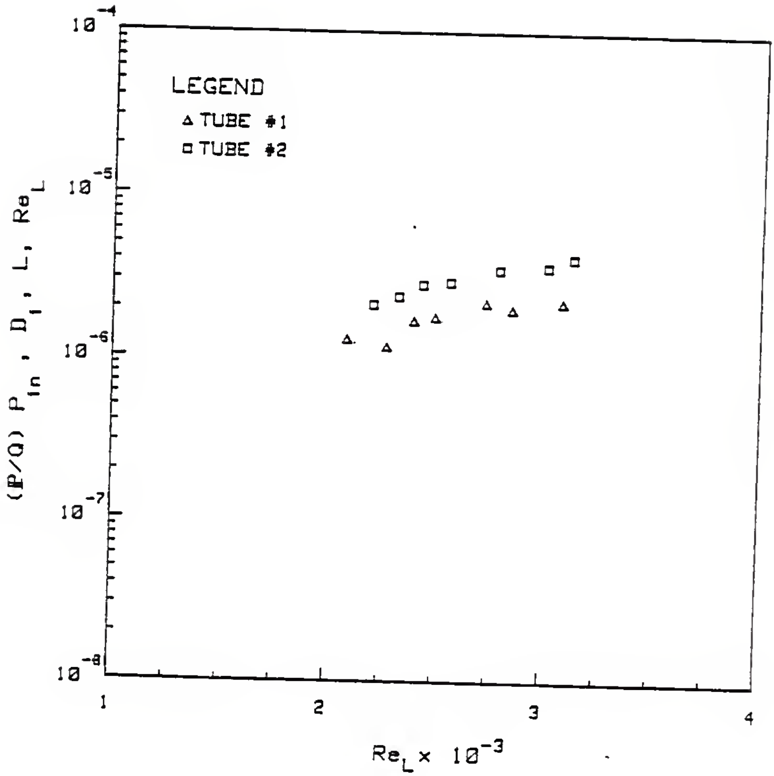

Fig 6.7 Pumping power per unit heat transfer rate versus Reynolds Number at P_{in}=1.67 bar (24.17 psia)

fer enhancement to the ratio of pressure drop increase. This ratio r was expressed by

$$r = \frac{(\bar{h})_{aug} \; / \; (\bar{h})_{sm}}{(\Delta p)_{aug} \; / \; (\Delta p)_{sm}} \tag{6-3}$$

This index was calculated at same constraints of Eq. (6-2). The higher the ratio r, the better the performance. Figures 6.8 and 6.9 show plots of r given by Eq. (6-3) versus Reynolds number at two nominal inlet pressures, 1.32 bar (19.19 psia) and 1.67 bar (24.17 psia), respectively. The plots indicate that the values of r are less than 1. The results also reinforce the conclusions drawn from Figs. 6.6, and 6.7, i.e., the enhancement in heat transfer was accompanied by an increase in the pressure drop. However, the trend in the data in Figs. 6.8 and 6.9 indicate that r increases with the increase of Re_L and it could become higher than 1. Because of the limitation of the test facility this observation could not be established experimentally.

Besides the objectives of increasing the heat transfer, reducing the pumping power, and reducing the heat transfer area, other important factors like initial cost, maintenance cost, etc., are to be considered by designer. The choice of an augmented versus a smooth tube for a given application must be based on the compromise between the improvements in heat transfer and the penalty of increasing the pressure drop.

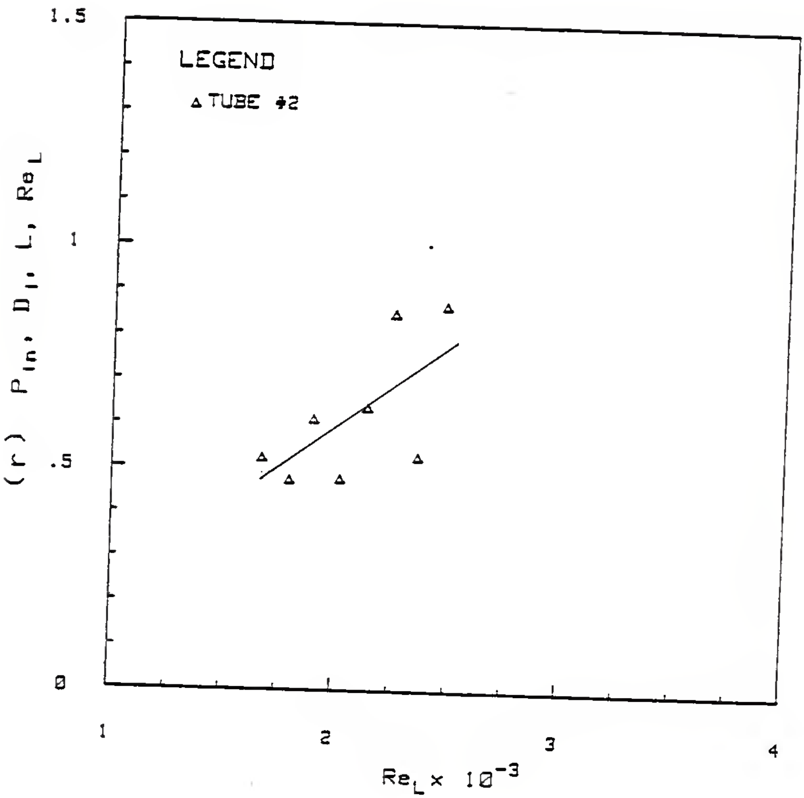

Fig. 6.8 The ratio r of heat transfer enhancement to the pressure drop increase versus Reynolds Number at P_{in}=1.32 bar (19.19 psia)

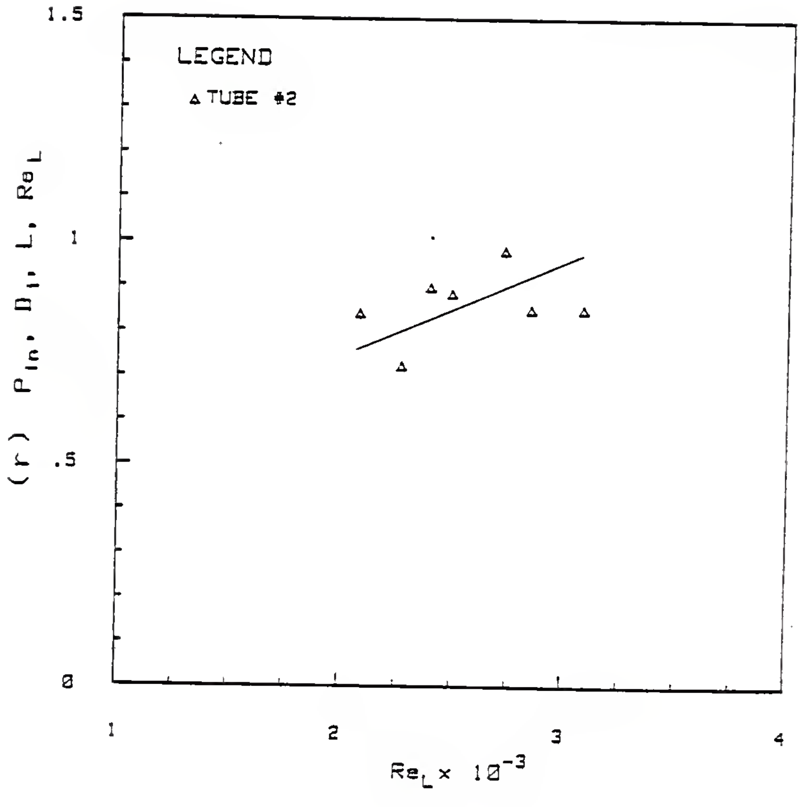

Fig. 6.9 The ratio r of heat transfer enhancement to the pressure drop increase versus Reynolds Number at P_{in}=1.67 bar (24.17 psia)

Chapter VII

SUMMARY, CONCLUSIONS, AND RECOMMENDATIONS

Heat transfer and pressure drop data were taken during condensation of R-11 inside five horizontal tubes. One tube was smooth and four were internally finned with different geometric parameters. The heat transfer and pressure drop data were compared with existing smooth tube and finned tube correlations.

The results are summarized in the following.

1. All the internally finned tubes tested yielded higher heat transfer coefficients than the smooth tube results. Over the mass flux range tested, an enhancement in the heat transfer coefficients as high as 55% over the smooth tube was obtained, on a nominal area basis. The heat transfer enhancement was accompanied by an increase in the pressure drop.
2. The best predictor of the sectional and overall average heat transfer coefficients of the smooth tube was the correlations of Akers et al. [6], Eq. (5-1).
3. The best predictors of the smooth tube and internally finned tube pressure drop were the frictional correlation of Lockhart-Martinelli [14], and Dukler II [16], combined with the void fraction correlation of Zivi [21].
4. The best predictor of the sectional and overall average heat transfer coefficients of the internally finned tubes was the correlation of Luu and Bergles [5,45,46], Eq. (5-30).

5. The pumping power per unit heat transfer subject to the constraints of fixed geometry, same inlet pressure, and flow rate, was used to evaluate the performance of the internally finned tubes. The ratio of pumping power per unit heat transfer for the internally finned tube to the same ratio of the smooth tube was greater than one. This indicated that the penalty of increased pressure drop was greater than the benefit of enhancement of the heat transfer coefficients for the internally finned tube. A similar performance index r, a ratio of heat transfer enhancement to the pressure drop increase yielded values less than one for internally finned tube. The trend of the variation of r with the mass flow rate suggested that a ratio greater than 1 is possible. This observation could not be verified experimentally because of the limitations of the test facility.

Recommendation for Future Studies

1. As pointed out earlier, before commercial usage of the existing heat transfer and pressure drop design correlations, additional experimental data for condensation inside internally finned tubes with different geometric parameters, and for different condensing fluids at wide flow ranges are needed. What is currently available can be considered limited. Also, the experimentation of future studies should be aimed at optimizing the fin geometry to obtain best heat transfer and pressure drop results.
2. More reliable pressure drop correlations need to be developed for condensation inside smooth tubes under different flow patterns. Once such correlations are established, better pressure drop correlations for internally finned tubes could also be developed.

3. Quantification of the performance of internally finned tubes is yet to be perfected. Most of the performance indices developed for single phase flow are not suited in two phase flow as the constraints with which these indices are evaluated cannot be achieved experimentally. More reliable and attainable performance criteria of augmented surfaces need to be defined for two-phase flow.

ACKNOWLEDGEMENTS

I wish to express my deepest appreciation and gratitude to Prof. Naim Z. Azer for his guidance and valuable advice during the course of this study.

Thanks are extended to Prof. Leonard E. Fuller and Prof. Robert E. Crank for being on my examination committee.

I wish to thank Dr. Paul L. Miller, Chairman, Department of Mechanical Engineering, for providing financial support during the present investigation.

Finally, I wish to thank my family for their patience, understanding and continuous encouragement during my graduate study.

SELECTED BIBLIOGRAPHY

1. Bergles, A. E., "Research Workshop on Augmentation of Convective Heat Transfer", Final Report HTL-8, ISU-ERI-AMES-76026 (1975).

2. Said, S., "Augmentation of Condensation Heat Transfer of R-113 by Internally Finned Tubes and Twisted Tape Inserts", Ph.D. dissertation, Dept. of Mechanical Engineering, Kansas State University (1982).

3. Bergles, A. E., Webb, R. L., Junken, G. H., and Jensen, M. K., "Bibliography on Augmentation of Convective Heat and Mass Transfer", Engineering Research Institute, Iowa State University, HTL-19-ISU-AMES-79206, (1979).

4. Royal, J., "Augmentation of Horizontal In-Tube Condensation of Steam", Ph.D. dissertation, Dept. of Mechanical Engineering, Iowa State University, Ames, Iowa (1980).

5. Luu, M., "Augmentation of In-Tube Condensation of R-113", Ph.D. dissertation, Dept. of Mechanical Engineering, Iowa State University, Ames, Iowa (1980).

6. Akers, W. W., Deans, H. A., and Crosser, O. K., "Condensing Heat Transfer Within Horizontal Tubes", Chemical Engineering Progress Symposium Series 55 (1959): 171-176.

7. Boyko, L. D. and Kruzhilin, G. M., "Heat Transfer and Hydraulic Resistance During Condensation of Steam in a Horizontal Tube and in a Bundle of Tubes", International Journal of Heat and Mass Transfer 10 (1967): 361-373.

8. Rosson, H. F. and Myers, J. A., "Point Values of Condensing Film Coefficients Inside a Horizontal Pipe", Chemical Engineering Progess Symposium Series 59 (1963): 190-199.

9. Travis, D. P., Rohsenow, W. M., and Baron, A. B., "Forced-Convenction Condensation Inside Tubes: A Heat Transfer Equation for Condenser Design", ASHRAE Transactions 79, Part 1 (1972): 157-165.

10. Soliman, M., Schuster, J. R., and Berenson, P. J., "A General Heat Transfer Correlation for Annular Flow Condensation," Journal of Heat Transfer 90 (1968): 267-276.

11. Azer, N. Z., Abis, L. V., and Swearingen, T. B., "Local Heat Transfer Coefficients During Forced Convection Condensation Inside Horizontal Tubes," ASHRAE Transactions 77, Part 1, (1971): 182-201.

12. Cavallini, A. and Zecchin, R., "High Velocity Condensation of Organic Refrigerants Inside Tubes", Reprint from the Proceedings of the 13th International Congress of Refrigeration, Washington, D.C., 2, Belgium:

International Institute of Refrigeration, (1971).

13. Shah, M. M., "A Ceneral Correlation for Heat Transfer During Film Condensation Inside Pipes", International Journal of Heat and Mass Transfer 22 (1979): 547-556.

14. Lockhart; R. W. and Martinelli, R. C., "Proposed Correlation of Data for Isothermal Two-Phase, Two-Component Flow in Pipes", Chemical Engineering Progress 45, (1) (1979): 39-48.

15. Dukler, A. E., Wicks, III, M., and Cleaveland, R. C., "Frictional Pressure Drop in Two-Phase Flow: A Comparison of Existing Correlations for Pressure Loss and Holdup", AIChE Journal 10, January (1964): 38-43.

16. Dukler, A. E., Wicks III, M., and Cleaveland, R. C., "Frictional Pressure Drop in Two-Phase Flow: An Approach Through Similarity Analysis", AIChE Journal 10, January (1964): 44-51.

17. Hughmark, C. A., "Pressure Drop in Horizontal and Vertical CO-Current Cas-Liquid Flow", I & EC Fundamentals 2, (4) (1963): 315-321.

18. Collier, J., Convective Boiling and Condensation, London: McGraw Hill, (1981).

19. Baroczy, C. J., "Correlation of Liquid Fraction in Two-Phase Flow with Application to Liquid Metals", North American Avaiation Report SR-8171, El Segundo, CA., (1963).

20. Thom, J. R. S., "Predictions of Pressure Drop During Forced Circulation Boiling Water", International Journal of Heat and Mass Transfer 7 (1964): 709-724.

21. Zivi, S. M., "Estimation of Steady-State Steam Void Fraction by Means of Minimum Entropy Production", Journal of Heat Transfer 86 (1964): 247-252.

22. Turner, J. M. and Wallis, C. B., "The Separate-Cylinder Model of Two-Phase Flow", Thayer's School of Engineering, Report No. NYO-3114-6, Darthmouth College, (1965).

23. Hughmark, C. A., "Holdup in Cas-Liquid Flow", Chemical Engineering Progress 58, April (1962), 62-65.

24. Watkinson, A. P., Miletti, D. L., and Kubanek, C. R., "Turbulent Heat Transfer and Pressure Drop of Internally Finned Tubes", AIChE Symposium Ser., Vol. 69, No. 131, (1973): 94-103.

25. Watkinson, A. P., Miletti, D. L., and Kubanek, C. R., "Heat Transfer and Pressure Drop of Internally Finned Tubes in Turbulent Air Flow," ASHRAE Transactions, Vol. 81, Part 1, (1975), 330-349.

26. Watkinson, A. P., Miletti, D. L., and Kubanek, C. R., "Heat Transfer and Pressure Drop of Internally Finned Tubes in Laminar Oil Flow", ASME

Paper 75-HT-41, Presented at the AIChE-ASME Heat Transfer Conference, San Francisco, California, August (1975).

27. Carnavos, T. C., "Cooling Air in Turbulent Flow with Internally Finned Tubes", Presented at the 17th Natl. Heat Transfer Conf., Salt Lake City, Utah, AIChE Paper 4, Aug. 14-17 (1977), also Heat Transfer Engineering, Vol. 1, No. 2, Oct.-Dec. (1979): 41-46.

28. Carnavos, T. C., "Cooling Air in Turbulent Flow Multi-Passage Internally Finned Tubes", ASME Paper 78-WA/HT-52, Presented at the Winter Annual Meeting, San Francisco, CA., Dec. 10-15 (1978).

29. Carnavos, T. C., "Heat Transfer Performance of Internally Finned Tubes in Turbulent Flow", Heat Transfer Engineering, Vol. 1., No. 4, April-June (1980): 32-37.

30. Hu, M. H. and Chang, Y. P., "Optimization of Finned Tubes for Heat Transfer in Laminar Flow", Transactions ASME, Journal of Heat Transfer, Vol. 95, Series C, (1973): 332-338.

31. Nandakumar, K. and Masliyah, J. H., "Fully Developed Viscous Flow in Internally Finned Tubes", The Chemical Engg. J., Vol. 10, (1975): 113-120.

32. Masliyah, J. H. and Nandakumar, K., "Heat Transfer in Internally Finned Tubes", Journal of Heat Transfer, Vol. 98, (1976): 257-261.

33. Soliman, H. M. and Feingold, A., "Analysis of Fully Developed Laminar Flow in Longitudinal Internally Finned Tubes", The Chemical Engineering Journal, Vol. 14, (1977): 119-128.

34. Soliman, H. M. and Feingold, A., "Analysis of Heat Transfer in Internally Finned Tubes Under Laminar Flow Conditions", Heat Transfer (1978), Vol. 2, Hemisphere Publishing Corporation, (1978): 571-576.

35. Reisbig, R. L., "Condensing Heat Transfer Augmentation Inside Splined Tubes", Paper 74-Ht-7, Presented at the AIAA/ASME Thermophysics and Heat Transfer Conference, Boston, July (1974).

36. Kroger, D. G., "Laminar Condensation Heat Transfer Inside Inclined Tubes", Paper No. AIChE-29, Presented at the 16th National Heat Transfer Conference, St. Louis, MO., Aug. 8-11, (1976).

37. Vrable, D. L., "Condensation Heat Transfer Inside Horizontal Tubes With Internal Axial Fins", Ph.D. dissertation, University of Michigan, (1974).

38. Vrable, D. L., Yang, Wen-Jei, and Clark, John A., "Condensation of Refrigerant-12 Inside Horizontal Tubes With Internal Axial Fins", In Heat Transfer (1974), Fifth International Heat Transfer Conference 3, pp. 250-254., Tokyo: Japan Society of Mechanical Engineers, (1974).

39. Yang, Wen-Jei, "Equivalent f and j Factors for Condensation Inside Horizontal Smooth and Finned Tubes", Letters in Heat and Mass Transfer 1 (1974): 127-130.

40. Cavallini, Alberto, and Zecchin, Reberto, "A Dimensionless Correlation for Heat Transfer in Forced Convection Condensation", pp. 309-313, In Heat Transfer (1974), Proceedings of the Fifth International Heat Transfer Conference 3. Tokyo: Japan Society of Mechanical Engineers, (1974).

41. Royal, J. H. and Bergles, A. E., "Experimental Study of Horizontal In-Tube Condensation", Presented at the ASHRAE Dallas Meeting, Feb. 1-5, ASHRAE Transactions 82, Part II (1976): 919-931.

42. Royal, J. H. and Bergles, A. E., "Augmentation of Horizontal In-Tube Condensation by Means of Twisted-Tape Inserts and Internally Finned Tubes", Journal of Heat Transfer 100, (1) (1978): 17-24.

43. Royal, J. H. and Bergles, A. E., "Pressure Drop Performance Evaluation of Augmented In-Tube Condensation", In Heat Transfer (1978), Sixth International Heat Transfer Conference, Vol. 3: 459-464. Toronto: Hemisphere Publishing Corporation, (1978).

44. Luu, M. and Bergles, A. E., "Experimental Study of Augmentation of In-Tube Condensation of R-113", ASHRAE Transactions Vol. 85, Pt. 2, (1979): 132-145.

45. Luu, M. and Bergles, A. E., "Enhancement of Horizontal In-Tube Condensation of Refrigerant-113", Paper Presented at the Session on Condensation Heat Transfer, National Heat Transfer Conference, ASME (1979).

46. Luu, M. and Bergles, A. E., "Enhancement of Horizontal In-Tube Condensation of Refrigerant-113", ASHRAE Transactions, 86, Part (1), (1980), pp. 293-312.

47. Said, S. A. and Azer, N. Z., "Heat Transfer and Pressure Drop During Condensation Inside Horizontal Finned Tubes", ASHRAE Transactions, (1983), Vol. 89, Pt. (1).

48. ASHRAE Handbook of Fundamentals, New York: ASHRAE (1981).

49. Silver, R. S. and Wallis, G. B., "A Simple Theory for Longitudinal Pressure Drop in the Presence of Lateral Condensation", Proceedings of the Institute of Mechanical Engineers 180, (1), (1965-66): 36-42.

50. Butterworth, D., "A Comparison of Some Void-Fraction Relationships for Co-Current Gas-Liquid Flow", International Journal of Multiphase Flow 1 (1975): 845-850.

51. Bergles, A. E., Blumenkrantz, A. R., and Taborek, J., "Performance Criteria for Enhanced Heat Transfer Surfaces", Presented at 13th National Transfer Conference, AIChE-ASME, Denver, CO., Aug. 6-9, (1972).

52. Bergles, A. E., Blumenkrantz, A. R., and Taborek, J., "Performance Evaluation Criteria for Enhanced Heat Transfer Surfaces", In Heat Transfer (1974), 5th International Heat Transfer Conference, Vol. 2, pp. 234-238. Tokyo: Japan Society of Mechanical Engineers, (1974).

53. Azer, N. Z., Fan, L. T., and Lin, S. T., "Augmentation of Condensation Heat Transfer With In-Line Static Mixers", Proceedings of 1976 HTFMI, (1976): 512-526.

54. Lin, S. T., "Augmentation of Two-Phase Heat Transfer With In-Line Static Mixers", Ph.D. dissertation, Dept. of Mechanical Engineering, Kansas State University, Manhattan, KS., (1979).

55. Azer, N. Z. and Shivakumar, V., "Enhancement of Saturated Boiling Heat Transfer by Internally Finned Tubes", ASHRAE Transactions (1984), V. 90, Pt. 1.

56. Kline, S. J. and McClintock, F. A., "Describing the Uncertainties in Single-Sample Experiments", Mechanical Engineering 75, January (1953): 3-8.

NOMENCLATURE

Symbol	
A	Flow cross-sectional area, m^2
A_1	Constant in Eq.(5-26) and Table (5.1)
A_a	Actual heat transfer area, m^2/m
A_{fa}	Actual free flow area, m^2
A_{fc}	Open core free flow area, m^2
A_{fn}	Nominal flow area based on inside tube diameter as if fins were not present, m^2
A_n	Nominal heat transfer area based on inside tube diameter as if fins were not present, m^2/m
b	Fin height, m
C	Constant in Eqs.(4-2) and (5-1)
C'	Constant in Eq.(4-3)
Cp_ℓ	Specific heat of liquid, W.hr/Kg.°C
Cp_{wa}	Specific heat of cooling water, W.hr/Kg.°C
D_e	Diameter of internally finned tube if fins melted down, m
D_h	Hydraulic diameter ($D_h = 4A_{fa}/A_a$), m
D_i	Inside tube diameter, m
D_o	Outside tube diameter, m
$\left(\frac{dp}{dz}\right)$	Pressure gradient, bar/m
$\left(\frac{dp}{dz}\right)_f$	Frictional pressure gradient, bar/m
$\left(\frac{dp}{dz}\right)_\ell$	Frictional pressure gradient assuming that liquid alone is flowing in the pipe, Eq.(5-10), bar/m
$\left(\frac{dp}{dz}\right)_m$	Momentum pressure gradient, bar/m
$\left(\frac{dp}{dz}\right)_v$	Frictional pressure gradient assuming that gas (or vapor) alone is flowing in the pipe, Eq.(5-10), bar/m
f	Friction factor

f_{co}	Friction factor in the presence of condensation, Eq.(5-23)
f_{fc}	Friction factor developed for finned tubes by Said and Azer, Eq.(5-43)
f_o	Friction factor defined in Eqs.(5-16) and (5-17)
F_1	Parameter defined in Eqs.(5-35) and (5-41)
F_2	Parameter defined in Eqs.(5-36) and (5-42)
F_3	Parameter defined in Eq.(5-37)
F_4	Paramter defined in Eq.(5-44)
g	Acceleration due to gravity, $g = 9.81$ m/sec^2
G	Mass flux, Kg/hr.m^2
G_e	Adjusted mass flux, Kg/hr.m^2
G_ℓ	Liquid mass flux ($G_\ell = G(1-x)$), Kg/hr.m^2
G_v	Vapor mass flux ($G_v = Gx$), Kg/hr.m^2
h	Heat transfer coefficient, W/m^2 °C
$\bar{h}$	Average heat transfer coefficient, W/m^2 °C
h_z	Local heat transfer coefficient, W/m^2 °C
H	Fin pitch (length per turn), m/360°, or enthalpy, Joule/Kg
H_f	Enthalpy of saturated liquid, Joule/Kg
H_{fg}	Latent heat of vaporization, Joule/Kg
k_ℓ	Thermal conductivity of saturated liquid, W/m °C
K	Thermal conductivity of condenser tube, W/m °C
L	Length of condenser, m
$\dot{m}_{wa}$	Mass flow rate of the cooling water, Kg/hr
$\dot{M}_\ell$	Saturated liquid flow rate of R-11 ($\dot{M}_\ell = \dot{M}_T(1-x)$), Kg/hr
$\dot{M}_T$	Mass flow rate of R-11, Kg/hr
$\dot{M}_v$	Saturated vapor flow rate of R-11 ($\dot{M}_v = \dot{M}_T x$), Kg/hr
n	Constant in Eq.(4-2) and (5-1), or number of internal fins
n'	Constant in Eq.(4-3)

P	System pressure, bar
P_{cr}	Critical pressure, bar
ΔP	Pressure drop, bar
P_{rc}	Reduced pressure ($P_{rc} = P/P_{cr}$)
Pr	Prandtl number of saturated liquid
$\mathbb{P}$	Pumping power, W
q_1	Constant in Eq.(5-26) and Table (5.1)
Q	Heat transfer rate to the coolant, W
Q_f	Heat transfer rate from the condensing fluid, W
r_1	Constant in Eq.(5-26) and Table (5.1)
$R_{\Delta P}$	Pressure drop index for the performance evaluation Eq.(6-2)
R_h	Reduction condenser size index for the performance evaluation, Eq.(6-1)
Re	Reynolds number
Re_e	Reynolds number based on adjusted mass velocity ($Re_e = G_e D_i/\mu_\ell$)
Re_ℓ	Reynolds number based on liquid or liquid phase alone flowing in the tube ($Re_\ell = G(1-x)\ D_i/\mu_\ell$)
Re_L	Reynolds number based on the liquid flowing alone ($Re_L = GD_i/\mu_\ell$)
s_1	Constant in Eq.(5-26) and Table (5.1)
t	Fin thickness, m
T	Temperature, $^\circ C$
$\overline{T}_s$	Average saturation temperature of R-11, $^\circ C$
T_{wai}	Water inlet temperature, $^\circ C$
T_{wao}	Water outlet temperature, $^\circ C$
$\overline{T}_{wo}$	Average wall temperature, $^\circ C$
ΔT	Temperature difference, $^\circ C$
w	Uncertainity
W	Channel width between internal fins
x	Dryness fraction (ratio of vapor mass to total mass)
$\overline{x}$	Mean dryness fraction

X_{tt} Lockhart-Martinelli parameter defined in Eq.(5-11)

Δz Length of the subsection, m

Z Axial distance, m

Greek Letters

α Spiral fin tube helix angle (angle between fin and tube axis), degrees

$\alpha(\lambda)$ Ratio of two-phase friction factor to single-phase friction factor at two-phase Reynolds number, Eq.(5-8)

β Ratio of two-phase density to no-slip density, Eq.(5-19)

ξ Parameter defined in Eq.(5-24)

λ Ratio of liquid volumetric flow to the total volumetric flow rate, Eq.(5-22)

μ Dynamic viscosity, Kg/hr.m

μ_ℓ Dynamic viscosity of saturated liquid, Kg/hr.m

μ_{NS} Dynamic viscosity of two-phase homogeneous mixture, Eq.(5-21) Kg/hr.m

μ_v Dynamic viscosity of saturated vapor, Kg/hr.m

ν_ℓ Kinematic viscosity of saturated liquid, m^2/hr

ρ Density, Kg/m^3

ρ_ℓ Desity of saturated liquid, Kg/m^3

ρ_m Density of two-phase homogeneous mixture, defined in Eq.(5-5), Kg/m^3

ρ_{NS} Density of two-phase homogeneous mixture, defined in Eq.(5-20), Kg/m^3

ρ_v Density of saturated vapor phase Kg/m^3

ϕ_v Lockhart-Martinelli parameter, Eq.(5-12)

ψ Void fraction

Subscripts

1-4 Subsection 1-4

aug Augmented surface

cal	Calculated
exp	Experimental
in	Inlet
NS	No-Slip
out	outlet
s	Saturated
sm	Smooth surface
tt	Turbulent-turbulent
z	Local, or axial

APPENDIX A

APPENDIX A

ADDITIONAL INFORMATION ON THE INSTRUMENTATION AND COMPONENTS USED IN THIS STUDY

1. R-11 FLOW CIRCUIT

A. Components:

1. Refrigerant-11 Liquid Circulating Gear Pump:

Sherwood Alear Siegler Company
Bronze Rotary Gear Pump
Model: S and V series
R.P.M.: 1725
Pipe Size: 1/4"
Shaft Diameter: 1/2"
H.P.: 1/3
Dripless Mechanical Shaft Seal, Self Lubricated.

2. Refrigerant-11 Liquid Circulating Pump Motor:

Dayton - Electric A.C. Motor
Model No.: 5K991
R.P.M.: 1725
H.P.: 1/2
HZ: 60

3. Refrigerant-11 Filter:

Sparlan - Catchall Refrigerant Filter
Type: C-304

4. Vapor Generator Heating Elements (Two):

Chromalox Immersion Type Heating Elements
Model: AH2745
Capacity: 240 V, 4.5 KW each

5. Refrigerant-11 Liquid Receiver:

Midland-Ross Refrigerant Type Circular Tank
Serial No.: 2193
Size: 3.5 gallons
Working Pressure: Maximum Allowable Working Pressure
400 psi at 650°F

6. Refrigerant-11 Valves:

Oiaphram Packless Line Valves
Superior Brand, Solder to Solder Type
A. Model No.: 214-4S (1/4")
B. Model No.: 216-10S (5/8")

7. Refrigerant-11 Vapor-Liquid Separator:

Penberty Co. V-L Separator
Serial No.: X-503070003000

8. Refrigerant-11 After-Condenser:

Dunham-Bush Bundle Type Condenser
Model No.: C1C-200-66-L

9. Refrigerant-11 Tube Connectors:

Standard Copper Tube
Sweat Fitting Type

10. Vibration Eliminators:

Anacond Vibration Eliminators Supplied by RECO
Specification: "Has Fatigue-Resistance Corrugated in Bronze Seamless Tubing Core with Bronze Braid Covering. Standard Copper Tube Fittings are Welded on Both Ends."

11. Refrigerant-11 Vapor Generator, Locally Constructed:

Material:

Steel Tubing: 17.78 cm 0.0. (16.51 cm I.D.), length 78.74 cm

Two Circular Steel Plates = 24.13 cm Diameter, 0.95 cm thick.

The two circular steel plates were welded to close the two ends of the horizontal steel tubing creating a tank. Holes were drilled and tapped in each steel plate to accommodate the threaded heater elements (one element in each plate, and positioned axially opposite to each other toward the bottom of of the tank). Holes were also drilled and tapped in a vertical plane on one plate to allow the connection of a liquid level indicator for the purpose of knowing if heaters were covered completely by the liquid. Two holes were drilled and tapped on one end of the tank to allow liquid R-11 to flow into the tank through the middle of the plate and vapor to exit at a level above the center.

12. Superheater, Locally Constructed:

Material:

Copper Tubing: 1.59 cm O.D. (1.27 cm I.D.), Length 101.6 cm
Heating Element: Ribbon type chromel of 0.204 Ω/30.48 cm
Teflon Tape: Saunder type S-17
Epoxy: Armstrong A-68 and B-68 Types

The teflon tape was wrapped around the copper tube with one thickness. The heating element was wound uniformly around the tape with 0.65 cm distance pitch. The epoxy was applied to secure the heating element.

13. Thermocouples:

Copper-Constantan thermocouples of type B&S 24 gage.

B. Instrumentation

1. Refrigerant-11 Liquid Level Gauge:

Brooks Rotameter View Meter
Type: 6-1355-VB
Serial No.: 6507-36340/4

2. Refrigerant-11 Flow Meters:

A. Fischer-Porter Variable Area Type Flow Meter

Range: 0∿0.35 GPM Liquid
Model: 10A3565S
Serial No.: 7207A4733A2
Tube No.: FP-1/2-27-G-10/55

B. Fischer-Porter Variable Area Type Flow Meter

Range: 0∿0.5 GPM Liquid
Model: 10A3565S
Serial No.: 7207A4733A1
Tube No.: FP-1/2-17-G-10/55

3. Refrigerant-11 Pressure Gauge:

Heise Pressure Gauge of Type H28832
Range: 0∿200 psig

4. Pressure Transducer:

   Pace Wiancko Division of Whittaker Corporation
   Model: KP15 Pressure Transducer
   Serial NO.: 150330

5. Transducer Indicator:

   Pace Wiancko Division of Whittaker Corporation
   Model: CD25
   Serial No.: 23449

6. Digital Multimeter

   Model: 168 Autoranging DMM
   Keithley Instruments, Inc.

7. Voltage Regulator

   Superior Electric Co.
   Powerstat Variable Autotransformer
   Input: 240 V, 60 HZ
   Output: 0-280 V, 28A, 7.8 KW

8. A.C. Ampere Meter:

   Daystrom, Incorporated Weston Instruments Div.
   Weston Instruments, Inc.
   New York, New Jersey
   Model: 433 No. 164330

9. A.C. Volt Meter:

   Daystrom, Incorporated Weston Instruments Div.
   Weston Instruments, Inc.
   New York, New Jersey.
   Model: 433 No. 146652

10. Data Acquisition System:

   Esterline Angus an Esterline Company
   Model: PD-2064
   Type: Key Programmable

   The system can gather analog and digital data from up to 64 channels under the control of tiny microprocessor. The system outputs the measured values in engineering or scientific units through various output devices. The solid-state integrated circuit microprocessor is combined with RAMs (random access memory devices), ROMs (read-only memory devices), and PROMs (programmable ROMs) to provide a keyboard-programmable system that permits the instrument to scan, measure, collect, identify, and record both analog and digital input signals.

Accuracy:

<u>.With Ambient Temperature at 77°F ∓ 9°F</u>

∓ 0.01% of reading, ∓ 0.015% full scale, ∓ 1 count on 4000 mV range;

∓ 0.01% of reading, ∓ 0.03% full scale, ∓ 1 count on 400 mV range;

∓ 0.01% of reading, ∓ 0.04% full scale, ∓ 1 count on 40 mV range.

<u>Over Full Operation Ambient Temperature Range of 32°F to 122°F</u>

∓ 0.5 μV per °C, ∓ 0.01% of reading, ∓ .04% full scale,

∓ 1 count on all ranges.

11. Manometer:

Meriam Instrument Co.
Type: W
Model: 30EC10
Serial No.: B23131
Range: 40"
Manometer with mercury as the indicating fluid.

12. Differential Pressure Cell:

Foxboro Type 13A
Range: -0.034∿0.184 bar (-.5∿2.67 psia)
D/P cell connections, locally constructed: Copper tubing of 0.64 cm O.D. was used to connect the pressure tap and the D/P cell.
Calibration: The differential pressure cell was calibrated according to the manufacturer's recommended calibration procedure before it was connected to the test condenser. A linear least squares regression correlation was used to obtain the calibration curve given by,

$$Y = 0.00021074\ x - 0.031749 \qquad \text{(A-1)}$$

where:

Y = pressure drop in bars

X = D/P cell output in mm of mercury.

A total of about 100 points were used to calibrate the pressure cell.

13. Vaccum Pump

Matheson Scientific
Division of Will Ross, Inc.
Serial No.: 1173
Power: 115 V, 60 HZ
Connections: 3 conductor power cord with 2-prong adapter. Inlet and outlet connector to 3/8" I.D. hose.
Function: Portable A.C. powered source of vaccum (to 686mm/27" Hg) or pressure (to 1.7 kg/cm^2, 25 psig).

All thermophysical and transport properties of R-11 were obtained from ASHRAE Handbook of Fundamentals [48].

2. WATER FLOW CIRCUIT

1. Cooling Water Flow Meters:

Brooks Rotameter
Type: 1110-09H3A1B
Serial No.: 7201-74650/1
Tube No.: R-9M-25-1 BR-3/4-14G10
Range: 0∿3 GPM

2. Cooling Water Pump:

A.O. Smith Co. Pump
Model No.: C48L2DA11A4
Serial No.: J69
H.P.: 1
R.P.M.: 3450
HZ: 60

APPENDIX B

APPENDIX B

SAMPLE OF DATA REDUCTION AND CALCULATION PROCEDURE OF HEAT TRANSFER COEFFICIENTS

The raw data of all experimental runs were fed into a digital computer prorgram which was written to reduce the data into useful forms. The computer program listing is given in Appendix C. The reduced data are given in Appendix D. The experimental runs in the reduced data are coded in three digit numbers. The first digit represents the tube number and the remaining two digits represent the run number. A sample of the calculation procedure for run number 146 is given below. Since all the experimental measurements like temperatures, pressures, flow rates etc. were in British units, the calculations for data reduction were done in British units and quantities of interest were converted into SI system of units. During the calculation procedure reference is made to the thermocouple stations and pressure tap locations in Fig B.1

<u>Recorded Experimental Data for Run number 146</u>

Reference (ambient) temperature	=	74^oF
Atmospheric pressure	=	14.10 psia
Tube I.D., D_i	=	0.545 in.
Tube O.D., D_o	=	0.625 in.
Tube length of each subsection, Δz	=	27.0 in.
Number of subsections in the tube	=	4
Tube thermal conductivity, K	=	$220 \frac{Btu}{hr\ ft^2\ ^oF}$
Test fluid flow rate, GPMF	=	$0.105 \frac{gal}{min}$
Water flow rate through the test condenser, GPMW	=	$1.58 \frac{gal}{min}$

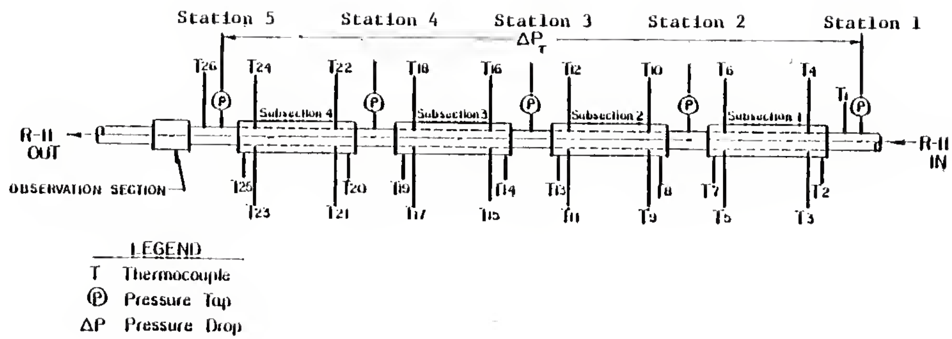

Fig. B.1 A Schematic Diagram of Thermocouples, Stations and Pressure Taps Locations.

Test section inlet pressure, P_{in}	=	24.10 psia
Total pressure drop, ΔP_T	=	0.066 psi

Coolant temperatures

Coolant inlet temperature at subsection 4, T_{25}	=	66.56 ^oF
Coolant outlet temperature at subsection 4, T_{20}	=	68.00 ^oF
Coolant inlet temperature at subsection 3, T_{19}	=	67.28 ^oF
Coolant outlet temperature at subsection 3, T_{14}	=	68.90 ^oF
Coolant inlet temperature at subsection 2, T_{13}	=	69.62 ^oF
Coolant outlet temperature at subsection 2, T_8	=	72.50 ^oF
Coolant inlet temperature at subsection 1, T_7	=	73.14 ^oF
Coolant outlet temperature at subsection 1, T_2	=	73.94 ^oF

R-11 Temperature

Test fluid inlet temperature, T_1	=	110.02 ^oF
Test fluid outlet temperature, T_{26}	=	96.98 ^oF
Test fluid temperature at flowmeter, T_{27}	=	86.72 ^oF

Wall Temperatures in ^oF

Subsection 1	Subsection 2	Subsection 3	Subsection 4
T_3 = 96.08	T_9 = 81.14	T_{15} = 74.84	T_{21} = 73.58
T_4 = 102.74	T_{10} = 90.32	T_{16} = 90.68	T_{22} = 83.66
T_5 = 94.46	T_{11} = 75.02	T_{17} = 73.22	T_{23} = 69.80
T_6 = 96.98	T_{12} = 82.76	T_{18} = 84.56	T_{24} = 84.92

Calculation Procedure

Sectional heat transfer area, A_n:

$$A_n = \pi D_i \Delta z = \frac{\pi(0.545)(27)}{144} = 0.321 \text{ ft}^2$$

Cross sectional flow area, A_{fn}:

$$A_{fn} = \frac{\pi D_i^2}{4} = \frac{(0.545)^2}{(4)(144)} = 1.62002 \times 10^{-3}\ ft^2$$

Coolant flow rate into the test condenser, $\dot{m}_{wa}$:

$$\dot{m}_{wa} = 1.58\ \frac{\text{gallons}}{\text{minute}} \times 60\ \frac{\text{minute}}{\text{hour}} \times 0.13368\ \frac{ft^3}{\text{gallon}} \times 62.3\ \frac{lbm}{ft^3}$$

$$= 789.52\ lbm/hr$$

Test fluid flow rate, $\dot{M}_T$:

Since the flow meter was calibrated for R-113, a correction factor of 1.036 was used for R-11 flow rate.

$$\dot{M}_T = (0.105 \times 1.036)\ \frac{\text{gallons}}{\text{minute}} \times 60\ \frac{\text{minute}}{\text{hour}} \times 0.13368\ \frac{ft^3}{\text{gallon}}$$

$$\times\ 91.33\ \frac{lbm}{ft^3}$$

$$= 79.70\ lbm/hr$$

Test fluid mass flux, G :

$$G = \dot{M}_T/A_{fn} = \frac{79.70}{1.62002\times10^{-3}} = 0.49197 \times 10^5\ lbm/hr.ft^2$$

Heat transfer rate at each subsection, Q_i:

$$Q_i = \dot{m}_{wa}\ Cp_{wa}\ (T_{wao} - T_{wai})$$

$$Q_1 = (789.52)(1)(73.94-72.14) = 1421.14\ Btu/hr$$

$$Q_2 = (789.52)(1)(72.50-69.62) = 2273.82\ Btu/hr$$

$$Q_3 = (789.52)(1)(68.90-67.28) = 1279.02\ Btu/hr$$

$$Q_4 = (789.52)(1)(68.00-66.56) = 1136.91\ Btu/hr$$

Total heat transfer rate, Q :

$$Q = Q_1 + Q_2 + Q_3 + Q_4 = 6110.88\ Btu/hr$$

Test fluid heat transfer, Q_f:

$$Q_f = \dot{M}_T\left[H_1(P_1,T_1) - H_{f5}\right]$$

$$= 79.70\ \left[105.36 - 28.07\right]$$

$$= 6160.18 \text{ Btu/hr}$$

where

H_1 is the specific enthalpy of the test fluid at station 1, Btu/lbm

H_{f5} is the specific enthalpy of the saturated R-11 at T_{26}, Btu/lbm

Energy balance error in percentage, Error % :

$$\text{Error \%} = 100 \times \frac{Q - Q_f}{Q}$$

$$= 100 \times \frac{6110.18-6160.18}{6110.18}$$

$$= -0.81\%$$

Quality at each station, x_i:

The quality was calculated from the energy balance for each substation in which the energy gained by coolant and the energy lost by condensing fluid were assumed to be equal.

$$Q_1 = \dot{M}_T(H_1-H_2)$$

$$Q_2 = \dot{M}_T(H_2-H_3)$$

$$Q_3 = \dot{M}_T(H_3-H_4)$$

$$Q_4 = \dot{M}_T(H_4-H_5)$$

Q_1 - Q_4 are known and proceeding from inlet to exit the above equations were solved for enthalpies H at each station. The results were

H_2 = 87.53 Btu/lbm

H_3 = 59.00 Btu/lbm

H_4 = 42.95 Btu/lbm

H_5 = 28.69 Btu/lbm

The qualities are determined as follows

$$x_1 = \frac{H_1 - H_{f1}}{H_{fg1}} = \frac{105.36-29.03}{75.02} = 1.017$$

$$x_2 = \frac{H_2 - H_{f2}}{H_{fg2}} = \frac{87.53-29.03}{75.02} = 0.779$$

$$x_3 = \frac{H_3 - H_{f3}}{H_{fg3}} = \frac{59.00-29.03}{75.02} = 0.339$$

$$x_4 = \frac{H_4 - H_{f4}}{H_{fg4}} = \frac{42.95-29.03}{75.02} = 0.186$$

$$x_5 = \frac{H_5 - H_{f5}}{H_{fg5}} = \frac{28.69-29.03}{75.02} = -0.004$$

where

H_f and H_{fg} are the saturated liquid enthalpy and the latent heat, respectively, corresponding to the saturation pressure at each station.

In the present study, the magnitude of the pressure drops was low and hence the effect of pressure drop on saturated liquid enthalpy and latent heat was neglected. It was assumed that

$$H_{f1} = H_{f2} = H_{f3} = H_{f4} = H_{f5}$$

and

$$H_{fg1} = H_{fg2} = H_{fg3} = H_{fg4} = H_{fg5}$$

<u>Heat Transfer Coefficients</u>

Average outside wall temperature, $\overline{T}_{wo}$:

Subsection 1 $$\overline{T}_{wo1} = \frac{T_3 + T_4 + T_5 + T_6}{4} = 97.57\ ^{o}F$$

Subsection 2 $$\overline{T}_{wo2} = \frac{T_9 + T_{10} + T_{11} + T_{12}}{4} = 82.31\ ^{o}F$$

Subsection 3 $\quad \overline{T}_{wo3} = \dfrac{T_{15} + T_{16} + T_{17} + T_{18}}{4} = 80.83\ ^{o}F$

Subsection 4 $\quad \overline{T}_{wo4} = \dfrac{T_{21} + T_{22} + T_{23} + T_{24}}{4} = 77.99\ ^{o}F$

Sectional average heat transfer coefficient, $\overline{h}_i$:

$$\overline{h}_i = \left[\frac{\pi\, D_i\, \Delta z\, (\overline{T}_{si} - \overline{T}_{woi})}{Q_i} - \frac{D_i}{2K}\ \ln\left(\frac{D_o}{D_i}\right)\right]^{-1} \qquad \text{(B-1)}$$

$\overline{T}_{si}$ and $\overline{T}_{woi}$ are the average saturation and average outside wall temperatures for the corresponding subsection respectively.

As discussed earliear in Chapter IV, the sectional heat transfer coefficient of section 1 was calculated by replacing $\overline{T}_{si}$ in Eq.(B-1) by $(T_1 + T_2)/2$

where

T_1 is the inlet superheat temperature of R-11

Since the effect of pressure drop on saturation temperature was neglected

$$\overline{T}_{si} = \overline{T}_{s1} = \overline{T}_{s2} = \overline{T}_{s3} = \overline{T}_{s4} = 101.53\ ^{o}F$$

For this run $T_1 = 110.02\ ^{o}F$

$$\overline{h}_1 = \left[\frac{\pi(0.545)(27)\left[(101.53+110.02)/2 - 97.57\right]}{(144)(1421.14)} - \frac{0.545}{(24)(220)}\ \ln\left(\frac{0.625}{0.545}\right)\right]^{-1}$$

$= 543.41\ \text{Btu/hr. ft}^2.^{o}F$

$$\overline{h}_2 = \left[\frac{\pi(0.545)(27)(101.53-82.31)}{(144)(2273.82)} - \frac{0.545}{(24)(220)}\ \ln\left(\frac{0.625}{0.545}\right)\right]^{-1}$$

$= 370.49\ \text{Btu/hr.ft}^2.^{o}F$

$$\bar{h}_3 = \left[\frac{\pi(0.545)(27)(101.53-80.83)}{(144)(1279.02)} - \frac{0.545}{(24)(220)}\ln\left(\frac{0.625}{0.545}\right)\right]^{-1}$$

$$= 192.97 \text{ Btu/hr.ft}^2.{}^oF$$

$$\bar{h}_4 = \left[\frac{\pi(0.545)(27)(101.53-77.99)}{(144)(1136.91)} - \frac{0.545}{(24)(220)}\ln\left(\frac{0.625}{0.545}\right)\right]^{-1}$$

$$= 150.78 \text{ Btu/hr.ft}^2.{}^oF$$

Overall average heat transfer coefficient (tube), $\bar{h}$:

$$\bar{h} = \left[\frac{\pi D_i L(\bar{T}_s - \bar{T}_{wo})}{Q} - \frac{D_i}{2K}\ln\left(\frac{D_o}{D_i}\right)\right]^{-1}$$

$\bar{T}_s$ is the average saturation temperature of the test condenser corresponding to the average pressure.

$\bar{T}_{wo}$ is the average wall temperature of the test condenser

$= (\bar{T}_{wo1} + \bar{T}_{wo2} + \bar{T}_{wo3} + \bar{T}_{wo4})/4.0$

L is the length of four subsections = 4 z.

Therfore,

$$\bar{h} = \left[\frac{\pi(0.545)(108)(101.53-84.68)}{(144)(6110.18)} - \frac{0.545}{(24)(220)}\ln\left(\frac{0.625}{0.545}\right)\right]^{-1}$$

$$= 283.46 \text{ Btu/hr.ft}^2.{}^oF$$

APPENDIX C

APPENDIX C

COMPUTER PROGRAM USED IN DATA REDUCTION

```
C      ****************************************************************
C      *                                                              *
C      *             DEFINITION OF SYMBOLS                            *
C      *                                                              *
C      ****************************************************************
C       AFLOW     -TEST CONDENSER CROSS SECTIONAL AREA,FT**2
C       AISF      -SECTIONAL HEAT TRANSFER AREA,FT**2
C       CPW       -COOLANT SPECIFIC HEAT,BTU/LBM DEG F
C       DPT       -TOTAL PRESSURE DROP, PSI
C       DPTS      -TOTAL PRESSURE DROP, BAR
C       DTD1-DTD4-SECTIONAL DRIVING TEMPERATURE DIFFERENCE,DEG F
C       DTDA      -TEST CONDENSER DRIVING TEMPERATURE DIFFERENCE, DEG F
C       DTDAS     -TEST CONDENSER DRIVING TEMPERATURE DIFFERFNCE, DEG C
C       ERROR     -PERCENTAGE DEVIATION BETWEEN THE HEAT GAINED BY COOLANT
C                   AND THE HEAT LOST BY CONDENSING FLUID
C       GPMF      -CONDENSING FLUID FLOW RATE THROUGH THE CONDENSER, GPM
C       GPMW      -COOLANT FLOW RATE THROUGH THE CONDENSER, GPM
C       GPMWS     -COOLANT FLOW RATE THROUGH THE CONDENSER IN SI UNITS,KG/HR
C       HTC1-HTC4-SECTIONAL AVERAGE HEAT TRANSFER COEFFICIENTS,BTU/HR FT**2 DEG F
C       HTCA      -OVERALL AVERAGE HEAT TRANSFER COEFFICIENT, BTD/HR FT**2 DEG F
C       HTCAS     -OVERALL AVERAGE HEAT TRANSFER COEFFICIENTS, W/M**2 DEG F
C       HF        -ENTHALPY OF SATURATED LIQUID AS A FUNCTION OF AVERAGE SATDRATED
C                   TEMPERATURE, BTU/LBM
C       HG        -ENTHALPY OF SATURATED VAPOUR AS A FUNCTION OF AVEPAGE SAT
C                   DRATED TEMPERATURE ,BTU/LHM
C       HIN       -ENTHALPY OF INLET TEST FLUID, BTU/LBM
C       HO1-HO4   -EXIT SECTIONAL ENTHALPY,BTU/LBM
C       K         -THERMAL CONDUCTIVITY OF THE SATURATED LIQUID,BTU/HR FT
C       IID       -INSIDE DIAMETER OF THE CONDENSER TUBE, FT
C       IOD       -OUTSIDE DIAMETER OF THE CONDENSER TUBE, FT
C       L         -SECTIONAL TEST CONDENSER LENGTH, FT
C       LDEN      -DENSITY OF SATURATED LIQUID AS A FUNCTION OF SATURATED
C                   TEMPERATURE, LBM/FT**3
C       LDENFM    -DENSITY OF LIQUID R-11 AT FLOW METER TEMPEPATURE, LBM/FT**3
C       N         -NDMBEP OF POINTS WITH DIFFENT MASS VELOCITIES
C       PI        -A CONSTANT
C       PA        -AVERAGE PRESSURE INSIDE THE CONDENSER, PSIA
C       PIN       -INLET PRESSURE OF THE CONDENSING FLDID, PSIA
C       PINS      -INLET PRESSURE OF THE CONDENSING FLUID IN SI DNITS, BAR
C       QF        -TOTAL HEAT TRANSFERED FROM THE TEST CONDENSER, BTU/HR
C       QFS       -TOTAL HEAT TRANSFERED FROM THE TEST FLDID, W
C       QW        -TOTAL HEAT TRANSFER RATE FROM THE TEST CONDENSER, BTU/HR
C       QWS       -TOTAL HEAT TRANSFER RATE FROM THE TEST CONDENSER, W
C       QW1-QW4   -SECTIONAL HEAT TRANSFER RATE, BTU/HR
C       T1-T27    -TEMPERATURE AT DIFFERENT LOCATIONS, DEG F
C       T1S       -INLET TEMPERATURE OF THE CONDENSING FLDID, DEG C
C       TG        -TEST FLUID TOTAL MASS VELOCITY, LBM/HR FT**2
C       TGS       -TEST FLUID TOTAL MASS VELOCITY, KG/S MT**2
C       TMF       -TEST FLUID MASS FLOW RATE, LBM/HR
C       TMW       -COOLANT MASS FLOW RATE, LBM/HR
C       TSA       -SATUBATION TEMPERATURE IN THE TEST CONDENSER, DEG F
C       TSAS      -SATURATION TEMPERATURE IN THE TEST CONDENSER, DEG C
C       TWA1-TWA4-AVERAGE SECTIONAL WALL TEMPERATURE, DEG F
C       TWA       -OVERALL AVERAGE WALL TEMPERATURE, DEG F
C       TWAS      -OVERALL AVERAGE WALL TEMPERATURE, DEG C
C       TVAP      -FUNCTION DSED TO CALCULATE SATURATION TEMPERATURE
C       XIN       -INLET TEST FLUID MASS QDALITY
C       X1-X4     -EXIT SECTIONAL TEST FLUID MASS QUALITY
1       REAL IID,IOD,LDEN,LDENFM
```

```
2          DIMENSION PIN(65),DPT(65),PINS(65),DPTS(65),GPMW(65),GPMWS(65),QW1
          1          (65),QW2(65),QW3(65),QW4(65),QW(65),QWS(65),T1(65),T1S(6
          2          5),TSA(65),TSAS(65),TWA1(65),TWA2(65),TWA3(65),TWA4(65),
          3          TWA(65),TWAS(65)
3          DIMENSION DTD1(65),DTD2(65),DTD3(65),DTD4(65),DTDA(65),DTDAS(65),
          1          GPMF(65),ERROR(65),HTC1(65),HTC2(65),HTC3(65),HTC4(65),
          2          HTCA(65),HTCAS(65),XIN(65),X1(65),X2(65),X3(65),X4(65),
          3          QF(65),QFS(65),GT(65),GTS(65),TMW(65),POUT(65),TCO(65),
          4          TCOS(65)
4          DIMENSION PIN2(5,65),PINS2(5,65),DPT2(5,65),DPTS2(5,65),
          1          GPMW2(5,65),GPMWS2(5,65),QW12(5,65),QW22(5,65),
          2          QW32(5,65),QW42(5,65),QWO2(5,65),QWS2(5,65),TO12(5,65),
          3          T1S2(5,65),TSAO2(5,65)
5          DIMENSION TSAS2(5,65),TWA12(5,65),TWA22(5,65),TWA32(5,65),
          1          TWA42(5,65),TWAO2(5,65),TWAS2(5,65),DTD12(5,65),
          2          DTD22(5,65),DTD32(5,65),DTD42(5,65),DTDA2(5,65),
          3          DTDAS2(5,65),GPMF2(5,65),ERROR2(5,65),HTC12(5,65),
          4          HTC22(5,65),HTC32(5,65),HTC42(5,65),HTCA2(5,65),
          5          HTCAS2(5,65)
6          DIMENSION XIN2(5,65),X12(5,65),X22(5,65),X32(5,65),X42(5,65),
          1          QF2(5,65),QFS2(5,65),GT2(5,65),GTS2(5,65),TMW2(5,65),
          2          POUT2(5,65),TCO2(5,65),TCOS2(5,65),NCOUNT(10)
     C
     C ******* FORMAT STATEMENTS
     C
7        10 FORMAT(4F10.5,3I10)
8        11 FORMAT(4F10.5)
9        12 FORMAT(10F8.2)
10      112 FORMAT(1H1)
11       21 FORMAT(/////,T13,'TABLE (D-1):-',/,'-',11X,80('-'),/)
12       22 FORMAT(T13,'RUN',T18,'INLET PRESS.',T31,'INLET TEMP.',T44,
           1'COND.FLUID MASS VEL.',T66,'COOLANT TIN',T80,'COOLANT RATE',/)
13       23 FORMAT(T14,'#',T18,'PSIA   BAR',T31,'DEG F DEG C',T44,'LBM/HR-FT2
           1  KG/S-M2  DEG F  DEG C   GPM    KG/HR',/,12X,80('-'),/)
14       25 FORMAT(T13,I3,T17,F5.2,T24,F5.3,T30,F6.1,T37,F5.1,T44,E11.5,T57,
           1F6.2,T66,F5.2,T73,F5.2,T80,F5.3,T87,F6.2)
15       26 FORMAT(/////,T10,'TABLE (D-2):-',/,'-',8X,97('-'),/)
16       27 FORMAT(T10,'RUN',T27,'QUALITIES',T53,'SAT. TEMP.',T66,'AVERAGE WAL
           1L TEMPEPATURES IN DEG F  DEG C')
17       50 FORMAT(T56,'TUBE')
18       28 FORMAT(T11,'#',T17,'XIN',T25,'I',T31,'II',T38,'III',T45,'IV',T52,
           1'DEG F',T59,'DEG C',T69,'I',T75,'II',T82,'III',T89,'IV',T95,'TUBE'
           2,T102,'TUBE',/,9X,97('-'),/)
19       30 FORMAT(T10,I3,T15,F6.3,T22,F6.3,T29,F6.3,T36,F6.3,T43,F6.3,T51,
           1F6.2,T59,F5.2,T66,F6.2,T73,F6.2,T80,F6.2,T87,F6.2,T94,F6.2,T102,
           2F5.2)
20       31 FORMAT(/////,T13,'TABLE (D-3):-',/,'-',11X,93('-'),/)
21       32 FORMAT(T13,'RUN  HEAT TRANSFER COEFFS. IN BTU/HR-SQFT*F',T58,
           1'W/SQM*C   DRIVING TEMP. DIFFERENCES DEG F DEG C',/)
22       33 FORMAT(T14,'#',T21,'I        II        III       IV       TUBE',T59,'TUBE'
           1,T68,'I      II      III     IV    TUBE   TUBE',/,12X,93('-'),/)
23       35 FORMAT(T13,I3,T17,F7.2,T25,F7.2,T33,F7.2,T41,F7.2,T49,F7.2,T58,
           1F6.1,T66,F5.2,T73,F5.2,T80,F5.2,T87,F5.2,T94,F5.2,T101,F5.2)
24       36 FORMAT(/////,T33,'TABLE (D-4):-',/,'-',31X,66('-'),/)
25       37 FORMAT(T33,'RUN',T49,'INLET PRESSURE',T77,'TOTAL PRESSURE DROP',
           1/)
26       38 FORMAT(T34,'#',T47,'PSIA',T62,'BAR',T78,'PSIA',T93,'PASCAL',/,
           132X,66('-'),/)
27       40 FORMAT(T33,I3,T46,F5.2,T60,F6.3,T74,F8.3,T91,F8.2)
28       41 FORMAT(/////,T13,'TABEL (D-5):-',/,12X,89('-'),/)
```

```
      42 FORMAT(T13,'RUN',T30,'COOLANT BTU/HR',T62,'TUBE',T78,'TEST FLUID',
     1T97,'ERROR',/)
      43 FORMAT(T14,'#',T21,'I          II        III         IV',T55,'BTU/HR
     1   W',T76,'BTU/HR        W                %',/,12X,89('-'),/)
      45 FORMAT(T13,I3,T18,F7.2,T27,F7.2,T36,F7.2,T45,F7.2,T54,F8.2,T65,
     1F7.2,T75,F8.2,T86,F7.2,T96,F6.2)
C     *****************************************************************
C
C     CALCULATION OF SATURATED LIQUID ENTHALPY IN BTU/LBM AS A FUNCTION OF
C      SATURATION TEMP. DEG F (CURVE FIT FROM ASHRAE TABLES )
C
       HFF(X)=8.0732+0.203944*X+1.495E-05*X*X+8.29E-08*X*X*X
C
C      CALCULATION OF SATURATED VAPOUR ENTHALPY IN BTU/LBM AS A FUNCTION
C      OF SATURATION TEMP. DEG F (CURVE FIT FROM ASHRAE TABLES )
C
       HGF(X)=91.942+0.121*X+9E-06*X*X-1.92E-07*X*X*X
C
C      CALCULATION OF SATURATED LIQUID DENSITY LBM/CU FT AS A FUNCTION OF
C      SATURATION TEMP DEG F (CURVE FIT FROM ASHRAE TABLES )
C
       LDEN(X)=96.734-0.02066*X-7.068E-04*X*X+2.611E-06*X*X*X
C
C      CALCULATION OF SATURATED TEMP. IN DEG F CORRESPONDING TO
C      SATURATION PR. IN PSIA (CURVE FIT FROM ASHRAE TABLES )
C
       TVAP(X)=5.4895+6.3303*X-0.127261*X*X+1.24322E-03*X*X*X
C
C     *****************************************************************
C
C ****** READ INPUT DATA
C
       ISTART=1
   800 CONTINUE
       READ(5,10) PI,IID,IOD,CPW,N,L,K
C      WRITE(6,10) PI,IID,IOD,CPW,N,L,K
       NCOUNT(ISTART)=N
       DO 1000 I=1,N
       READ(5,11) PIN(I),DPT(I),GPMW(I),GPMF(I)
C      WRITE(6,11) PIN(I),DPT(I),GPMW(I),GPMF(I)
       READ(5,12) T1(I),T2,T3,T4,T5,T6,T7,T8,T9,T10,T11,T12,T13,T14,T15,
     1T16,T17,T18,T19,T20,T21,T22,T23,T24,T25,T26,T27,HIN
C      WRITE(6,12)T1(I),T2,T3,T4,T5,T6,T7,T8,T9,T10,T11,T12,T13,T14,T15,
C     1T16,T17,T18,T19,T20,T21,T22,T23,T24,T25,T26,T27,HIN
C
C ****** CALCULATION OF THE AREAS
C
       AFLOW=PI*IID*IID/576
       AISF=PI*IID*L/144
C
C ****** CALCULATION OF HEAT GAINED BY WATER
C
       TCO(I)=T25
       TMW(I)=GPMW(I)*60*0.13368*62.3
       QW1(I)=TMW(I)*CPW*(T2-T7)
       QW2(I)=TMW(I)*CPW*(T8-T13)
       QW3(I)=TMW(I)*CPW*(T14-T19)
       QW4(I)=TMW(I)*CPW*(T20-T25)
       QW(I)=QW1(I)+QW2(I)+QW3(I)+QW4(I)
C
```

```
C ****** CALCULATION OF SATURATION TEMPERATURE
C
      POUT(I)=PIN(I)-DPT(I)
      TSA(I)=TVAP(PIN(I))
C
C ****** CALCULATION OF HEAT TRANSFER COEFFICIENTS
C
      B=IID/24./K*ALOG(IOD/IID)
      TWA1(I)=(T3+T4+T5+T6)/4.
      TWA2(I)=(T9+T10+T11+T12)/4.
      TWA3(I)=(T15+T16+T17+T18)/4.
      TWA4(I)=(T21+T22+T23+T24)/4.
      TWA(I)=(TWA1(I)+TWA2(I)+TWA3(I)+TWA4(I))/4.
      DTD1(I)=(TSA(I)+T1(I))*0.5-TWA1(I)
      DTD2(I)=TSA(I)-TWA2(I)
      DTD3(I)=TSA(I)-TWA3(I)
      DTD4(I)=TSA(I)-TWA4(I)
      DTDA(I)=TSA(I)-TWA(I)
      C1=PI*IID*L*DTD1(I)/(QW1(I)*144.)
      C2=PI*IID*L*DTD2(I)/(QW2(I)*144.)
      C3=PI*IID*L*DTD3(I)/(QW3(I)*144.)
      C4=PI*IID*L*DTD4(I)/(QW4(I)*144.)
      CA=4.*PI*IID*L*DTDA(I)/(QW(I)*144.)
      HTC1(I)=1.0/(C1-B)
      HTC2(I)=1.0/(C2-B)
      HTC3(I)=1.0/(C3-B)
      HTC4(I)=1.0/(C4-B)
      HTCA(I)=1.0/(CA-B)
C
C ****** CALCULATION OF QUALITIES
C
      HF=HFF(TSA(I))
      HG=HGF(TSA(I))
      XIN(I)=(HIN-HF)/(HG-HF)
      LDENFM=LDEN(T27)
      TMF=60.0*0.13368*GPMF(I)*LDENFM
      GT(I)=TMF/AFLOW
      HO1=HIN-QW1(I)/TMF
      X1(I)=(HO1-HF)/(HG-HF)
      HO2=HO1-QW2(I)/TMF
      X2(I)=(HO2-HF)/(HG-HF)
      HO3=HO2-QW3(I)/TMF
      X3(I)=(HO3-HF)/(HG-HF)
      HO4=HO3-QW4(I)/TMF
      X4(I)=(HO4-HF)/(HG-HF)
C
C ****** OVERALL HEAT BALANCE
C
      HFO=HFF(T26)
      QF(I)=TMF*(HIN-HFO)
      ERROR(I)=100.0*(QW(I)-QF(I))/QW(I)
C
C ****** CONVERSION TO SI UNITS
C
      PINS(I)=PIN(I)/14.5
      T1S(I)=(T1(I)-32.0)/1.8
      TCOS(I)=(TCO(I)-32.0)/1.8
      GTS(I)=GT(I)/737.339
      GPMWS(I)=GPMW(I)*226.662
      TSAS(I)=(TSA(I)-32.0)/1.8
```

```
      TWAS(I)=(TWA(I)-32.0)/1.8
      HTCAS(I)=HTCA(I)*5.6783
      DTDAS(I)=DTDA(I)/1.8
      DPTS(I)=DPT(I)*6.894757E+03
      QWS(I)=QW(I)*0.2928751
      QFS(I)=QF(I)*0.2928751
      PIN2(ISTART,I)=PIN(I)
      PINS2(ISTART,I)=PINS(I)
      T012(ISTART,I)=T1(I)
      T1S2(ISTART,I)=T1S(I)
      GT2(ISTART,I)=GT(I)
      GTS2(ISTART,I)=GTS(I)
      TCO2(ISTART,I)=TCO(I)
      TCOS2(ISTART,I)=TCOS(I)
      GPMW2(ISTART,I)=GPMW(I)
      GPMWS2(ISTART,I)=GPMWS(I)
      TSAO2(ISTART,I)=TSA(I)
      TSAS2(ISTART,I)=TSAS(I)
      TWA12(ISTART,I)=TWA1(I)
      TWA22(ISTART,I)=TWA2(I)
      TWA32(ISTART,I)=TWA3(I)
      TWA42(ISTART,I)=TWA4(I)
      TWAO2(ISTART,I)=TWA(I)
      TWAS2(ISTART,I)=TWAS(I)
      HTC12(ISTART,I)=HTC1(I)
      HTC22(ISTART,I)=HTC2(I)
      HTC32(ISTART,I)=HTC3(I)
      HTC42(ISTART,I)=HTC4(I)
      HTCA2(ISTART,I)=HTCA(I)
      HTCAS2(ISTART,I)=HTCAS(I)
      DTD12(ISTART,I)=DTD1(I)
      DTD22(ISTART,I)=DTD2(I)
      DTD32(ISTART,I)=DTD3(I)
      DTD42(ISTART,I)=DTD4(I)
      DTDA2(ISTART,I)=DTDA(I)
      DTDAS2(ISTART,I)=DTDAS(I)
      DPT2(ISTART,I)=DPT(I)
      DPTS2(ISTART,I)=DPTS(I)
      XIN2(ISTART,I)=XIN(I)
      X12(ISTART,I)=X1(I)
      X22(ISTART,I)=X2(I)
      X32(ISTART,I)=X3(I)
      X42(ISTART,I)=X4(I)
      QW12(ISTART,I)=QW1(I)
      QW22(ISTART,I)=QW2(I)
      QW32(ISTART,I)=QW3(I)
      QW42(ISTART,I)=QW4(I)
      QWO2(ISTART,I)=QW(I)
      QWS2(ISTART,I)=QWS(I)
      QF2(ISTART,I)=QF(I)
      QFS2(ISTART,I)=QFS(I)
      ERROR2(ISTART,I)=ERROR(I)
 1000 CONTINUE
      ISTART=ISTART+1
      IF(ISTART-5) 800,800,900
  900 CONTINUE
      IPRINT=0
      WRITE(6,112)
      WRITE(6,21)
      WRITE(6,22)
```

```
      WRITE(6,23)
      DO 241 ISTART=1,5
      II=ISTART*100
      N=NCOUNT(ISTART)
      DO 24 I=1,N
      III=II+I
      PIN(I)=PIN2(ISTART,I)
      PINS(I)=PINS2(ISTART,I)
      T1(I)=TO12(ISTART,I)
      T1S(I)=T1S2(ISTART,I)
      GT(I)=GT2(ISTART,I)
      GTS(I)=GTS2(ISTART,I)
      TCO(I)=TCO2(ISTART,I)
      TCOS(I)=TCOS2(ISTART,I)
      GPMW(I)=GPMW2(ISTART,I)
      GPMWS(I)=GPMWS2(ISTART,I)
      IPRINT=IPRINT+1
      IF(IPRINT.EQ.26) GO TO 1001
      GO TO 1002
 1001 CONTINUE
      WRITE(6,112)
      WRITE(6,21)
      WRITE(6,22)
      WRITE(6,23)
      IPRINT=0
 1002 CONTINUE
   24 WRITE(6,25) III,PIN(I),PINS(I),T1(I),T1S(I),GT(I),GTS(I),TCO(I),
     1TCOS(I),GPMW(I),GPMWS(I)
  241 CONTINUE
      IPRINT=0
      WRITE(6,112)
      WRITE(6,26)
      WRITE(6,27)
      WRITE(6,50)
      WRITE(6,28)
      DO 291 ISTART=1,5
      II=ISTART*100
      N=NCOUNT(ISTART)
      DO 29 I=1,N
      III=II+I
      XIN(I)=XIN2(ISTART,I)
      X1(I)=X12(ISTART,I)
      X2(I)=X22(ISTART,I)
      X3(I)=X32(ISTART,I)
      X4(I)=X42(ISTART,I)
      TSA(I)=TSAO2(ISTART,I)
      TSAS(I)=TSAS2(ISTART,I)
      TWA1(I)=TWA12(ISTART,I)
      TWA2(I)=TWA22(ISTART,I)
      TWA3(I)=TWA32(ISTART,I)
      TWA4(I)=TWA42(ISTART,I)
      TWA(I)=TWAO2(ISTART,I)
      TWAS(I)=TWAS2(ISTART,I)
      IPRINT=IPRINT+1
      IF(IPRINT.EQ.26) GO TO 1011
      GO TO 1012
 1011 CONTINUE
      WRITE(6,112)
      WRITE(6,26)
      WRITE(6,27)
```

```
      WRITE(6,50)
      WRITE(6,28)
      IPRINT=0
 1012 CONTINUE
   29 WRITE(6,30) III,XIN(I),X1(I),X2(I),X3(I),X4(I),TSA(I),TSAS(I),
     1TWA1(I),TWA2(I),TWA3(I),TWA4(I),TWA(I),TWAS(I)
  291 CONTINUE
      IPRINT=0
      WRITE(6,112)
      WRITE(6,31)
      WRITE(6,32)
      WRITE(6,33)
      DO 341 ISTART=1,5
      II=ISTART*100
      N=NCOUNT(ISTART)
      DO 34 I=1,N
      III=II+I
      HTC1(I)=HTC12(ISTART,I)
      HTC2(I)=HTC22(ISTART,I)
      HTC3(I)=HTC32(ISTART,I)
      HTC4(I)=HTC42(ISTART,I)
      HTCA(I)=HTCA2(ISTART,I)
      HTCAS(I)=HTCAS2(ISTART,I)
      DTD1(I)=DTD12(ISTART,I)
      DTD2(I)=DTD22(ISTART,I)
      DTD3(I)=DTD32(ISTART,I)
      DTD4(I)=DTD42(ISTART,I)
      DTDA(I)=DTDA2(ISTART,I)
      DTDAS(I)=DTDAS2(ISTART,I)
      IPRINT=IPRINT+1
      IF(IPRINT.EQ.26) GO TO 1013
      GO TO 1014
 1013 CONTINUE
      WRITE(6,112)
      WRITE(6,31)
      WRITE(6,32)
      WRITE(6,33)
      IPRINT=0
 1014 CONTINUE
   34 WRITE(6,35) III,HTC1(I),HTC2(I),HTC3(I),HTC4(I),HTCA(I),HTCAS(I),
     1DTD1(I),DTD2(I),DTD3(I),DTD4(I),DTDA(I),DTDAS(I)
  341 CONTINUE
      IPRINT=0
      WRITE(6,112)
      WRITE(6,36)
      WRITE(6,37)
      WRITE(6,38)
      DO 391 ISTART=1,5
      II=ISTART*100
      N=NCOUNT(ISTART)
      DO 39 I=1,N
      III=II+I
      PIN(I)=PIN2(ISTART,I)
      PINS(I)=PINS2(ISTART,I)
      DPT(I)=DPT2(ISTART,I)
      DPTS(I)=DPTS2(ISTART,I)
      IF(DPT(I).GT.0.0) IPRINT=IPRINT+1
      IF(IPRINT.EQ.26) GO TO 1015
      GO TO 1016
 1015 CONTINUE
```

```
      WRITE(6,112)
      WRITE(6,36)
      WRITE(6,37)
      WRITE(6,38)
      IPRINT=0
 1016 CONTINUE
   39 IF(DPT(I).GT.0.0) WRITE(6,40) III,PIN(I),PINS(I),DPT(I),DPTS(I)
  391 CONTINUE
      IPRINT=0
      WRITE(6,112)
      WRITE(6,41)
      WRITE(6,42)
      WRITE(6,43)
      DO 441 ISTART=1,5
      II=ISTART*100
      N=NCOUNT(ISTART)
      DO 44 I=1,N
      III=II+I
      QW1(I)=QW12(ISTART,I)
      QW2(I)=QW22(ISTART,I)
      QW3(I)=QW32(ISTART,I)
      QW4(I)=QW42(ISTART,I)
      QW(I)=QWO2(ISTART,I)
      QWS(I)=QWS2(ISTART,I)
      QF(I)=QF2(ISTART,I)
      QFS(I)=QFS2(ISTART,I)
      ERROR(I)=ERROR2(ISTART,I)
      IPRINT=IPRINT+1
      IF(IPRINT.EQ.26) GO TO 1017
      GO TO 1018
 1017 CONTINUE
      WRITE(6,112)
      WRITE(6,41)
      WRITE(6,42)
      WRITE(6,43)
      IPRINT=0
 1018 CONTINUE
      IF(X4(I).GT.0.0) WRITE(6,45) III,QW1(I),QW2(I),QW3(I),QW4(I),QW(I)
     1,QWS(I),QF(I),QFS(I),ERROR(I)
      IF(X4(I).LT.0.0) WRITE(6,45) III,QW1(I),QW2(I),QW3(I),QW4(I),QW(I)
     1,QWS(I),QF(I),QFS(I),ERROR(I)
   44 CONTINUE
  441 CONTINUE
      WRITE(6,112)
      STOP
      END

$ENTRY
```

APPENDIX D

TABLE (D-1) :- REDUCED DATA - INLET PRESSURES, TEMPERATURES AND FLOW RATES

RUN	INLET PRESS.		INLET TEMP.		COND.FLUID MASS VEL.		COOLANT TIN		COOLANT RATE	
#	PSIA	BAR	DEG F	DEG C	LBM/HR-FT2	KG/S-M2	DEG F	DEG C	GPM	KG/HR
101	19.47	1.343	101.5	38.6	0.37511E 05	50.87	62.42	16.90	2.100	475.99
102	19.57	1.350	101.3	38.5	0.39871E 05	54.07	62.42	16.90	2.260	512.26
103	19.56	1.349	104.0	40.0	0.42115E 05	57.12	63.14	17.30	2.500	566.65
104	19.72	1.360	103.5	39.7	0.44465E 05	60.30	63.50	17.50	2.550	577.99
105	19.31	1.332	103.6	39.8	0.46869E 05	63.57	62.96	17.20	2.750	623.32
106	19.61	1.353	102.0	38.9	0.49172E 05	66.69	63.68	17.60	2.950	668.65
107	19.61	1.353	104.0	40.0	0.51512E 05	69.86	62.96	17.20	3.110	704.92
108	18.91	1.304	104.0	40.0	0.30477E 05	41.33	62.96	17.20	1.330	301.46
109	18.87	1.301	103.1	39.5	0.32827E 05	44.52	61.16	16.20	1.120	253.86
110	19.07	1.315	99.8	37.7	0.35216E 05	47.76	60.98	16.10	1.220	276.53
111	18.88	1.302	102.9	39.4	0.53944E 05	73.16	60.26	15.70	3.150	713.99
112	21.38	1.474	106.7	41.5	0.37467E 05	50.81	60.44	15.80	0.810	183.60
113	21.57	1.488	106.2	41.2	0.39759E 05	53.92	61.16	16.20	0.910	206.26
114	21.68	1.495	105.8	41.0	0.42017E 05	56.98	61.34	16.30	1.480	335.46
115	21.48	1.481	109.6	43.1	0.44398E 05	60.21	61.16	16.20	1.860	421.59
116	21.48	1.481	109.0	42.8	0.46729E 05	63.37	62.96	17.20	2.030	460.12
117	21.46	1.480	108.0	42.2	0.48935E 05	66.37	64.40	18.00	2.220	503.19
118	21.29	1.468	109.6	43.1	0.51426E 05	69.75	60.62	15.90	1.820	412.52
119	21.29	1.468	106.5	41.4	0.53738E 05	72.88	61.52	16.40	2.060	466.92
120	21.18	1.461	108.7	42.6	0.56150E 05	76.15	60.80	16.00	2.250	509.99
121	21.28	1.468	107.6	42.0	0.58518E 05	79.36	62.06	16.70	2.540	575.72
122	21.28	1.468	108.9	42.7	0.60833E 05	82.50	62.06	16.70	2.760	625.59
123	23.88	1.647	114.4	45.8	0.36396E 05	49.36	62.96	17.20	0.530	120.13
124	23.98	1.654	115.2	46.2	0.39182E 05	53.14	62.96	17.20	0.590	133.73
125	23.98	1.654	112.1	44.5	0.41919E 05	56.85	62.96	17.20	0.660	149.60

TABLE (D-1) :- (CONTINUED)

RUN	INLET PRESS.		INLET TEMP.		COND. FLUID MASS VEL.		COOLANT TIN		COOLANT RATE	
#	PSIA	BAR	DEG F	DEG C	LBM/HR-FT2	KG/S-M2	DEG F	DEG C	GPM	KG/HR
126	23.78	1.640	112.8	44.9	0.44198E 05	59.94	63.68	17.60	0.860	194.93
127	23.68	1.633	113.2	45.1	0.46635E 05	63.25	62.42	16.90	1.050	238.00
128	23.81	1.642	115.9	46.6	0.48960E 05	66.40	63.68	17.60	1.120	253.86
129	23.81	1.642	115.0	46.1	0.51306E 05	69.58	63.32	17.40	1.310	296.93
130	23.51	1.622	111.2	44.0	0.53720E 05	72.86	60.62	15.90	1.480	335.46
131	23.51	1.622	113.2	45.1	0.56084E 05	76.06	61.70	16.50	1.630	369.46
132	23.71	1.635	112.6	44.8	0.58372E 05	79.17	62.78	17.10	1.750	396.66
133	23.71	1.635	114.4	45.8	0.60732E 05	82.37	62.96	17.20	2.020	457.86
134	18.98	1.309	101.3	38.5	0.35204E 05	47.75	62.64	17.02	1.740	394.39
135	19.58	1.350	100.6	38.1	0.37548E 05	50.92	62.96	17.20	1.780	403.46
136	19.08	1.316	101.7	38.7	0.39944E 05	54.17	61.52	16.40	2.080	471.46
137	19.48	1.343	102.0	38.9	0.42248E 05	57.30	61.34	16.30	2.170	491.86
138	19.28	1.329	102.2	39.0	0.44796E 05	60.75	61.70	16.50	2.290	519.06
139	19.38	1.336	104.7	40.4	0.47086E 05	63.86	61.34	16.30	2.510	568.92
140	19.48	1.343	101.8	38.8	0.49417E 05	67.02	61.70	16.50	2.680	607.45
141	19.48	1.343	104.0	40.0	0.51785E 05	70.23	61.34	16.30	2.740	621.05
142	18.99	1.309	101.3	38.5	0.54131E 05	73.41	60.62	15.90	3.150	713.99
143	24.09	1.661	113.4	45.2	0.41132E 05	55.78	66.92	19.40	0.850	192.66
144	24.80	1.710	111.0	43.9	0.44435E 05	60.26	67.28	19.60	1.110	251.59
145	24.90	1.717	112.8	44.9	0.46830E 05	63.51	68.00	20.00	1.460	330.93
146	24.10	1.662	110.0	43.3	0.49197E 05	66.72	66.56	19.20	1.580	358.13
147	24.51	1.690	112.6	44.8	0.51537E 05	69.90	67.28	19.60	1.820	412.52
148	24.11	1.662	112.1	44.5	0.53837E 05	73.01	67.10	19.50	2.100	475.99
149	24.11	1.662	112.1	44.5	0.56253E 05	76.29	67.28	19.60	2.250	509.99
150	24.20	1.669	113.7	45.4	0.58489E 05	79.32	67.82	19.90	2.370	537.19
151	24.30	1.676	114.4	45.8	0.60772E 05	82.42	68.90	20.50	2.570	582.52

TABLE (D-1) :- (CONTINUED)

RUN	INLET PRESS.		INLET TEMP.		COND.FLUID MASS VEL.		COOLANT TIN		COOLANT RATE	
#	PSIA	BAR	DEG F	DEG C	LBM/HR-FT2	KG/S-M2	DEG F	DEG C	GPM	KG/HR
152	24.70	1.704	118.0	47.8	0.63078E 05	85.55	69.98	21.10	2.840	643.72
201	19.05	1.314	103.6	39.8	0.40069E 05	54.34	62.60	17.00	1.410	319.59
202	18.65	1.287	101.7	38.7	0.42396E 05	57.50	62.24	16.80	1.460	330.93
203	18.72	1.291	103.5	39.7	0.44540E 05	60.41	62.06	16.70	2.120	480.52
204	18.93	1.306	103.8	39.9	0.46753E 05	63.41	62.60	17.00	2.180	494.12
205	18.74	1.292	104.4	40.2	0.49017E 05	66.48	62.78	17.10	2.490	564.39
206	21.39	1.475	109.0	42.8	0.39936E 05	54.16	63.32	17.40	1.300	294.66
207	21.59	1.489	107.2	41.8	0.42199E 05	57.23	62.42	16.90	1.350	305.99
208	21.49	1.482	105.8	41.0	0.44459E 05	60.30	63.32	17.40	1.510	342.26
209	21.92	1.511	112.5	44.7	0.46659E 05	63.28	62.96	17.20	1.460	330.93
210	24.15	1.665	116.6	47.0	0.39816E 05	54.00	62.24	16.80	0.710	160.93
211	23.85	1.644	113.5	45.3	0.44244E 05	60.00	61.88	16.60	1.030	233.46
212	23.74	1.638	114.1	45.6	0.42016E 05	56.98	61.88	16.60	0.960	217.60
213	23.45	1.617	114.6	45.9	0.46504E 05	63.07	62.78	17.10	1.140	258.39
214	18.65	1.286	100.9	38.3	0.51238E 05	69.49	61.34	16.30	2.100	475.99
215	18.45	1.272	102.9	39.4	0.53564E 05	72.64	60.08	15.60	2.300	521.32
216	18.65	1.286	102.9	39.4	0.55740E 05	75.60	61.16	16.20	2.440	553.06
217	18.65	1.286	105.1	40.6	0.57983E 05	78.64	61.34	16.30	2.720	616.52
218	18.65	1.286	102.9	39.4	0.60203E 05	81.65	61.34	16.30	2.750	623.32
219	20.96	1.445	108.3	42.4	0.48952E 05	66.39	61.34	16.30	1.900	430.66
220	20.96	1.446	108.7	42.6	0.51076E 05	69.27	63.50	17.50	1.550	351.33
221	21.15	1.459	108.1	42.3	0.53386E 05	72.40	61.70	16.50	1.690	383.06
222	22.04	1.520	108.0	42.2	0.55592E 05	75.40	61.34	16.30	1.800	407.99
223	21.34	1.472	106.3	41.3	0.57762E 05	78.34	61.88	16.60	1.830	414.79
224	21.34	1.472	105.6	40.9	0.60044E 05	81.43	61.88	16.60	1.900	430.66
225	21.54	1.486	106.5	41.4	0.62246E 05	84.42	62.42	16.90	2.110	478.26

TABLE (D-1) :- (CONTINUED)

RUN	INLET PRESS.		INLET TEMP.		COND.FLUID MASS VEL.		COOLANT TIN		COOLANT RATE	
#	PSIA	BAR	DEG F	DEG C	LBM/HR-FT2	KG/S-M2	DEG F	DEG C	GPM	KG/HR
226	23.63	1.630	116.1	46.7	0.48570E 05	65.87	63.14	17.30	1.170	265.19
227	23.63	1.630	116.6	47.0	0.50821E 05	68.92	62.60	17.00	1.320	299.19
228	23.70	1.634	114.1	45.6	0.53217E 05	72.18	61.70	16.50	1.250	283.33
229	23.90	1.648	116.2	46.8	0.55397E 05	75.13	61.88	16.60	1.370	310.53
230	23.90	1.648	118.4	48.0	0.57647E 05	78.18	62.24	16.80	1.520	344.53
231	23.26	1.604	111.7	44.3	0.59874E 05	81.20	61.70	16.50	1.500	339.99
232	23.55	1.624	114.1	45.6	0.62132E 05	84.26	60.98	16.10	1.600	362.66
233	18.76	1.293	102.0	38.9	0.62360E 05	84.57	62.78	17.10	3.080	698.12
234	19.79	1.365	102.6	39.2	0.33438E 05	45.35	68.72	20.40	1.440	326.39
235	19.69	1.358	102.0	38.9	0.35314E 05	47.89	67.82	19.90	1.680	380.79
236	19.65	1.355	100.8	38.2	0.38215E 05	51.83	68.36	20.20	1.850	419.32
237	19.95	1.376	100.2	37.9	0.40042E 05	54.31	68.90	20.50	2.060	466.92
238	19.36	1.335	101.8	38.8	0.42347E 05	57.43	67.28	19.60	2.160	489.59
239	19.66	1.356	101.3	38.5	0.44511E 05	60.37	68.72	20.40	2.330	528.12
240	19.26	1.328	100.4	38.0	0.46768E 05	63.43	68.00	20.00	2.590	587.05
241	19.36	1.335	100.6	38.1	0.48985E 05	66.43	67.64	19.80	2.620	593.85
242	19.46	1.342	100.9	38.3	0.51331E 05	69.62	67.82	19.90	2.930	664.12
243	24.18	1.667	113.4	45.2	0.39976E 05	54.22	69.98	21.10	0.800	181.33
244	24.74	1.706	112.1	44.5	0.42108E 05	57.11	73.22	22.90	1.040	235.73
245	25.04	1.727	112.8	44.9	0.44214E 05	59.96	69.08	20.60	1.370	310.53
246	24.54	1.692	111.9	44.4	0.46581E 05	63.17	73.40	23.00	1.520	344.53
247	25.04	1.727	113.5	45.3	0.48732E 05	66.09	68.90	20.50	1.730	392.13
248	24.74	1.706	111.9	44.4	0.50957E 05	69.11	73.76	23.20	1.940	439.72
249	25.22	1.740	112.6	44.8	0.53013E 05	71.90	73.40	23.00	2.160	489.59
250	24.72	1.705	112.3	44.6	0.55333E 05	75.04	75.56	24.20	2.220	503.19
251	24.82	1.712	112.3	44.6	0.57512E 05	78.00	70.52	21.40	2.450	555.32

TABLE (D-1) :- (CONTINUED)

RUN	INLET PRESS.		INLET TEMP.		COND.FLUID MASS VEL.		COOLANT TIN		COOLANT RATE	
#	PSIA	BAR	DEG F	DEG C	LBM/HR-FT2	KG/S-M2	DEG F	DEG C	GPM	KG/HR
252	24.52	1.691	113.5	45.3	0.59774E 05	81.07	70.52	21.40	2.660	602.92
301	18.47	1.274	99.1	37.3	0.30615E 05	41.52	59.90	15.50	1.450	328.66
302	21.03	1.451	101.8	38.8	0.30039E 05	40.74	59.90	15.50	0.790	179.06
303	23.53	1.623	115.0	46.1	0.30549E 05	41.43	59.54	15.30	0.520	117.86
304	18.53	1.278	102.4	39.1	0.31937E 05	43.31	59.36	15.20	1.590	360.39
305	21.13	1.458	110.7	43.7	0.31895E 05	43.26	58.64	14.80	0.840	190.40
306	23.66	1.632	109.0	42.8	0.32099E 05	43.53	59.36	15.20	0.473	107.21
307	18.76	1.294	99.7	37.6	0.34123E 05	46.28	59.90	15.50	1.620	367.19
308	21.06	1.453	110.7	43.7	0.33681E 05	45.68	60.98	16.10	1.100	249.33
309	23.56	1.625	113.9	45.5	0.33637E 05	45.62	58.82	14.90	0.560	126.93
310	23.67	1.632	115.2	46.2	0.35155E 05	47.68	59.18	15.10	0.610	138.26
311	21.07	1.453	101.1	38.4	0.35271E 05	47.84	59.36	15.20	0.970	219.86
312	18.77	1.294	100.0	37.8	0.35317E 05	47.90	60.62	15.90	1.870	423.86
313	18.63	1.285	95.4	35.2	0.36866E 05	50.00	59.18	15.10	1.740	394.39
314	21.53	1.485	102.2	39.0	0.36714E 05	49.79	61.16	16.20	1.170	265.19
315	21.44	1.479	104.9	40.5	0.36775E 05	49.87	59.00	15.00	0.980	222.13
316	23.84	1.644	108.9	42.7	0.36358E 05	49.31	59.54	15.30	0.620	140.53
317	19.04	1.313	102.7	39.3	0.38000E 05	51.54	60.08	15.60	2.020	457.86
318	21.19	1.462	105.4	40.8	0.38332E 05	51.99	59.00	15.00	1.130	256.13
319	23.79	1.641	110.1	43.4	0.38237E 05	51.86	59.00	15.00	0.750	170.00
320	18.86	1.301	97.2	36.2	0.39881E 05	54.09	60.26	15.70	2.220	503.19
321	21.26	1.466	108.3	42.4	0.39789E 05	53.96	60.80	16.00	1.380	312.79
322	23.56	1.625	111.9	44.4	0.39684E 05	53.82	61.16	16.20	0.950	215.33
323	23.79	1.641	112.8	44.9	0.41176E 05	55.84	61.16	16.20	1.080	244.79
324	21.35	1.472	99.1	37.3	0.41265E 05	55.96	61.34	16.30	1.560	353.59
325	19.24	1.327	97.5	36.4	0.41354E 05	56.08	60.98	16.10	2.930	664.12

TABLE (D-1) :- (CONTINUED)

RUN	INLET PRESS.		INLET TEMP.		COND. FLUID MASS VEL.		COOLANT TIN		COOLANT RATE	
#	PSIA	BAR	DEG F	DEG C	LBM/HR-FT2	KG/S-M2	DEG F	DEG C	GPM	KG/HR
326	19.24	1.327	96.8	36.0	0.42948E 05	58.25	60.98	16.10	2.980	675.45
327	21.34	1.472	106.5	41.4	0.42800E 05	58.05	62.24	16.80	1.700	385.33
328	23.65	1.631	112.1	44.5	0.42714E 05	57.93	61.88	16.60	1.090	247.06
329	23.74	1.637	113.5	45.3	0.44165E 05	59.90	62.42	16.90	1.260	285.59
330	18.74	1.293	99.0	37.2	0.44547E 05	60.42	59.90	15.50	3.040	689.05
331	21.34	1.472	104.0	40.0	0.44415E 05	60.24	59.90	15.50	1.610	364.93
332	23.94	1.651	113.2	45.1	0.44232E 05	59.99	61.16	16.20	1.080	244.79
333	21.14	1.458	104.4	40.2	0.45530E 05	61.75	60.98	16.10	2.140	485.06
334	23.74	1.638	114.4	45.8	0.45717E 05	62.00	61.52	16.40	1.200	271.99
335	18.74	1.293	98.1	36.7	0.46051E 05	62.46	59.90	15.50	2.910	659.59
336	18.90	1.303	96.6	35.9	0.47453E 05	64.36	60.80	16.00	2.940	666.39
337	21.20	1.462	105.3	40.7	0.47343E 05	64.21	60.80	16.00	2.020	457.86
338	19.09	1.317	97.7	36.5	0.49007E 05	66.46	60.98	16.10	3.060	693.59
339	21.09	1.455	105.4	40.8	0.48950E 05	66.39	61.52	16.40	2.030	460.12
340	23.39	1.613	113.5	45.3	0.48861E 05	66.27	60.80	16.00	1.420	321.86
341	23.49	1.620	110.7	43.7	0.47320E 05	64.18	60.98	16.10	1.360	308.26
342	19.50	1.345	100.2	37.9	0.27528E 05	37.33	60.44	15.80	1.850	419.32
343	19.70	1.358	102.7	39.3	0.29074E 05	39.43	62.78	17.10	1.910	432.92
344	19.60	1.352	100.8	38.2	0.30585E 05	41.48	62.96	17.20	2.030	460.12
345	19.63	1.354	101.7	38.7	0.32178E 05	43.64	64.40	18.00	2.050	464.66
346	19.13	1.320	98.4	36.9	0.33720E 05	45.73	63.32	17.40	2.250	509.99
347	19.23	1.326	99.9	37.7	0.35271E 05	47.84	63.86	17.70	2.350	532.66
348	18.93	1.306	100.0	37.8	0.36799E 05	49.91	63.32	17.40	2.500	566.65
349	18.63	1.285	100.4	38.0	0.38439E 05	52.13	62.42	16.90	2.710	614.25
350	19.03	1.313	101.3	38.5	0.40240E 05	54.57	64.04	17.80	2.810	636.92
351	24.75	1.707	113.7	45.4	0.27432E 05	37.20	68.72	20.40	0.530	120.13

TABLE (D-1) :- (CONTINUED)

RUN	INLET PRESS.		INLET TEMP.		COND.FLUID MASS VEL.		COOLANT TIN		COOLANT RATE	
#	PSIA	BAR	DEG F	DEG C	LBM/HR-FT2	KG/S-M2	DEG F	DEG C	GPM	KG/HR
352	24.75	1.707	112.8	44.9	0.28953E 05	39.27	69.44	20.80	0.600	136.00
353	24.75	1.707	112.6	44.8	0.30524E 05	41.40	68.90	20.50	0.690	156.40
354	24.85	1.714	113.2	45.1	0.31997E 05	43.40	70.52	21.40	0.820	185.86
355	24.35	1.679	112.1	44.5	0.33620E 05	45.60	67.10	19.50	0.960	217.60
356	23.75	1.638	113.7	45.4	0.35196E 05	47.73	66.38	19.10	1.080	244.79
357	24.99	1.723	113.5	45.3	0.36568E 05	49.59	72.86	22.70	1.100	249.33
358	24.59	1.696	111.2	44.0	0.38186E 05	51.79	69.44	20.80	1.160	262.93
359	24.49	1.689	114.8	46.0	0.39730E 05	53.88	68.36	20.20	1.250	283.33
401	19.49	1.344	97.3	36.3	0.34664E 05	47.01	60.62	15.90	3.000	679.99
402	23.79	1.640	114.1	45.6	0.21634E 05	29.34	61.52	16.40	0.510	115.60
403	23.79	1.640	113.4	45.2	0.19426E 05	26.35	61.52	16.40	0.500	113.33
404	21.26	1.466	103.5	39.7	0.19504E 05	26.45	60.44	15.80	0.700	158.66
405	21.16	1.459	107.6	42.0	0.21680E 05	29.40	60.08	15.60	0.850	192.66
406	23.56	1.625	113.9	45.5	0.21623E 05	29.33	60.62	15.90	0.500	113.33
407	21.56	1.487	104.4	40.2	0.22731E 05	30.83	62.06	16.70	0.950	215.33
408	19.05	1.314	100.9	38.3	0.20842E 05	28.27	59.18	15.10	1.100	249.33
409	19.05	1.314	99.7	37.6	0.21723E 05	29.46	59.36	15.20	1.300	294.66
410	23.85	1.645	115.2	46.2	0.22689E 05	30.77	62.06	16.70	0.560	126.93
411	18.93	1.305	97.9	36.6	0.22877E 05	31.03	59.54	15.30	1.290	292.39
412	18.65	1.286	93.9	34.4	0.23934E 05	32.46	59.54	15.30	1.570	355.86
413	21.35	1.472	102.9	39.4	0.23847E 05	32.34	60.80	16.00	0.900	204.00
414	19.13	1.319	97.7	36.5	0.24969E 05	33.86	60.98	16.10	1.700	385.33
415	21.03	1.450	106.7	41.5	0.24948E 05	33.84	61.70	16.50	1.050	238.00
416	23.93	1.650	115.9	46.6	0.24870E 05	33.73	62.60	17.00	0.680	154.13
417	21.45	1.479	106.3	41.3	0.25978E 05	35.23	61.70	16.50	1.400	317.33
418	23.91	1.649	113.7	45.4	0.25840E 05	35.04	63.86	17.70	0.800	181.33

TABLE (D-1) :- (CONTINUED)

RUN	INLET PRESS.		INLET TEMP.		COND. FLUID MASS VEL.		COOLANT TIN		COOLANT RATE	
#	PSIA	BAR	DEG F	DEG C	LBM/HR-FT2	KG/S-M2	DEG F	DEG C	GPM	KG/HR
419	19.14	1.320	99.1	37.3	0.26051E 05	35.33	61.16	16.20	1.760	398.93
420	19.14	1.320	100.9	38.3	0.27096E 05	36.75	60.98	16.10	1.790	405.72
421	19.34	1.334	102.6	39.2	0.28265E 05	38.33	60.08	15.60	1.940	439.72
422	21.33	1.471	105.8	41.0	0.27100E 05	36.75	60.08	15.60	1.090	247.06
423	21.33	1.471	107.8	42.1	0.28205E 05	38.25	59.18	15.10	1.220	276.53
424	21.33	1.471	104.7	40.4	0.29246E 05	39.66	61.16	16.20	1.300	294.66
425	23.93	1.651	113.9	45.5	0.27037E 05	36.67	61.16	16.20	0.720	163.20
426	24.23	1.671	112.8	44.9	0.28102E 05	38.11	59.90	15.50	0.760	172.26
427	19.14	1.320	101.1	38.4	0.29280E 05	39.71	60.26	15.70	2.190	496.39
428	23.74	1.638	113.9	45.5	0.29135E 05	39.51	60.98	16.10	0.840	190.40
429	19.02	1.312	99.1	37.3	0.30404E 05	41.23	59.36	15.20	2.410	546.26
430	21.24	1.465	105.3	40.7	0.30309E 05	41.11	59.90	15.50	1.320	299.19
431	23.82	1.643	114.8	46.0	0.29159E 05	39.55	60.62	15.90	0.840	190.40
432	23.72	1.636	116.8	47.1	0.30198E 05	40.96	62.06	16.70	0.960	217.60
433	19.04	1.313	101.3	38.5	0.31515E 05	42.74	58.64	14.80	2.390	541.72
501	19.78	1.364	101.7	38.7	0.12863E 05	17.45	61.70	16.50	1.320	299.19
502	21.61	1.491	106.0	41.1	0.12715E 05	17.25	60.62	15.90	1.000	226.66
503	23.66	1.632	113.4	45.2	0.12642E 05	17.14	60.44	15.80	0.820	185.86
504	21.56	1.487	106.2	41.2	0.13942E 05	18.91	61.34	16.30	1.170	265.19
505	23.96	1.652	115.2	46.2	0.13952E 05	18.92	60.80	16.00	0.830	188.13
506	19.37	1.336	97.3	36.3	0.13995E 05	18.98	60.62	15.90	1.620	367.19
507	19.27	1.329	97.2	36.2	0.14692E 05	19.93	61.70	16.50	1.760	398.93
508	21.67	1.494	104.7	40.4	0.14629E 05	19.84	60.98	16.10	1.110	251.59
509	19.04	1.313	97.9	36.6	0.15371E 05	20.85	60.98	16.10	1.900	430.66
510	21.45	1.479	107.1	41.7	0.15338E 05	20.80	61.52	16.40	1.200	271.99
511	24.15	1.665	113.9	45.5	0.14612E 05	19.82	60.62	15.90	0.790	179.06

TABLE (D-1) :- (CONTINUED)

RUN	INLET PRESS.		INLET TEMP.		COND.FLUID MASS VEL.		COOLANT TIN		COOLANT RATE	
#	PSIA	BAR	DEG F	DEG C	LBM/HR-FT2	KG/S-M2	DEG F	DEG C	GPM	KG/HR
512	24.04	1.658	114.4	45.8	0.15284E 05	20.73	61.34	16.30	0.950	215.33
513	18.96	1.308	99.9	37.7	0.16083E 05	21.81	61.34	16.30	2.000	453.32
514	21.86	1.508	106.9	41.6	0.16124E 05	21.87	62.24	16.80	1.300	294.66
515	23.76	1.639	117.9	47.7	0.16004E 05	21.70	60.80	16.00	0.970	219.86
516	18.65	1.287	102.7	39.3	0.16819E 05	22.81	62.06	16.70	2.200	498.66
517	19.55	1.349	103.5	39.7	0.17494E 05	23.73	62.06	16.70	2.300	521.32
518	21.04	1.451	106.7	41.5	0.16752E 05	22.72	60.98	16.10	1.070	242.53
519	20.96	1.445	108.3	42.4	0.17597E 05	23.87	61.70	16.50	1.240	281.06
520	23.59	1.627	114.3	45.7	0.16722E 05	22.68	61.16	16.20	0.660	149.60
521	18.65	1.286	95.4	35.2	0.18179E 05	24.66	61.34	16.30	2.140	485.06
522	21.04	1.451	106.7	41.5	0.18104E 05	24.55	60.62	15.90	1.250	283.33
523	23.85	1.644	116.4	46.9	0.17392E 05	23.59	61.16	16.20	0.730	165.46
524	18.65	1.287	103.3	39.6	0.18907E 05	25.64	60.98	16.10	2.420	548.52
525	21.54	1.485	105.1	40.6	0.18819E 05	25.52	61.34	16.30	1.200	271.99
526	23.74	1.637	115.9	46.6	0.18086E 05	24.53	60.98	16.10	0.850	192.66
527	21.15	1.459	104.9	40.5	0.19539E 05	26.50	62.06	16.70	1.270	287.86
528	21.15	1.459	105.3	40.7	0.20281E 05	27.51	60.26	15.70	1.430	324.13
529	23.76	1.638	116.1	46.7	0.18772E 05	25.46	60.98	16.10	0.830	188.13
530	23.13	1.596	113.7	45.4	0.19493E 05	26.44	61.70	16.50	0.950	215.33
531	23.76	1.638	116.8	47.1	0.20196E 05	27.39	60.80	16.00	0.960	217.60
532	23.65	1.631	115.5	46.4	0.20791E 05	28.20	60.80	16.00	1.050	238.00
533	21.18	1.461	106.2	41.2	0.20912E 05	28.36	59.72	15.40	1.490	337.73
534	19.18	1.323	100.6	38.1	0.19594E 05	26.57	61.16	16.20	2.460	557.59
535	18.85	1.300	102.9	39.4	0.20273E 05	27.49	61.88	16.60	2.610	591.59
536	19.18	1.323	102.4	39.1	0.20978E 05	28.45	61.88	16.60	2.640	598.39

TABLE (D-2):- REDUCED DATA - EXIT QUALITIES AND TEMPERATURES

RUN	QUALITIES					SAT. TEMP. TUBE		AVERAGE WALL TEMPERATURES IN DEG F					DEG C
#	XIN	I	II	III	IV	DEG F	DEG C	I	II	III	IV	TUBE	TUBE
101	1.022	0.737	0.288	0.084	-0.079	89.67	32.04	88.25	72.18	71.64	70.88	75.74	24.30
102	1.021	0.856	0.650	0.360	-0.012	89.95	32.20	86.09	73.31	74.12	70.74	76.07	24.48
103	1.027	0.724	0.421	0.161	-0.055	89.93	32.18	89.60	73.13	71.69	69.80	76.05	24.47
104	1.025	0.732	0.397	0.104	-0.063	90.38	32.43	89.01	72.36	70.56	69.08	75.26	24.03
105	1.027	0.728	0.472	0.301	0.001	89.23	31.80	88.83	72.50	70.43	68.76	75.13	23.96
106	1.023	0.804	0.541	0.235	-0.027	90.07	32.26	82.80	76.41	72.63	69.35	75.30	24.06
107	1.026	0.762	0.498	0.190	-0.030	90.07	32.26	88.56	72.00	69.44	68.18	74.55	23.64
108	1.030	0.744	0.490	0.205	-0.018	88.10	31.17	89.64	73.44	70.34	69.39	75.71	24.28
109	1.028	0.756	0.458	0.259	-0.039	87.97	31.10	89.33	73.17	70.74	68.90	75.54	24.19
110	1.021	0.769	0.315	0.114	-0.038	88.54	31.41	83.79	74.79	71.64	68.36	74.65	23.69
111	1.028	0.858	0.518	0.264	0.009	88.00	31.11	80.91	71.60	69.93	68.22	72.67	22.59
112	1.023	0.785	0.468	0.230	-0.008	94.80	34.89	94.19	77.81	73.85	71.06	79.23	26.24
113	1.021	0.769	0.399	0.181	-0.020	95.31	35.17	94.10	77.67	73.71	71.46	79.24	26.24
114	1.019	0.760	0.605	0.295	0.037	95.57	35.32	89.42	80.96	76.32	74.84	80.39	26.88
115	1.028	0.782	0.475	0.198	-0.017	95.06	35.03	93.65	75.42	74.03	72.72	78.96	26.09
116	1.027	0.708	0.294	0.071	-0.025	95.06	35.03	93.33	74.52	74.39	74.12	79.09	26.16
117	1.025	0.692	0.359	0.127	-0.007	95.00	35.00	93.20	74.30	73.35	73.22	78.52	25.84
118	1.029	0.769	0.614	0.328	0.017	94.56	34.76	93.33	75.51	73.80	70.74	78.35	25.75
119	1.023	0.717	0.464	0.239	-0.014	94.56	34.76	92.48	74.52	72.90	70.83	77.69	25.38
120	1.027	0.792	0.557	0.234	-0.001	94.30	34.61	93.02	73.63	70.02	69.30	76.49	24.72
121	1.025	0.770	0.516	0.198	0.007	94.56	34.75	92.75	73.53	70.47	69.53	76.57	24.76
122	1.027	0.728	0.428	0.229	-0.071	94.56	34.75	85.95	77.27	74.03	69.08	76.58	24.77
123	1.026	0.822	0.617	0.316	0.036	101.02	38.35	96.30	88.70	83.48	76.23	86.18	30.10
124	1.028	0.794	0.538	0.271	0.015	101.26	38.48	101.43	85.28	80.55	76.28	85.89	29.94
125	1.022	0.848	0.568	0.289	0.022	101.26	38.48	96.17	87.03	82.26	76.41	85.47	29.71

TABLE (D-2):- (CONTINUED)

RUN		QUALITIES				SAT. TEMP. TUBE		AVERAGE WALL TEMPERATURES IN DEG F					DEG C
#	XIN	I	II	III	IV	DEG F	DEG C	I	II	III	IV	TUBE	TUBE
126	1.023	0.765	0.535	0.290	0.032	100.78	3B.21	99.50	83.34	79.57	75.65	84.51	29.17
127	1.025	0.792	0.542	0.326	0.044	100.55	38.08	99.50	82.44	80.15	74.39	84.12	28.96
128	1.029	0.809	0.488	0.252	0.032	100.85	38.25	100.71	82.35	79.57	74.57	84.30	29.06
129	1.027	0.801	0.556	0.292	0.028	100.85	38.25	99.18	81.77	79.74	74.03	83.68	28.71
130	1.021	0.838	0.553	0.289	0.004	100.13	37.85	91.62	82.63	80.60	73.44	82.07	27.82
131	1.025	0.780	0.565	0.265	0.029	100.13	37.85	97.65	80.60	78.03	71.51	81.95	27.75
132	1.023	0.758	0.514	0.248	0.005	100.61	38.12	97.70	80.46	78.21	72.23	82.15	27.86
133	1.026	0.781	0.486	0.216	-0.030	100.61	38.12	91.04	82.40	79.63	68.74	80.45	26.92
134	1.022	0.698	0.267	0.159	0.023	88.29	31.27	81.18	72.14	76.95	68.67	74.74	23.74
135	1.020	0.640	0.363	0.156	-0.017	89.98	32.21	88.25	73.22	71.01	69.75	75.56	24.20
136	1.026	0.685	0.533	0.230	0.002	88.58	31.43	80.64	77.09	71.46	68.18	74.34	23.52
137	1.023	0.724	0.537	0.200	-0.025	B9.70	32.06	88.43	71.33	68.90	68.13	74.20	23.44
138	1.025	0.802	0.504	0.206	-0.017	89.13	31.74	80.55	76.95	72.36	68.32	74.55	23.64
139	1.028	0.718	0.485	0.213	-0.020	89.41	31.90	80.78	77.09	72.54	67.82	74.56	23.64
140	1.023	0.707	0.509	0.232	-0.005	89.69	32.05	87.66	71.51	69.21	67.82	74.05	23.36
141	1.027	0.680	0.410	0.140	-0.091	89.69	32.05	78.80	76.73	72.09	67.55	73.79	23.22
142	1.024	0.685	0.516	0.304	-0.034	88.31	31.28	77.00	75.88	71.51	67.73	73.03	22.79
143	1.023	0.763	0.565	0.259	-0.001	101.50	38.61	101.03	B5.19	81.63	80.60	87.11	30.62
144	1.016	0.794	0.386	0.201	-0.002	103.16	39.54	96.26	85.95	85.37	80.73	87.08	30.60
145	1.018	0.718	0.395	0.187	-0.044	103.39	39.66	95.20	85.73	84.65	80.51	86.52	30.29
146	1.017	0.779	0.399	0.186	-0.004	101.53	38.63	97.56	82.31	80.82	77.99	84.67	29.26
147	1.020	0.707	0.445	0.158	-0.051	102.49	39.16	94.14	83.93	82.89	77.09	84.51	29.17
148	1.020	0.761	0.501	0.271	0.011	101.55	38.64	97.88	81.32	79.20	75.96	83.59	28.66
149	1.021	0.784	0.488	0.163	-0.074	101.55	38.64	90.59	85.01	80.42	75.60	82.91	28.28
150	1.023	0.753	0.574	0.304	0.004	101.78	38.77	98.91	82.17	77.85	75.65	83.65	28.69
151	1.024	0.680	0.398	0.148	-0.071	102.02	38.90	90.09	85.86	78.26	75.69	82.48	28.04

TABLE (D-2):- (CONTINUED)

RUN		QUALITIES				SAT. TEMP. TUBE		AVERAGE WALL TEMPERATURES IN DEG F					DEG C
#	XIN	I	II	III	IV	DEG F	DEG C	I	II	III	IV	TUBE	TUBE
152	1.029	0.829	0.563	0.296	0.062	102.95	39.42	95.45	86.27	78.98	77.04	84.44	29.13
201	1.028	0.688	0.493	0.225	-0.018	88.51	31.39	91.26	77.27	75.96	71.73	79.06	26.14
202	1.027	0.908	0.694	0.289	-0.044	87.36	30.76	82.44	79.43	76.10	73.08	77.76	25.42
203	1.030	0.767	0.405	0.142	-0.089	87.55	30.86	90.05	76.05	73.22	69.13	77.11	25.06
204	1.030	0.772	0.288	0.095	-0.099	88.17	31.20	90.72	75.38	72.86	69.44	77.10	25.06
205	1.031	0.855	0.610	0.259	-0.057	87.59	30.89	83.25	79.83	74.03	73.35	77.62	25.34
206	1.027	0.687	0.347	0.120	-0.016	94.83	34.90	96.26	83.21	81.77	77.09	84.58	29.21
207	1.022	0.732	0.442	0.108	-0.049	95.34	35.19	94.86	83.57	81.27	76.30	84.00	28.89
208	1.020	0.713	0.428	0.121	-0.045	95.08	35.05	94.55	83.70	81.81	77.00	84.27	29.04
209	1.031	0.747	0.463	0.179	-0.017	96.19	35.66	98.24	84.15	82.31	77.81	85.63	29.79
210	1.029	0.766	0.440	0.177	0.001	101.64	38.69	96.21	91.58	89.46	84.24	90.38	32.43
211	1.024	0.730	0.485	0.207	-0.038	100.93	38.30	101.21	89.15	87.66	80.51	89.63	32.02
212	1.026	0.689	0.425	0.168	-0.008	100.69	38.16	93.29	89.91	88.88	83.93	89.00	31.67
213	1.028	0.702	0.427	0.100	-0.020	99.97	37.76	101.75	87.44	85.73	80.15	88.77	31.54
214	1.026	0.686	0.318	0.120	-0.050	87.34	30.74	89.28	75.38	74.25	70.88	77.45	25.25
215	1.030	0.852	0.556	0.259	-0.037	86.76	30.42	81.99	76.68	74.79	71.33	76.20	24.56
216	1.029	0.697	0.485	0.183	-0.029	87.34	30.74	89.78	74.25	73.13	69.30	76.62	24.79
217	1.033	0.709	0.353	0.061	-0.069	87.34	30.74	90.68	73.26	71.87	68.22	76.01	24.45
218	1.029	0.871	0.524	0.240	-0.044	87.34	30.74	81.45	77.32	76.41	71.42	76.65	24.81
219	1.028	0.623	0.298	-0.215	-0.647	93.70	34.28	95.58	81.63	79.65	73.80	82.67	28.15
220	1.028	0.712	0.353	0.120	-0.028	93.73	34.29	95.49	79.97	78.30	76.95	82.68	28.16
221	1.026	0.718	0.343	0.101	-0.054	94.22	34.57	95.13	79.25	80.01	75.69	82.52	28.07
222	1.022	0.773	0.456	0.140	-0.041	96.50	35.83	88.07	81.68	80.55	78.13	82.11	27.84
223	1.022	0.735	0.360	0.161	-0.038	94.71	34.84	94.73	80.51	80.82	75.42	82.87	28.26
224	1.021	0.845	0.521	0.257	-0.030	94.71	34.84	87.89	81.54	83.21	79.38	83.01	28.34
225	1.022	0.738	0.502	0.242	-0.018	95.22	35.12	94.41	81.95	80.19	75.45	83.00	28.33

TABLE (D-2) :- (CONTINUED)

RUN #	XIN	QUALITIES I	II	III	IV	SAT. TEMP. TUBE DEG F	DEG C	AVERAGE WALL TEMPERATURES IN DEG F I	II	III	IV	TUBE	DEG C TUBE
226	1.030	0.810	0.522	0.235	-0.019	100.43	38.02	94.77	89.91	87.57	83.30	88.89	31.61
227	1.031	0.703	0.448	0.175	0.011	100.43	38.02	101.75	87.84	85.68	80.01	88.82	31.57
228	1.026	0.713	0.416	0.136	-0.012	100.58	38.10	100.89	87.93	84.96	79.29	88.27	31.26
229	1.030	0.700	0.387	0.161	-0.013	101.05	38.36	102.51	88.29	86.22	80.10	89.28	31.82
230	1.034	0.848	0.534	0.256	-0.003	101.05	38.36	96.12	89.82	87.75	81.41	88.78	31.54
231	1.024	0.690	0.374	0.146	0.005	99.51	37.51	98.69	86.49	84.96	78.98	87.28	30.71
232	1.026	0.718	0.339	0.122	-0.022	100.24	37.91	99.68	86.04	83.88	78.26	86.97	30.54
233	1.027	0.685	0.412	0.173	-0.031	87.65	30.92	88.79	74.48	73.80	70.38	76.86	24.92
234	1.023	0.664	0.426	0.216	0.007	90.56	32.53	92.34	81.86	80.51	76.86	82.89	28.27
235	1.035	0.772	0.541	0.244	-0.020	90.28	32.38	84.56	85.37	81.95	77.32	82.30	27.94
236	1.020	0.752	0.483	0.215	0.013	90.17	32.31	84.42	85.41	81.45	76.73	82.01	27.78
237	1.017	0.732	0.518	0.197	-0.018	90.99	32.77	91.44	82.22	80.06	75.88	82.40	28.00
238	1.023	0.706	0.494	0.246	-0.036	89.38	31.88	82.85	82.04	80.37	77.45	80.68	27.04
239	1.021	0.694	0.440	0.150	0.005	90.21	32.34	91.53	80.96	79.02	74.88	81.60	27.56
240	1.022	0.830	0.447	0.255	0.025	89.09	31.72	82.58	81.00	82.59	76.50	80.67	27.04
241	1.021	0.836	0.577	0.280	-0.016	89.38	31.88	85.10	80.78	78.26	75.33	79.87	26.59
242	1.022	0.785	0.468	0.152	-0.046	89.65	32.03	83.66	80.28	79.02	74.61	79.40	26.33
243	1.023	0.798	0.558	0.263	0.010	101.71	38.73	95.99	95.72	89.46	81.32	90.62	32.57
244	1.018	0.774	0.409	0.183	-0.026	103.03	39.46	102.69	92.66	90.23	82.94	92.13	33.41
245	1.018	0.734	0.428	0.210	-0.030	103.73	39.85	95.40	96.66	94.64	83.66	92.59	33.66
246	1.018	0.766	0.421	0.146	-0.038	102.57	39.21	101.97	91.40	89.06	82.13	91.14	32.86
247	1.019	0.744	0.519	0.269	-0.006	103.73	39.85	96.48	96.03	92.61	82.94	92.02	33.34
248	1.017	0.696	0.535	0.240	-0.028	103.03	39.46	101.16	91.62	89.55	82.53	91.22	32.90
249	1.017	0.758	0.471	0.184	0.040	104.15	40.08	95.99	96.21	91.62	86.85	92.67	33.71
250	1.018	0.764	0.509	0.199	-0.027	103.00	39.44	101.93	91.49	87.71	82.71	90.96	32.76
251	1.018	0.748	0.478	0.238	-0.032	103.23	39.57	94.68	93.42	91.08	83.03	90.56	32.53

TABLE (D-2) :- (CONTINUED)

RUN		QUALITIES				SAT. TEMP. TUBE		AVERAGE WALL TEMPERATURES IN DEG F					DEG C
#	XIN	I	II	III	IV	DEG F	DEG C	I	II	III	IV	TUBE	TUBE
252	1.021	0.771	0.552	0.176	-0.043	102.53	39.18	94.68	95.09	86.36	84.69	90.21	32.34
301	1.023	0.732	0.440	0.216	-0.053	86.82	30.46	77.27	74.03	71.51	71.73	73.64	23.13
302	1.015	0.726	0.488	0.161	-0.102	93.91	34.39	83.12	79.02	75.69	75.15	78.25	25.69
303	1.030	0.841	0.579	0.342	-0.035	100.19	37.88	90.68	85.46	80.64	79.43	84.05	28.92
304	1.018	0.735	0.428	0.145	-0.114	87.02	30.56	76.01	72.95	70.56	70.29	72.45	22.47
305	1.032	0.831	0.541	0.214	-0.063	94.17	34.54	84.20	79.79	75.69	74.43	78.53	25.85
306	1.018	0.833	0.564	0.322	-0.018	100.50	38.05	91.40	86.63	81.68	79.88	84.90	29.39
307	1.022	0.775	0.437	0.145	-0.080	87.67	30.93	76.37	73.85	71.73	71.15	73.28	22.93
308	1.029	0.857	0.623	0.327	0.030	93.98	34.43	81.68	78.80	76.32	75.74	78.14	25.63
309	1.028	0.835	0.571	0.306	-0.038	100.26	37.92	90.45	85.55	80.19	78.98	83.79	28.77
310	1.030	0.821	0.529	0.286	-0.039	100.51	38.06	89.87	85.19	80.46	79.38	83.73	28.74
311	1.014	0.804	0.541	0.252	-0.010	94.00	34.44	82.71	78.66	75.15	75.02	77.89	25.49
312	1.018	0.742	0.441	0.165	-0.061	87.69	30.94	75.74	73.49	71.69	71.19	73.03	22.79
313	1.015	0.769	0.456	0.165	-0.081	87.29	30.72	75.38	73.08	70.52	70.61	72.40	22.44
314	1.013	0.800	0.526	0.221	-0.069	95.19	35.11	83.39	80.01	76.86	76.28	79.14	26.19
315	1.019	0.777	0.547	0.280	0.012	94.98	34.99	81.99	78.62	75.20	74.88	77.67	25.37
316	1.015	0.802	0.555	0.284	-0.028	100.93	38.29	89.28	85.59	80.64	79.83	83.84	28.80
317	1.020	0.793	0.541	0.238	-0.014	88.48	31.38	76.41	73.85	71.10	71.06	73.11	22.84
318	1.018	0.736	0.454	0.173	-0.067	94.32	34.62	81.23	77.85	74.21	74.04	76.83	24.91
319	1.018	0.829	0.546	0.272	0.026	100.81	38.23	88.02	83.70	78.57	77.45	81.94	27.74
320	1.018	0.807	0.464	0.226	-0.064	87.96	31.09	75.20	72.86	70.83	70.52	72.35	22.42
321	1.026	0.811	0.529	0.247	-0.034	94.51	34.73	81.00	78.17	75.20	74.66	77.26	25.14
322	1.022	0.758	0.493	0.205	-0.049	100.26	37.92	86.36	82.71	78.80	78.75	81.66	27.59
323	1.023	0.783	0.492	0.189	-0.152	100.81	38.23	87.89	83.84	79.86	78.53	82.53	28.07
324	1.008	0.792	0.539	0.195	-0.058	94.72	34.84	81.50	78.39	75.24	74.52	77.42	25.23
325	1.016	0.915	0.545	0.242	-0.094	89.04	31.69	75.29	73.44	71.06	70.11	72.48	22.49

TABLE (D-2) :- (CONTINUED)

RUN #	XIN	QUALITIES I	QUALITIES II	QUALITIES III	QUALITIES IV	SAT. TEMP. TUBE DEG F	SAT. TEMP. TUBE DEG C	AVERAGE WALL TEMPERATURES IN DEG F I	II	III	IV	TUBE	DEG C TUBE
326	1.014	0.751	0.421	0.158	-0.073	89.04	31.69	74.34	72.36	70.29	69.89	71.72	22.07
327	1.023	0.795	0.491	0.206	-0.022	94.71	34.84	81.14	78.71	75.56	75.15	77.64	25.36
328	1.022	0.838	0.556	0.285	0.015	100.47	38.04	86.63	83.30	79.74	78.84	82.13	27.85
329	1.025	0.819	0.544	0.269	-0.005	100.69	38.16	86.90	82.94	79.38	78.66	81.97	27.76
330	1.021	0.762	0.504	0.180	-0.046	87.62	30.90	73.85	71.47	68.67	68.67	70.67	21.48
331	1.018	0.758	0.532	0.221	-0.022	94.72	34.84	80.96	78.13	73.89	73.89	76.72	24.84
332	1.023	0.800	0.517	0.259	-0.012	101.17	38.43	87.62	83.70	82.17	79.07	83.14	28.41
333	1.019	0.884	0.570	0.301	-0.014	94.19	34.55	79.92	77.27	74.12	73.44	76.19	24.55
334	1.027	0.787	0.521	0.268	-0.010	100.69	38.16	87.21	83.21	79.38	78.48	82.07	27.82
335	1.020	0.763	0.464	0.164	-0.075	87.62	30.90	73.94	71.87	69.71	69.39	71.23	21.79
336	1.016	0.663	0.428	0.164	-0.071	88.06	31.14	74.12	72.68	70.70	70.74	72.06	22.26
337	1.021	0.817	0.633	0.369	0.124	94.33	34.63	79.20	75.92	72.86	73.26	75.31	24.06
338	1.017	0.780	0.454	0.187	-0.020	88.62	31.45	75.51	73.40	70.81	71.01	72.68	22.60
339	1.022	0.784	0.467	0.190	-0.028	94.06	34.48	80.01	77.27	74.52	74.25	76.52	24.73
340	1.026	0.775	0.481	0.230	-0.022	99.85	37.69	84.92	80.82	76.91	76.68	79.83	26.57
341	1.020	0.813	0.523	0.232	-0.031	100.09	37.83	86.58	82.26	77.76	76.82	80.86	27.14
342	1.020	0.605	0.413	0.221	-0.066	89.75	32.09	78.57	79.20	77.08	74.88	77.44	25.24
343	1.023	0.711	0.524	0.243	-0.038	90.31	32.39	79.52	80.15	77.72	75.38	78.19	25.66
344	1.020	0.705	0.484	0.200	-0.052	90.03	32.24	80.46	80.78	78.35	73.89	78.37	25.76
345	1.022	0.780	0.537	0.234	-0.008	90.13	32.29	81.05	80.73	78.21	73.89	78.47	25.82
346	1.018	0.765	0.575	0.227	-0.027	88.73	31.52	79.74	79.20	75.24	72.18	76.59	24.77
347	1.020	0.767	0.578	0.230	-0.023	89.01	31.67	80.73	79.02	74.30	71.87	76.48	24.71
348	1.022	0.636	0.410	0.152	-0.041	88.16	31.20	79.29	77.04	72.99	72.14	75.37	24.09
349	1.025	0.757	0.490	0.123	-0.044	87.30	30.72	79.11	74.88	70.97	70.88	73.96	23.31
350	1.024	0.693	0.527	0.229	-0.069	88.45	31.36	79.52	75.96	73.71	72.36	75.39	24.11
351	1.021	0.844	0.638	0.377	0.041	103.06	39.48	95.81	93.92	86.76	85.59	90.52	32.51

TABLE (D-2) :- (CONTINUED)

RUN		QUALITIES				SAT. TEMP. TUBE		AVERAGE WALL TEMPERATURES IN DEG F					DEG C
#	XIN	I	II	III	IV	DEG F	DEG C	I	II	III	IV	TUBE	TUBE
352	1.019	0.849	0.639	0.379	0.048	103.06	39.48	95.49	93.74	87.39	86.27	90.72	32.62
353	1.019	0.811	0.560	0.287	0.036	103.06	39.48	95.58	93.24	86.40	85.37	90.15	32.31
354	1.019	0.834	0.586	0.289	0.029	103.29	39.60	95.49	93.60	87.17	86.27	90.63	32.57
355	1.020	0.758	0.538	0.290	0.014	102.12	38.96	92.39	90.27	83.16	83.03	87.21	30.67
356	1.025	0.818	0.612	0.272	-0.009	100.70	38.17	92.34	89.51	81.77	81.86	86.37	30.21
357	1.019	0.860	0.598	0.293	0.046	103.61	39.78	95.94	93.51	86.94	86.94	90.84	32.69
358	1.017	0.797	0.562	0.240	0.020	102.68	39.27	94.01	91.35	84.24	83.97	88.40	31.33
359	1.024	0.781	0.569	0.265	0.022	102.45	39.14	93.24	90.81	83.43	83.07	87.64	30.91
401	1.014	0.753	0.462	0.200	-0.062	89.72	32.07	75.02	74.25	72.41	67.23	72.23	22.35
402	1.026	0.817	0.568	0.279	0.022	100.79	38.22	90.81	87.71	83.43	75.33	84.32	29.07
403	1.026	0.842	0.728	0.465	0.035	100.79	38.22	90.95	85.95	80.55	75.56	83.25	28.47
404	1.017	0.798	0.495	0.252	-0.015	94.49	34.72	82.53	79.29	75.07	71.33	77.06	25.03
405	1.026	0.920	0.549	0.231	-0.021	94.23	34.57	94.46	78.26	73.67	69.93	79.08	26.16
406	1.026	0.798	0.546	0.318	0.027	100.24	37.91	101.21	85.64	79.82	74.25	85.23	29.57
407	1.017	0.735	0.466	0.240	-0.015	95.27	35.15	92.70	78.98	74.93	71.64	79.56	26.42
408	1.023	0.669	0.262	0.067	-0.110	88.48	31.38	87.98	72.36	69.26	66.69	74.07	23.37
409	1.021	0.780	0.499	0.238	-0.023	88.48	31.38	87.12	73.53	70.16	66.69	74.38	23.54
410	1.028	0.826	0.591	0.330	0.036	100.94	38.30	102.06	86.40	80.78	75.33	86.15	30.08
411	1.019	0.754	0.375	0.243	0.016	88.14	31.19	81.68	74.34	71.64	67.59	73.82	23.23
412	1.013	0.727	0.441	0.177	-0.043	87.34	30.75	82.98	71.73	68.90	66.15	72.44	22.47
413	1.016	0.761	0.506	0.161	-0.082	94.72	34.85	91.89	79.02	74.52	70.97	79.10	26.17
414	1.017	0.765	0.491	0.148	-0.103	88.71	31.51	86.85	73.53	70.34	67.10	74.46	23.59
415	1.024	0.797	0.541	0.271	0.029	93.89	34.38	93.20	78.75	74.48	70.70	79.28	26.27
416	1.035	0.840	0.569	0.299	0.029	101.13	38.40	94.95	87.80	81.14	76.86	85.19	29.55
417	1.022	0.766	0.420	0.147	-0.090	95.00	35.00	92.16	76.64	73.04	69.93	77.94	25.52
418	1.025	0.772	0.550	0.308	0.023	101.08	38.38	101.07	85.64	80.96	76.32	86.00	30.00

TABLE (D-2):- (CONTINUED)

RUN #	XIN	QUALITIES I	II	III	IV	SAT. TEMP. TUBE DEG F	DEG C	AVERAGE WALL TEMPERATURES IN DEG F I	II	III	IV	TUBE	DEG C TUBE
419	1.020	0.725	0.589	0.238	-0.011	88.75	31.53	81.59	77.27	70.92	69.44	74.81	23.78
420	1.025	0.825	0.426	0.160	-0.062	88.75	31.53	82.22	75.24	72.41	68.27	74.54	23.63
421	1.024	0.794	0.586	0.264	-0.036	89.31	31.84	83.66	76.59	72.00	67.41	74.92	23.84
422	1.020	0.789	0.599	0.245	-0.081	94.69	34.83	89.78	82.49	75.24	68.58	79.02	26.12
423	1.025	0.806	0.542	0.264	0.001	94.69	34.83	93.96	77.63	73.22	68.99	78.45	25.81
424	1.018	0.763	0.432	0.207	-0.019	94.69	34.83	87.98	77.36	75.83	71.91	78.27	25.71
425	1.025	0.744	0.517	0.191	-0.064	101.14	38.41	92.66	88.16	80.82	75.55	84.30	29.06
426	1.023	0.829	0.580	0.276	-0.019	101.85	38.81	99.32	84.60	78.53	73.13	83.90	28.83
427	1.023	0.722	0.320	0.169	-0.082	88.76	31.53	87.17	71.96	69.66	66.69	73.87	23.26
428	1.026	0.751	0.505	0.299	-0.015	100.69	38.16	92.61	88.38	81.77	74.57	84.33	29.07
429	1.020	0.728	0.488	0.222	-0.017	88.42	31.34	85.19	71.10	68.94	65.88	72.78	22.66
430	1.021	0.770	0.476	0.211	-0.039	94.46	34.70	91.31	76.82	73.22	69.35	77.67	25.37
431	1.027	0.811	0.566	0.291	-0.004	100.88	38.27	99.54	83.66	77.99	73.22	83.60	28.67
432	1.031	0.782	0.533	0.208	-0.051	100.64	38.14	94.14	86.67	78.65	74.57	83.51	28.62
433	1.023	0.704	0.373	0.093	-0.111	88.48	31.38	81.05	71.96	68.99	66.42	72.11	22.28
501	1.021	0.731	0.486	0.219	-0.115	90.54	32.52	90.99	78.53	77.40	71.78	79.68	26.49
502	1.020	0.745	0.505	0.299	-0.062	95.41	35.23	94.95	81.27	79.88	74.97	82.77	28.21
503	1.025	0.740	0.540	0.341	0.013	100.48	38.05	101.61	85.59	79.11	79.79	86.53	30.29
504	1.021	0.728	0.582	0.398	-0.023	95.27	35.15	94.95	81.32	80.42	73.80	82.62	28.12
505	1.027	0.752	0.569	0.386	-0.007	101.20	38.44	103.37	87.13	85.19	78.39	88.52	31.40
506	1.015	0.739	0.438	0.212	-0.089	89.38	31.88	88.43	76.77	75.15	70.02	77.60	25.33
507	1.015	0.730	0.522	0.236	-0.075	89.10	31.72	88.38	77.90	76.68	70.92	78.47	25.82
508	1.018	0.736	0.537	0.355	-0.010	95.55	35.30	95.67	82.63	81.23	75.02	83.64	28.69
509	1.018	0.723	0.509	0.295	-0.026	88.48	31.38	88.07	76.46	76.14	69.35	77.51	25.28
510	1.022	0.731	0.527	0.322	-0.037	94.98	34.99	96.35	83.21	82.44	73.71	83.93	28.85
511	1.024	0.750	0.548	0.346	-0.011	101.64	38.69	103.05	87.48	86.00	77.36	88.47	31.37

TABLE (D-2) :- (CONTINUED)

RUN		QUALITIES				SAT. TEMP. TUBE		AVERAGE WALL TEMPERATURES IN DEG F					DEG C
#	XIN	I	II	III	IV	DEG F	DEG C	I	II	III	IV	TUBE	TUBE
512	1.025	0.738	0.588	0.410	-0.027	101.41	38.56	103.05	87.03	86.09	77.00	88.29	31.27
513	1.022	0.726	0.537	0.322	-0.001	88.24	31.24	89.73	77.13	76.50	69.13	78.12	25.62
514	1.021	0.721	0.510	0.298	-0.054	96.04	35.58	97.11	83.84	83.07	73.94	84.49	29.16
515	1.033	0.727	0.514	0.300	-0.033	100.73	38.18	105.03	86.63	84.74	73.76	87.54	30.86
516	1.029	0.746	0.435	0.152	-0.046	87.36	30.76	90.18	72.54	70.11	68.40	75.31	24.06
517	1.026	0.683	0.427	0.198	-0.058	89.91	32.17	91.31	72.54	70.52	68.22	75.65	24.25
518	1.024	0.788	0.565	0.272	-0.048	93.94	34.41	97.16	82.89	76.86	71.28	82.05	27.81
519	1.028	0.782	0.521	0.306	0.014	93.70	34.28	96.93	77.81	75.65	71.69	80.52	26.96
520	1.027	0.845	0.576	0.307	-0.005	100.31	37.95	103.37	85.23	80.46	74.43	85.88	29.93
521	1.015	0.684	0.404	0.175	-0.054	87.34	30.74	86.99	74.52	70.57	68.13	75.05	23.92
522	1.024	0.814	0.543	0.257	-0.059	93.94	34.41	96.08	81.95	74.84	70.29	80.79	27.11
523	1.030	0.864	0.642	0.347	0.024	100.93	38.30	105.08	89.78	82.22	74.52	87.90	31.06
524	1.030	0.725	0.420	0.171	-0.050	87.36	30.76	90.27	70.88	69.53	67.46	74.54	23.63
525	1.019	0.782	0.490	0.253	-0.025	95.21	35.12	96.17	81.59	75.92	71.38	81.26	27.37
526	1.030	0.823	0.575	0.286	-0.045	100.67	38.15	104.27	87.93	79.79	73.53	86.38	30.21
527	1.020	0.779	0.510	0.255	-0.014	94.22	34.57	95.59	79.47	76.32	71.91	80.83	27.13
528	1.021	0.790	0.498	0.222	-0.024	94.22	34.57	95.36	77.72	73.67	69.44	79.05	26.14
529	1.030	0.845	0.544	0.291	-0.010	100.72	38.18	104.36	86.54	79.88	73.85	86.16	30.09
530	1.028	0.825	0.568	0.312	0.002	99.22	37.35	102.74	87.08	80.19	73.98	86.00	30.00
531	1.021	0.833	0.592	0.310	-0.024	100.72	38.18	104.81	87.98	80.06	73.58	86.61	30.34
532	1.029	0.840	0.607	0.307	-0.003	100.48	38.04	103.50	87.26	79.07	73.22	85.76	29.87
533	1.023	0.790	0.463	0.152	-0.158	94.30	34.61	96.08	81.54	73.44	69.66	80.18	26.77
534	1.022	0.723	0.505	0.179	-0.066	88.87	31.60	89.10	74.07	70.25	67.59	75.26	24.03
535	1.028	0.694	0.415	0.164	-0.059	87.94	31.08	90.41	73.22	70.83	68.54	75.75	24.31
536	1.025	0.725	0.453	0.180	-0.065	88.87	31.60	90.14	73.04	70.70	68.49	75.59	24.22

TABLE (D-3) :- REDUCED DATA - HEAT TRANSFER COEFFICIENTS AND TEMPERATURE DIFFERENCES

RUN	HEAT TRANSFER COEFFS. IN BTU/HR-SQFT*F					W/SQM*C	DRIVING TEMP. DIFFERENCES DEG F					DEG C
#	I	II	III	IV	TUBE	TUBE	I	II	III	IV	TUBE	TUBE
101	566.60	372.01	163.55	125.45	286.17	1625.0	7.33	17.49	18.03	18.79	13.93	7.74
102	266.60	190.75	281.07	297.95	286.15	1624.8	9.54	16.64	15.83	19.21	13.89	7.71
103	671.92	293.01	231.12	174.38	316.86	1799.2	7.37	16.80	18.24	20.13	13.88	7.71
104	638.52	318.77	253.34	134.45	308.48	1751.6	7.90	18.01	19.81	21.30	15.12	8.40
105	716.60	277.33	164.27	264.46	329.33	1870.1	7.60	16.73	18.80	20.47	14.10	7.83
106	313.50	365.00	333.37	240.13	337.35	1915.5	13.24	13.66	17.44	20.72	14.77	8.21
107	622.61	290.56	296.87	199.57	338.38	1921.4	8.47	18.07	20.63	21.89	15.52	8.62
108	527.36	203.95	189.30	139.70	248.84	1413.0	6.41	14.66	17.76	18.71	12.40	6.89
109	560.58	255.39	146.02	197.99	272.32	1546.3	6.21	14.80	17.23	19.07	12.43	6.91
110	330.34	450.44	162.16	101.77	259.27	1472.2	10.40	13.75	16.90	20.18	13.89	7.72
111	243.59	433.28	294.42	268.86	347.20	1971.5	14.54	16.40	18.06	19.77	15.33	8.51
112	522.89	268.21	162.89	143.70	237.66	1349.5	6.56	16.99	20.95	23.74	15.57	8.65
113	580.98	319.44	153.79	128.52	246.70	1400.8	6.64	17.64	21.60	23.85	16.07	8.93
114	370.01	170.70	259.50	200.59	260.38	1478.5	11.27	14.61	19.25	20.73	15.18	8.44
115	484.27	266.47	223.77	163.74	276.24	1568.5	8.67	19.63	21.03	22.33	16.10	8.94
116	658.86	361.98	193.18	81.59	295.17	1676.1	8.71	20.53	20.67	20.94	15.96	8.87
117	759.08	301.70	201.69	114.40	293.62	1667.3	8.28	20.70	21.65	21.78	16.49	9.16
118	588.52	160.99	271.25	257.85	307.99	1748.8	8.74	19.05	20.76	23.82	16.21	9.01
119	788.27	260.19	213.84	219.60	316.80	1798.9	8.06	20.04	21.66	23.73	16.88	9.38
120	600.39	244.75	286.79	202.33	311.10	1766.5	8.47	20.68	24.28	25.00	17.81	9.89
121	590.22	271.85	296.74	171.02	317.97	1805.5	8.33	21.02	24.08	25.03	17.99	9.99
122	444.55	404.88	226.75	274.22	356.73	2025.6	15.75	17.29	20.53	25.48	17.97	9.99
123	247.78	229.70	237.81	156.10	230.85	1310.8	11.43	12.32	17.54	24.79	14.84	8.25
124	516.10	238.72	192.13	152.53	245.48	1393.9	6.78	15.98	20.71	24.98	15.37	8.54
125	264.90	313.36	234.41	171.60	252.70	1434.9	10.51	14.23	19.00	24.85	15.79	8.77

TABLE (D-3) :- (CONTINUED)

RUN	HEAT TRANSFER COEFFS. IN BTU/HR-SQFT*F					W/SQM*C	DRIVING TEMP. DIFFERENCES DEG F					DEG C
#	I	II	III	IV	TUBE	TUBE	I	II	III	IV	TUBE	TUBE
126	598.97	221.75	193.57	172.98	256.40	1455.9	7.30	17.44	21.22	25.13	16.27	9.04
127	563.84	244.64	188.01	191.73	265.19	1505.8	7.36	18.10	20.40	26.16	16.42	9.12
128	537.16	323.78	206.96	155.55	280.73	1594.1	7.65	18.50	21.29	26.28	16.55	9.20
129	508.02	250.91	244.27	192.08	284.35	1614.6	8.73	19.08	21.11	26.82	17.17	9.54
130	266.76	333.10	277.03	218.18	288.15	1636.2	14.04	17.51	19.53	26.69	18.06	10.03
131	585.37	234.56	290.49	175.93	292.80	1662.6	9.00	19.53	22.10	28.62	18.19	10.10
132	665.25	268.68	263.65	190.52	306.73	1741.7	8.93	20.15	22.40	28.38	18.46	10.26
133	344.94	374.83	297.99	178.00	303.06	1720.9	16.49	18.21	20.98	31.87	20.16	11.20
134	323.80	364.00	129.21	94.00	250.63	1423.2	13.61	16.15	11.34	19.62	13.56	7.53
135	789.04	238.85	158.13	123.50	260.34	1478.3	7.03	16.76	18.97	20.23	14.42	8.01
136	364.23	203.49	273.48	171.83	277.46	1575.5	14.47	11.49	17.11	20.40	14.23	7.91
137	660.65	165.85	264.03	169.55	275.58	1564.8	7.43	18.37	20.80	21.57	15.50	8.61
138	255.66	423.98	307.42	185.40	309.25	1756.0	15.11	12.18	16.77	20.82	14.59	8.10
139	347.12	344.03	293.02	195.94	320.99	1822.7	16.29	12.32	16.87	21.59	14.86	8.25
140	749.28	207.08	257.60	206.57	313.42	1779.7	8.10	18.18	20.48	21.87	15.64	8.69
141	384.93	416.97	306.68	208.62	351.79	1997.5	18.05	12.96	17.60	22.14	15.90	8.83
142	398.91	285.07	263.66	344.77	362.88	2060.5	17.80	12.43	16.80	20.58	15.28	8.49
143	638.20	190.31	240.56	194.22	278.33	1580.5	6.40	16.31	19.87	20.90	14.39	7.99
144	346.21	399.83	175.21	152.85	266.87	1515.4	10.83	17.21	17.79	22.43	16.08	8.94
145	414.57	325.68	196.95	179.20	279.93	1589.5	12.90	17.66	18.74	22.88	16.87	9.37
146	543.41	370.49	192.97	150.78	283.46	1609.6	8.21	19.22	20.70	23.54	16.86	9.36
147	458.91	275.81	287.41	160.97	291.97	1657.9	13.42	18.56	19.60	25.40	17.98	9.99
148	596.93	262.71	211.26	207.56	287.83	1634.4	8.95	20.23	22.35	25.59	17.96	9.98
149	311.99	383.16	329.68	194.90	314.13	1783.7	16.24	16.54	21.13	25.95	18.65	10.36
150	682.84	203.78	250.65	255.01	312.62	1775.2	8.84	19.61	23.93	26.13	18.13	10.07
151	439.49	403.49	243.30	192.00	323.93	1839.4	18.13	16.15	23.76	26.32	19.54	10.85

TABLE (D-3) :- (CONTINUED)

RUN	HEAT TRANSFER COEFFS. IN BTU/HR-SQFT*F					W/SQM*C	DRIVING TEMP. DIFFERENCES DEG F					DEG C
#	I	II	III	IV	TUBE	TUBE	I	II	III	IV	TUBE	TUBE
152	318.75	383.68	266.56	215.66	312.96	1777.1	15.05	16.68	23.97	25.91	18.51	10.29
201	1136.14	275.06	339.11	230.24	440.44	2500.9	4.81	11.24	12.54	16.77	9.45	5.25
202	165.56	454.75	606.11	392.78	469.93	2668.4	12.07	7.93	11.26	14.28	9.60	5.33
203	857.38	557.53	324.40	220.52	473.99	2691.5	5.46	11.50	14.33	18.43	10.44	5.80
204	913.85	704.29	234.06	191.21	473.47	2688.5	5.27	12.79	15.31	18.73	11.07	6.15
205	268.14	617.98	504.36	432.04	531.66	3018.9	12.72	7.76	13.56	14.24	9.98	5.54
206	949.35	461.03	272.86	120.30	400.54	2274.4	5.67	11.62	13.06	17.74	10.24	5.69
207	752.53	409.16	395.02	135.77	392.01	2226.0	6.43	11.77	14.07	19.04	11.34	6.30
208	919.77	437.18	406.01	159.95	431.14	2448.1	5.89	11.38	13.27	18.08	10.82	6.01
209	860.79	433.08	375.25	195.76	455.69	2587.5	6.08	12.03	13.88	18.38	10.56	5.87
210	316.71	503.99	335.72	156.34	354.30	2011.8	12.91	10.06	12.18	17.40	11.27	6.26
211	848.67	359.67	362.02	207.14	406.55	2308.5	6.03	11.78	13.27	20.42	11.30	6.28
212	392.41	401.92	356.62	172.41	362.92	2060.8	14.10	10.78	11.81	16.76	11.69	6.49
213	1080.06	399.36	417.39	110.10	425.86	2418.2	5.55	12.53	14.24	19.82	11.21	6.23
214	1442.24	628.28	308.06	209.66	554.80	3150.3	4.85	11.96	13.08	16.46	9.89	5.49
215	294.50	628.32	528.43	409.18	539.01	3060.7	12.84	10.07	11.96	15.43	10.56	5.86
216	1393.14	358.15	471.74	259.53	547.57	3109.2	5.35	13.08	14.21	18.03	10.72	5.95
217	1365.41	584.78	434.55	155.79	561.25	3186.9	5.53	14.07	15.47	19.11	11.33	6.29
218	275.57	832.57	623.55	426.88	601.77	3417.0	13.67	10.02	10.92	15.92	10.68	5.94
219	1459.53	519.36	707.93	419.44	735.63	4177.1	5.42	12.06	14.04	19.89	11.03	6.13
220	1127.30	526.47	303.09	177.09	481.90	2736.3	5.71	13.76	15.42	16.77	11.04	6.14
221	1082.24	527.31	358.87	174.75	486.06	2760.0	6.05	14.97	14.21	18.53	11.70	6.50
222	383.64	466.96	433.85	214.58	403.25	2289.8	14.16	14.82	15.95	18.38	14.39	8.00
223	1136.60	602.81	325.33	233.96	509.91	2895.4	5.79	14.20	13.88	19.28	11.83	6.57
224	339.63	582.29	545.19	442.64	531.94	3020.5	12.27	13.16	11.50	15.32	11.70	6.50
225	1084.68	436.42	423.94	321.82	521.92	2963.6	6.46	13.27	15.03	19.77	12.22	6.79

TABLE (D-3) :- (CONTINUED)

RUN	HEAT TRANSFER COEFFS. IN BTU/HR-SQFT*F					W/SQM*C	DRIVING TEMP. DIFFERENCES DEG F					DEG C
#	I	II	III	IV	TUBE	TUBE	I	II	III	IV	TUBE	TUBE
226	309.54	519.79	424.71	280.75	431.43	2449.8	13.47	10.52	12.86	17.13	11.54	6.41
227	970.15	402.96	368.35	159.24	437.11	2482.1	6.77	12.59	14.75	20.42	11.61	6.45
228	1020.37	488.92	373.42	144.64	439.29	2494.4	6.43	12.64	15.61	21.28	12.30	6.84
229	1175.39	531.20	329.32	179.00	479.62	2723.4	6.13	12.76	14.83	20.95	11.77	6.54
230	306.33	633.21	470.87	296.92	476.16	2703.8	13.60	11.23	13.30	19.64	12.28	6.82
231	1137.11	570.27	367.68	159.93	488.50	2773.8	6.94	13.02	14.55	20.53	12.23	6.80
232	1005.00	651.30	321.90	159.38	480.14	2726.4	7.48	14.20	16.35	21.98	13.27	7.37
233	1414.42	514.03	427.42	293.34	608.73	3456.5	6.05	13.17	13.85	17.27	10.79	5.99
234	1134.85	363.29	274.89	201.55	438.52	2490.0	4.21	8.70	10.05	13.69	7.66	4.26
235	317.89	658.95	498.55	284.04	462.32	2625.2	11.59	4.91	8.33	12.97	7.98	4.44
236	367.81	859.42	466.60	226.25	467.00	2651.7	11.04	4.75	8.71	13.44	8.16	4.53
237	1095.63	386.61	465.76	223.92	477.44	2711.1	4.16	8.77	10.93	15.12	8.59	4.77
238	418.25	485.34	461.35	397.64	511.87	2906.5	12.76	7.34	9.00	11.93	8.70	4.83
239	1379.08	484.33	457.62	166.44	520.62	2956.3	4.22	9.25	11.19	15.33	8.61	4.78
240	291.71	883.53	547.29	338.49	549.33	3119.3	12.17	8.09	6.50	12.59	8.42	4.68
241	363.79	586.83	518.19	409.72	530.22	3010.8	9.88	8.60	11.12	14.04	9.51	5.28
242	414.62	688.83	606.60	266.90	529.86	3008.7	11.64	9.37	10.63	15.04	10.26	5.70
243	303.86	624.23	376.27	193.30	356.13	2022.2	11.55	5.99	12.25	20.39	11.09	6.16
244	824.11	578.90	289.39	169.98	392.60	2229.3	4.87	10.37	12.80	20.09	10.90	6.06
245	379.72	748.42	413.84	205.63	405.24	2301.1	12.87	7.06	9.09	20.07	11.13	6.19
246	875.47	561.21	370.38	162.81	419.83	2383.9	5.27	11.17	13.51	20.44	11.43	6.35
247	430.03	556.55	427.41	250.80	415.73	2360.6	12.15	7.69	11.11	20.79	11.71	6.50
248	1019.36	279.58	434.63	259.28	439.55	2495.9	6.31	11.41	13.48	20.50	11.81	6.56
249	430.25	750.29	473.76	170.94	439.23	2494.1	12.40	7.93	12.52	17.29	11.48	6.38
250	966.76	476.90	438.56	239.85	468.57	2660.7	5.71	11.51	15.29	20.28	12.04	6.69
251	463.33	618.78	443.14	299.22	464.57	2638.0	13.07	9.80	12.14	20.20	12.67	7.04

TABLE (D-3) :- (CONTINUED)

RUN	HEAT TRANSFER COEFFS. IN BTU/HR-SQFT*F					W/SQM*C	DRIVING TEMP. DIFFERENCES DEG F					DEG C
#	I	II	III	IV	TUBE	TUBE	I	II	III	IV	TUBE	TUBE
252	437.58	688.87	542.52	286.08	504.03	2862.0	13.35	7.44	16.17	17.84	12.32	6.85
301	262.61	322.77	207.11	252.39	288.91	1640.5	15.71	12.79	15.31	15.09	13.19	7.33
302	269.61	220.66	246.83	193.48	245.68	1395.0	14.75	14.88	18.21	18.75	15.66	8.70
303	154.65	247.26	168.70	252.20	229.18	1301.4	16.90	14.73	19.54	20.76	16.13	8.96
304	223.38	321.94	253.86	228.87	286.94	1629.3	18.69	14.07	16.45	16.72	14.56	8.09
305	161.30	294.24	258.77	204.83	255.70	1451.9	18.21	14.38	18.47	19.73	15.64	8.69
306	201.20	283.79	186.89	240.98	242.18	1375.2	13.37	13.87	18.82	20.62	15.60	8.67
307	225.27	385.38	289.31	214.46	301.85	1714.0	17.31	13.82	15.94	16.52	14.40	8.00
308	128.09	237.81	259.08	250.74	243.05	1380.1	20.64	15.18	17.66	18.24	15.85	8.80
309	176.77	275.08	201.46	247.67	247.53	1405.5	16.62	14.71	20.06	21.28	16.46	9.15
310	185.63	305.23	193.00	246.46	254.58	1445.6	17.96	15.32	20.04	21.12	16.78	9.32
311	228.78	277.05	247.88	223.67	257.03	1459.5	14.84	15.33	18.84	18.98	16.11	8.95
312	248.38	346.32	281.50	223.24	300.30	1705.2	18.12	14.20	16.00	16.49	14.66	8.14
313	262.76	375.95	295.39	251.15	313.54	1780.4	15.94	14.20	16.77	16.68	14.89	8.27
314	234.14	303.85	279.50	257.24	283.18	1608.0	15.31	15.18	18.33	18.92	16.06	8.92
315	227.05	236.00	227.69	224.11	244.83	1390.2	17.94	16.36	19.78	20.09	17.30	9.61
316	225.93	265.51	220.66	244.41	252.10	1431.5	15.61	15.34	20.29	21.10	17.09	9.49
317	207.19	302.47	305.62	253.85	295.02	1675.2	19.19	14.63	17.37	17.42	15.37	8.54
318	265.24	300.55	245.91	207.21	272.31	1546.2	18.65	16.47	20.11	20.28	17.49	9.72
319	188.09	288.06	214.00	182.54	228.28	1296.2	17.44	17.10	22.23	23.36	18.87	10.48
320	223.82	419.20	255.35	306.66	319.38	1813.5	17.36	15.10	17.13	17.44	15.61	8.67
321	192.25	314.58	266.01	258.75	280.30	1591.6	20.41	16.34	19.31	19.85	17.25	9.58
322	242.36	272.68	242.21	212.62	259.92	1475.9	19.73	17.54	21.46	21.50	18.60	10.33
323	237.24	320.59	270.81	286.54	300.78	1707.9	18.93	16.97	20.95	22.28	18.28	10.16
324	265.59	292.98	333.48	236.66	291.21	1653.6	15.43	16.32	19.47	20.19	17.30	9.61
325	106.75	453.41	321.21	339.17	319.66	1815.1	17.99	15.60	17.98	18.93	16.57	9.20

TABLE (D-3) :- (CONTINUED)

RUN	HEAT TRANSFER COEFFS. IN BTU/HR-SQFT*F					W/SQM*C	DRIVING TEMP. DIFFERENCES DEG F					DEG C
#	I	II	III	IV	TUBE	TUBE	I	II	III	IV	TUBE	TUBE
326	281.04	391.96	278.52	238.42	311.06	1766.3	18.57	16.67	18.74	19.15	17.31	9.62
327	229.18	372.64	291.57	228.24	299.90	1702.9	19.48	16.00	19.15	19.56	17.07	9.48
328	181.88	319.78	253.20	242.63	266.66	1514.1	19.66	17.17	20.73	21.63	18.34	10.19
329	204.51	311.02	258.94	250.45	276.38	1569.4	20.21	17.75	21.30	22.02	18.71	10.40
330	273.88	329.91	351.65	245.82	324.09	1840.3	19.44	16.15	18.95	18.95	16.95	9.42
331	287.42	276.27	304.84	236.88	293.86	1668.6	18.40	16.59	20.82	20.82	18.00	10.00
332	229.61	325.17	273.88	246.00	288.63	1638.9	19.55	17.46	18.99	22.10	18.03	10.01
333	145.01	388.12	280.08	316.28	299.34	1699.7	19.35	16.92	20.07	20.75	18.00	10.00
334	245.18	315.76	246.51	260.22	289.33	1642.9	20.35	17.48	21.31	22.21	18.62	10.34
335	288.44	405.19	356.09	279.67	355.57	2019.1	18.90	15.75	17.91	18.23	16.39	9.11
336	424.81	335.17	334.04	297.56	372.73	2116.5	18.22	15.38	17.36	17.31	15.99	8.89
337	214.61	216.02	267.74	251.84	255.72	1452.1	20.59	18.41	21.47	21.07	19.02	10.57
338	303.87	485.59	338.86	266.38	368.36	2091.7	17.64	15.22	17.81	17.60	15.93	8.85
339	270.19	424.25	318.62	246.70	335.85	1907.0	19.74	16.79	19.54	19.81	17.55	9.75
340	256.92	343.46	243.83	241.45	291.29	1654.0	21.78	19.03	22.94	23.17	20.02	11.12
341	237.56	351.10	280.07	242.99	294.21	1670.6	18.79	17.83	22.33	23.27	19.23	10.68
342	321.00	230.21	191.52	245.04	279.48	1587.0	16.41	10.55	12.67	14.87	12.32	6.84
343	245.83	246.92	299.08	252.04	293.46	1666.4	17.00	10.16	12.59	14.93	12.11	6.73
344	297.76	336.59	342.76	220.19	324.26	1841.2	14.93	9.25	11.68	16.14	11.66	6.48
345	241.76	382.71	377.18	221.00	327.51	1859.7	14.84	9.39	11.91	16.23	11.66	6.48
346	284.97	310.41	402.47	238.05	335.13	1903.0	13.83	9.53	13.49	16.55	12.14	6.74
347	300.50	309.20	385.21	239.98	339.02	1925.1	13.70	9.99	14.71	17.14	12.53	6.96
348	444.56	344.90	288.72	204.75	353.27	2006.0	14.81	11.12	15.17	16.02	12.79	7.11
349	322.28	382.73	400.21	180.40	356.14	2022.3	14.74	12.42	16.33	16.42	13.34	7.41
350	401.34	246.32	376.31	344.58	389.31	2210.6	15.35	12.48	14.73	16.08	13.06	7.25
351	175.05	279.45	199.24	239.13	242.93	1379.4	12.58	9.14	16.29	17.46	12.53	6.96

TABLE (D-3) :- (CONTINUED)

RUN	HEAT TRANSFER COEFFS. IN BTU/HR-SQFT*F					W/SQM*C	DRIVING TEMP. DIFFERENCES DEG F					DEG C
#	I	II	III	IV	TUBE	TUBE	I	II	III	IV	TUBE	TUBE
352	179.24	296.21	217.92	258.19	258.28	1466.6	12.44	9.32	15.66	16.79	12.33	6.85
353	233.93	354.54	226.67	196.26	263.36	1495.4	12.26	9.81	16.65	17.69	12.90	7.17
354	211.22	371.33	267.31	221.39	283.83	1611.7	12.74	9.68	16.12	17.02	12.65	7.03
355	271.24	283.85	199.35	219.99	257.22	1460.6	14.72	11.85	18.96	19.09	14.91	8.28
356	222.51	295.81	287.27	238.29	288.76	1639.6	14.87	11.19	18.93	18.84	14.33	7.96
357	209.59	430.42	303.64	245.62	316.07	1794.7	12.63	10.09	16.66	16.66	12.77	7.09
358	294.67	359.14	303.16	203.45	302.33	1716.7	12.93	11.33	18.44	18.71	14.29	7.94
359	284.74	329.57	287.91	225.86	305.09	1732.4	15.38	11.63	19.01	19.37	14.81	8.23
401	268.55	357.57	287.25	220.95	292.21	1659.2	18.51	15.46	17.31	22.48	17.49	9.72
402	146.65	222.37	194.56	117.80	177.97	1010.5	16.62	13.08	17.36	25.46	16.47	9.15
403	119.65	80.46	136.23	178.56	148.06	840.7	16.13	14.84	20.24	25.23	17.54	9.74
404	140.87	211.88	132.46	122.19	156.86	890.7	16.44	15.19	19.42	23.16	17.43	9.69
405	193.77	274.40	182.48	122.16	203.86	1157.6	6.45	15.97	20.56	24.29	15.15	8.42
406	456.49	201.54	130.45	130.83	194.49	1104.3	5.86	14.60	20.43	25.99	15.01	8.34
407	493.47	203.86	137.37	133.04	203.11	1153.3	7.11	16.29	20.34	23.62	15.70	8.72
408	604.16	289.02	115.65	92.73	224.74	1276.1	6.73	16.12	19.22	21.79	14.41	8.01
409	413.56	224.00	169.58	142.56	220.43	1251.7	6.96	14.95	18.32	21.79	14.11	7.84
410	414.28	198.47	158.33	140.71	205.46	1166.7	5.98	14.53	20.16	25.60	14.79	8.22
411	293.50	344.56	100.55	138.46	219.50	1246.4	11.33	13.80	16.50	20.55	14.33	7.96
412	492.85	240.68	187.89	136.20	232.71	1321.4	7.65	15.61	18.44	21.19	14.90	8.28
413	479.67	210.93	221.35	132.30	227.94	1294.3	6.93	15.70	20.20	23.75	15.62	8.68
414	543.99	247.41	255.50	159.08	268.98	1527.3	6.35	15.18	18.37	21.61	14.25	7.92
415	436.91	229.81	189.05	141.49	231.52	1314.7	7.09	15.13	19.41	23.19	14.60	8.11
416	193.85	272.42	181.44	149.41	211.93	1203.4	13.55	13.33	19.99	24.26	15.94	8.85
417	425.21	266.78	175.88	133.47	230.41	1308.3	8.50	18.36	21.96	25.06	17.05	9.47
418	560.92	200.14	168.15	160.42	231.85	1316.5	6.33	15.44	20.12	24.75	15.08	8.38

TABLE (D-3) :- (CONTINUED)

RUN	HEAT TRANSFER COEFFS. IN BTU/HR-SQFT*F					W/SQM*C	DRIVING TEMP. DIFFERENCES DEG F					DEG C
#	I	II	III	IV	TUBE	TUBE	I	II	III	IV	TUBE	TUBE
419	341.28	169.17	280.82	184.40	264.03	1499.2	12.35	11.48	17.82	19.31	13.94	7.75
420	234.84	440.25	241.96	160.71	284.11	1613.3	12.62	13.50	16.34	20.48	14.21	7.90
421	291.04	252.74	289.01	211.90	285.45	1620.9	12.28	12.72	17.31	21.90	14.39	8.00
422	326.22	230.16	268.31	184.29	259.37	1472.8	10.47	12.20	19.45	26.11	15.67	8.70
423	464.56	236.88	198.59	157.09	241.96	1373.9	7.27	17.06	21.47	25.70	16.24	9.02
424	347.35	303.96	190.16	157.40	251.39	1427.5	11.73	17.33	18.86	22.78	16.42	9.12
425	276.02	255.18	234.75	144.81	235.87	1339.4	14.86	12.98	20.32	25.59	16.84	9.36
426	366.98	218.89	197.79	155.66	219.98	1249.1	8.02	17.25	23.32	28.72	17.96	9.98
427	625.53	384.56	126.46	182.53	298.03	1692.3	7.77	16.80	19.09	22.06	14.89	8.27
428	295.05	314.34	171.42	189.26	250.49	1422.4	14.68	12.31	18.92	26.12	16.36	9.09
429	570.36	230.51	227.71	177.00	276.65	1570.9	8.59	17.31	19.47	22.53	15.64	8.69
430	484.62	275.61	205.82	164.33	260.64	1480.0	8.55	17.64	21.24	25.11	16.78	9.32
431	410.83	224.36	188.96	167.50	234.84	1333.5	8.30	17.22	22.89	27.66	17.28	9.60
432	279.09	291.09	241.05	162.46	257.86	1464.2	14.57	13.97	21.99	26.07	17.13	9.52
433	399.89	346.67	248.32	159.41	299.52	1700.7	13.84	16.52	19.49	22.05	16.37	9.09
501	497.76	178.52	178.07	155.80	228.89	1299.7	5.10	12.01	13.13	18.76	10.86	6.03
502	412.16	146.12	113.97	151.63	183.90	1044.3	5.74	14.14	15.53	20.44	12.64	7.02
503	457.31	113.76	79.24	134.49	153.93	874.1	5.31	14.89	21.37	20.69	13.95	7.75
504	481.12	99.00	116.26	185.10	194.70	1105.6	5.76	13.95	14.85	21.46	12.64	7.02
505	536.65	121.82	107.08	161.16	190.87	1083.8	4.81	14.07	16.01	22.80	12.68	7.04
506	535.03	227.69	151.23	148.20	223.25	1267.7	4.93	12.61	14.23	19.36	11.79	6.55
507	604.32	185.54	230.24	171.50	256.82	1458.3	4.75	11.20	12.42	18.18	10.63	5.91
508	627.15	152.12	125.83	175.60	213.31	1211.2	4.46	12.92	14.32	20.53	11.91	6.62
509	606.05	186.70	181.92	175.94	249.37	1416.0	5.11	12.02	12.33	19.13	10.97	6.10
510	647.59	180.63	169.59	174.94	248.67	1412.0	4.67	11.77	12.53	21.26	11.05	6.14
511	570.57	139.97	126.67	144.03	192.63	1093.8	4.72	14.16	15.64	24.28	13.17	7.32

TABLE (D-3) :- (CONTINUED)

RUN	HEAT TRANSFER COEFFS. IN BTU/HR-SQFT*F					W/SQM*C	DRIVING TEMP. DIFFERENCES DEG F					DEG C
#	I	II	III	IV	TUBE	TUBE	I	II	III	IV	TUBE	TUBE
512	607.12	107.26	118.96	183.87	205.93	1169.3	4.87	14.37	15.32	24.41	13.11	7.28
513	756.60	186.15	201.35	185.38	277.58	1576.2	4.31	11.10	11.73	19.11	10.11	5.62
514	754.24	188.71	177.56	173.63	253.51	1439.5	4.35	12.20	12.97	22.10	11.55	6.42
515	777.11	162.46	143.24	132.68	217.21	1233.4	4.26	14.10	15.99	26.97	13.19	7.33
516	670.07	241.19	188.28	119.84	256.16	1454.6	4.87	14.82	17.25	18.96	12.05	6.70
517	761.77	175.96	140.03	140.86	226.27	1284.8	5.38	17.37	19.39	21.69	14.26	7.92
518	855.33	229.00	194.33	160.36	256.02	1453.7	3.16	11.04	17.07	22.65	11.88	6.60
519	722.19	195.88	141.94	157.99	229.30	1302.0	4.07	15.89	18.05	22.01	13.18	7.32
520	524.12	200.38	152.15	135.50	200.84	1140.4	3.92	15.08	19.85	25.88	14.43	8.02
521	948.65	271.47	169.51	148.03	270.28	1534.7	4.36	12.81	16.77	19.20	12.28	6.82
522	612.61	277.35	183.61	163.89	252.87	1435.9	4.23	11.99	19.10	23.64	13.14	7.30
523	541.06	232.01	184.29	142.78	225.43	1280.1	3.60	11.15	18.71	26.41	13.03	7.24
524	782.62	238.50	180.28	143.53	271.73	1543.0	5.05	16.48	17.83	19.90	12.83	7.13
525	761.35	273.34	156.08	148.60	238.27	1353.0	3.98	13.62	19.29	23.84	13.95	7.75
526	629.02	236.58	168.24	147.93	228.43	1297.1	4.01	12.73	20.88	27.13	14.29	7.94
527	807.80	241.64	188.55	159.64	255.57	1451.2	3.97	14.75	17.90	22.31	13.40	7.44
528	726.04	243.16	184.87	136.23	236.58	1343.4	4.38	16.50	20.55	24.78	15.18	8.43
529	579.81	268.10	152.84	141.32	225.18	1278.7	4.03	14.18	20.84	26.87	14.56	8.09
530	717.52	277.44	176.89	161.12	254.72	1446.4	3.73	12.14	19.03	25.24	13.22	7.35
531	650.24	256.05	185.23	167.08	251.24	1426.6	3.94	12.74	20.66	27.14	14.11	7.84
532	588.37	246.39	195.51	159.19	245.04	1391.4	4.49	13.22	21.41	27.26	14.71	8.17
533	799.06	362.64	210.97	178.55	296.30	1682.5	4.15	12.76	20.86	24.64	14.12	7.84
534	713.74	196.32	234.08	153.55	266.85	1515.2	5.62	14.80	18.62	21.28	13.62	7.57
535	927.14	261.96	202.78	158.87	308.58	1752.2	5.02	14.72	17.10	19.40	12.19	6.77
536	785.30	246.25	214.49	172.09	293.72	1667.8	5.49	15.83	18.17	20.38	13.28	7.38

TABLE (D-4) :- REDUCED DATA - PRESSURE DROP

RUN	INLET PRESSURE		TOTAL PRESSURE DROP	
#	PSIA	BAR	PSIA	PASCAL
134	18.98	1.309	0.020	135.83
135	19.58	1.350	0.021	141.69
136	19.08	1.316	0.029	197.88
137	19.48	1.343	0.023	159.27
138	19.28	1.329	0.034	233.73
139	19.38	1.336	0.049	340.60
140	19.48	1.343	0.032	224.08
141	19.48	1.343	0.065	449.54
142	18.99	1.309	0.033	230.28
143	24.09	1.661	0.048	333.36
144	24.80	1.710	0.043	295.10
145	24.90	1.717	0.065	448.50
146	24.10	1.662	0.066	452.64
147	24.51	1.690	0.072	493.66
148	24.11	1.662	0.080	548.13
149	24.11	1.662	0.080	553.65
150	24.20	1.669	0.061	417.82
151	24.30	1.676	0.088	604.67
152	24.70	1.704	0.081	561.92
234	19.79	1.365	0.072	492.98
235	19.69	1.358	0.071	486.77
236	19.65	1.355	0.080	548.13
237	19.95	1.376	0.082	568.82
238	19.36	1.335	0.090	622.60
239	19.66	1.356	0.090	620.53

TABLE (D-4) :- (CONTINUED)

RUN	INLET PRESSURE		TOTAL PRESSURE DROP	
#	PSIA	BAR	PSIA	PASCAL
240	19.26	1.328	0.099	679.13
241	19.36	1.335	0.103	712.57
242	19.46	1.342	0.113	775.66
243	24.18	1.667	0.082	564.68
244	24.74	1.706	0.081	558.48
245	25.04	1.727	0.091	626.73
246	24.54	1.692	0.109	748.08
247	25.04	1.727	0.110	761.53
248	24.74	1.706	0.121	831.51
249	25.22	1.740	0.125	864.60
250	24.72	1.705	0.137	946.65
251	24.82	1.712	0.140	962.51
252	24.52	1.691	0.162	1114.19
342	19.50	1.345	0.090	623.98
343	19.70	1.358	0.099	685.68
344	19.60	1.352	0.098	678.79
345	19.63	1.354	0.106	728.78
346	19.13	1.320	0.112	772.21
347	19.23	1.326	0.116	799.79
348	18.93	1.306	0.137	943.89
349	18.63	1.285	0.139	957.68
350	19.03	1.313	0.140	964.58
351	24.75	1.707	0.086	592.95
352	24.75	1.707	0.097	669.48
353	24.75	1.707	0.096	665.34
354	24.85	1.714	0.105	721.88

TABLE (D-4):- (CONTINUED)

RUN	INLET PRESSURE		TOTAL PRESSURE DROP	
#	PSIA	BAR	PSIA	PASCAL
355	24.35	1.679	0.115	794.28
356	23.75	1.638	0.114	786.00
357	24.99	1.723	0.130	899.42
358	24.59	1.696	0.137	942.51
359	24.49	1.689	0.132	912.87

TABEL (D-5) :- REDUCED DATA - ENERGY TRANSFER AND HEAT BALANCE

RUN	COOLANT BTU/HR				TUBE		TEST FLUID		ERROR
#	I	II	III	IV	BTU/HR	W	BTU/HR	W	%
101	1322.19	2077.75	944.43	755.54	5099.91	1493.64	4797.26	1405.00	5.93
102	813.11	1016.37	1422.93	1829.48	5081.88	1488.36	5085.11	1489.30	-0.06
103	1574.05	1574.03	1349.18	1124.31	5621.57	1646.42	5433.71	1591.40	3.34
104	1605.51	1834.89	1605.51	917.44	5963.36	1746.52	5657.47	1656.93	5.13
105	1731.44	1484.10	989.40	1731.44	5936.37	1738.62	5952.93	1743.46	-0.28
106	1326.71	1592.03	1857.36	1592.03	6368.13	1865.07	6207.63	1818.06	2.52
107	1678.38	1678.38	1958.10	1398.64	6713.49	1966.21	6538.83	1915.06	2.60
108	1076.64	957.02	1076.64	837.39	3947.69	1156.18	3948.95	1156.55	-0.03
109	1108.12	1208.87	805.90	1208.87	4331.75	1268.66	4203.14	1231.00	2.97
110	1097.33	1975.19	877.87	658.40	4608.79	1349.80	4500.95	1318.22	2.34
111	1133.31	2266.62	1699.97	1699.97	6799.86	1991.51	6878.20	2014.45	-1.15
112	1092.84	1457.11	1092.83	1092.83	4735.61	1386.94	4784.39	1401.23	-1.03
113	1227.76	1800.70	1064.05	982.20	5074.71	1486.26	5018.02	1469.65	1.12
114	1331.19	798.71	1597.42	1331.19	5058.52	1481.51	5318.57	1557.68	-5.14
115	1338.39	1672.98	1505.68	1171.08	5688.13	1665.91	5663.87	1658.81	0.43
116	1825.89	2373.65	1278.11	547.76	6025.41	1764.69	5972.20	1749.11	0.88
117	1996.79	1996.79	1397.74	798.71	6190.02	1812.90	6183.50	1810.99	0.11
118	1637.01	982.20	1800.70	1964.41	6384.31	1869.81	6548.73	1917.96	-2.58
119	2017.56	1667.58	1482.30	1667.58	6835.02	2001.81	6759.02	1979.55	1.11
120	1619.02	1619.02	2226.14	1619.02	7083.18	2074.49	7109.26	2082.13	-0.37
121	1827.69	1827.69	2284.59	1370.77	7310.73	2141.13	7400.37	2167.38	-1.23
122	2234.23	2234.25	1489.50	2234.23	8192.21	2399.29	7733.80	2265.04	5.60
123	905.75	905.75	1334.78	1239.44	4385.72	1284.47	4574.04	1339.62	-4.29
124	1114.42	1220.56	1273.63	1220.56	4829.16	1414.34	4951.73	1450.24	-2.54
125	890.46	1424.73	1424.73	1365.37	5105.29	1495.21	5268.32	1542.96	-3.19

TABEL (D-5) :- (CONTINUED)

RUN	COOLANT BTU/HR				TUBE		TEST FLUID		ERROR
#	I	II	III	IV	BTU/HR	W	BTU/HR	W	%
126	1392.35	1237.65	1315.00	1392.35	5337.35	1563.18	5532.70	1620.39	-3.66
127	1322.20	1416.64	1227.76	1605.52	5572.11	1631.93	5856.52	1715.23	-5.10
128	1309.60	1914.04	1410.33	1309.61	5943.58	1740.73	6208.43	1818.29	-4.46
129	1413.94	1531.77	1649.59	1649.59	6244.88	1828.97	6454.47	1890.35	-3.36
130	1198.07	1863.67	1730.54	1863.67	6655.95	1949.36	6791.13	1988.95	-2.03
131	1677.88	1466.11	2052.55	1612.71	6809.25	1994.26	7068.00	2070.04	-3.80
132	1888.85	1731.44	1888.85	1731.44	7240.59	2120.59	7321.92	2144.41	-1.12
133	1816.90	2180.28	1998.58	1816.88	7812.63	2288.12	7656.34	2242.35	2.00
134	1408.55	1878.06	469.51	591.25	4347.36	1273.23	4526.81	1325.79	-4.13
135	1761.12	1280.82	960.62	800.51	4803.07	1406.70	4755.35	1392.72	0.99
136	1683.77	748.35	1496.68	1122.52	5051.30	1479.40	5136.24	1504.28	-1.68
137	1561.45	975.91	1756.62	1171.09	5465.07	1600.58	5426.58	1589.31	0.70
138	1235.85	1647.80	1647.80	1235.85	5767.29	1689.10	5708.74	1671.95	1.02
139	1806.10	1354.58	1580.33	1354.58	6095.58	1785.24	6061.22	1775.18	0.56
140	1928.43	1205.28	1687.37	1446.32	6267.39	1835.56	6266.99	1835.44	0.01
141	2218.04	1725.14	1725.16	1478.70	7147.04	2093.19	6666.44	1952.43	6.72
142	2266.62	1133.31	1416.63	2266.62	7083.18	2074.49	6842.20	2003.91	3.40
143	1299.71	993.90	1529.06	1299.71	5122.38	1500.22	5170.41	1514.28	-0.94
144	1198.07	2196.47	998.39	1098.23	5491.16	1608.22	5507.46	1613.00	-0.30
145	1707.17	1838.48	1181.88	1313.20	6040.73	1769.18	5842.54	1711.13	3.28
146	1421.14	2273.82	1279.02	1136.91	6110.88	1789.72	6160.18	1804.16	-0.81
147	1964.39	1637.01	1800.70	1309.60	6711.70	1965.69	6470.07	1894.92	3.60
148	1699.96	1699.96	1511.08	1699.96	6610.96	1936.18	6770.57	1982.93	-2.41
149	1619.02	2023.77	2226.15	1619.02	7487.95	2193.03	7030.69	2059.11	6.11
150	1918.52	1279.02	1918.54	2131.69	7247.77	2122.69	7363.18	2156.49	-1.59
151	2542.75	2080.43	1849.28	1618.13	8090.57	2369.53	7586.25	2221.82	6.23

TABEL (D-5) :- (CONTINUED)

RUN	COOLANT BTU/HR				TUBE		TEST FLUID		ERROR
#	I	II	III	IV	BTU/HR	W	BTU/HR	W	%
152	1532.67	2043.56	2043.56	1788.13	7407.91	2169.59	7952.14	2328.99	-7.35
201	1775.52	1014.58	1395.05	1268.22	5453.37	1597.16	5481.24	1605.32	-0.51
202	656.61	1181.88	2232.44	1838.47	5909.39	1730.71	5786.17	1694.62	2.09
203	1525.47	2097.52	1525.46	1334.80	6483.24	1898.78	6119.77	1792.33	5.61
204	1568.63	2941.20	1176.49	1176.47	6862.78	2009.94	6410.63	1877.51	6.59
205	1119.81	1567.74	2239.64	2015.67	6942.85	2033.39	6723.67	1969.20	3.16
206	1753.93	1753.93	1169.29	701.56	5378.71	1575.29	5396.21	1580.42	-0.33
207	1578.54	1578.54	1821.39	849.98	5828.44	1707.00	5663.55	1658.71	2.83
208	1765.62	1629.81	1765.63	950.72	6111.78	1789.99	5971.00	1748.76	2.30
209	1707.16	1707.16	1707.16	1181.88	6303.34	1846.09	6305.45	1846.71	-0.03
210	1341.08	1660.39	1341.08	894.05	5236.60	1533.67	5325.80	1559.79	-1.70
211	1667.59	1389.65	1574.95	1389.65	6021.83	1763.64	5931.07	1737.06	1.51
212	1813.29	1419.93	1381.56	949.82	5564.60	1629.73	5603.69	1641.18	-0.70
213	1948.21	1640.60	1948.21	717.76	6254.79	1831.87	6269.11	1836.07	-0.23
214	2266.61	2455.50	1322.19	1133.31	7177.60	2102.14	6967.87	2040.72	2.92
215	1241.25	2068.74	2068.74	2068.74	7447.47	2181.18	7356.62	2154.57	1.22
216	2414.12	1536.28	2194.65	1536.26	7681.30	2249.66	7617.35	2230.93	0.83
217	2446.51	2691.16	2201.87	978.61	8318.14	2436.18	7979.43	2336.98	4.07
218	1236.74	2720.84	2226.14	2226.16	8409.87	2463.04	8209.89	2404.47	2.38
219	2563.44	2050.74	3247.02	2734.34	10595.53	3103.17	6626.64	1940.78	37.46
220	2091.24	2370.05	1533.57	975.90	6970.76	2041.56	6902.21	2021.49	0.98
221	2128.11	2584.12	1672.08	1064.06	7448.36	2181.44	7206.19	2110.51	3.25
222	1780.91	2266.62	2266.61	1295.21	7609.36	2228.59	7490.87	2193.89	1.56
223	2139.79	2798.19	1481.39	1481.39	7900.77	2313.94	7733.29	2264.89	2.12
224	1367.17	2506.47	2050.75	2221.64	8146.04	2385.77	8026.71	2350.82	1.46
225	2277.42	1897.85	2087.64	2087.62	8350.52	2445.66	8346.59	2444.51	0.05

TABEL (D-5) :- (CONTINUED)

RUN	COOLANT BTU/HR				TUBE		TEST FLUID		ERROR
#	I	II	III	IV	BTU/HR	W	BTU/HR	W	%
226	1368.06	1789.01	1789.01	1578.54	6524.62	1910.90	6546.76	1917.38	-0.34
227	2137.09	1662.19	1780.91	1068.55	6648.73	1947.25	6836.30	2002.18	-2.82
228	2136.20	2023.76	1911.33	1011.89	7083.18	2074.49	7128.53	2087.77	-0.64
229	2341.27	2218.04	1601.93	1232.24	7393.48	2165.37	7420.45	2173.27	-0.36
230	1367.17	2324.18	2050.76	1914.03	7656.14	2242.29	7752.17	2270.42	-1.25
231	2563.45	2428.51	1753.93	1079.34	7825.23	2291.81	8006.66	2344.95	-2.32
232	2446.52	3022.16	1726.95	1151.30	8346.93	2444.61	8309.10	2433.53	0.45
233	2770.32	2216.25	1939.23	1662.19	8587.99	2515.21	8466.28	2479.56	1.42
234	1554.26	1036.16	906.64	906.64	4403.70	1289.73	4485.94	1313.82	-1.87
235	1208.87	1057.75	1359.98	1208.85	4835.45	1416.18	4852.25	1421.10	-0.35
236	1331.19	1331.19	1331.19	998.39	4991.97	1462.02	5200.80	1523.18	-4.18
237	1482.30	1111.72	1667.59	1111.72	5373.34	1573.72	5406.84	1583.53	-0.62
238	1748.53	1165.69	1359.97	1554.26	5828.44	1707.00	5742.89	1681.95	1.47
239	1886.14	1467.00	1676.58	838.29	5868.01	1718.59	6011.71	1760.68	-2.45
240	1164.78	2329.58	1164.80	1397.75	6056.92	1773.92	6336.51	1855.81	-4.62
241	1178.27	1649.61	1885.25	1885.25	6598.39	1932.50	6624.95	1940.28	-0.40
242	1581.22	2108.32	2108.32	1317.69	7115.54	2083.96	6949.34	2035.29	2.34
243	1151.30	1223.25	1511.08	1295.21	5180.85	1517.34	5345.25	1565.49	-3.17
244	1309.60	1964.40	1216.06	1122.52	5612.58	1643.78	5595.62	1638.82	0.30
245	1601.92	1725.15	1232.24	1355.47	5914.78	1732.29	5894.46	1726.34	0.34
246	1503.88	2050.75	1640.60	1093.74	6288.96	1841.88	6207.25	1817.95	1.30
247	1711.65	1400.44	1556.05	1711.67	6379.81	1868.49	6469.86	1894.86	-1.41
248	2093.93	1046.96	1919.43	1744.94	6805.25	1993.09	6759.20	1979.60	0.68
249	1748.55	1942.80	1942.82	971.42	6605.59	1934.61	6993.34	2048.18	-5.87
250	1797.10	1797.12	2196.46	1597.43	7388.10	2163.79	7329.18	2146.53	0.80
251	1983.29	1983.29	1762.91	1983.29	7712.77	2258.88	7604.03	2227.03	1.41

TABEL (D-5) :- (CONTINUED)

RUN	COOLANT BTU/HR				TUBE		TEST FLUID		ERROR
#	I	II	III	IV	BTU/HR	W	BTU/HR	W	%
252	1914.04	1674.79	2871.03	1674.77	8134.63	2382.43	7988.64	2339.67	1.79
301	1695.46	1695.48	1304.20	1565.05	6260.18	1833.45	6056.21	1773.71	3.26
302	1634.30	1350.08	1847.47	1492.19	6324.04	1852.15	5842.50	1711.12	7.61
303	1075.74	1496.69	1356.37	2151.49	6080.29	1780.77	5911.47	1731.32	2.78
304	1716.16	1859.17	1716.16	1573.14	6864.62	2010.48	6298.42	1844.65	8.25
305	1208.86	1737.74	1964.41	1662.19	6573.20	1925.13	6287.86	1841.56	4.34
306	1106.15	1616.67	1446.50	2042.12	6211.43	1819.17	6147.09	1800.33	1.04
307	1602.83	2185.68	1894.24	1457.11	7139.86	2091.09	6685.21	1957.93	6.37
308	1088.33	1484.09	1879.86	1879.85	6332.14	1854.53	6582.80	1927.94	-3.96
309	1208.86	1662.19	1662.19	2165.88	6699.11	1962.00	6530.16	1912.52	2.52
310	1371.66	1920.33	1591.13	2139.80	7022.92	2056.84	6815.17	1995.99	2.96
311	1395.94	1744.94	1919.43	1744.94	6805.25	1993.09	6783.09	1986.60	0.33
312	1850.17	2018.37	1850.17	1513.79	7232.50	2118.22	6921.31	2027.08	4.30
313	1721.55	2191.07	2034.56	1721.56	7668.73	2245.98	7186.22	2104.67	6.29
314	1473.30	1894.25	2104.72	1999.48	7471.75	2188.29	7055.98	2066.52	5.56
315	1674.79	1586.64	1851.07	1851.07	6963.56	2039.45	7140.15	2091.17	-2.54
316	1449.91	1672.98	1840.28	2119.11	7082.28	2074.22	6980.83	2044.51	1.43
317	1635.20	1816.90	2180.26	1816.90	7449.25	2181.70	7428.21	2175.54	0.28
318	2032.77	2032.77	2032.76	1727.85	7826.13	2292.08	7405.82	2168.98	5.37
319	1349.18	2023.76	1956.30	1753.93	7083.17	2074.48	7424.93	2174.58	-4.82
320	1597.43	2595.81	1797.10	2196.47	8186.81	2397.71	7847.57	2298.36	4.14
321	1613.63	2110.11	2110.11	2110.11	7943.96	2326.59	7810.25	2287.43	1.68
322	1965.30	1965.30	2136.20	1879.85	7946.65	2327.38	7670.37	2246.46	3.48
323	1845.67	2234.24	2331.38	2622.80	9034.09	2645.86	7983.38	2338.13	11.63
324	1683.78	1964.41	2665.98	1964.41	8278.57	2424.59	8005.86	2344.72	3.29
325	790.63	2898.93	2371.85	2635.40	8696.80	2547.08	8172.45	2393.51	6.03

TABEL (D-5) :- (CONTINUED)

RUN	COOLANT BTU/HR				TUBE		TEST FLUID		ERROR
#	I	II	III	IV	BTU/HR	W	BTU/HR	W	%
326	2144.30	2680.35	2144.30	1876.27	8845.21	2590.54	8500.90	2489.70	3.89
327	1834.89	2446.51	2293.61	1834.87	8409.88	2463.05	8381.53	2454.74	0.34
328	1470.61	2254.93	2156.88	2156.88	8039.30	2354.51	8258.29	2418.65	-2.72
329	1699.96	2266.61	2266.61	2266.62	8499.81	2489.38	8636.15	2529.31	-1.60
330	2187.45	2187.45	2734.34	1914.05	9023.28	2642.69	8868.49	2597.36	1.72
331	2172.17	1882.55	2606.62	2027.37	8688.70	2544.70	8593.82	2516.91	1.09
332	1845.68	2331.38	2137.09	2234.24	8548.38	2503.61	8509.04	2492.09	0.46
333	1154.90	2694.75	2309.80	2694.76	8854.20	2593.18	8956.34	2623.09	-1.15
334	2050.75	2266.63	2158.68	2374.55	8850.60	2592.12	8861.48	2595.31	-0.12
335	2239.33	2617.41	2617.41	2093.93	9568.07	2802.25	9121.17	2671.36	4.67
336	3173.27	2115.49	2379.96	2115.51	9784.23	2865.56	9299.89	2723.71	4.95
337	1816.88	1635.20	2361.96	2180.28	7994.31	2341.33	9276.64	2716.90	-16.04
338	2201.86	3027.55	2477.08	1926.64	9633.13	2821.30	9627.20	2819.57	0.06
339	2191.07	2921.42	2556.25	2008.47	9677.20	2834.21	9617.05	2816.59	0.62
340	2299.00	2682.17	2299.00	2298.99	9579.16	2805.50	9482.51	2777.19	1.01
341	1834.88	2568.83	2568.83	2324.18	9296.72	2722.78	9195.94	2693.26	1.08
342	2163.18	998.38	998.39	1497.58	5657.54	1656.95	5536.62	1621.54	2.14
343	1717.96	1030.77	1546.15	1546.15	5841.04	1710.69	5864.65	1717.61	-0.40
344	1825.89	1278.11	1643.31	1460.70	6208.01	1818.17	6165.22	1805.64	0.69
345	1475.10	1475.10	1843.88	1475.10	6269.18	1836.09	6484.91	1899.27	-3.44
346	1619.02	1214.26	2226.15	1619.00	6678.43	1955.94	6765.00	1981.30	-1.30
347	1690.97	1268.21	2325.08	1690.97	6975.23	2042.87	7110.07	2082.36	-1.93
348	2698.34	1574.03	1798.91	1349.16	7420.44	2173.26	7378.23	2160.90	0.57
349	1950.02	1950.02	2681.26	1218.77	7800.06	2284.44	7735.19	2265.44	0.83
350	2527.46	1263.72	2274.73	2274.73	8340.64	2442.77	8093.63	2370.42	2.96
351	905.75	1048.76	1334.78	1716.15	5005.45	1465.97	5298.66	1551.85	-5.86

TABEL (D-5) :- (CONTINUED)

RUN	COOLANT BTU/HR				TUBE		TEST FLUID		ERROR
#	I	II	III	IV	BTU/HR	W	BTU/HR	W	%
352	917.44	1133.31	1403.15	1780.92	5234.81	1533.15	5546.39	1624.40	-5.95
353	1179.18	1427.44	1551.56	1427.43	5585.60	1635.88	5857.20	1715.43	-4.86
354	1106.33	1475.10	1770.12	1548.86	5900.40	1728.08	6175.45	1808.63	-4.66
355	1640.60	1381.55	1554.26	1726.94	6303.35	1846.09	6545.45	1917.00	-3.84
356	1359.97	1359.97	2234.24	1845.67	6799.86	1991.51	6878.25	2014.47	-1.15
357	1088.33	1780.92	2077.73	1681.97	6628.96	1941.46	6986.78	2046.25	-5.40
358	1565.04	1669.38	2295.41	1565.04	7094.87	2077.91	7388.16	2163.81	-4.13
359	1798.91	1574.04	2248.63	1798.91	7420.49	2173.28	7736.38	2265.79	-4.26
401	2428.54	2698.36	2428.51	2428.54	9983.94	2924.05	9718.55	2846.32	2.66
402	1192.67	1422.03	1651.39	1467.90	5734.00	1679.35	5993.67	1755.40	-4.53
403	944.42	584.64	1349.18	2203.66	5081.90	1488.36	5359.57	1569.69	-5.46
404	1133.31	1574.04	1259.23	1385.15	5351.73	1567.39	5389.84	1578.55	-0.71
405	611.63	2140.69	1834.88	1452.61	6039.81	1768.91	6079.99	1780.68	-0.67
406	1304.21	1439.12	1304.21	1663.99	5711.52	1672.76	5973.38	1749.45	-4.58
407	1708.96	1623.52	1367.17	1538.07	6237.71	1826.87	6310.75	1848.26	-1.17
408	1978.79	2275.61	1088.34	989.40	6332.14	1854.53	5880.21	1722.17	7.14
409	1403.15	1637.01	1520.07	1520.07	6080.29	1780.77	6112.08	1790.08	-0.52
410	1208.86	1410.34	1561.45	1762.93	5943.57	1740.72	6243.35	1828.52	-5.04
411	1624.40	2320.59	812.20	1392.35	6149.55	1801.05	6401.00	1874.69	-4.09
412	1835.78	1835.78	1694.57	1412.14	6778.27	1985.19	6714.16	1966.41	0.95
413	1619.01	1619.02	2185.67	1538.06	6961.75	2038.92	6609.68	1935.81	5.06
414	1681.97	1834.89	2293.60	1681.98	7492.44	2194.35	7016.34	2054.91	6.35
415	1511.07	1699.97	1794.41	1605.52	6610.96	1936.19	6922.73	2027.49	-4.72
416	1284.42	1773.72	1773.72	1773.72	6605.58	1934.61	6947.61	2034.78	-5.18
417	1762.93	2392.54	1888.86	1637.00	7681.32	2249.67	7279.70	2132.04	5.23
418	1726.95	1511.08	1654.99	1942.82	6835.83	2002.04	7139.91	2091.10	-4.45

TABEL (D-5) :- (CONTINUED)

RUN	COOLANT BTU/HR				TUBE		TEST FLUID		ERROR
#	I	II	III	IV	BTU/HR	W	BTU/HR	W	%
419	2057.94	949.82	2444.91	1741.34	7194.01	2106.95	7277.87	2131.51	-1.17
420	1449.01	2898.04	1932.03	1610.02	7889.09	2310.52	7634.75	2236.03	3.22
421	1744.94	1570.44	2442.92	2268.41	8026.71	2350.82	7973.57	2335.26	0.66
422	1666.68	1372.57	2549.04	2352.96	7941.25	2325.80	7520.27	2202.50	5.30
423	1646.01	1975.19	2084.93	1975.20	7681.32	2249.67	7892.13	2311.41	-2.74
424	1987.79	2572.43	1753.93	1753.93	8068.07	2362.94	8083.88	2367.57	-0.20
425	2003.98	1619.01	2331.38	1813.29	7767.66	2274.96	7468.23	2187.26	3.85
426	1435.52	1845.68	2255.83	2187.47	7724.49	2262.31	7782.41	2279.27	-0.75
427	2363.76	3151.67	1181.88	1969.80	8667.11	2538.38	8247.30	2415.43	4.84
428	2115.51	1888.85	1586.63	2417.73	8008.72	2345.55	8024.42	2350.15	-0.20
429	2384.46	1950.91	2167.68	1950.91	8453.95	2475.95	8563.05	2507.90	-1.29
430	2018.37	2374.56	2137.10	2018.38	8548.40	2503.61	8422.63	2466.78	1.47
431	1662.19	1888.85	2115.51	2266.62	7933.16	2323.43	8078.06	2365.86	-1.83
432	1985.99	1985.99	2590.42	2072.34	8634.74	2528.90	8389.84	2457.17	2.84
433	2699.05	2794.59	2364.65	1719.76	9578.05	2805.17	8953.28	2622.19	6.52
501	1543.46	1306.00	1424.73	1780.91	6055.10	1773.39	5541.45	1622.95	8.48
502	1439.13	1259.23	1079.34	1888.85	5666.55	1659.59	5439.79	1593.18	4.00
503	1475.10	1032.57	1032.57	1696.37	5236.61	1533.67	5387.54	1577.87	-2.88
504	1683.78	841.89	1052.36	2420.43	5998.45	1756.80	5978.23	1750.88	0.34
505	1567.74	1045.16	1045.16	2239.63	5897.70	1727.29	5998.59	1756.84	-1.71
506	1602.82	1748.54	1311.40	1748.54	6411.29	1877.71	6043.25	1769.92	5.74
507	1741.34	1266.43	1741.34	1899.65	6648.75	1947.25	6306.96	1847.15	5.14
508	1697.26	1198.07	1098.23	2196.47	6190.03	1812.90	6181.39	1810.37	0.14
509	1879.85	1367.17	1367.17	2050.75	6664.94	1952.00	6630.21	1941.82	0.52
510	1834.88	1295.20	1295.21	2266.62	6691.91	1959.89	6492.29	1901.43	2.98
511	1634.30	1207.96	1207.96	2131.70	6181.93	1810.53	6150.48	1801.32	0.51

TABEL (D-5) :- (CONTINUED)

RUN	COOLANT BTU/HR				TUBE		TEST FLUID		ERROR
#	I	II	III	IV	BTU/HR	W	BTU/HR	W	%
512	1794.41	939.93	1110.82	2734.34	6579.49	1926.97	6437.77	1885.46	2.15
513	1978.79	1259.23	1439.11	2158.69	6835.81	2002.04	6913.69	2024.85	-1.14
514	1987.79	1403.15	1403.15	2338.57	7132.65	2088.98	6839.50	2003.12	4.11
515	2006.68	1395.95	1395.95	2181.17	6979.75	2044.19	6873.67	2013.13	1.52
516	1978.78	2176.67	1978.78	1385.17	7519.39	2202.24	7335.24	2148.31	2.45
517	2482.49	1861.88	1654.98	1861.86	7861.20	2302.35	7668.97	2246.05	2.45
518	1636.10	1539.86	2021.07	2213.55	7410.57	2170.37	7200.11	2108.73	2.84
519	1784.51	1896.04	1561.45	2119.11	7361.11	2155.88	7488.85	2193.30	-1.74
520	1246.65	1840.27	1840.28	2137.10	7064.29	2068.95	7145.09	2092.62	-1.14
521	2502.27	2117.32	1732.34	1732.36	8084.29	2367.69	7742.26	2267.51	4.23
522	1574.04	2023.76	2136.21	2361.06	8095.07	2370.84	7773.60	2276.69	3.97
523	1181.88	1575.84	2101.12	2298.10	7156.93	2096.09	7371.85	2159.03	-3.00
524	2394.34	2394.34	1959.00	1741.34	8489.01	2486.22	8243.30	2414.26	2.89
525	1834.88	2266.62	1834.89	2158.69	8095.07	2370.84	8009.09	2345.66	1.06
526	1529.06	1834.89	2140.69	2446.51	7951.15	2328.69	7744.36	2268.13	2.60
527	1941.92	2170.38	2056.15	2170.38	8338.82	2442.23	8286.24	2426.83	0.63
528	1929.33	2443.81	2315.18	2057.95	8746.27	2561.57	8718.36	2553.39	0.32
529	1418.43	2314.29	1941.01	2314.29	7988.03	2339.49	7944.05	2326.61	0.55
530	1623.51	2050.75	2050.75	2477.99	8203.00	2402.46	8345.14	2444.08	-1.73
531	1554.26	1985.99	2331.38	2763.11	8634.74	2528.90	8497.59	2488.73	1.59
532	1605.52	1983.29	2549.95	2644.39	8783.14	2572.36	9079.26	2659.09	-3.37
533	2010.27	2814.38	2680.37	2680.37	10185.40	2983.05	8914.92	2610.96	12.47
534	2433.91	1770.12	2655.17	1991.38	8850.58	2592.11	8484.26	2484.83	4.14
535	2817.09	2347.57	2112.81	1878.06	9155.52	2681.42	8739.55	2559.60	4.54
536	2612.00	2374.56	2374.54	2137.09	9498.18	2781.78	9126.30	2672.87	3.92

APPENDIX E

APPENDIX E

UNCERTAINITY ANALYSIS IN EXPERIMENTAL MEASUREMENTS OF OVERALL HEAT TRANSFER COEFFICIENTS

Due to the limits in the accuracy with which the measurements were taken, the final result of intrest is associated with certain uncertainity. The attempt was made to determine the uncertainity in the experimental measurements of the condensation heat transfer coefficients. The method outlined by Kline and McClintock [56] was used in estimating the uncertainity associated with overall heat transfer coefficient $\overline{h}$ for the smooth tube, run 144.

The overall average heat transfer coefficient is calculated by

$$\overline{h} = \frac{Q}{A_n(\overline{T}_s - \overline{T}_{wi})} \tag{E-1}$$

The experimental uncertainity for the overall average heat transfer coefficient is given by

$$w_{\overline{h}} = \left[\left(\frac{\partial \overline{h}}{\partial Q} w_Q\right)^2 + \left(\frac{\partial \overline{h}}{\partial A_n} w_{A_n}\right)^2 + \left(\frac{\partial \overline{h}}{\partial \overline{T}_s} w_{\overline{T}_s}\right)^2 + \left(\frac{\partial \overline{h}}{\partial \overline{T}_{wi}} w_{\overline{T}_{wi}}\right)^2 \right]^{1/2} \tag{E-2}$$

From Eq. (E-1)

$$\frac{\partial \overline{h}}{\partial Q} = \frac{1}{A_n(\overline{T}_s - \overline{T}_{wi})} \tag{E-3}$$

$$\frac{\partial \overline{h}}{\partial A_n} = - \frac{Q}{A_n^2(\overline{T}_s - \overline{T}_{wi})} \tag{E-4}$$

$$\frac{\partial \overline{h}}{\partial \overline{T}_s} = - \frac{Q}{A_n(\overline{T}_s - \overline{T}_{wi})^2} \tag{E-5}$$

$$\frac{\partial \bar{h}}{\partial \bar{T}_{wi}} = \frac{Q}{A_n(\bar{T}_s - \bar{T}_{wi})^2} \tag{E-6}$$

For this run

$$A_n = \pi D_i L = \left(\frac{0.545}{12}\right)(9.0) = 1.284 \text{ ft}^2$$

$$\bar{T}_s = 103.16\ ^oF$$

From the one dimensional heat conduction equation, the inside wall temperature can be estimated as

$$\bar{T}_{wi} = \bar{T}_{wo} + \frac{Q}{2\ \ LK} \ln\left(\frac{D_o}{D_i}\right) \tag{E-7}$$

Also, neglecting the temperature drop in the tube wall, it can be approximated as

$$\bar{T}_{wi} \cong \bar{T}_{wo} = 87.08\ ^oF$$

For this run, the heat gained by the cooling water

$$Q = 5491.16 \text{ Btu/hr}$$

Substituting in Eqs.(E-3) to (E-6) we get

$$\frac{\partial \bar{h}}{\partial Q} = \frac{1}{1.284(103.16-87.08)} = \frac{1}{20.67} \tag{E-8}$$

$$\frac{\partial \bar{h}}{\partial A_n} = \frac{-5491.16}{(1.284)^2(103.16-87.08)} = -207.12 \tag{E-9}$$

$$\frac{\partial \bar{h}}{\partial \bar{T}_s} = \frac{-5491.16}{(1.284)(103.16-87.08)^2} = -16.52 \tag{E-10}$$

$$\frac{\partial \bar{h}}{\partial \bar{T}_{wi}} = \frac{5491.16}{(1.284)(103.16-87.08)^2} = 16.52 \tag{E-11}$$

The estimation of the uncertainity of energy transfer, w_Q:

The energy transfer is given by

$$Q = \dot{m}_{wa}\ Cp_{wa}\ (T_{wao} - T_{wai}) \tag{E-12}$$

The uncertainity in Q is given by

$$w_Q = \left[\left(\frac{\partial Q}{\partial \dot{m}_{wa}} w_{\dot{m}_{wa}}\right)^2 + \left(\frac{\partial Q}{\partial Cp_{wa}} w_{Cp_{wa}}\right)^2 + \left(\frac{\partial Q}{\partial T_{wao}} w_{T_{wao}}\right)^2 + \left(\frac{\partial Q}{\partial T_{wai}} w_{T_{wai}}\right)^2\right]^{1/2} + \text{heat exchange with the environment} \qquad \text{(E-13)}$$

For this particular run

$\dot{m}_{wa}$ = 554.66 lbm/hr

Cp_{wa} = 1.0 Btu/lbm.°F

T_{wao} = 76.64 °F

T_{wai} = 67.28 °F

Therefore

$$\frac{\partial Q}{\partial \dot{m}_{wa}} = Cp_{wa}(T_{wao} - T_{wai}) = 1.0(76.64-67.28)$$

$$= 9.36 \text{ Btu/lbm}$$

$$\frac{\partial Q}{\partial Cp_{wa}} = \dot{m}_{wa}(T_{wao} - T_{wai}) = 554.66(76.64-67.28)$$

$$= 5191.63 \text{ lbm.}^{\circ}\text{F/hr}$$

$$\frac{\partial Q}{\partial T_{wao}} = \dot{m}_{wa} Cp_{wa} = (554.66)(1.0)$$

$$= 554.66 \text{ Btu/hr.}^{\circ}\text{F}$$

$$\frac{\partial Q}{\partial T_{wai}} = -\dot{m}_{wa} Cp_{wa} = -(554.66)(1.0)$$

$$= -554.66 \text{ Btu/hr.}^{\circ}\text{F}$$

The uncertainity associated with the water flow was assumed to be within ∓ 1% of the flow rate. Therefore,

$$w_{\dot{m}_{wa}} = 0.01 \times 554.66 = 5.54 \text{ lbm/hr}$$

and the uncertainity of the specific heat $w_{Cp_{wa}}$ was assumed to be

$$w_{Cp_{wa}} = 0.004 \text{ Btu/lbm.}^{o}\text{F}$$

The uncertainities in T_{wao}, and T_{wai} were determined from the uncertainities of thermocouples and data acquisition system reading as follows :

Uncertainity due to thermocouple wire inaccuracies $\mp$ 0.75 ^{o}F
Uncertainity due to data acquisition system $\mp$ 0.01 % of the reading

Therefore,

$$w_{T_{wao}} = \left[(0.75)^2 + (76.64 \times 0.0001)^2\right]^{1/2} = 0.75 \ ^{o}\text{F}$$

and

$$w_{T_{wai}} = \left[(0.75)^2 + (67.28 \times 0.0001)^2\right]^{1/2} = 0.75 \ ^{o}\text{F}$$

For this particular run, heat balance error of -0.3% obtained and it was considered to be the estimate of the heat transferred to the ambient. Substituting the values in Eq.(E-13) yields

$$w_Q = \Big[(9.36 \times 5.54)^2 + (5191.63 \times 0.004)^2 + (554.66 \times 0.75)^2$$
$$(-554.66 \times 0.75)^2\Big]^{1/2} + (0.003 \times 5491.16)$$
$$= 607.43 \text{ Btu/hr}$$

The estimation of the uncertainity of heat transfer area, w_{A_n} :

$$A_n = \pi D_i L \tag{E-14}$$

Thus, the uncertainity

$$w_{A_n} = \left[\left(\frac{\partial A_n}{\partial D_i} w_{D_i}\right)^2 + \left(\frac{\partial A_n}{\partial L} w_L\right)^2\right]^{1/2}$$

$$= \left[(\pi L w_{D_i})^2 + (\pi D_i w_L)^2\right]^{1/2} \tag{E-15}$$

For this particular run,

$$D_i = 0.0454 \text{ ft}$$

$L = 4\Delta z = 9.0$ ft

The uncertainities in measuring the inside diameter and the length of the tube were estimated by

$w_{D_i} = 0.001$ ft

$w_L = 0.01$ ft

Therefore,

$$w_{A_n} = \left[(\pi \times 9.0 \times 0.001)^2 + (\pi \times 0.0454 \times 0.01)^2\right]^{1/2}$$
$$= 0.028 \text{ ft}^2$$

The estimation of the uncertainity for the average saturation temperature, $w_{\overline{T}_s}$:

The average saturation temperature is a function of the saturation pressure P_s

$$\overline{T}_s = \overline{T}_s(P_s) \qquad \text{(E-16)}$$

The uncertainity is estimated by

$$w_{\overline{T}_s} = \left[\frac{\partial \overline{T}_s}{\partial P_s} \; w_{P_s}\right] \qquad \text{(E-17)}$$

The uncertainity, w_{P_s} , results from the following uncertainities

Uncertainity due to the pressure gage reading: ∓0.2 psia
Uncertainity due to the pressure gage resolution: ∓ 0.2 psia
Uncertainity associated with the pressure fluctuations in the system: ∓ 0.25 psia

Therefore,

$$w_{P_s} = \left[(0.2)^2 + (0.2)^2 + (0.25)^2\right]^{1/2} = 0.377 \text{ psia}$$

From the thermophysical property tables given in ASHRAE Handbook of Fundamentals, and at the pressure range of interest to this experimental run, it was estimated that

$$\frac{\partial \overline{T}_s}{\partial P_s} = \frac{\Delta T}{\Delta P} = 2.27 \ ^oF/psia$$

Therfore,

$$w_{\overline{T}_s} = \left[(2.27 \times 0.377)\right] = 0.856$$

The estimation of the uncertainity of the average inside wall temperature, $w_{\overline{T}_{wi}}$:

As shown earliear in this Appendix

$$\overline{T}_{wi} \cong \overline{T}_{wo}$$

The factors which contribute to the uncertainity of the average outside wall temperature, were

Uncertainity due to thermocouple wire inaccuracies $\mp$ 0.75 ^oF
Uncertainity associated with the attatchment method $\mp$ 1.5 ^oF
Uncertainity due to the data acquisition system $\mp$ 0.01% of the reading

Therefore,

$$w_{\overline{T}_{wi}} \cong w_{\overline{T}_{wo}} = \left[(0.75)^2 + (1.5)^2 + (87.08 \times 0.0001)^2\right]^{1/2}$$

$$= 1.67 \ ^oF$$

The values of w_Q, w_{A_n}, $w_{\overline{T}_s}$, and $w_{\overline{T}_{wi}}$ are substituted in Eq.(E-2) to yield

$$w_{\overline{h}} = \left[\left(\frac{1}{20.67} \times 607.43\right)^2 + (-207.12 \times 0.028)^2 + (-16.52 \times 0.856)^2 + (16.52 \times 1.67)^2\right]^{1/2}$$

$$= \mp 43.10 \ Btu/hr.ft^2.^oF$$

Thus for this run,

$$\overline{h} = 266.87 \mp 43.10 \quad Btu/ft^2.hr.^oF$$

Therefore, the uncertainity for the experimental condensation overall average heat transfer coefficient of this run is about ∓ 16.15%. It can also be assumed that this uncertainity holds true for all other runs.

The main reason for such a high value of uncertainity can be attributed to the fact that the driving temperature difference ($\overline{T}_s - \overline{T}_{wi}$) was low for this run.

APPENDIX F

APPENDIX F

Table F.1: Tabulation of Stastistical Information for the Curve Fits to the Experimental Overall Heat Transfer Coefficient

$$h = C\,G^{n}$$

Nominal Inlet Pressure (bar)	Tube No.	n	C	Correlation Coefficient
1.32	1	0.654	0.281	0.934
	2	0.507	2.197	0.908
	3	0.372	6.465	0.664
	4	0.820	6.238 E-02	0.924
	5	0.519	1.681	0.870
1.47	1	0.736	0.104	0.972
	2	0.675	0.309	0.976
	3	0.614	0.420	0.906
	4	1.015	7.638 E-03	0.929
	5	0.666	0.361	0.796
1.67	1	0.531	0.905	0.938
	2	0.711	0.198	0.961
	3	0.330	8.420	0.673
	4	1.031	6.172 E-03	0.935
	5	0.860	4.964 E-02	0.942

Table F.2: Tabulation of Stastical Information for the Curve Fits to the Experimental Overall Pressure Drop

$$p = C' G^{n'}$$

Nominal Inlet Pressure (bar)	Tube No.	n'	C'	Correlation Coefficient
1.32	1	1.200	1.617 E-11	0.759
	2	1.052	1.199 E-06	0.985
	3	1.253	2.440 E-07	0.973
1.67	1	1.357	2.668 E-08	0.809
	2	1.700	1.184 E-09	0.986
	3	1.242	2.671 E-07	0.973

CURRICULUM VITA

K.S. VENKATESH

Candidate for the degree of

Master of Science

THESIS: AUGMENTATION OF CONDENSATION HEAT TRANSFER OF R-11 BY INTERNALLY FINNED TUBES

MAJOR FIELD: Mechanical Engineering

BIOGRAPHICAL:

PERSONAL DATA: Born in Kanakpur, Karnataka, India, February 7, 1957.

EDUCATION: Bachelor of Engineering degree with Distinction, in Mechanical Engineering, B.M. Srinivasiah College of Engineering, Bangalore University, 1979; completed requirements for Master of Science, Kansas State University, 1984.

EXPERIENCE: Graduate Research Assistant, Dept. of Mechanical Engg., Kansas State University, 1982 - 1984.

Quality Control Engineer, Control Equipment Division, Barath Heavy Electricals Limited, 1979 - 1982.

AUGMENTATION OF CONDENSATION HEAT TRANSFER OF R-11
BY INTERNALLY FINNED TUBES

by

K.S. VENKATESH

B.E., Mechanical Engineering, Bangalore University, India, 1979

AN ABSTRACT OF MASTER'S THESIS

Submitted in partial fulfillment of the

requirements for the degree

MASTER OF SCIENCE

Department of Mechanical Engineering

KANSAS STATE UNIVERSITY

Manhattan, Kansas

1984

AUGMENTATION OF CONDENSATION HEAT TRANSFER OF R-11 BY INTERNALLY FINNED TUBES

ABSTRACT

The continuous demand for more efficient heat exchangers has stimulated the interest of investigators to explore the use of different techniques to augment the heat transfer. Before incorporating any of the augmentation techniques into a full scale industrial use, a considerable amount of testing is necessary. The ultimate objective is the development of reliable design correlations for predicting the heat transfer and pressure drop in heat exchangers with heat transfer augmented surfaces. The present study was concerned with augmentation of in-tube condensation of R-11 by internally finned tubes.

Heat transfer and pressure drop data were taken during condensation of R-11 inside five horizontal tubes. One tube was smooth, one had straight internal fins and the remaining three had spiral internal fins with different outside diameters and fin geometries. The smooth tube was used as a basis for comparison with the results of the finned tubes. The experimental results of all tubes tested were compared with predictions of numerous existing correlations in order to identify the correlation which best predicted the results of the present study.

The results are summarized below.

1. On a nominal area basis, an enhancement in heat transfer as high as 55% over the smooth tube results was obtained by internally finned tubes, over the mass flux range tested. The heat transfer was accompanied by a modest increase in the pressure drop.

2. The best predictor of the smooth tube sectional and overall heat transfer coefficients was the correlation of Akers et al.[6]. For internally

finned tubes, the correlation of Luu and Bergles [45,46] predicted the sectional and overall heat transfer coefficient best.

3. The best predictor of the pressure drop of the smooth tube was the combination of the frictional drop correlation of Lockhart-Martinelli [14] and the void fraction correlation of Zivi [21]. Good correlation was also obtained by replacing the correlation of Lockhart-Martinelli by the correlation of Dukler [16], for the frictional pressure drop.

4. The same combinations of frictional pressure gradient and void fraction correlations of the smooth tube predicted the finned tubes pressure drop by replacing the nominal inside diameter by the hydraulic diameter.

5. The ratio of the pumping power per unit heat transfer, subject to the constraints of fixed geometry, same inlet pressure and flow rate was used to evaluate the performance of one of the finned tubes in relation to the smooth tube. The results showed that over the mass flow rate tested, the smooth tube required less pumping power per unit heat transfer.

6. The ratio of heat transfer enhancement of the finned tube to smooth tube to a similar ratio for the pressure drop was also used to evaluate the performance of the same finned tube. The ratio was also subject to the same constraints as the ratio of the pumping power per unit heat transfer. This ratio was lower than 1 but increased with the increase in mass flow rate. The result suggested that this ratio could exceed 1 at higher mass flow rates. However, such observation could not be confirmed because of the limitation of the test facility. A ratio greater than one indicates that the increase in heat transfer of the internally finned tube is accompanied only by a modest increase in pressure drop. Hence, in the flow range where this ratio could be greater than one, internally finned tubes could be advantageous compared to smooth tubes.